Predictive Medicine for Chronic Patients in an Integrated Care Scenario

Chronic Obstructive Pulmonary Disease as Use Case

Isaac Cano Franco

UNIVERSITAT DE BARCELONA

Predictive Medicine for Chronic Patients in an Integrated Care Scenario

Chronic Obstructive Pulmonary Disease as Use Case

Report of the Doctoral Thesis presented by
Isaac Cano Franco
to obtain the PhD degree

under the direction of
Prof. Josep Roca Torrent
Co-directed by
Prof. Peter D. Wagner

Thesis registered at the Doctoral Program of Medicine 2010
Department of Medicine, School of Medicine

Memoria de la tesis doctoral presentada por
Isaac Cano Franco
para optar al grado de doctor en medicina

Trabajo realizado bajo la dirección de
Prof. Josep Roca Torrent
y la codirección de
Prof. Peter D. Wagner

Tesis inscrita en el programa de Doctorado de Medicina
Departamento de Medicina, Facultad de Medicina, Universidad de Barcelona

Barcelona 2014

Contents

Dedicatoria

Sin el apoyo constante, tanto moral como económico, por parte de mi familia,
sin los ratos de diversión y desconexión mental con mis amigos,
sin la ayuda de todos aquellos que día a día demuestran ser los mejores compañeros,
sin la conmemorable ayuda de ambos directores de esta tesis doctoral,
y sobretodo, sin el cariño recibido durante casi 14 años de mi pareja y compañera,
el logro académico y profesional reflejado en esta tesis no tendría valor.

Without the constant support, both moral and financial, from my family,
without the moments of fun and mental disconnection with my Friends,
without the everyday help of all of you that every day prove to be the best work-mates,
without the tremendous help of both directors of this dissertation,
and above all, without the love received during almost 14 years from my life partner,
the academic and professional achievements reflected in this thesis would be worthless.

Grants and support

This PhD thesis was partly supported by:

- Synergy-COPD (Modeling and Simulation Environment for Systems Medicine: Chronic Obstructive Pulmonary Disease (COPD) as a use case): grant FP7-ICT-2011-270086.

- NEXES (Supporting Healthier and Independent Living for Chronic Patients and Elderly; grant CIP-ICTPSP- 2007-225025).

- FIS PI09/90634 - Servicios Innovadores de Atención Integrada para Pacientes Crónicos - PITES- ISCIII 2010-12.

- FIS PI12/01241 - Escalabilidad Regional de los Servicios de Atención Integrada y Ayuda a la Decisión Clínica - PITES-ISA ISCIII 2013-15.

Glossary

4P	Predictive, Preventive, Personalized and Participatory
ACO	Accountable Care Organizations
CDSS	Clinical Decision Support Systems
COPD	Chronic Obstructive Pulmonary Disease
COPDkb	COPD knowledge base
CT	Computed Tomography
CVD	Cardiovascular Disorders
DHF	Digital Health Framework
DM	Diabetes Mellitus
ECLIPSE	The Evaluation of COPD Longitudinally to Identify Predictive Surrogate End-points
EHR	Electronic Health Record
EIP-AHA	European Innovation Partnership for Active and Healthy Ageing
FEV_1	Forced expiratory volume in the first second
GOLD	Global initiative for chronic Obstructive Lung Disease
HIE	Health Information Exchange
HIS	Hospital Information Systems
ICS	Integrated Care Services
ICS-ICT	ICS supported by ICT
ICT	Information and Communications Technologies
NCDs	Non-Communicable Diseases
NEXES	Supporting Healthier and Independent Living for Chronic Patients and Elderly
PmO_2	Mitochondrial Partial Pressure of Oxygen
ROS	Reactive Oxygen Species
Synergy-COPD	Modeling and Simulation Environment for Systems Medicine: Chronic Obstructive Pulmonary Disease (COPD) as a use case
T2DM	Type 2 Diabetes Mellitus
WHO	World Health Organization

A new scenario for patients with chronic disorders

The need for an operational frame facilitating a continuous interplay between integrated care and novel systems-oriented biomedical research is a pivotal unmet need for an effective deployment of 4P (Predictive, Preventive, Personalized and Participatory) medicine for patients with chronic diseases [1, 2].

The five major non-communicable diseases (NCDs) prioritized by the Chronic Care program of the World Health Organization [3] are: cardiovascular disorders (CVD), cancer, chronic respiratory diseases, diabetes mellitus (DM) and mental disorders. Among these NCDs, Chronic Obstructive Pulmonary Disease (COPD) has a high prevalence - ~ 9% of the adult population above 45 yrs. [4] – and it is the fourth leading cause of mortality worldwide [5], imposing a high burden on healthcare systems. For the reasons described above and other factors that will be presented in this introductory section, COPD is taken as the use case in the PhD Thesis.

The current research work aims to explore a systems medicine [2, 6] orientation to analyze the potential of computer-based modeling to improve knowledge on underlying mechanisms of COPD heterogeneity, both in terms of clinical manifestations and progress. The proposed approach should lead to generation of biomedical knowledge to enhance patient management while exploring applicable strategies to foster cross talk between healthcare and biomedical research, resulting in a quick transfer of research achievements into clinical practice.

Deployment of integrated care: barriers & opportunities

Over the last years, the epidemics of NCDs and the need for cost-containment are triggering factors for a profound reshaping of the way we approach delivery of care for chronic patients [7]. Integrated care, following the Chronic Care model, is widely accepted [8]. In the new scenario, conventional disease-oriented approaches, centered on the management of clinical episodes, are being replaced by novel patient-centered services. Such a transition has proven successful in areas wherein one organization is providing care [9-11], but extensive deployment of integrated care services (ICS) in settings with heterogeneous healthcare providers is still a challenge.

The three major barriers for adoption of ICS [12] are: *i)* change management; *ii)* lack of reimbursement incentives; and, *iii)* organizational interoperability among professional teams, from different providers and healthcare tiers, working around the patient.

Change management - The complexity of healthcare systems [13] requires change management strategies with a building blocks approach [7, 14], and based on complicities between top-down policies and bottom-up initiatives [12]; as opposed to massive transitional changes of healthcare driven by top-down designs.

Economic incentives - Novel reimbursement modalities, based on payment by results with a bundle approach, including risk sharing among actors, seem to facilitate adoption of ICS. The main limiting factor for implementation is the lack of experience in the technicalities for implementing bundle-based payments. The current situation could be progressively overcome by the steady consolidation of experiences like the Accountable Care Organizations (ACO) in USA [15, 16], as well as different pilots in the EU [17].

ICT-enabled organizational interoperability - Last but not least, information and communication technologies (ICT) have a major role to facilitate interoperability among heterogeneous providers, each one using proprietary health information systems, as extensively analyzed in the current PhD thesis. Moreover, the use of appropriate ICT has shown to be essential to support continuity of care through collaborative tools, facilitating accessibility of citizens and patients to healthcare and generating a disruptive scenario in terms of information management.

Different on-going initiatives aiming at enforcing the transition toward adoption of the novel healthcare model, such as the EIP-AHA (European Innovation Partnership for Active and Healthy Ageing) [18], are generating and disseminating specific proposals to foster extensive deployment of integrated care. It is currently well accepted that deployment of ICS supported by ICT (ICS-ICT) may contribute to enhance health outcomes without increasing overall costs of the system. Such a generation of healthcare efficiencies is partly achieved by the transfer of complexities from specialized to primary care.

However, it is hypothesized that the generation of health efficiencies can be markedly boosted by promoting a more active role of citizens and patients, and fostering cost-effective preventive strategies aiming at modulating disease progress. These two strategic proposals require adoption of a novel health paradigm that involves bridging traditional healthcare delivery (i.e. formal care) and informal care (e.g. patient self-management, wellness programs, social care, etc.) through adoption of citizen's (patient's) personal health records as management tools. In this new scenario, the correct articulation of patient gateways and mobile devices, also known as mHealth [19], is promising to empower for the first time an efficient channel enhancing accessibility to the health system, facilitating monitoring and including patient's behavioral and environmental factors into health management. The ultimate goal of patient gateways is

to support cost-effective preventive interventions to modulate the evolution of the disease, which might represent tremendous sources of efficiencies if in-place.

Toward health risk assessment & stratification for patient's management

Adoption of proper strategies for patient's health risk assessment and stratification constitute a key element for deployment of ICS-ICT, aiming at transferring complexity to primary care and the community. Current stratification tools rely on population analyses generally based on past use of healthcare resources. They are useful to support interventions and/or to define health policies at group level, but they show limitations for clinical applicability at patient level.

Current changes in the landscape of risk assessment are driven largely by the convergence of two events: *i)* the phenomenal advances in molecular and systems biology; and, *ii)* ICS-ICT facilitating novel scenarios for data management, including longitudinal analyses combining biological and non-biological phenomena. These drivers are prompting to consider adoption of the emerging methods in systems medicine as tools to inform risk assessment and decision-making in the clinical arena.

From systems biology to systems medicine

Briefly, systems biology [20] is the study of an organism as a whole living system, viewed as an integrated and interacting network of genes, proteins, biochemical reactions and environmental factors at different levels, which together give rise to life, as depicted in Figure 1. Systems biology differs from previous biological reductionist approaches as it does not focus on individual components of the living system, but considers the interaction among all components and how they work as a whole organism. Hence, there are properties of biology that cannot be discovered by analyzing individual components. These are known as emergent properties.

Another pivotal component is the use of mathematical modeling, using huge amounts of data, as a tool to explore biological systems and their interactions with the environment. In this regard, the discipline has expanded through the development of high-throughput technologies such as high-throughput sequencing and mass spectrometry, which has enabled scientists and clinicians to examine genomes, transcriptomes, proteomes, metabolomes, and other "omics" information in unprecedented manner. Furthermore, application of the systems biology approach into health has generated a new paradigm, systems medicine, that is actively transforming the field of modern healthcare from symptom-based disease diagnosis and treatment to precision/personalized medicine in which patients are treated based on underlying disease mechanisms [22-24].

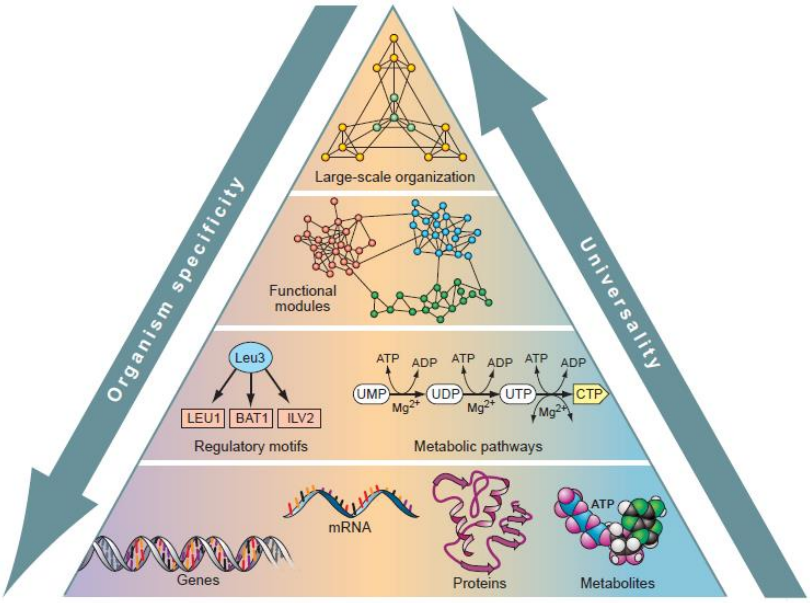

Figure 1: *The Systems Biology view of life states that insights into the logic of cellular organization can be achieved when the cell is studied considering the universal organizing principles of complex networks, in which the components, unique to a given organism, are connected by functional links. Partially reproduced with permission from [21].*

The new orientation provides the basis for future individualized risk assessment and prediction, facilitating patient stratification as a first step to a further personalized healthcare that should optimize treatment. Most human diseases are complex and/or polygenic, and many have several external (environmental, life style, societal, etc.) influences, so the study of genes and proteins as part of a system should help to understand the basis of complex disease [25-29], and to personalize therapies [30].

In this context, systems patho-biology is defined as the discipline that integrates genetic, "omics", cellular, physiological, and clinical data to create a network that can be used to model disease expression and response to therapy for prediction purposes, as illustrated in **Figure 2**. In order to understand best disease manifestations, one needs not only to define the architecture or topology of the disease network within the context of the universe of complex interplay of factors in a cell or organism, but also to explore its dynamic response to perturbations. The characteristically nonlinear responses of these complex systems underlie their emergent properties, which can only be appreciated when the system is viewed in a holistic context. This leads to the introduction of the two principal categories of systems medicine modeling approaches: statistical (network-driven) [31] and mechanistic (causal-driven) [32] models. The key difference between them is that whereas statistical modeling represents associations within the system organization, mechanistic modeling provides representations of information flow through the system, which can in turn be translated into dynamic equations. In other words,

statistical models provide a qualitative and data-driven view of the system mainly based on correlations, while mechanistic models pick a defined problem and focus on how it works considering causative and quantitative relationships and temporal dynamics.

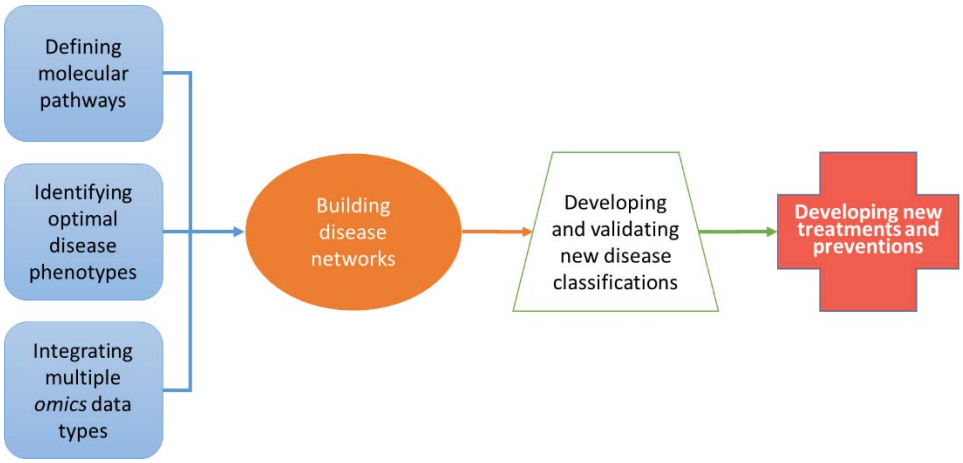

Figure 2: *Approaches to complex diseases in network medicine.*

Ultimately, transforming medicine into a modeling driven endeavor will require quantitative measurements. In this way, one begins to define the discipline of network medicine [33]. This scenario of network-based thinking might result in better understanding chronic disease mechanisms and co-morbidity clustering that will foster predictive medicine for chronic patients with relevant implications on management.

It is well accepted that network medicine is opening entirely new and fascinating scenarios, however, at the same time; it is generating novel requirements with impact on adoption [34]. Firstly, the need for a proper management of the huge amount of information from the multiple levels of data [35-37], as listed in **Figure 3**, which are mainly stored in electronic resources and in the scientific literature, and the need for highly applicable user-profiled functionalities to manage this knowledge [38, 39]. Secondly, the need for strategies combining mechanistic and statistical modeling approaches to investigate the complexity of chronic diseases with a threefold objective: *i)* to infer distributions for model parameters from available prior knowledge and experimental data; *ii)* to employ models to predict possible outcomes of new experiments (consistently propagating uncertainty); and *iii)* to compare alternative models of the system to assess validity of working hypothesis. Ultimately, converging mechanistic and statistical modeling might enable posterior inference, model inference and characterization of uncertainty, leading to a better understanding of disease mechanisms and facilitating to

enable future rule-based clinical decision-making. This is, rules derived from such approaches should be expected to feed Clinical Decision Support Systems (CDSS).

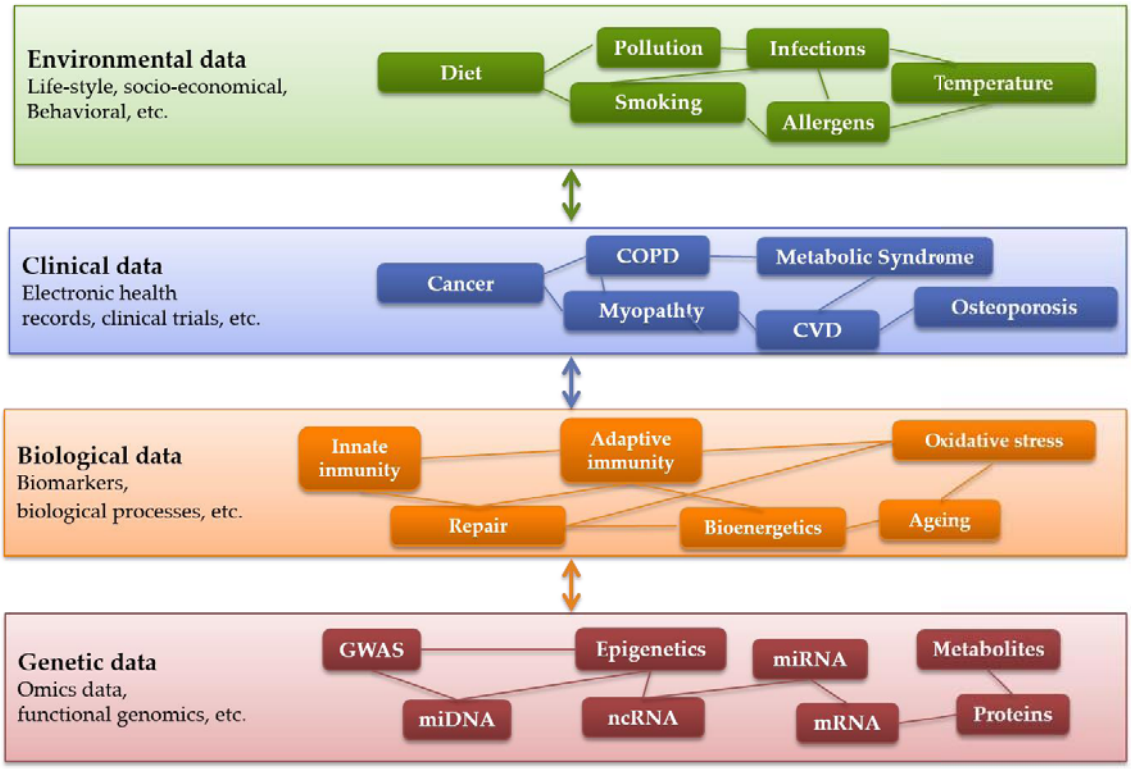

Figure 3: *The holistic approach of system medicine prompts the need for multilevel integration of heterogeneous patient information generated by different data sources, namely: environmental, clinical, biological and genetic data.*

CDSS, as active knowledge systems, use several items of patient data (e.g. physiological, environmental, genomic, etc.) to generate case-specific advice [40] based on validated knowledge (e.g. clinical guidelines, novel patient stratification approaches, etc.). CDSS ought to be used as supporting tools embedded into clinical decision-making processes (e.g. novel ICS clinical processes) involving early interventions and patient management for chronic conditions, such as Chronic Obstructive Pulmonary Disease (COPD), the target chronic condition of the current PhD Thesis.

COPD as a highly heterogeneous major chronic disease

COPD is a prevalent chronic respiratory disease that imposes a high burden on healthcare systems worldwide and it is currently the fourth leading cause of mortality [5]. Current diagnosis of COPD is based on three concurrent criteria [4]: *i)* presence of respiratory symptoms, mainly shortness of breath and/or chronic cough/sputum; *ii)* history of inhalation of irritants; and, *iii)* forced spirometry testing indicating an obstructive ventilatory defect. The expiratory flow limitation observed in COPD patients is due to

increased airways resistance and/or reduced lung elasticity caused by destruction of pulmonary parenchyma.

The most common cause of COPD is the inhalation of irritants, mainly tobacco smoke. Smoking, however, is far from the only cause of COPD, with a number of other environmental factors playing important roles. Among these, exposure to environmental toxins, either fumes or particulates, are the most important [41]. In some parts of the world, exposure to indoor air pollution, consequent to the use of biomass for heating and cooking, is the major etiologic factor for COPD [42, 43]. In the developed world, air pollution has a substantial adverse effect on lung function [44], measured as the forced expiratory volume in one second (FEV_1). However, although FEV_1 falls gradually over adult lifespan, in most non-smokers and in many smokers clinically significant airflow obstruction never develops [45]. Hence, factors other than exposure to inhaled irritants may also contribute to COPD risk, such as bronchial hyper-responsiveness [46], low birth weight [47], aging [48], low socioeconomic status [49], nutrition [50, 51] and genetic factors [52], among others [53]. Overall, although the inhalation of tobacco smoke is the main cause of COPD, only approximately 15 to 20% of all tobacco smokers are prone to develop the disease and there is marked individual variability of both clinical manifestations and COPD progression [4, 54, 55] with relevant implications in terms of health risk assessment and patient management [56].

Repeated episodes of exacerbations are observed in some COPD patients, constituting a well-established disease subgroup, with an associated negative impact on use of healthcare resources and prognosis [4, 57-59]. Moreover, COPD patients can also show systemic effects of the disease - being skeletal muscle dysfunction/wasting a characteristic one [56, 60] – and co-morbid conditions [61]. Highly prevalent chronic conditions such as cardiovascular disorders (CVD) and type 2 diabetes mellitus (T2DM) – metabolic syndrome (MS) often occur as a co-morbidity cluster in COPD patients [56, 62]. There is evidence that both skeletal muscle dysfunction/wasting and co-morbidity clustering are independently associated with poor prognosis [56].

Main challenges on COPD heterogeneity

There are several major challenges to be taken into account in the design of a systems approach to better understanding COPD heterogeneity. Firstly, the overlap among different chronic obstructive airways diseases (COPD, asthma, bronchiectasis, bronchiolitis, etc.) requires novel disease taxonomies based on a better knowledge of underlying mechanisms, which may result in a re-definition of COPD as a pulmonary disease. Such an approach should solve three current deficits, namely: *i)* overlap

between COPD and lung ageing; *ii)* availability of operational diagnostic criteria differentiating COPD from other obstructive pulmonary diseases; and, *iii)* a proper capture of pulmonary heterogeneity of the disease.

Another major challenge is to clarify the current confusion between systemic effects of COPD and some co-morbid conditions due to the descriptive nature of the reporting [56]. As an example, is anxiety-depression a systemic effect, a COPD complication or a co-morbid condition? Likely, a proper understanding of the mechanisms involved in the relationships between systemic inflammation in COPD and depression [56, 63, 64] may help to clarify this type of questions.

Last, but not least, a major challenge is a proper understanding of the phenomenon of co-morbidity clustering that is strongly associated with a high use of healthcare resources and survival. There is evidence indicating that co-morbidity clustering is only partly explained by shared risk factors among the concurrent diseases [61, 65, 66], namely: tobacco smoking, unhealthy diet and sedentarism. A better understanding of the risks associated to the occurrence of co-morbidity clustering may likely have relevant implications on patient management [64].

Overall, there is a strong rationale for further research on subject-specific health risk prediction and stratification aiming at enhancing cost-effective management of COPD patients. The ability to better understand heterogeneity of COPD [67] should permit the development and implementation of therapeutic strategies that are specific for subgroups of patients, as well as the development of new therapies [68]. Thus, future patient-oriented guidelines for the management of COPD may have to revise their definitions to encompass the heterogeneity of the disease.

The Global initiative for Obstructive Lung Disease (GOLD) [4] has played a major role in raising COPD awareness and defining standards for COPD management. GOLD has faced the challenge of COPD heterogeneity by evolving from an initial disease staging, based only on the degree of airflow limitation (FEV_1, forced expiratory volume during the first second) [69], to the incorporation of symptoms and frequency of severe exacerbations into the scoring system (2011 GOLD update) [57, 58] and acknowledging the negative impact of co-morbid conditions on prognosis. Evidence-based data using the 2011 GOLD classification are currently emerging, but the results are not yet consolidated [70, 71]. Alternative options for COPD risk assessment [4, 72-75] seem also insufficient for subject-specific prediction and stratification of management.

COPD heterogeneity and its clinical implications have been further assessed by ECLIPSE (The Evaluation of COPD Longitudinally to Identify Predictive Surrogate End-points) study [56]. ECLIPSE has been a 3-year follow-up project of a large cohort of well-

characterized COPD GOLD II-IV patients [76] that has generated a relevant body of knowledge on several major aspects of the disease. The recent summary report (2014) on clinical implications of the project outcomes [56] stresses the impact of COPD heterogeneity observed in both the cross-sectional and the longitudinal study assessments and highlights the multi-facetted nature of the disease [77]. It is of note, however, that ECLIPSE has not generated relevant information on underlying mechanisms of COPD heterogeneity.

The need for a systems perspective of COPD heterogeneity

The classical theory of relevant bio-pathological processes involved in COPD heterogeneity to explain the systemic effects of the disease follows the *"spill over"* hypothesis [78]. That is, lung injury caused by inhaled irritants (e.g. tobacco smoking) generates peripheral lung inflammation that may cause "spill over" of different types of cytokines into the systemic circulation. According to this hypothesis, systemic inflammation causes skeletal muscle dysfunction and muscle wasting, but it may also cause and worsen co-morbidities. Two main limitations of this hypothesis are its over-simplistic explanation of the phenomenon of systemic low-grade inflammation, not confirmed by ECLIPSE [62] and other studies [79-81], and lack of a proper consideration of the co-morbidity challenge. An implicit assumption of the hypothesis is that COPD heterogeneity is ultimately driven by the pulmonary events of the disease.

Alternatively, the Synergy-COPD project [82] proposed that COPD heterogeneity is explained by the interplay of conceptually independent events occurring at three different levels: *i)* *Pulmonary disease* – determined by the effects of lung injury and local remodeling processes; *ii)* Systemic effects of the disease with different manifestations, such as skeletal muscle dysfunction/wasting [83]; and, *iii)* Co-morbidity clustering that refers to observed associations of different chronic disorders.

Synergy-COPD [82] explored underlying mechanisms of COPD heterogeneity focusing on skeletal muscle dysfunction/wasting and co-morbidity clustering targeting the analysis of COPD associations with CVD, and T2DM. The project only marginally addressed pulmonary events of the disease.

As indicated above, COPD is certainly a target for a systems approach. The current definition of COPD – poorly reversible airflow limitation – is being questioned from a systems perspective because it does not take into account the different non-pulmonary manifestations of the disease with prognostic implications. The classical approach to the disease is not operational to properly address COPD heterogeneity and the boundaries with other obstructive airway diseases are poorly defined.

Depending upon the interplay among genetic background, epigenetic changes and post-translational abnormalities different subtypes of COPD patients with clear clinical and prognostic implications seem to emerge. For example, in COPD patients with skeletal-muscle abnormalities and mechanical-energetic uncoupling [84, 85] seem reasonable to hypothesize that increased skeletal-muscle ROS-generation [60] likely impairs regulation of inflammatory signaling and generates abnormal skeletal-muscle remodeling ultimately leading to muscle wasting. There is evidence indicating that impairment of the central organ (lung) in patients with COPD only partly explains disease prognosis. In this context, it can be hypothesized that abnormal interactions between lung, cardiovascular system and peripheral tissues are determinants of disease subtypes associated with poor prognosis, such as skeletal muscle dysfunction/wasting [56, 60]. Consequently, identification of underlying mechanisms associated to clinical subtypes of COPD patients constitutes a major goal for risk stratification and it is likely a first step to define future strategies aiming at modulating disease evolution.

The Synergy-COPD project

In 2010, under FP7 Call 6, the Virtual Physiological Human project Synergy-COPD (Modeling and Simulation Environment for Systems Medicine – Chronic Obstructive Pulmonary Disease – COPD – as a use case) was selected for funding, which facilitated the development of the current PhD thesis.

The general aim of Synergy-COPD was to explore the potential of computer-based modeling techniques using a systems medicine approach to improve knowledge on underlying mechanisms of COPD heterogeneity, focusing on the systemic effects of the disease and the co-morbidity clustering.

The transfer of a better knowledge of disease heterogeneity to enhance individual health risk assessment and stratification, leading to innovative patient management strategies, was also a core aim of the project. Also within the translational scope of the project, Synergy-COPD aimed to identify novel modalities for the interplay between healthcare and biomedical research aiming at fostering deployment of 4P Medicine for patients with chronic disorders [1, 2, 86, 87].

The project design (**Figure 4**) was based on several iterations among the three main project pillars: (i) development of the COPD knowledge base (COPDkb); (ii) different modeling strategies; and, (iii) generation of tools for users: either clinicians (CDSS) or translational researchers (Simulation Environment). The iterations facilitated the design of appropriate evaluation strategies carried out throughout the project lifetime which were

based on experimental designs (animal models and cell cultures) [82] exploring targeted disease mechanisms.

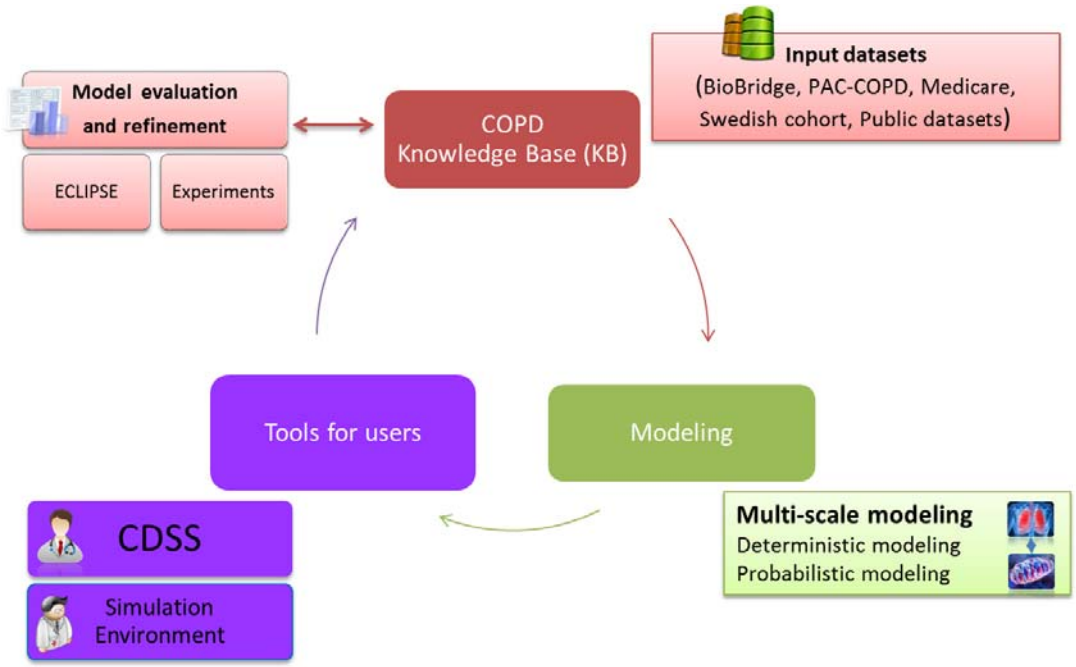

Figure 4: *The Synergy-COPD translational research design.*

The use of part of the ECLIPSE dataset was considered in the evaluation plan for the final phase of the project. With this project design, the different biomedical aims were addressed using a building blocks strategy that facilitated the learning process in a rather novel research approach. The project generated outcomes in three different dimensions: *i)* biomedical area; *ii)* information and communication technologies (ICT); and, *iii)* transfer into healthcare.

Biomedical area

As alluded to above, Synergy-COPD used a network medicine approach to investigate the underlying mechanisms of two different actionable phenomena showing negative impact on prognosis of COPD patients: skeletal muscle dysfunction/wasting, as a hallmark of systemic manifestations of the disease; and co-morbidity clustering in these patients.

Skeletal muscle dysfunction - The project explored three relevant aspects of skeletal muscle dysfunction and muscle wasting in COPD patients.

Firstly, the degree of dissociation between classical COPD GOLD stages (I to IV) [69] and estimations of both cellular oxygenation (PmO_2) and mitochondrial reactive oxygen

species (ROS) levels in skeletal muscle exercising maximally (VO_2max). The study was done using a COPD dataset wherein VO_2max, cardiac output (QT), pulmonary ventilation-perfusion mismatching (VA/Q inequalities) and blood oxygenation, arterial and mixed venous blood, had been measured [88]. The analysis was carried out using the deterministic integrated model developed in the project wherein an integrated physiological O_2 pathway model was made interoperable with a biochemical model characterizing mitochondrial ROS generation. This integrated model is the target of the first three manuscripts of this PhD thesis covering the first objective; that is a "*quantitative analysis of the relationships between cellular oxygenation and mitochondrial ROS generation*". Likewise, such an analysis was also done using the BioBridge dataset [79] wherein healthy subjects and COPD patients had a multilevel (omics, biochemical, physiological and clinical data) characterization of lower limb skeletal muscle, blood and whole-body physiological changes from pre- to post- high intensity supervised resistance training during 8 weeks.

A second study enriched the initial network medicine analysis [79] reported in the BioBridge project [89] by including additional "omics" information [80, 81], as well as an extended set of measurements on nitroso-redox balance carried out in blood and in skeletal muscle [80]. The purpose of the network approach was to compare healthy subjects and COPD patients at baseline (pre-training) in terms of the relationships among relevant metabolic pathways governing cellular bioenergetics, protein balance, and skeletal muscle remodeling paying particular attention to the role of nitroso-redox disequilibrium in the network modeling.

Finally, a third study on skeletal muscle dysfunction in COPD addressed the analysis of abnormal training adaptations comparing healthy subjects and COPD from the BioBridge dataset. Two different modeling strategies were undertaken: targeted probabilistic network modeling [90] and a Thomas network approach [91].

Co-morbidity analyses – Two different studies were undertaken. Firstly, a data driven approach aimed at assessing different indices of relative risk for co-morbidity clustering in COPD patients aged +65-yrs. compared to non-COPD patients. The study was done using the Medicare dataset (13 million people)[92] and the Swedish cohort (5 million people). The research also identified genes and pathways associated with clusters of co-morbidities. A second independent study compared the outcomes of the data driven study with the pathway analysis of the co-morbidity clustering targeted in Synergy-COPD, namely: CVD, T2DM and COPD as reported in [61, 65, 93]. Moreover, the project explored shared abnormalities between the two phenomena: skeletal muscle dysfunction and risk of co-morbidity clustering. The relevant abnormally regulated pathways

identified in the analysis of skeletal muscle dysfunction/wasting were compared with those seen in the co-morbidity clustering to explore commonalities.

An ancillary biomedical aim was to explore specific pulmonary events of COPD. In 2011, a multicenter longitudinal study on COPD patients assessed after the first hospital admission (PAC_COPD [93]), reported an unbiased cluster analysis identifying three subtypes of COPD patients with clinical and prognostic implications. The study [93] reported dissociations between relatively low central airways resistance and high emphysema score as a distinctive trait in approximately one third of the PAC_COPD patients (Group II from PAC_COPD). Because of the potential interest of the finding in terms of patient stratification for lung cancer screening [94, 95], we used modeling techniques exploring spatial pulmonary heterogeneities to address the issue. The study was done in close collaboration with the AIRPROM project [96].

Targeted ICT developments

Three well-differentiated ICT developments were carried out during the project lifetime. Firstly, the **COPD Knowledge-Base** (COPDkb) [39] fed with multi-level data from previous experimental studies (BioBridge [89]), data from a multicenter longitudinal study on COPD subtypes (PAC-COPD [93]), and public datasets (e.g. Gene Expression Omnibus (GEO), Gene Ontology (GO), Ensembl, KEGG pathways, etc.). The COPDkb was designed, as an extension of the developments done within the BioBridge project [80], to include COPD-specific expression and co-morbidity networks connecting over 6.000 genes/proteins with physiological parameters and disease states. Three mathematical models describing different aspects of systemic effects of COPD were connected to clinical and experimental data. The technical architecture was completely re-designed to enhance the user interface and provide browser-based access and form-based searches. In addition, network search approaches were considered to enable the use of interconnecting information and the generation of disease-specific sub-networks from general knowledge. Moreover, integration with a Simulation Environment was expected to enable multi-scale integrated simulation of individual computational models. Ultimately, integration with Clinical Decision Support Systems (CDSS) was a key pillar of the COPDkb design, supporting delivery into clinical practice. The COPDkb is the target of the **fourth manuscript** of this PhD thesis covering part of the second objective that is "*ICT-support to the deployment of integrated care services (ICS-ICT) and to the cross talk between healthcare and systems-oriented biomedical research*".

The second group of ICT developments was associated with different types of **mathematical modeling** aiming at addressing the biomedical questions alluded to above. They encompassed the following different types of qualitative and semi-quantitative network analyses, classical mechanistic modeling based on ordinary differential equations, as well as research on the interplay between network analysis and mechanistic modeling.

Qualitative and semi-quantitative network analyses - The first type of mathematical modeling considered in Synergy-COPD can be categorized as qualitative scale-free network modeling [90] approaches, as well as semi-quantitative Bayesian [97] and Thomas [91] networks. The first objective of the network approaches was to compare healthy subjects and COPD patients in terms of the relationships among relevant metabolic pathways governing cellular bioenergetics, protein balance, and skeletal muscle remodeling paying particular attention to the role of nitroso-redox disequilibrium in the network modeling. The second objective addressed the analysis of abnormal training adaptations comparing healthy subjects and COPD from the BioBridge database [89]. Finally, the third objective of the network approaches was to assess different indices of relative risk for co-morbidity clustering in COPD patients compared to non-COPD patients.

Classical mechanistic modeling based on ordinary differential equations - The Synergy-COPD project considered different multi-level mechanistic models, as describe below:

- Spatial heterogeneities of lung ventilation and perfusion. It derives, from lung x-ray CT scan data, patient specific geometric models of the lung parenchyma, airways and blood vessels used to predict the regional distribution of ventilation (VA) and blood flow (Q) within the lung. This modeling of spatial pulmonary heterogeneities [98, 99] was used in Synergy-COPD to explore the characteristics of patients from the PAC-COPD study [93] in whom moderate to severe emphysema score, assessed by high resolution CT scan, was not accompanied by significant central airway remodeling. The model provides estimations of arterial oxygenation from spatial heterogeneities. But, estimations of pulmonary functional heterogeneities (lung VA/Q inequalities) [100] was the option considered in the project for the integrated O_2 pathway modeling approach described below.
- Oxygen transport and utilization. This well-established mechanistic model considers the O_2 transport/utilization pathway as an integrated system (i.e. Central and peripheral O_2 transport and utilization) and predicts O_2 transport from air to mitochondria [101, 102]. Synergy-COPD, and this PhD thesis, aimed at expanding this previous model of O_2 transport and utilization in heath to additionally allow for

both lung ventilation/perfusion and tissue metabolism/perfusion heterogeneities, in order to estimate whole body oxygen uptake/delivery capacity and cellular oxygenation during maximal exercise, in health and in disease (i.e. COPD).

- Cell Bioenergetics, mitochondrial respiration and ROS generation. This model [103] takes into account the mechanisms governing mitochondrial ROS (Reactive Oxygen Species) generation. It is well accepted that ROS have important roles in terms of both cell signaling and potential nitroso-redox damage of cellular components.

The integration of the last two mechanistic models (O_2 pathway and mitochondrial ROS generation) has been the focus of the first objective of this PhD thesis: *quantitative analysis between cellular oxygenation and mitochondrial ROS generation*.

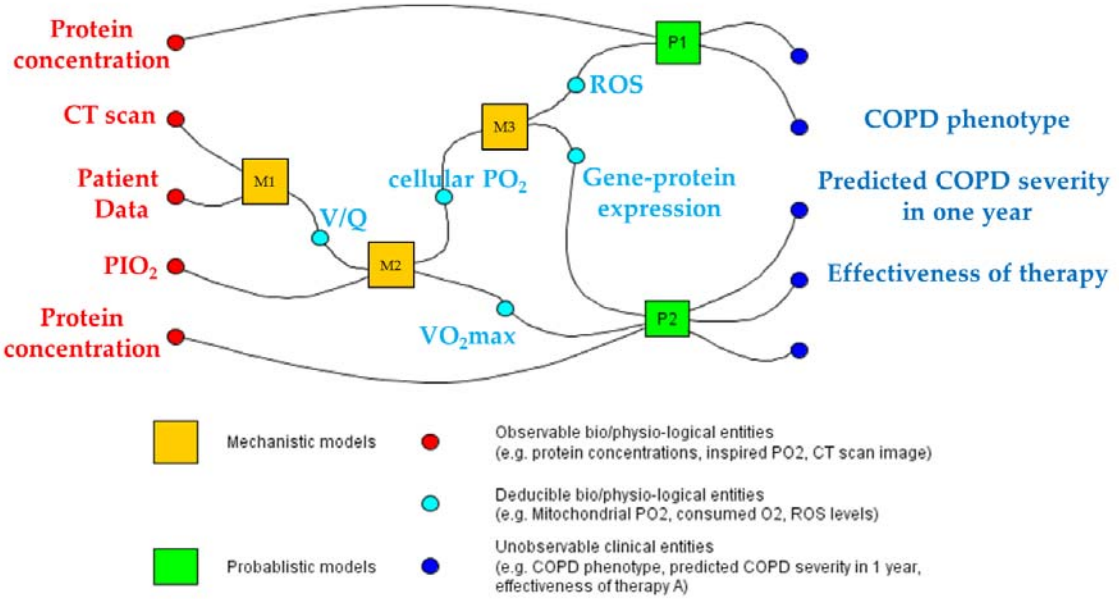

Figure 5: *Synergy-COPD framework that links data and models, establishing the key link between basic low-level observable physiological or biological parameters (such as protein concentrations, CT scan image or inspired PO_2) and high-level unobservable outputs (such as a subtype of COPD, disease progression, etc.). In the generic sense, mechanistic models (M1 to M3 in the figure) are used to study the values of some entities; while probabilistic models (P1 and P2) are key linking patient-specific measures and predictions. Specific implementation of this framework depend in the different biological question of we aim to address.*

Research on the interplay between network analysis and mechanistic modeling. Synergy-COPD aimed at combining several modeling approaches, probabilistic [79, 104] and mechanistic [98, 99, 101-103], to address the biomedical questions alluded to above. Specifically, the project addressed the interplay between probabilistic (network-based) and mechanistic modeling, following the framework depicted in **Figure 5**, with a twofold objective: *i)* to contribute to parameter refinement of the mechanistic models (e.g. enhanced parameter estimation for mitochondrial function); and, *ii)* to assess the multi-

scale impact of the outcomes generated by the mechanistic modeling (e.g. consequences of abnormally high mitochondrial ROS generation on inflammatory responses or tissue remodeling).

The third ICT product was the **Simulation Environment** [105] aiming at supporting biomedical researchers to concurrently run heterogeneous modeling approaches that may have complementary roles in exploring a given biomedical phenomenon.

Transfer to healthcare

A last and most important aspect of the project was the transfer of the acquired knowledge, as novel rules for patient management, into the clinical practice through the generation of Clinical Decision Support Systems (CDSS). The CDSS are relevant ICT tools supporting integrated healthcare strategies in terms of diagnosis, stratification and management. The families of CDSS that were considered in Synergy-COPD are described in the following **Table**.

1. **Early diagnosis – COPD case finding program**
   The suite of CDSS supports the regional deployment of a program of early COPD diagnosis targeting citizens at risk examined in pharmacy offices and non-diagnosed patients studied in primary care. Additional objectives of the program are to ensure high quality forced spirometry accessible across healthcare tiers, as well as prevention of over-diagnosis of COPD in elderly due to the GOLD diagnostic criteria [106].
2. **Enhanced stratification of COPD patients**
   It includes three families of CDSS with well differentiated objectives: i) to enhance applicability of the 2011 GOLD Update criteria for COPD staging [106]; ii) to facilitate off-line comparisons with other COPD staging and survival criteria [73, 74, 107]; and, iii) to enhance stratification combining acquired knowledge in Synergy-COPD and consolidated findings from ECLIPSE [56].
3. **Community-based integrated care program**
   This suite of CDSS aims at supporting different integrated care services fostering the transfer of complexity from specialized care to the community with an active role of patients. The two programs being deployed are targeting sustainability of training-induced effects and promotion of physical activity [108], and management of patients under long-term oxygen therapy (LTOT). The two programs were assessed within NEXES [12, 109], as part of the deployment of integrated care services in the health district of Hospital Clinic.

Three main steps were considered in the project for the development of the CDSS: *i)* generation of novel rules feeding the CDSS either automatically from computer modeling and/or through existing knowledge; *ii)* clinical validation and acceptability of the rules by the clinical users; and *iii)* interoperability with the ICT tools supporting integrated care services (ICS-ICT). Such development strategy assumes the Synergy-COPD's CDSS to be embedded into the clinical process and to show both usability and applicability. CDSS embedded within novel ICS-ICT platforms represents another basic pillar to accomplish the second objective of this PhD thesis: to provide *ICT-support to the deployment of integrated care services (ICS-ICT) and to the cross talk between healthcare and systems-oriented biomedical research*.

Main challenges beyond Synergy-COPD

The project run smoothly from February 2011 to end-of-April 2014 with significant achievements and some gaps. Major lessons learnt from the analysis of the limitations faced during the development of the project can be grouped in three major clusters: *i)* available datasets; *ii)* maturity of the field; and, *iii)* need for societal changes. The assessment of these three areas helped to identify major challenges to be faced beyond Synergy-COPD:

Available datasets - Despite the current exponential generation of large amounts of biomedical data of different nature, several factors associated to availability of appropriate datasets have limited the transfer of the project outcomes on mechanisms of skeletal muscle dysfunction and co-morbidity clustering closer to clinical application. The following limiting aspects were identified: *i)* insufficient harmonization of medical coding across countries and within large longitudinal datasets [110-112]; *ii)* gaps in semantic interoperability with large variations in disease definitions and coding; *iii)* publicly available information biased toward well established and expected diseases and their underlying mechanisms [113-115]; *iv)* lack of multilevel "omics" information bridging between Genome-Wide Association Studies (GWAS) information and phenotypic characterization [116]; and, (v) lack of accompanying non-clinical information (environmental, lifestyle, socioeconomic factors) in bio-banking data.

In summary, the characteristics of the available datasets had a negative impact on the project precluding the generation of subject-specific predictive modeling. They also constituted a limit for the validation of the novel semi-quantitative modeling approaches explored in Synergy-COPD (e.g. Bayesian analysis and Thomas formalism), that should facilitate the interplay between probabilistic and mechanistic modeling for further characterization of complex biological processes. In this regard, policies promoting data sharing are highly recommended.

Maturity of the field – Mechanistic modeling techniques have shown usefulness to characterize biological mechanisms and to provide quantitative assessment of the phenomena analyzed [60, 61], but they have serious limitations to address complex biological phenomena. In contrast, network medicine approaches [28, 104] based on statistical predictive models [31, 117] seem suitable to address complex biomedical phenomena when large amount of data are available. Moreover, high-throughput analysis [118, 119] have shown that canonical analysis of biological pathways is too simplistic, not reflecting the real complexity of interconnectedness of biological networks [120]. It is of note, however, that the high expectations generated by emerging high-throughput methods are not balanced by a sufficient degree of maturity yet [121, 122].

Societal changes – The project clearly identified that major organizational and technological changes are required to pave the way for a credible transition toward 4P medicine. Some of the key requirements for such a transition are described in **Manuscript 6** of this PhD thesis within the concept of the Digital Health Framework. But, cultural factors such as workforce preparation, evolving concepts in terms of ethical factors relative to privacy of information transfer and information sharing, and development of novel business environments fulfilling the requirements of the upcoming scenario are relevant elements to be taken into account in the definition of strategies leading to a successful implementation of the change.

It must be emphasized that the identification of the limiting elements alluded to above does not define at all a negative landscape for systems-oriented research in the biomedical area. On the contrary, one of the most important outcomes of Synergy-COPD has been the identification of the challenges to be faced and the definition of innovative strategies to adequately overcome the limiting factors alluded to above that should lead to unprecedented developments in the medical practice.

Summary of the introductory section

The epidemics of non-communicable diseases and the widely extended need for cost-containment are triggering factors for a profound reshaping of the way we approach delivery of care toward adoption of the Chronic Care model [8]. In this scenario, enhanced health risk assessment and patient's stratification play a relevant role.

The two drivers alluded to above are prompting to consider adoption of the emerging methods in systems medicine to improve the current healthcare delivery through a mechanism-based approach to diseases. To this end, the use of appropriate ICT has shown to be essential to support continuity of care through the extensive deployment of

ICS-ICT, facilitating accessibility of citizens and patients to healthcare and generating a disruptive scenario in terms of knowledge management.

Moreover, this approach generates the need for cross talk between healthcare and systems-oriented biomedical research, which opens new challenges also partly addressed in the current PhD thesis that benefited from the Synergy-COPD project described above. Nevertheless, the aims of the current PhD thesis were not only to generate biomedical knowledge, but also, to examine applicable strategies for a quick transfer of biomedical research achievements into the clinical practice contributing to enhanced patient health-risk and stratification strategies. The need for an operational frame facilitating a continuous interplay between healthcare and novel biomedical systems-oriented research was identified as a pivotal unmet need for an effective deployment of 4P (Predictive, Preventive, Personalized and Participatory) medicine.

Hypothesis

The overarching hypothesis of Synergy-COPD is that a systems-oriented research of COPD heterogeneity may provide better understanding of underlying disease mechanisms than a conventional reductionist approach.

Subject-specific health risk assessment and stratification may lead to novel and more efficient patient-oriented healthcare delivery. Moreover, the systems medicine orientation adopted in the Synergy-COPD project may facilitate the transfer of the acquired knowledge to healthcare, as well as the cross talk between healthcare and biomedical research.

Specifically, the current PhD thesis hypothesizes that predictive mechanistic modeling integrating the oxygen pathway and the mitochondrial function can contribute to assess the biological effects of cellular hypoxia and its role on skeletal muscle dysfunction in COPD. The underlying biological hypothesis is that mismatching between oxygen transport and skeletal muscle oxygen requirements during maximum exercise lead to cellular hypoxia and increased mitochondrial ROS production. The phenomenon may have a relevant role in the abnormal regulation among cellular bioenergetics, inflammatory signaling and skeletal muscle remodeling observed in COPD patients.

Moreover, it is hypothesized that a holistic design of the ICT support may contribute to a successful deployment of integrated care services (ICS) for chronic patients, and may foster the transfer of the achievements of systems-oriented research into healthcare if a Digital Health Framework were in place.

The first objective of the current PhD thesis is to examine the potential of the integration of the physiological modeling of the O_2 pathway and the biochemical modeling of mitochondrial ROS generation to quantitatively analyze the relationships between skeletal muscle oxygenation and mitochondrial ROS generation.

The second objective addressed the design and development of the ICT support required for the effective deployment of Integrated Care Services (ICS) for chronic patients, as well as for the innovative cross talk between systems-oriented biomedical research and healthcare.

The ultimate aim of this PhD thesis is to use the knowledge gained with the systems medicine approach of chronic diseases to generate subject-specific predictive modeling facilitating patient-oriented management at community level through enhanced stratification.

Specific objectives

Objective 1 – Quantitative analysis between cellular oxygenation and mitochondrial ROS generation

Rationale

There is evidence of systemic nitroso-redox disequilibrium in COPD patients [123]. It has been hypothesized that abnormal mitochondrial ROS generation leading to nitroso-redox disequilibrium can be a pivotal underlying mechanism of systemic effects of COPD, as well as in the co-morbidity clustering.

We believe that a quantitative assessment of the relationships between skeletal muscle oxygenation and mitochondrial ROS generation can contribute to the analysis of the impact of the nitroso-redox disequilibrium on non-pulmonary effects of COPD that have a negative impact on patient's prognosis.

Manuscript 1

Cano I, Mickael M, Gomez-Cabrero D, Tegnér J, Roca J, Wagner PD. *Importance of mitochondrial in maximal O2 transport and utilization: A theoretical analysis*. Respiratory Physiology & Neurobiology. 2013;189(3):477-83.

Manuscript 2

Cano I, Wagner PD, Roca J. *Effects of Lung and Muscle Heterogeneities on Maximal O2 Transport and Utilization*. Submitted to The Journal of Physiology. 2014 (2nd revision).

Manuscript 3

Cano I, Selivanov V, Gomez-Cabrero D, Tegnér J, Roca J, Wagner PD, M. Cascante. *Oxygen pathway modeling estimates high reactive oxygen species production above the highest permanent human habitation*. Submitted to PLoS One. 2014 (submitted).

Objective 2 – ICT-support to the deployment of integrated care services (ICS-ICT) and to the cross talk between healthcare and systems-oriented biomedical research

Rationale

A holistic design of the ICT support to deployment of ICS-ICT constitutes a key enabling element for the convergence between integrated care and 4P medicine for chronic patients. The current PhD thesis presents an open and modular ICT platform, based on shared knowledge management, enabling deployment of ICS-ICT. The challenges faced for extensive regional deployment of ICS-ICT are addressed and the design and development of ICT-supporting tools (i.e. COPDkb) for systems-oriented biomedical research within a Digital Health Framework are presented.

Manuscript 4

Cano I, Tényi A, Schueller C, Wolff M, Huertas M, Gomez-Cabrero D, Antczak P, Roca J, Cascante M, Falicani F, Maier D. *The COPD Knowledge Base: enabling data analysis and computational simulation in translational COPD research.* BMC Journal of Translational Medicine (accepted) 2014.

Manuscript 5

Cano I, Alonso A, Hernandez C, Burgos F, Martinez-Roldan J, Roca J. *A Multi-tier ICT Framework to Deploy Integrated Care Services*. Submitted to BMC Medical Informatics and Decision Making. 2014 (submitted).

Manuscript 6

Cano I, Lluch-Ariet M, Gomez-Cabrero D, Maier D, Kalko S. G, Cascante M, Tégner J, Miralles F, Herrera D, Roca J and the Synergy-COPD consortium. *Biomedical Research in a Digital Health Framework.* BMC Journal of Translational Medicine (accepted). 2014.

Manuscript 1:

Importance of mitochondrial in maximal O2 transport and utilization: A theoretical analysis.

Cano I, Mickael M, Gomez-Cabrero D, Tegnér J, Roca J, Wagner PD.

Published in Respiratory Physiology & Neurobiology

Respir Physiol Neurobiol 2013; 189: 477–483

IMPORTANCE OF MITOCHONDRIAL PO2 IN MAXIMAL O2 TRANSPORT AND UTILIZATION

I Cano[a*], Mickael M[b], D. Gomez-Cabrero[b], J Tegnér[b], J Roca[a], PD Wagner[c]

[a]Hospital Clinic, IDIBAPS, CIBERES, Universitat de Barcelona, Barcelona, Catalunya, Spain. [b]Unit of Computational Medicine, Center for Molecular Medicine, Karolinska Institute and Karolinska University Hospital, Stockholm, Sweden. [c]School of Medicine University of California, San Diego, San Diego, CA 92093-0623A.

*Corresponding author: Isaac Cano, iscano@clinic.ub.es, IDIBAPS, C/Villarroel 170, 08036, Barcelona, Spain.

ABSTRACT

In previous computational analyses of how the O2 transport system limits $\dot{V}O_2$ max, we have made the approximation that mitochondrial PO_2 (Pm_{O_2}) is sufficiently low that it can be neglected. We investigated the putative influence of a non-zero Pm_{O_2} on these calculations. To this end, we developed an integrative model of O_2 transport and utilization by coupling previously used equations for mass transport to that for mitochondrial respiration. Inputs are ventilation, cardiac output, lung and muscle diffusing capacity, [Hb] and acid base status for the transport portion, and now mitochondrial P_{50} and $\dot{V}_{MAX}$ for the hyperbolic mitochondrial respiration curve relating mitochondrial $\dot{V}O_2$ to PO_2. Outputs are, $\dot{V}O_2$max, alveolar, arterial and venous PO_2, and now also Pm_{O_2}. Simulations of healthy fit subjects exercising at sea level and altitude showed that depending on the effective balance between O_2 transport capacity and mitochondrial oxidative metabolic function, Pm_{O_2} may vary over a wide range and, especially at elevated levels, contribute significantly to limiting $\dot{V}O_2$max.

Keywords: bioenergetics, mitochondrial respiration, mitochondrial PO_2, oxygen transport, $\dot{V}O_2$max.

1. Introduction

At rest or during exercise, production of ATP requires both physical O_2 transport from the environment to the mitochondria and subsequent chemical utilization of O_2 by oxidative phosphorylation. Oxygen transport has been well described (Dejours, 1966; Gnaiger et al., 1998; Weibel et al., 1981) based on the O_2 transport pathway, consisting of the lungs/chest wall, the heart, vascular tree and blood, and the tissues. These structures conduct O_2 as an in-series system in which the main sequential transport steps are ventilation, alveolar-capillary diffusion, circulatory transport, and tissue capillary to mitochondrial diffusion. At each step, the mass of O_2 must be conserved, and this allows a set of simple equations to be defined that quantifies how the transport process at each step integrates with those of the other steps to determine how much O_2 is delivered to the mitochondria per minute (Wagner, 1993, 1996b).

A central conclusion from such analyses is that maximal mitochondrial O_2 availability is governed by the integrated behavior of this system rather than by any single step. Systems physiological investigations (Wagner, 1993, 1996b) targeting the understanding of the limits to maximal $\dot{V}O_2$, have previously been performed on the basis of an important simplifying approximation. This has been that the downstream mitochondrial PO_2 (Pm_{O_2}) is so small in comparison to tissue capillary PO_2 that it can be ignored and therefore set to zero, thus making the analyses of O_2 transport much more tractable. However, because O_2 is one of the molecules that drive oxidative phosphorylation according to the law of mass action, this approximation cannot be physiologically correct, or otherwise $\dot{V}O_2$ would itself be zero.

Given that Pm_{O_2} must be larger than zero, the PO_2 difference between red cells and mitochondria must be less than when Pm_{O_2} is assumed to be zero, and thus the diffusive movement of O_2 between them must also be reduced. Therefore, if Pm_{O_2} is now considered as greater than zero, there is an additional resistance, from the process of mitochondrial respiration, to O_2 movement through the entire pathway of O_2 transport and utilization. This additional resistance must reduce maximal $\dot{V}O_2$ below that which would be expected if this resistance were ignored. Clearly, the degree to which $\dot{V}O_2$max would be reduced will depend on how the high mitochondrial PO_2 rises above zero. This in turn will depend broadly on the capacity for O_2 transport (how many O_2 molecules can be delivered to the mitochondria per minute) compared to the capacity for metabolism (how many O_2 molecules can be consumed by the mitochondria per minute).

The importance of including consideration of oxidative phosphorylation goes beyond asking how much does mitochondrial respiration contribute to the overall impedance to $\dot{V}O_2$. Because the value of Pm_{O_2} is dependent on the mitochondrial respiration curve/O_2 transport interaction, hypoxia-induced biological changes may be affected by this interaction.

The purpose of the present paper is therefore to expand the prior theoretical analysis of the integrated O_2 transport pathway (Wagner, 1993, 1996a) by analyzing the consequences of allowing mitochondrial PO_2 to be greater than zero. This requires integration of the previously described O_2 transport equations

with an equation for mitochondrial respiration, followed by the application of mass conservation principles to solve this new equation system.

2. Material and methods

2.1. Principles

Oxidative phosphorylation ensues via the following equation 1 that embodies the law of mass action:

$$3\mathrm{ADP} + 3\mathrm{P}i + \mathrm{NADH} + \mathrm{H}^+ + 1/2\,\mathrm{O}_2 \rightarrow 3\mathrm{ATP} + \mathrm{NAD}^+ + \mathrm{H}_2\mathrm{0} \qquad \textbf{eq. 1}$$

In this equation, Pm_{O_2} corresponds to O_2. Clearly, this mass action equation can only move from left to right and produce ATP if Pm_{O_2} is greater than zero.

To illustrate this effect, a graphical depiction of mitochondrial respiration is presented in **Figure 1.** Here, the solid line is the relationship between velocity of the reaction (i.e., mitochondrial $\dot{\mathrm{V}}\mathrm{O}_2$), and Pm_{O_2}, similar to what has been found experimentally (Gnaiger et al., 1998; Scandurra and Gnaiger, 2010; Wilson et al., 1977). It shows how $\dot{\mathrm{V}}\mathrm{O}_2$ is a positive but non-linear function of mitochondrial PO_2, and indicates that at low Pm_{O_2}, $\dot{\mathrm{V}}\mathrm{O}_2$ is very sensitive to (and thus limited by) PO_2, while at higher Pm_{O_2}, $\dot{\mathrm{V}}\mathrm{O}_2$ becomes independent of PO_2, and is limited by factors other than O_2.

The hyperbolic curve through the origin displayed in **Figure 1** represents mitochondrial respiration. It is of note that despite mitochondrial respiration kinetics is not really a Michaelis-Menten type (Johnson and Goody, 2011; Michaelis and Menten, 1913), experimental data (Gnaiger et al., 1998; Scandurra and Gnaiger, 2010) are well fitted by such a curve. As a hyperbola, it can be represented by equation 2:

$$\dot{\mathrm{V}}\mathrm{O}_2 = \dot{\mathrm{V}}_{\mathrm{MAX}} \cdot \mathrm{Pm}_{O_2} / \left(\mathrm{Pm}_{O_2} + P_{50}\right) \qquad \textbf{eq. 2}$$

Where $\dot{\mathrm{V}}\mathrm{O}_2$ is mitochondrial $\dot{\mathrm{V}}\mathrm{O}_2$ (the ordinate in **Figure 1**); $\dot{\mathrm{V}}_{\mathrm{MAX}}$ is the asymptote of the curve, and represents the maximal rate of use of O_2 when O_2 is in excess; Pm_{O_2} is mitochondrial PO_2 (the abscissa in **Figure 1**) and P_{50} is the PO_2 at 50% of $\dot{\mathrm{V}}_{\mathrm{MAX}}$. Thus, the mitochondrial respiration curve is defined by two parameters: $\dot{\mathrm{V}}_{\mathrm{MAX}}$ and P_{50}.

Also shown in **Figure 1** is a straight (dashed) line of negative slope. It represents the Fick law of diffusion and depicts diffusive O_2 transport between the tissue capillary and the mitochondria as a function of mitochondrial PO_2 for a given tissue O_2 diffusional conductance (DM) and a given tissue mean capillary PO_2 ($\mathrm{P}\bar{\mathrm{c}}_{O_2}$), both at maximal exercise. We previously utilized this representation as a tool for interpreting intracellular oxygenation data obtained using magnetic resonance spectroscopy (Richardson et al., 1999). The equation is as follows:

$$\dot{V}O_2 = DM \cdot \left(P\bar{c}_{O_2} - Pm_{O_2}\right) \quad \textbf{eq. 3}$$

As the figure indicates, as Pm_{O_2} is increased, $\dot{V}O_2$ in eq (3) must fall because the PO_2 difference between mean capillary and mitochondrial PO_2 is reduced. Thus, **Figure 1** shows how $\dot{V}O_2$ *increases* with mitochondrial PO_2 according to oxidative phosphorylation, but *decreases* with mitochondrial PO_2 according to the laws of diffusion.

The key concept in **Figure 1** is that in a steady state of O_2 consumption, $\dot{V}O_2$ given by both equations 2 and 3 must be the same at the same mitochondrial PO_2 (i.e., the law of mass conservation applies). This can occur only at the single point of intersection between the two relationships, as indicated by the solid circle placed there. If, as previously approximated (Wagner, 1996b), mitochondrial PO_2 were truly zero, $\dot{V}O_2$ would be higher, as indicated by the open circle at the left end of the dashed straight line in **Figure 1**. For a given O_2 transport system defined by the conductances for O_2 allowed by ventilation, alveolar-capillary diffusion, circulation, and capillary to mitochondrial diffusion, the values of mitochondrial $\dot{V}_{MAX}$ and P_{50} (equation 2) will thereby influence maximal rate of O_2 utilization, $\dot{V}O_2max$. In the remainder of this paper, it will be important to distinguish between $\dot{V}_{MAX}$ (the asymptote to the mitochondrial respiration curve) and $\dot{V}O_2max$ (actual maximal rate of O_2 utilization, solid circle in **Figure 1**) to avoid confusion. In general, $\dot{V}_{MAX}$ can exceed $\dot{V}O_2max$, but $\dot{V}O_2max$ cannot exceed $\dot{V}_{MAX}$.

2.2. Modeling the O_2 transport/utilization system

The present study augments our prior approach (Wagner, 1993, 1996b) by adding equation (2) to the equation system used previously. **Figure 2** recapitulates the O_2 transport pathway, and the associated four mass conservation equations governing O_2 transport at each step. It adds Equation (2), describing O_2 utilization as a function of Pm_{O_2}. The important point is that in this way, the system has expanded from four equations with four unknowns into a system of five equations and five unknowns.

Briefly, using specified input values for O_2 transport step parameters (i.e., values of inspired O_2 fraction (FI_{O_2}), ventilation ($\dot{V}I$, inspired; $\dot{V}A$, expired), lung diffusing capacity (DL), cardiac output ($\dot{Q}$), [Hb], acid base status, tissue (muscle) diffusing capacity (DM), and mitochondrial respiration curve parameters ($\dot{V}_{MAX}$ and P_{50})), five mass conservation equations are written for O_2 (see **Figure 2**). They describe (a) ventilatory transport; (b) alveolar-capillary diffusion; (c) circulatory transport; (d) muscle capillary-mitochondrial diffusion; and (e) mitochondrial respiration. There are five unknowns in these equations: Alveolar PO_2 (PA_{O_2}), arterial PO_2 (Pa_{O_2}), venous PO_2 ($P\bar{v}_{O_2}$), mitochondrial PO_2 (Pm_{O_2}) and $\dot{V}O_2$ itself. In **Figure 2**, equations (b) and (d) are differential equations describing the process of diffusion across the lung blood: gas barrier and across the tissue capillary wall respectively. They specifically describe the time rate of change of O_2 concentration, $[O_2]$, along the respective capillary as a function of the diffusing capacity, blood flow, red cell capillary transit time (T_L (lungs); T_M (tissues)) and the instantaneous difference between upstream and downstream PO_2 values (alveolar and pulmonary

capillary in (b); capillary and mitochondrial in (d)). The two equations are each expressions of the Fick law of diffusion.

The additional **inputs** of mitochondrial $\dot{V}_{MAX}$ and P_{50}, and the additional coding for the fifth equation were added to the prior model, and the same (numerical) method of solution employed before (Wagner, 1996b) was used to find the solutions for any set of input variables, defined as the unique values of the five unknowns listed above that simultaneously satisfy all five equations for the given input data defining O_2 transport and utilization.

2.3. Input data for simulations

The input data defining the O_2 pathway parameters used in this analysis were essentially identical to those used previously (Wagner, 1996b), and come from Operation Everest II (Sutton et al., 1988). They reflect maximal exercise by normal subjects at sea level, at a chamber "altitude" of 4,573 m (approximately 15,000 ft.) and at the chamber altitude of the Everest summit, 8,848 m (approximately 29,000 ft.). They are reproduced in **Table 1**. It is clear that data do not exist for the two new key variables: mitochondrial $\dot{V}_{MAX}$ and P_{50}. Therefore, for each of the three data sets we computed solutions to the equation system over a systematic range of five mitochondrial $\dot{V}_{MAX}$ (1000, 2000, 3000, 4000, and 5000 ml/min) and four mitochondrial P_{50} values (0.1, 0.3, 0.5 and 1.0 mm Hg), resulting in 20 combinations of the two, and thus 20 mitochondrial respiration curves. The values of $\dot{V}_{MAX}$ were chosen to encompass the range of $\dot{V}O_2max$ from the very sedentary to the elite athlete. Values of P_{50} on the other hand were based on physiological studies inscribing the mitochondrial respiration curve from samples of normal muscle (Gnaiger et al., 1998; Scandurra and Gnaiger, 2010).

A typical example from one of these papers is reproduced with permission in **Figure 3**, where the hyperbolic character of the curve and its P_{50} can both be seen by the fitted curve. In this and other similar published cases (Gnaiger et al., 1998; Scandurra and Gnaiger, 2010), P_{50} is close to 0.3 mm Hg. This accounts for our choice of P_{50} values - from a third of this typical value to about threefold greater. However it should be stressed that the modeling can be based on any combination of P_{50} and $\dot{V}_{MAX}$, and need not be limited to the choice of specific parameters appearing here.

2.4. Analysis

Across the matrix of $\dot{V}_{MAX}$ and P_{50} values, we posed two questions: First we asked how much would Pm_{O_2} have to rise above zero to satisfy mass conservation and drive mitochondrial respiration for the given set of physiological O_2 transport variables, $\dot{V}_{MAX}$ and P_{50} - and as a result, how much would that cause $\dot{V}O_2$ to be reduced (compared to assuming $Pm_{O_2} = 0$) as per **Figure 1** (comparing the open and closed circles). This question allows a quantitative description of the theoretical consequences for $\dot{V}O_2max$ of any combination of mitochondrial $\dot{V}_{MAX}$ and P_{50}. While this is a very useful question to answer, in reality $\dot{V}O_2max$ is a directly measured variable. Therefore, asking how much would it be

reduced by any pair of $\dot{V}_{MAX}$ and P_{50} values is hypothetical. On the other hand, muscle diffusing capacity, DM, is a variable calculated on the assumption that mitochondrial PO_2 can be neglected and set to zero – the very approximation that the present study is addressing.

Thus, another way to interrogate the model system can be proposed, leading to a second question: It recognizes that the muscle O_2 diffusion step was previously modeled, and muscle diffusing capacity estimated, on the basis of $Pm_{O_2} = 0$. However, if Pm_{O_2} is greater than zero, the capillary to mitochondrial O_2 diffusion gradient would be reduced, and this would necessitate, by the Fick law of diffusion, a higher value of DM to accomplish a given, measured $\dot{V}O_2max$ (compared to the value calculated assuming $Pm_{O_2} = 0$).

Therefore, for each of the combinations of $\dot{V}_{MAX}$ and P_{50}, we asked how much would muscle diffusing capacity have to increase to maintain $\dot{V}O_2$ constant at the measured value as a result of Pm_{O_2} being greater than zero.

3. Results

3.1. Effects of mitochondrial respiration on Pm_{O_2} and maximal $\dot{V}O_2$

Figure 4 shows how the different combinations of mitochondrial $\dot{V}_{MAX}$ and P_{50} affect $\dot{V}O_2max$. The upper panel covers the mitochondrial PO_2 (Pm_{O_2}) range from zero to 20 mm Hg; the lower panel shows the same data, but expands the abscissa to better reflect the lower Pm_{O_2} range between zero and 5 mm Hg. In both panels, each solid curved line emanating from the origin represents one of the twenty mitochondrial respiration curves (as in **Figure 3**) for a particular $\dot{V}_{MAX}$ and P_{50} combination. Solid circles reflect sea level conditions; solid squares represent moderate altitude and solid triangles are for the equivalent of the Everest summit. It turns out that at each altitude, an approximately straight line can be drawn through the resulting $\dot{V}O_2max/Pm_{O_2}$ solution points for each mitochondrial respiration curve. These are the dashed lines in the figure.

The values of $\dot{V}O_2max$ at each altitude at the point where Pm_{O_2} equals zero (open symbols at zero Pm_{O_2}) are the same as those described in (Wagner, 1996b) where Pm_{O_2} was taken to be zero. The figure shows how relaxing that approximation affects $\dot{V}O_2max$ for each combination of mitochondrial $\dot{V}_{MAX}$ and P_{50}. At sea level (solid circles), results show that allowing for a non-zero Pm_{O_2} has a small but significant impact on $\dot{V}O_2max$. For example, $\dot{V}O_2max$ at $Pm_{O_2} = 0$ mm Hg (open circle) would be 3,827 ml/min, but if $\dot{V}_{MAX}$ were 4,000 ml/min and P_{50} 1.0 mm Hg, $\dot{V}O_2max$ would be significantly less, by 9%, and would be 3,477 ml/min. Moreover, this would require a mitochondrial PO_2 of 6.7 mm Hg to drive oxidative phosphorylation, as the figure shows. In general, for the fixed set of O_2 transport parameters used (see Table 1), the lower the $\dot{V}_{MAX}$ and the higher the P_{50}, the greater is the reduction in $\dot{V}O_2$, and the higher is the Pm_{O_2} required to drive ATP generation. The range of possible values of mitochondrial PO_2 is considerable, from a fraction of a mm Hg to more than 10 mm Hg, depending on $\dot{V}_{MAX}$ and P_{50}.

The same outcome is seen at each altitude, but with $\dot{V}O_2$ lower at any Pm_{O_2} as PI_{O_2} is reduced. The reduction in $\dot{V}O_2$ per unit change in Pm_{O_2} is somewhat less at altitude than at sea level, but if examined as a percent of $\dot{V}O_2$ at $Pm_{O_2} = 0$ at each altitude, the effects of allowing for mitochondrial respiration on maximal $\dot{V}O_2$ are relatively similar across altitudes.

In summary, the higher the mitochondrial $\dot{V}_{MAX}$ and the lower the P_{50}, the more O_2 can be metabolized for a given upstream (heart, lungs, blood, muscle) transport system. Mitochondrial PO_2 at $\dot{V}O_2max$ can be neglected when considering O_2 transport only when mitochondrial P_{50} is low and mitochondrial $\dot{V}_{MAX}$ is high. When $\dot{V}_{MAX}$ is low and/or P_{50} is high, the mitochondrial PO_2 required to drive oxidative phosphorylation may reach double digit values, and the impact on $\dot{V}O_2max$ can be considerable.

3.2. Maintenance of maximal $\dot{V}O_2$ in the face of non-zero Pm_{O_2}

The preceding subsection showed how $\dot{V}O_2max$ would have to decrease as a function of mitochondrial $\dot{V}_{MAX}$ and P_{50} with constant values for all O_2 transport conductances. In this subsection we investigate how much higher the muscle O_2 diffusing capacity would have to be to maintain $\dot{V}O_2max$ constant over the same range of $\dot{V}_{MAX}$ and P_{50} values as Pm_{O_2} increases above zero.

The results are shown in **Figure 5**, which displays the simulation outcomes across the entire matrix of $\dot{V}_{MAX}$ and P_{50} values, using $\dot{V}_{MAX}$ on the abscissa and isopleths for each P_{50}. Results are shown for each altitude as indicated by the different symbols. The top panel shows mitochondrial PO_2 for every combination of $\dot{V}_{MAX}$ and P_{50} examined, and the bottom panel the corresponding values of muscle diffusing capacity (DM), that would have to exist to maintain $\dot{V}O_2max$ at measured levels (indicated at each altitude by the vertical dashed lines). Comparing panels shows that when Pm_{O_2} is high (thus reducing the PO_2 gradient between capillaries and mitochondria), DM must also be high to maintain diffusive O_2 transport.

Also, when mitochondrial $\dot{V}_{MAX}$ substantially exceeds measured $\dot{V}O_2max$ (at each altitude), Pm_{O_2} remains low, and therefore DM does not need to be substantially increased to maintain O_2 flux. However, the closer mitochondrial $\dot{V}_{MAX}$ is to measured $\dot{V}O_2max$, the higher Pm_{O_2} must be (see **Figure 4**), and therefore, DM is also required to be elevated to maintain O_2 transport. When $\dot{V}_{MAX}$ and actual $\dot{V}O_2max$ are very close, the required DM may be as much as four times the value needed when Pm_{O_2} is (close to) zero, and the associated Pm_{O_2} would reach double digit values.

4. Discussion

4.1. Summary of major findings

In this simulation of normal fit subjects exercising maximally at sea level and at altitude, incorporating mitochondrial respiration kinetics into a systems analysis of O_2 transport and utilization reveals that mitochondrial respiration generally poses only a small additional resistance to the system (over that of

the transport pathway alone). Nevertheless, this must reduce $\dot{V}O_2max$ below that computed ignoring this contribution (**Figure 4**). The associated mitochondrial PO_2 would also be low, generally < 1 mm Hg. This finding is based on the evident low muscle mitochondrial P_{50} of 0.30 mm Hg (Gnaiger et al., 1998; Scandurra and Gnaiger, 2010). If however mitochondrial $\dot{V}_{MAX}$ was low in relation to O_2 transport capacity, or if mitochondrial P_{50} were higher than reported values (Gnaiger et al., 1998; Scandurra and Gnaiger, 2010), $\dot{V}O_2max$ would fall more. Mitochondrial PO_2 would then rise more, and could reach double digit values. In order to maintain $\dot{V}O_2max$ in the face of reduced $\dot{V}_{MAX}$ or increased P_{50}, muscle diffusing capacity (DM) would need to be higher than when Pm_{O_2} is assumed to be zero. Under most conditions examined in the present study, the necessary increase in DM would be minimal, and only when Pm_{O_2} is considerably elevated would DM have to be comparably increased to overcome the loss of the PO_2 gradient driving diffusion between capillaries and mitochondria. This would happen when mitochondrial $\dot{V}_{MAX}$ and actual $\dot{V}O_2max$ are closely similar (**Figure 5**).

4.2. Unifying principles

The main principle demonstrated in the present study is that the final step in the O_2 pathway – mitochondrial respiration – may contribute a non-negligible resistance to O_2 movement through the system from the air to its conversion to CO_2, resulting in a lower $\dot{V}O_2max$ compared to a system where metabolism imposed no resistance to overall O_2 flow. The higher the mitochondrial PO_2 required to drive oxidative phosphorylation, the greater would be the relative resistance and thus the more effect there will be on reduction in $\dot{V}O_2max$. When mitochondrial P_{50} is about 0.30 mm Hg as reported by Gnaiger (Gnaiger et al., 1998; Scandurra and Gnaiger, 2010) the effects are generally minor.

The simulations at the three inspired PO_2 values shown here demonstrate that it is the relative capacities (rather than individual absolute values) of the physiological transport system and the mitochondrial respiratory chain that effectively determine both the mitochondrial PO_2 and the associated effect on $\dot{V}O_2max$, and that both variables, but especially mitochondrial PO_2, may vary over a wide range depending on mitochondrial respiratory function.

An additional important principle is shown in **Figure 6**: Even when O_2 transport capacity (i.e., potential for O_2 delivery) is considerably greater than mitochondrial respiratory capacity (i.e., potential for O_2 utilization), as illustrated in concept in the top panel, a change in the former will change overall $\dot{V}O_2$. The converse is also true – that when mitochondrial respiratory capacity exceeds O_2 transport capacity, (lower panel), a change in the former will have an effect on $\dot{V}O_2$. It is thus not correct to think that when one component is greater than the other, only the lesser of the two determines overall $\dot{V}O_2max$. This conclusion is much the same as described for individual components of the physiological transport pathway of the lungs and chest wall, the heart, blood and circulation, and the muscles, where we previously showed (Wagner, 1996a, b) that all components affect $\dot{V}O_2max$, not just the step with the least transport capacity.

4.3. Effects of mitochondrial respiration kinetics on both $\dot{V}O_2max$ and Pm_{O_2} may be small or large

For the examples shown – fit normal subjects – the effects of considering mitochondrial respiration are generally less on $\dot{V}O_2$ than on the associated Pm_{O_2} (**Figure 4**). Examining the sea level results for the example of $\dot{V}_{MAX}$ = 4,000 ml/min and P_{50} increasing from 0.1 to 1.0 mm Hg, $\dot{V}O_2max$ would fall by 9% while Pm_{O_2} would increase by an order of magnitude, from less than 1 mm Hg to more than 6 mm Hg. Just how much variation there is in mitochondrial P_{50} in the normal population is unknown, let alone whether this may change systematically with training, or in chronic diseases such as chronic obstructive pulmonary disease (COPD) or chronic heart failure. The calculations presented herein however point out that the quantitative nature of the mitochondrial respiration curve may be a critical determinant of the values of mitochondrial PO_2 and $\dot{V}O_2max$, over and above any influence of upstream O_2 transport. Even if the effects on $\dot{V}O_2max$ are numerically small, they would likely be important in the competitive endurance athlete where very small differences may separate success from failure. But possibly even more significant might be the potentially large variation in mitochondrial PO_2 depending on P_{50} and $\dot{V}_{MAX}$ due to known hypoxia-induced biological effects (Semenza, 2011). Thus, hypoxia-induced gene expression or reactive O_2 species generation may vary according to mitochondrial PO_2.

4.4. Potential for estimating mitochondrial P_{50} based on the current modeling approach

The analysis presented here suggests a possible method for estimating the characteristics of the mitochondrial respiration curve in vivo. Currently, mitochondrial $\dot{V}_{MAX}$ and P_{50} are measured in vitro in respirometers where mitochondria are exposed to different levels of O_2 and $\dot{V}O_2$ measured (as in **Figure 3**), (Gnaiger et al., 1998; Scandurra and Gnaiger, 2010; Wilson et al., 1977). To obtain this information in humans would therefore necessitate a muscle biopsy, and even if that were done, the result would be subject to the usual sampling constraints as for any other measure of muscle structure or function determined from a single biopsy.

The fitting of a hyperbolic function to paired measured values of $\dot{V}O_2max$ and mitochondrial PO_2 has the potential for estimating P_{50} and $\dot{V}_{MAX}$ in vivo, and this is illustrated in **Figure 7**. The intervention to garner several points on the curve would come from acutely varying FI_{O_2} and measuring $\dot{V}O_2$ and mitochondrial PO_2 during maximal exercise at each FI_{O_2}, as indicated by the theoretical example of the two solid circles in the **upper panel of Figure 7**. These two points reflect a mitochondrial respiration curve with P_{50} of 0.30 mm Hg and $\dot{V}_{MAX}$ of 4,000 ml/min. If such data were to span both the steep and flat parts of the respiration curve, as shown in the figure, identifying the $\dot{V}_{MAX}$ and P_{50} of a hyperbola that resulted in a least squares best fit to the data points would be possible, as shown in the **lower panel of Figure 7**. Here, over a range of trial values of both $\dot{V}_{MAX}$ and P_{50}, the root mean square (RMS) residual $\dot{V}O_2$ between the data and the hyperbola corresponding to each trial combination of P_{50} (and the

$\dot{V}_{MAX}$ providing the lowest RMS for that P_{50}) is shown. In this error-free theoretical case, one could quite accurately estimate $\dot{V}_{MAX}$ (4,000 ml/min) and P_{50} (0.3 mm Hg) from the values at the nadir of the relationship in the figure. However, if measured data happened to lie on only the flat or only on the steep parts of the curve, ability to estimate $\dot{V}_{MAX}$ and/or P_{50} would be considerably reduced.

While whole body or large muscle mass $\dot{V}O_2$ can be measured relatively easily, the experimental challenge would be to measure mitochondrial PO_2 (during exercise) (Mik, 2013). The closest approach to date in intact subjects has used MRS-based determination of myoglobin O_2 saturation (Jue et al., 1994; Richardson et al., 1995), where the signal comes from a relatively large muscle region**.** This approach gives intracellular PO_2 estimates of 3-4 mm Hg during exercise (Richardson et al., 1995), but this is the PO_2 associated with myoglobin, inferred from the finding of about 50% myoglobin saturation during peak exercise combined with accepted values of myoglobin P_{50} of about 3 mm Hg (Rossi-Fanelli and Antonini, 1958). This PO_2 is an order of magnitude greater than that projected at the mitochondria based on the preceding discussion. In the end, a method would have to be developed for direct measurement of mitochondrial PO_2. Whether a candidate signaling atom or molecule can be found for an MRS-based approach is currently unknown**.**

5. Conclusions

Considering the hindrance to overall O_2 flux caused by mitochondrial respiration using an established model of O_2 transport to the mitochondria revealed that in normal subjects exercising maximally, the step of oxidative phosphorylation, with its requirement for a mitochondrial $PO_2 > 0$, likely plays only a small role in total O_2 flux resistance. However, we identified conditions in which mitochondrial PO_2 can rise to double digit values. This occurs particularly when the mitochondrial respiration curve has either a low $\dot{V}_{MAX}$ (relative to O_2 transport), or a high P_{50}, and under such conditions, mitochondrial function may significantly impair O_2 flux.

ACKNOWLEDGEMENT

We would like to acknowledge the contributions made by the Synergy-COPD consortium and NIH P01 HL091830.

REFERENCES

Dejours P, and Kayser C. Respiration. Oxford University Press, 1966.

Gnaiger, E., Lassnig, B., Kuznetsov, A., Rieger, G., Margreiter, R., 1998. Mitochondrial oxygen affinity, respiratory flux control and excess capacity of cytochrome c oxidase. J Exp Biol 201, 1129-1139.

Johnson, K.A., Goody, R.S., 2011. The Original Michaelis Constant: Translation of the 1913 Michaelis–Menten Paper. Biochemistry 50, 8264-8269.

Jue, T., Kreutzer, U., Chung, Y., 1994. 1H NMR approach to observe tissue oxygenation with the signals of myoglobin. Adv Exp Med Biol 361, 111-118.

Michaelis, L., Menten, M.L., 1913. Die kinetik der invertinwirkung. Biochem. Z 49, 352.

Mik, E.G., 2013. Measuring Mitochondrial Oxygen Tension: From Basic Principles to Application in Humans. Anesthesia and analgesia.

Richardson, R.S., Leigh, J.S., Wagner, P.D., Noyszewski, E.A., 1999. Cellular PO2 as a determinant of maximal mitochondrial O2 consumption in trained human skeletal muscle. J Appl Physiol 87, 325-331.

Richardson, R.S., Noyszewski, E.A., Kendrick, K.F., Leigh, J.S., Wagner, P.D., 1995. Myoglobin O2 desaturation during exercise. Evidence of limited O2 transport. J Clin Invest 96, 1916-1926.

Rossi-Fanelli, A., Antonini, E., 1958. Studies on the oxygen and carbon monoxide equilibria of human myoglobin. Arch Biochem Biophys 77, 478-492.

Scandurra, F.M., Gnaiger, E., 2010. Cell respiration under hypoxia: facts and artefacts in mitochondrial oxygen kinetics. Adv Exp Med Biol 662, 7-25.

Semenza, G.L., 2011. Oxygen Sensing, Homeostasis, and Disease. New England Journal of Medicine 365, 537-547.

Sutton, J.R., Reeves, J.T., Wagner, P.D., Groves, B.M., Cymerman, A., Malconian, M.K., Rock, P.B., Young, P.M., Walter, S.D., Houston, C.S., 1988. Operation Everest II: oxygen transport during exercise at extreme simulated altitude. J Appl Physiol 64, 1309-1321.

Wagner, P.D., 1993. Algebraic analysis of the determinants of VO2max. Respiration physiology 93, 221-237.

Wagner, P.D., 1996a. Determinants of maximal oxygen transport and utilization. Annu Rev Physiol 58, 21-50.

Wagner, P.D., 1996b. A theoretical analysis of factors determining VO2 MAX at sea level and altitude. Respiration physiology 106, 329-343.

Weibel, E.R., Taylor, C.R., Gehr, P., Hoppeler, H., Mathieu, O., Maloiy, G.M., 1981. Design of the mammalian respiratory system. IX. Functional and structural limits for oxygen flow. Respiration physiology 44, 151-164.

Wilson, D.F., Erecinska, M., Drown, C., Silver, I.A., 1977. Effect of oxygen tension on cellular energetics. American Journal of Physiology - Cell Physiology 233, C135-C140.

FIGURES

Figure 1: Graphical analysis of diffusive transport of O_2 from muscle capillary to the mitochondria (dashed line) and subsequent utilization of O_2 through oxidative phosphorylation (solid line). See text for details.

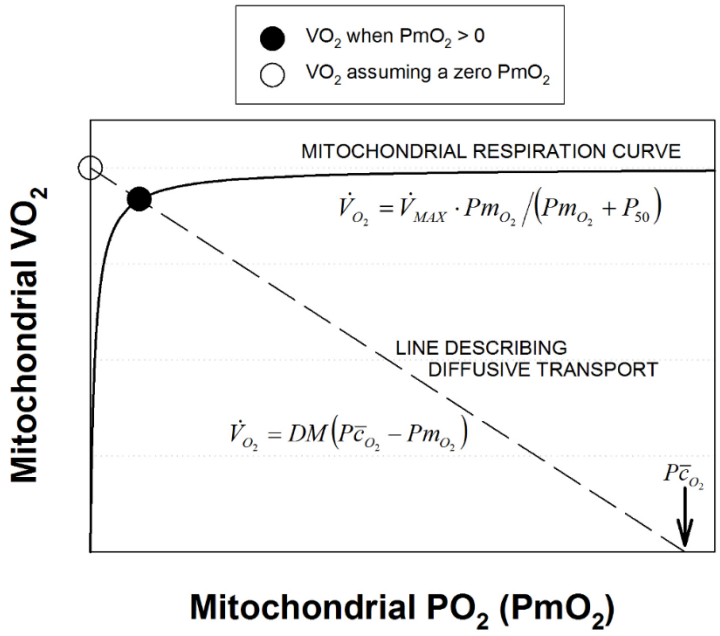

Figure 2: Schematic representation of the oxygen transport and utilization system considered in this study and the five associated mass conservation equations governing O_2 transport (equations a-d) and utilization (equation e).

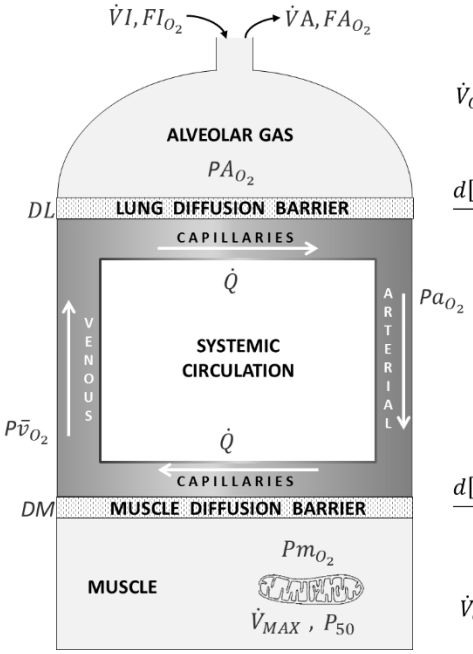

$$\dot{V}_{O_2} = \dot{V}I \cdot FI_{O_2} - \dot{V}A \cdot FA_{O_2} \quad \textbf{(a)}$$

$$\frac{d[O_2]_{(t)}}{dt} = \frac{DL}{T_L \cdot \dot{Q}} \cdot \left(PA_{O_2} - Pc_{O_2(t)}\right) \quad \textbf{(b)}$$

$$\dot{V}_{O_2} = \dot{Q}\left(Ca_{O_2} - C\bar{v}_{O_2}\right) \quad \textbf{(c)}$$

$$\frac{d[O_2]_{(t)}}{dt} = \frac{DM}{T_M \cdot \dot{Q}} \cdot \left(Pc_{O_2(t)} - Pm_{O_2}\right) \quad \textbf{(d)}$$

$$\dot{V}_{O_2} = \frac{\dot{V}_{MAX} \cdot Pm_{O_2}}{\left(Pm_{O_2} + P_{50}\right)} \quad \textbf{(e)}$$

Figure 3: Graphical depiction of the hyperbolic equation for oxidative phosphorylation fitted to the data of Scandurra & Gnaiger (Scandurra and Gnaiger, 2010). p16. fig 3B).

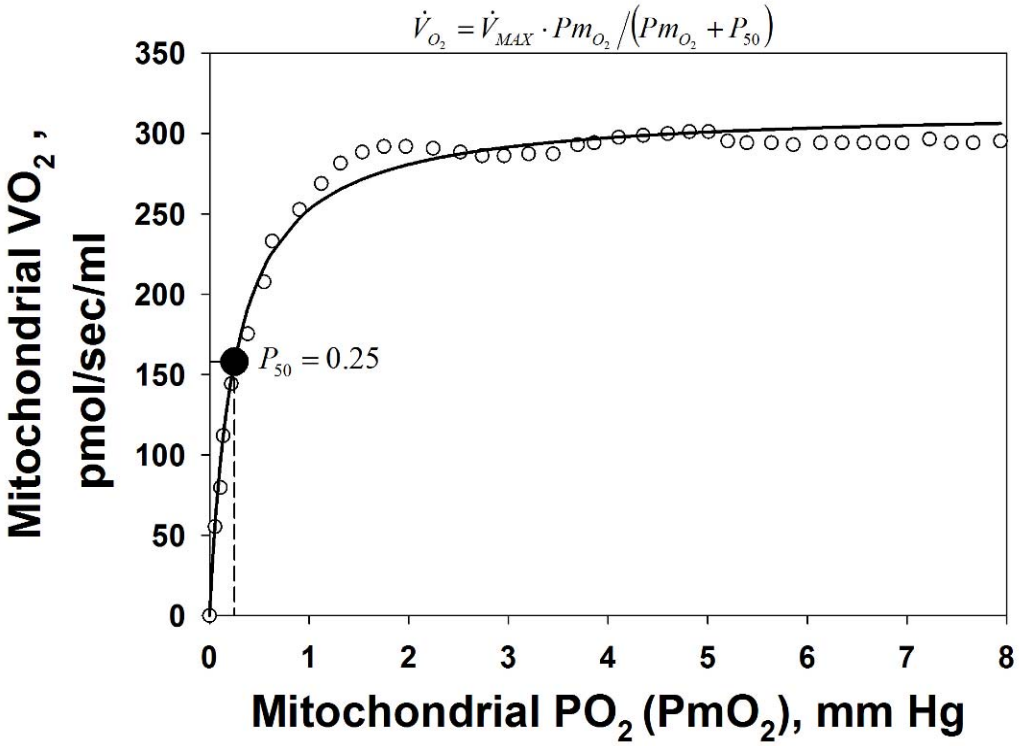

Figure 4: Effects of considering mitochondrial respiration on maximal $\dot{V}O_2$ and mitochondrial PO_2. For each $\dot{V}_{MAX}$ value, the four hyperbolic curves represent P_{50} values of 0.1, 0.3, 0.5 and 1.0 mm Hg, left to right. See text for details.

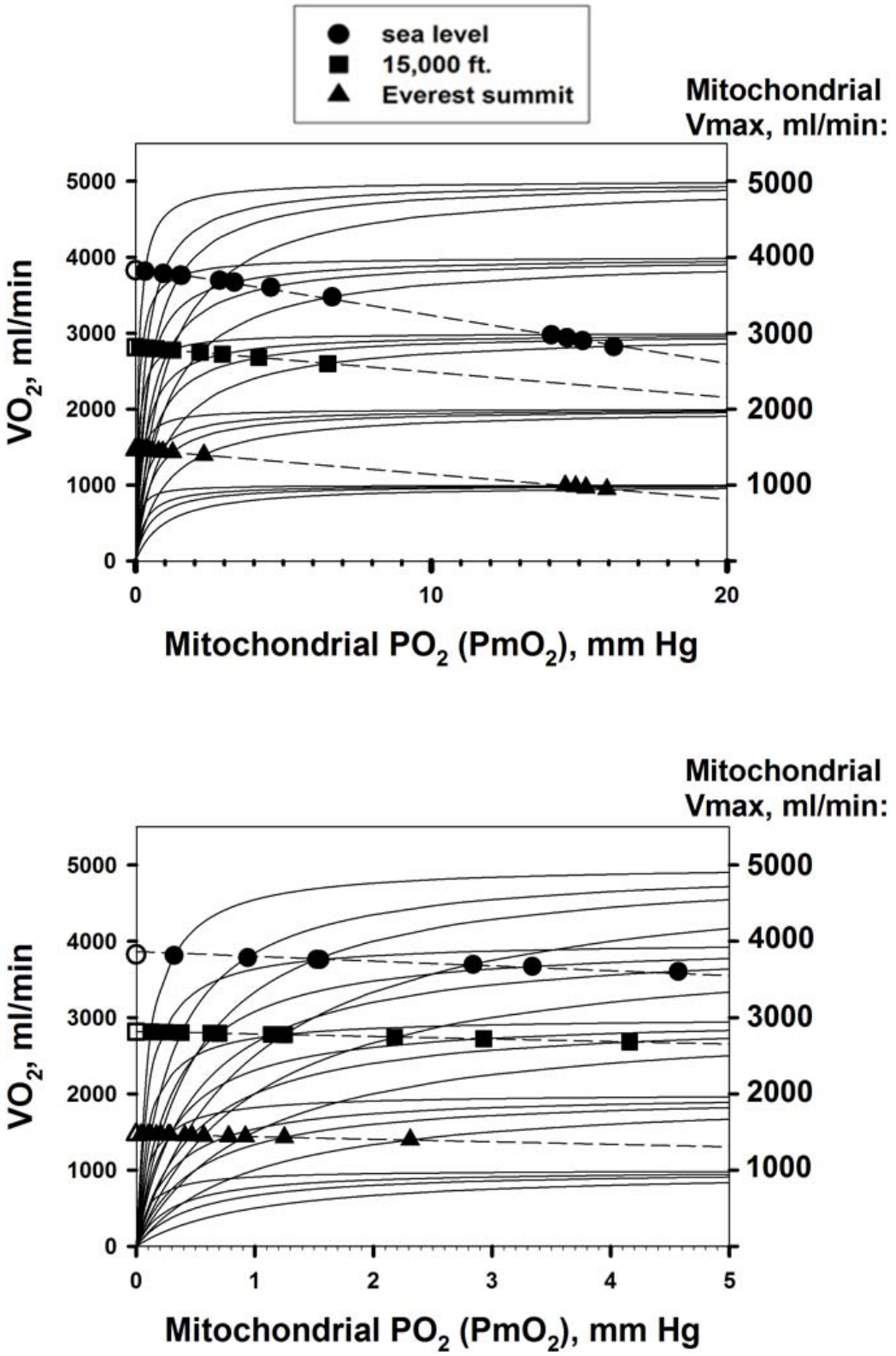

Figure 5: Mitochondrial PO_2 (upper panel) and muscle O_2 diffusing capacity (lower panel) required to maintain $\dot{V}O_2$ constant at the measured value across the domain of $\dot{V}_{MAX}$ and P_{50} values at each altitude studied (see text for details).

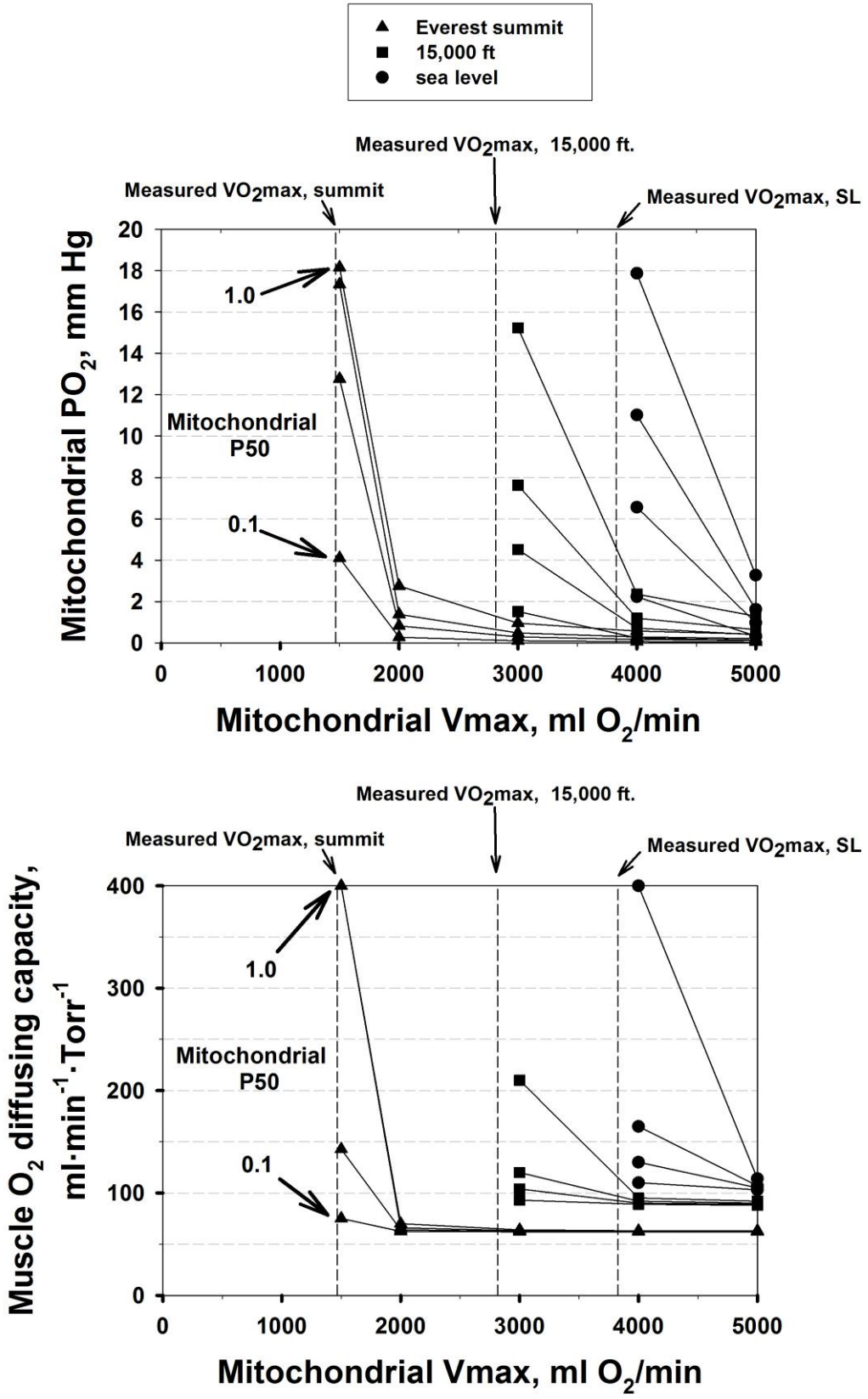

Figure 6: Graphical depiction of the concept that even when the capacity for O_2 delivery exceeds O_2 utilization (upper panel) a change in O_2 delivery will change actual $\dot{V}O_2$. Conversely, when the capacity for O_2 utilization exceeds O_2 delivery (lower panel) a change in O_2 utilization (increase in P_{50} in this example) will change actual $\dot{V}O_2$. Open circles: maximal O_2 delivery to mitochondria if Pm_{O_2} was zero. Closed circles: actual $\dot{V}O_2$. Solid and dashed lines: as in Figure 1.

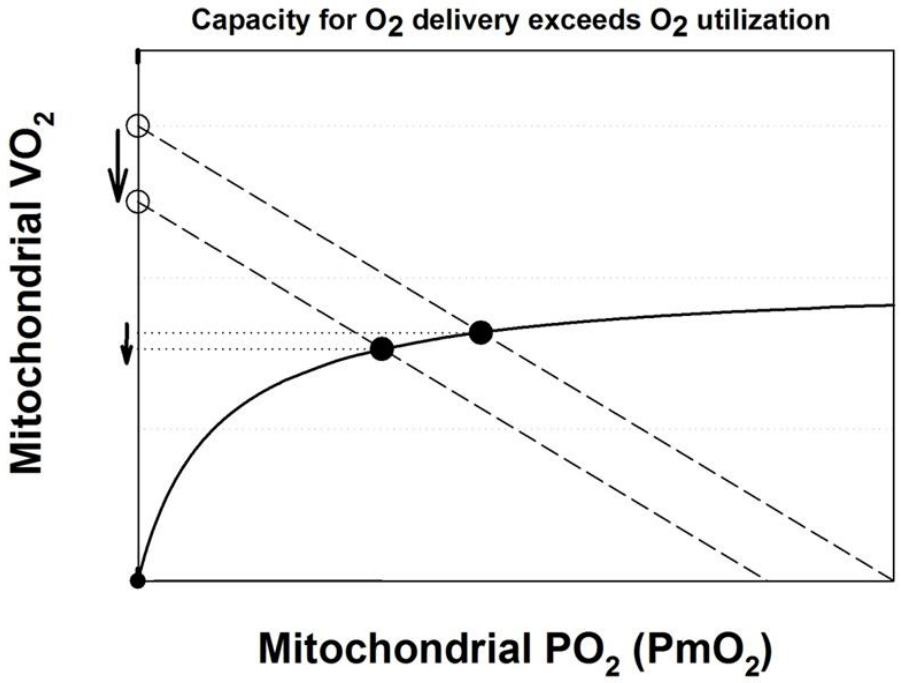

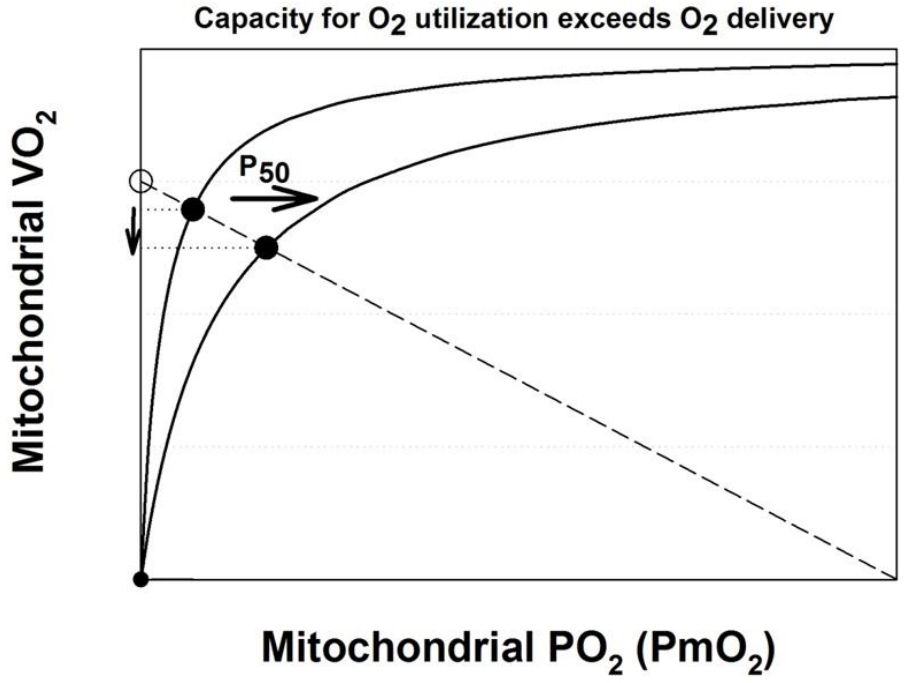

Figure 7: Estimation of mitochondrial P_{50}. Upper panel: least squares best fit (solid lines) to data (solid circles) for five trial P_{50} values. Lower panel: closeness of fit to data reflected by the Root Mean Square error, showing that a P_{50} of 0.30 mm Hg provides the best estimate.

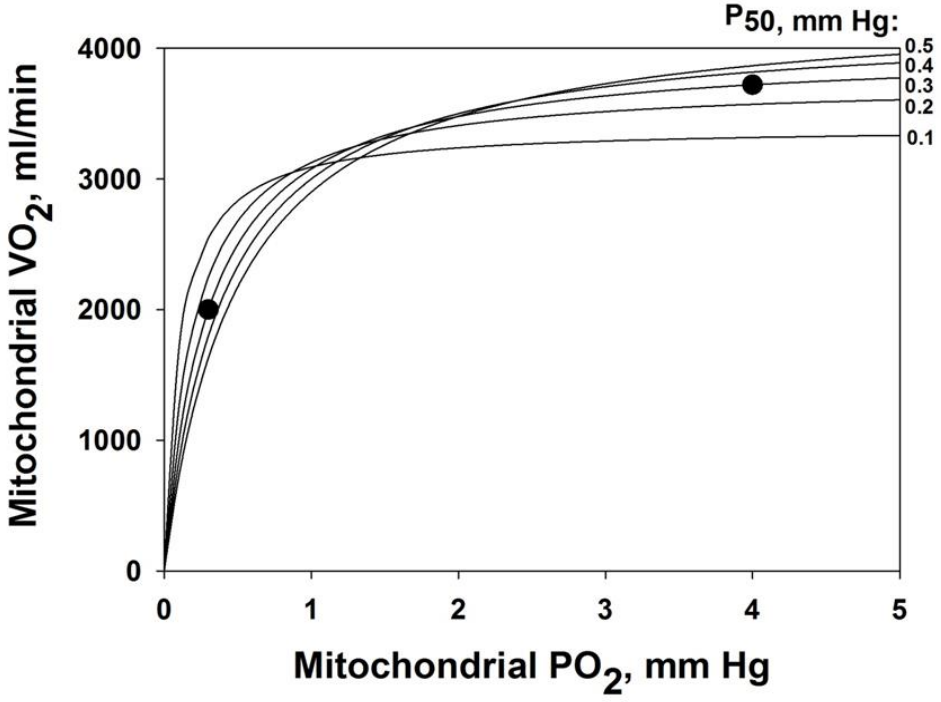

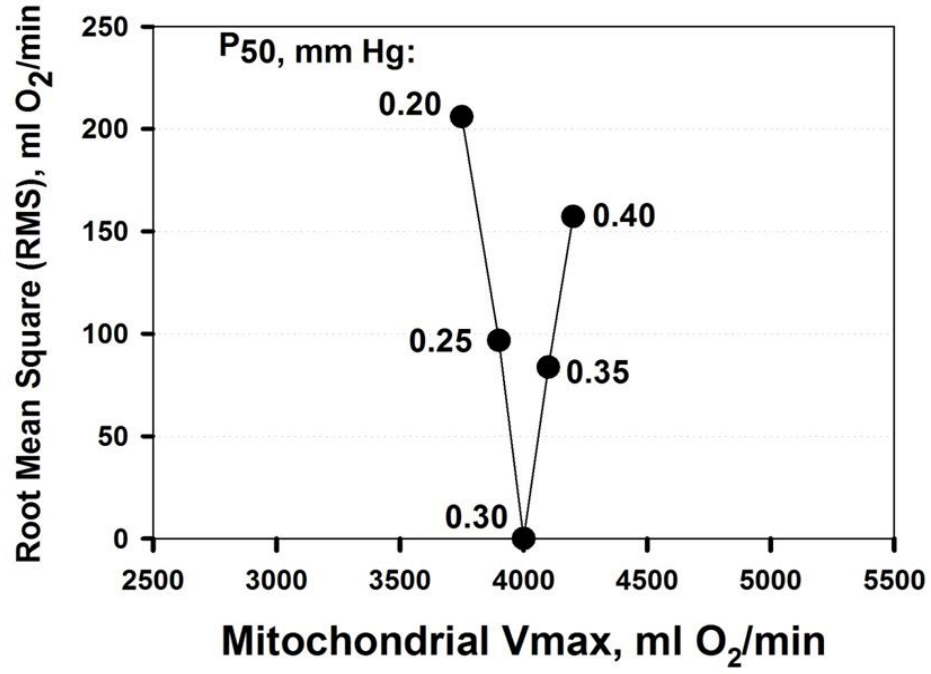

TABLE 1

Parameter	*Normal subjects at…* Sea Level	15,000 ft.	Everest summit
Barometric pressure (PB), Torr	760	464	253
Fractional Inspired Oxygen (FI_{O_2})	0.2093	0.2093	0.2093
Alveolar ventilation ($\dot{\mathrm{V}}$), BTPS, *L·min^{-1}*	112	125	165
Blood flow ($\dot{\mathrm{Q}}$), *L·min^{-1}*	23	21	16
Hemoglobin concentration ($[\mathrm{Hb}]$), g·dl^{-1}	14.5	15.5	18.0
Body temperature (T), °C	38	38	37
O_2 dissociation curve P_{50} , Torr	26.8	26.8	26.8
Total Lung O_2 diffusing capacity (DL), *ml·min^{-1}·Torr^{-1}*	51	80	100
Total muscle O_2 diffusing capacity (DM), *ml·min^{-1}·Torr^{-1}*	102	88	62
Maximum O_2 uptake ($\dot{\mathrm{V}}\mathrm{O}_2\mathrm{max}$), L·min^{-1}	3.82	2.81	1.46

Manuscript 2:

Effects of Lung and Muscle Heterogeneities on Maximal O2 Transport and Utilization.

Cano I, Wagner PD, Roca J.

Submitted to The Journal of Physiology, 2014 (2nd revision).

EFFECTS OF LUNG AND MUSCLE HETEROGENEITIES ON MAXIMAL O_2 TRANSPORT AND UTILIZATION

I Cano[ab], J Roca[ab], PD Wagner[c]

[a]Hospital Clinic, IDIBAPS, CIBERES, Universitat de Barcelona, Barcelona, Catalunya, Spain.

[b]Centro de Investigación en Red de Enfermedades Respiratorias (CibeRes), Palma de Mallorca.

[c] School of Medicine University of California, San Diego, San Diego, CA 92093-0623A.

*Corresponding author: Isaac Cano, iscano@clinic.ub.es, IDIBAPS, C/Villarroel 170, 08036, Barcelona, Spain.

Key points summary

- We expanded a prior model of whole-body O_2 transport and utilization based on diffusive O_2 exchange in the lungs and tissues to additionally allow for both lung ventilation/perfusion and tissue metabolism/perfusion heterogeneities, in order to estimate $\dot{V}_{O_2}$ and mitochondrial P_{O_2} ($P_{m_{O_2}}$) during maximal exercise.
- Simulations were performed using data from a) healthy fit subjects exercising at sea level and at altitudes up to the equivalent of Mount Everest and b) patients with mild and severe chronic obstructive pulmonary disease (COPD) exercising at sea level.
- A given degree of heterogeneity in the skeletal muscle reduces overall O_2 transfer more than does lung heterogeneity, but actually observed heterogeneity in lung is greater than in muscle, so that lung heterogeneity has a greater impact on overall O_2 transport. Muscle heterogeneity increases the range of skeletal muscle $P_{m_{O_2}}$ values, and in regions with a low ratio of metabolic capacity to blood flow, $P_{m_{O_2}}$ can exceed that of mixed tissue venous blood.
- The combined effects of lung and peripheral heterogeneities on the resistance to O_2 flow in health decreases with altitude.

Abstract

Previous models of O_2 transport and utilization in health considered diffusive exchange of O_2 in lung and muscle, but, reasonably, neglected functional heterogeneities in these tissues. However, in disease, disregarding such heterogeneities would not be justified. Here, pulmonary ventilation/perfusion and skeletal muscle metabolism/perfusion mismatching were added to a prior model of only diffusive exchange. Previously ignored O_2 exchange in non-exercising tissues was also included. We simulated maximal exercise in a) healthy subjects at sea level and altitude, and b) COPD patients at sea level, to assess the separate and combined effects of pulmonary and peripheral functional heterogeneities on overall muscle O_2 uptake ($\dot{V}_{O_2}$) and on mitochondrial P_{O_2} ($P_{m_{O_2}}$). In healthy subjects at maximal exercise, the combined effects of pulmonary and peripheral heterogeneities reduced arterial P_{O_2} ($P_{a_{O_2}}$) at sea level by 32 mm Hg, but muscle $\dot{V}_{O_2}$ by only 122 ml/min (-3.5%). At the altitude of Mt Everest, lung and tissue heterogeneity together reduced $P_{a_{O_2}}$ by less than 1 mm Hg and $\dot{V}_{O_2}$ by 32 ml/min (-2.4%). Skeletal muscle heterogeneity led to a wide range of $P_{m_{O_2}}$ among muscle regions, and in regions with a low ratio of metabolic capacity to blood flow, $P_{m_{O_2}}$ exceeded P_{O_2} of mixed muscle venous blood. For patients with severe COPD, peak $\dot{V}_{O_2}$ was insensitive to substantial changes in the mitochondrial characteristics for O_2 consumption or the extent of muscle heterogeneity. This integrative computational model of O_2 transport and utilization offers the potential for estimating profiles of $P_{m_{O_2}}$ both in health and in diseases such as COPD if the extent of pulmonary and peripheral heterogeneity is known.

Key words: Altitude, COPD; Exercise; Health, Gas exchange; Lung ventilation-perfusion mismatching; Maximal O_2 uptake; Skeletal muscle perfusion-metabolism mismatching

Abbreviations $\dot{V}_{O_2}$max, maximum oxygen delivery-uptake; COPD, chronic obstructive pulmonary disease; $P_{m_{O_2}}$, mitochondrial P_{O_2}, $\dot{V}_{MAX}$ mitochondrial maximal capacity for O_2 consumption.

1. Introduction

Current modeling of the O_2 pathway (Wagner, 1993, 1996; Cano *et al.*, 2013) is based on the concept that it is the functional integration amongst all individual components of the oxygen transport and utilization system (i.e. lungs and chest wall, heart, blood and circulation, and tissue mitochondria) which determines maximal overall O_2 uptake ($\dot{V}_{O_2}$max). In these models, important simplifying assumptions were made. In particular, O_2 exchange within the lungs was simplified by ignoring ventilation/perfusion ($\dot{V}_A/\dot{Q}$) inequality, and exchange focused only on alveolar-capillary diffusion. This was felt to be reasonable as the minimal $\dot{V}_A/\dot{Q}$ inequality found in health (Wagner *et al.*, 1974) is normally of minor importance to O_2 exchange, while allowing for such inequality greatly increased model complexity. However, this would be an unacceptable simplification in cardiopulmonary diseases where $\dot{V}_A/\dot{Q}$ inequality can be substantial. Similarly, within the muscles, potential heterogeneity of local metabolic capacity and demand ($\dot{V}_{O_2}$) in relation to blood flow distribution ($\dot{Q}$) was not considered, and while diffusive movement of O_2 from the muscle microcirculation to the mitochondria was modeled, the muscles were considered to be functionally homogeneous, i.e., with blood flow perfectly matched to O_2 demand throughout. Much less information exists about normal $\dot{V}_{O_2}/\dot{Q}$ heterogeneity in muscle (Richardson *et al.*, 2001), but using NIRS, preliminary unpublished data in normal subjects (Vogiatzis et al, J. Applied Physiol, under review) suggest that $\dot{V}_{O_2}/\dot{Q}$ matching is much tighter than is $\dot{V}_A/\dot{Q}$ matching. Additional unpublished data (Louvaris et al, in preparation) from patients with moderate chronic obstructive pulmonary disease suggest that $\dot{V}_{O_2}/\dot{Q}$ heterogeneity in muscle is not greater than in health. Thus, $\dot{V}_{O_2}/\dot{Q}$ dispersion in muscle appears to be only about ¼ of $\dot{V}_A/\dot{Q}$ dispersion in normal lung.

Another simplifying assumption was that all of the cardiac output flowed to the exercising muscles, which is clearly untrue. This is not of great quantitative importance to muscle O_2 transport in health because of the ability to increase cardiac output to over 20 L/min, rendering the fraction of cardiac output perfusing non-exercising tissue small. However, such an assumption would pose a substantial limitation if the models were applied to patients with chronic cardiorespiratory disease where peak exercise may elicit less than a doubling of the resting cardiac output and resting $\dot{V}_{O_2}$.

The purpose of the study reported in the current paper was therefore to first expand the prior O_2 transport pathway model (Wagner, 1993, 1996; Cano *et al.*, 2013) by allowing for a) $\dot{V}_A/\dot{Q}$ heterogeneity in the lung, b) $\dot{V}_{O_2}/\dot{Q}$ heterogeneity in the muscle, and c) perfusion and metabolism in non-exercising tissues, and then to analyze the impact of possible

heterogeneity in lungs and in peripheral exercising tissues, separately and combined, on overall O_2 transport and utilization at maximum exercise, both in health and in disease. In health, we simulated exercise not just at sea level but at altitudes up to the summit of Mt. Everest using as input data variables obtained in Operation Everest II (Sutton *et al.*, 1988). In disease, we chose COPD as the example of pulmonary gas exchange heterogeneity because of availability of O_2 transport data (Blanco *et al.*, 2010), and because of general interest in muscle function in this disease.

We then posed four questions: a) in health, what are the potential effects of lung and muscle heterogeneity (each modeled over a wide range) on oxygen flux and partial pressures at all steps in the O_2 pathway at sea level; b) what is the impact of typical normal levels of heterogeneity on these variables when O_2 availability is reduced by exposure to high altitude; c) how substantial variations of the three least well established determinants of O_2 flux and partial pressures in the transport/utilization pathway ($\dot{V}_{MAX}$ and P_{50} of the mitochondrial respiration curve and the extent of muscle heterogeneity) would affect both $\dot{V}_{O_2}$ and mitochondrial P_{O_2} estimates; and d) what is the effect of (measured) lung and possible muscle heterogeneity on overall oxygen uptake and mitochondrial P_{O_2} in mild and severe COPD, where O_2 transport is less than normal.

2. Methods

2.1. The prior O_2 transport and utilization model

In the absence of heterogeneity in lungs or tissues, and ignoring metabolism and blood flow to non-exercising tissues, the system describing maximal O_2 transport and utilization (Wagner, 1993, 1996; Cano *et al.*, 2013) was composed of five mass conservation equations as shown in **Figure 1**, which is reproduced from (Cano *et al.*, 2013) for the convenience of the reader. These equations represent: 1) O_2 transport by ventilation from the atmosphere to alveolar gas (**Eq. (a)** in **Figure 1**); 2) O_2 diffusion from the alveolar gas to the lung capillaries (**Eq. (b)** in **Figure 1**); 3) O_2 transport through the systemic circulation (**Eq. (c)** in **Figure 1**); 4) O_2 diffusion from systemic capillary blood to the muscle mitochondria (**Eq. (d)** in **Figure 1**); and 5) mitochondrial O_2 utilization (**Eq. (e)** in **Figure 1**).

The inputs to these equations are, at maximal exercise: inspired O_2 fraction (FI_{O_2}), ventilation ($\dot{V}$I, inspired; $\dot{V}$A, expired), lung diffusing capacity (DL), cardiac output ($\dot{Q}$), [Hb], acid base status, tissue (muscle) diffusing capacity (DM) and the characteristics of mitochondrial respiration (modeled as a hyperbolic curve with its two parameters, $\dot{V}_{MAX}$ and P_{50}, as defined

below). The five outputs, or unknowns, in these equations are the maximal rate of O_2 uptake ($\dot{V}_{O_2}$max) and alveolar, systemic arterial, venous and mitochondrial P_{O_2} values.

While the focus is clearly on O_2 transport, CO_2 cannot be ignored in such a model because of the effects of CO_2 on the O_2Hb dissociation curve. Thus, the same processes and equations are used for CO_2 (except for mitochondrial respiration, where, because the mitochondrial respiration curve for O_2 consumption does not apply to CO_2; CO_2 production is related to $\dot{V}_{O_2}$ through a stipulated value of the respiratory quotient) and the solutions for both gases sought simultaneously.

2.2. Modeling lung ventilation-perfusion inequality

To expand the model and allow for ventilation/perfusion ($\dot{V}_A/\dot{Q}$) inequality, ventilation and perfusion within the lung were distributed amongst a set of virtual lung compartments, each defined by its own ratio of ventilation ($\dot{V}_A$) to blood flow ($\dot{Q}$), with the compartments connected in parallel. This is exactly the same approach as first advanced by West in 1969 (West, 1969). Then, the computation for diffusive alveolar-capillary exchange, previously applied to just a single lung compartment representing the homogeneous lung, is now applied to all compartments in turn. The entering mixed venous blood is the same for all compartments, and the task is to compute the P_{O_2} and P_{CO_2} values expected at the end of the capillary in each compartment of different $\dot{V}_A/\dot{Q}$ ratio. This is done with a forward numerical integration procedure (Wagner *et al.*, 1974), also used in (Cano *et al.*, 2013), and the outcome for each compartment depends on the compartmental $DL/\dot{Q}$ and $\dot{V}_A/\dot{Q}$ ratios, the inspired gas and mixed venous blood O_2 and CO_2 composition, and the shape and position of the respective binding curves in blood. This approach is in fact the same as developed by Hammond and Hempleman (Hammond & Hempleman, 1987), and which is also contained within the multiple inert gas elimination technique (Wagner, 2008). Once all compartments have been subjected to this numerical integration, O_2 and CO_2 concentrations in their effluent blood are averaged in a perfusion-weighted manner to compute the O_2 and CO_2 profile of the systemic arterial blood that will reach both the exercising muscles and non-exercising tissues and organs.

In the present application, two means of data entry are possible for specifying the features of the $\dot{V}_A/\dot{Q}$ distribution, allowing flexibility: Individual compartmental values for ventilation and blood flow can be used, or the compartments can be calculated based on a $\dot{V}_A/\dot{Q}$ distribution containing one or more modes, using for each mode its first three moments (mean, dispersion and skewness) as originally programmed by West (West, 1969). Both types of inputs end up providing a multi-compartmental $\dot{V}_A/\dot{Q}$ distribution (indicated in **Figure 1**).

For simplicity, when computing the lung compartments based on a $\dot{V}_A/\dot{Q}$ distribution, the lung diffusing capacity (DL) was always distributed in proportion to compartmental blood flow, so that compartmental $DL/\dot{Q}$ remains constant throughout the lung. This decision does not eliminate the opportunity to introduce actual data on $DL/\dot{Q}$ distribution when available.

In summary, to allow for $\dot{V}_A/\dot{Q}$ heterogeneity, the single homogeneous lung "compartment" in the prior model has been replaced by a multi-compartment model built from the algorithms of West (West, 1969) as modified by Hammond and Hempleman (Hammond & Hempleman, 1987) and which allows for both $\dot{V}_A/\dot{Q}$ inequality and diffusive exchange. Just as in the prior model, necessary inputs remain the composition of inspired gas and mixed venous blood, and the output remains the composition of systemic arterial blood destined for the muscles and other tissues.

2.3. Modeling peripheral heterogeneity

Similarly to lung ventilation/perfusion mismatch, tissue heterogeneities are considered as (regional) variability in a functional ratio. However, instead of $\dot{V}_A/\dot{Q}$ being that ratio as in the lung, it is the ratio of mitochondrial metabolic capacity ($\dot{V}_{MAX}$) to blood flow ($\dot{Q}$) that is important in the muscles. Here, $\dot{V}_{MAX}$ is the local mitochondrial maximal metabolic capacity to use O_2, and is the very same parameter as $\dot{V}_{MAX}$ in equation 5, **Figure 1**. The ratio $\dot{V}_{MAX}/\dot{Q}$ in essence expresses the balance between O_2 supply and O_2 demand, reflected by $\dot{Q}$ and $\dot{V}_{MAX}$ respectively. In the prior model, the muscle was considered homogeneous in terms of $\dot{V}_{MAX}/\dot{Q}$ ratios, but now the muscle is considered as a parallel collection of muscle "units" each with its own ratio of $\dot{V}_{MAX}/\dot{Q}$. Exactly as with the lung, the $\dot{V}_{MAX}/\dot{Q}$ distribution can be specified either as a set of individual compartmental values for $\dot{Q}$ and $\dot{V}_{MAX}$, or computed from the moments of a (multimodal) $\dot{V}_{MAX}/\dot{Q}$ distribution. While it would be possible to assign every $\dot{V}_{MAX}/\dot{Q}$ compartment a unique mitochondrial P_{50} (see equation 5, **Figure 1**), this has not been modeled to date, and P_{50} has been taken to be constant throughout any single muscle. Also as in the lung, diffusion is considered in every $\dot{V}_{MAX}/\dot{Q}$ unit, with the diffusing capacity DM distributed in proportion to $\dot{Q}$, just as for the lung. The algorithm however can accommodate different values across compartments for both P_{50} and DM if desired. The same forward integration procedure is used as in the prior model (Cano *et al.*, 2013), when it was applied to the entire muscle considered as one homogeneous unit to compute each muscle compartment's effluent venous O_2 and CO_2 levels for the given inflowing arterial blood composition, and the $\dot{V}_{MAX}/\dot{Q}$ and $DM/\dot{Q}$ ratios of the unit. Again as in the lung, the effluent venous blood from all muscle units is combined, or mixed, in terms of both O_2 and CO_2 concentrations, and a resulting mixed muscle venous P_{O_2} and P_{CO_2} is then calculated. Finally,

this blood is mixed with that from the non-exercising tissues (see below). This mixed venous blood returns to the lungs for re-oxygenation.

In summary, to allow for $\dot{V}_{MAX}/\dot{Q}$ heterogeneity, the single homogeneous muscle "compartment" in the prior model has been replaced by a multi-compartment model which allows for both $\dot{V}_{MAX}/\dot{Q}$ inequality and diffusion impairment. Similarly to the prior model, necessary additional inputs remain the composition of arterial blood, and the blood binding characteristics of O_2 and CO_2. The output remains the composition of mixed muscle venous blood destined for return to the lungs for re-oxygenation.

2.4 Modeling metabolism and blood flow to non-exercising tissues

Non-exercising tissue blood flow and metabolism are incorporated simply by assigning values for total non-exercising tissue $\dot{V}_{O_2}$ and $\dot{Q}$, and using the Fick principle to compute the tissue venous O_2 concentration. Then, a mixing equation combines venous blood from this non-exercising tissue with that from the mixed muscle venous blood (see above) in proportion to the blood flow rates assigned to the non-exercising tissues and muscles respectively, to form what will be pulmonary arterial blood reaching the lungs for re-oxygenation.

2.5 Achieving a solution for the model

In the prior model it was explained (Cano *et al.*, 2013) how the model was run and a solution achieved. The same process is used with the above-described expansions in the current paper. In brief, a starting estimate is made for the composition of mixed venous blood entering the lungs, and for that estimate, the lung component is executed over the many $\dot{V}_A/\dot{Q}$ compartments and the end-capillary O_2 and CO_2 concentrations averaged over all compartments (weighted by compartmental blood flow) to yield an estimate of systemic arterial P_{O_2} and P_{CO_2}. These are then used as input data for the muscle part of the system, and that component is run once for each $\dot{V}_{MAX}/\dot{Q}$ compartment. The effluent compartmental venous O_2 and CO_2 levels are then averaged (again blood flow-weighted), and mixed with the blood draining the non-exercising tissues (**see 2.4**). It is the P_{O_2} and P_{CO_2} of this mixed blood that is the new estimate at mixed venous P_{O_2} and P_{CO_2} for the next iteration (or cycle) of pulmonary gas exchange: To this point, all that has changed between the first and second cycles is the composition of mixed venous blood. After pulmonary gas exchange calculations using this new venous blood composition are complete, new values of arterial blood P_{O_2} and P_{CO_2} are calculated, and now muscle O_2 exchange is recomputed, from which new values of mixed venous P_{O_2} and P_{CO_2} are calculated. This cycling back and forth between the lungs and the tissues is continued until the five $\dot{V}_{O_2}$ estimates - one computed from each of the 5

equations in **Figure 1** - are identical (to within +/- 0.1 ml/min). At this point, stability of all P_{O_2} values (alveolar, arterial, muscle venous and mitochondrial) in the face of further cycling between the lungs and tissues is also achieved. When this is observed, the governing requirement for conservation of mass has been achieved, and this signals the end of the run.

2.6 Analysis and input data for simulations

As mentioned, four questions were posed:

First, in health, we first assessed the effects of a wide range of lung and tissue heterogeneities on oxygen tensions and utilization at all steps of the O_2 pathway. This extensive exploration was carried out for conditions of maximal exercise breathing room air at sea level. To this end, input data defining O_2 transport conductances (i.e., ventilation, cardiac output, lung and muscle diffusional conductances) from normal subjects exercising maximally at sea level in Operation Everest II (Sutton et al., 1988) were used just as for the previous models (Wagner, 1993, 1996). Lung heterogeneity was analyzed from complete homogeneity ($\log \mathrm{SD}\ \dot{Q} = 0$), to very high inhomogeneity ($\log \mathrm{SD}\ \dot{Q} = 2$) as might be seen in the critically ill. We also explored the effects of skeletal muscle heterogeneity on overall O_2 uptake (VO_2 max) using a similar wide range of $\log \mathrm{SD}\ \dot{V}_{max}$, from 0 to 2.0**.**.

However, in all the subsequent analyses, for each level of lung heterogeneity (from $\log \mathrm{SD}\ \dot{Q} = 0$ to $\log \mathrm{SD}\ \dot{Q} = 2$), the impact of muscle tissue heterogeneity was assessed from a completely homogenous exercising muscle ($\log \mathrm{SD}\ \dot{V}_{max} = 0$), to a likely high degree of muscle metabolism/perfusion inhomogeneity ($\log \mathrm{SD}\ \dot{V}_{max} = 0.5$), taking into account that recent experimental studies suggests a $\log \mathrm{SD}\ \dot{V}_{max}$ of only 0.1 in normal subjects exercising maximally at sea level (Vogiatzis et al, J. Applied Physiol, under review)).

The second question examined the effects of heterogeneity in healthy lungs and muscle on O_2 transport and utilization at altitude. For the lung we used $\log \mathrm{SD}\ \dot{Q} = 0.5$ as a value commonly seen during exercise (Wagner *et al.*, 1987b). This value is near the upper end of the normal range, which is 0.3-0.6 (Wagner *et al.*, 1987a). In muscle, we used preliminary unpublished estimates of $\log \mathrm{SD}\ \dot{V}_{max} = 0.1$. For non-exercising body tissues we used typical resting total values of $\dot{V}_{O_2}$ (300 ml/min), $\dot{V}_{CO_2}$ (240 ml/min) and blood flow (5 L/min) for normal subjects. The input data defining the O_2 transport conductances again came from normal subjects exercising maximally at sea level and altitude in Operation Everest II (Sutton et al., 1988) as used above and also in our prior work 2013. However, to study the consequences at more altitudes than were examined in Operation Everest II (which were sea level, 4600m, 6100m, 7600m and 8848m), O_2 transport conductance parameters were linearly

interpolated at 305m (1000 ft.) elevation increments from the data obtained at each of the 5 altitudes studied in Operation Everest II (Sutton et al., 1988).

Data from experimental human exercise studies do not exist for the two variables defining the hyperbolic mitochondrial respiration curve: $\dot{V}_{max}$ and P_{50}. Therefore, we executed the simulations mentioned above using a value for $\dot{V}_{max}$ (4.6 L/min) that is 20% higher than the measured $\dot{V}_{O_2}$max at sea level in Operation Everest II (Sutton et al., 1988) of 3.8 L/min. We chose this value as a reasonable estimate for $\dot{V}_{max}$ because it is known that measured $\dot{V}_{O_2max}$ is less than mitochondrial capacity to use O_2 (i.e., $\dot{V}_{MAX}$) in healthy fit subjects since exercise capacity is known to be increased when breathing 100% O_2 (Welch, 1982; Knight *et al.*, 1992). For P_{50}, we used a value of 0.3 mm Hg, similar to what has been found experimentally in vitro (Wilson *et al.*, 1977; Gnaiger *et al.*, 1998; Scandurra & Gnaiger, 2010). Little is known about $\dot{V}_{MAX}/\dot{Q}$ heterogeneity in muscle except for measurements made by Richardson using magnetic resonance spectroscopy (Richardson *et al.*, 2001) and recent unpublished data using NIRS that yield dispersion values of about 0.1 as explained earlier.

For the third and fourth question we assessed how substantial variations of the three least well-established determinants of O_2 flux and partial pressures in the transport/utilization pathway ($\dot{V}_{MAX}$ and P_{50} of the mitochondrial respiration curve and log SD $\dot{V}_{MAX}$) would affect both $\dot{V}_{O_2}$ and mitochondrial P_{O_2} estimates, in health (third question) and in COPD (fourth question). Input data defining O_2 transport conductances and lung heterogeneity (i.e. $\log \text{SD } \dot{Q} = 0.5$) from normal subjects exercising maximally at sea level in Operation Everest II (Sutton et al., 1988) were used in health. In disease, measured O_2 conductances and lung heterogeneity data came from two previously studied COPD patients (Blanco *et al.*, 2010) exercising maximally (**Table II**), one with mild (FEV_1 = 66 % predicted post-bronchodilator) and one with severe (FEV_1 = 23 % predicted post-bronchodilator) COPD. However, even if reasonable, the values of $\dot{V}_{MAX}$ and P_{50} assumed to answer the previous question are uncertain, let alone whether there is significant $\dot{V}_{MAX}/\dot{Q}$ heterogeneity. Because of this, we carried out simulations over a wide range of possible values of these variables. In the case of $\dot{V}_{max}$, it is known that acutely increasing inspired O_2 concentration increases exercise capacity, both in health and in COPD (Welch, 1982; Knight *et al.*, 1992; Richardson *et al.*, 2004). How much higher is not known, and so to determine how important knowing $\dot{V}_{MAX}$ is to the outcomes of the model we compared outcomes using the previously-used $\dot{V}_{MAX}$ value (20% higher than actual $\dot{V}_{O_2max}$) to results obtained when $\dot{V}_{MAX}$ was set to 10 % and 30% above measured $\dot{V}_{O_2max}$. For mitochondrial P_{50}, we used values lower (0.14 mm Hg) and higher (0.46 mm Hg) than 0.3 mm Hg, the value found experimentally in vitro (Wilson

et al., 1977; Gnaiger *et al.*, 1998; Scandurra & Gnaiger, 2010)**.** Finally, to assess how sensitive the outcomes are to the degree of heterogeneity, we also carried out calculations with log SD $\dot{V}_{MAX}$ values of 0.1 (healthy subject estimates), 0.2 and 0.3. With respect to non-exercising body tissues, we used typical resting total values of $\dot{V}_{O_2}$ (300 ml/min), $\dot{V}_{CO_2}$ (240 ml/min) and blood flow (5 L/min) for normal subjects.

For the two previously studied COPD patients (Blanco *et al.*, 2010) exercising maximally we used measured resting values of whole body $\dot{V}_{O_2}$ ($\dot{V}_{O_2}$rest) and $\dot{V}_{CO_2}$ (**Table II**), along with a blood flow estimate ($\dot{Q}_{non-exercising}$) from the following formula, which expresses the concept that blood flow is proportional to metabolic rate: $\dot{Q}_{non-exercising} = \dot{Q}_{max} * (\dot{V}_{O_2}rest/\dot{V}_{O_2}max)$.

3. Results

3.1. Effects of potential lung and muscle heterogeneities on O_2 transport and utilization in healthy subjects exercising maximally at sea level

Figure 2 shows the independent effects of lung $\dot{V}_A/\dot{Q}$ heterogeneity (solid circles) and muscle $\dot{V}_{MAX}/\dot{Q}$ heterogeneity (empty circles) on maximal muscle oxygen uptake ($\dot{V}_{O_2}$max), in normal subjects exercising maximally at sea level**.** In this figure, both $\dot{V}_A/\dot{Q}$ and $\dot{V}_{MAX}/\dot{Q}$ heterogeneity has been varied over a wide range of LOG SD, from 0 to 2.0. Healthy subjects show pulmonary log SD Q between 0.30 and 0.60 (refs), whereas skeletal muscle heterogeneity (log SD Vmax) presents a average value of 0.10 (Vogiatzis et al, J. Applied Physiol, under review). In patients with moderate to severe COPD, log SD Q can present values close to 1.0, but no published data on log SD Vmax are available. However, recent studies in patients with COPD (Louvaris et al, in preparation) suggest similar degrees of muscle heterogeneity as in health. Finally, critically ill patients admitted in the Intensive Care Unit (ICU) may show lung heterogeneity values close to 2.0, but no information on log SD Vmax is available. The main result from Figure 2 is that for any given degree of heterogeneity, that in muscle affects O2 transport more than does that in the lungs. However, because muscle heterogeneity appears to be much less than that in the lung, both in health and COPD, based on a combination of published and unpublished data as mentioned, actual muscle heterogeneity has less of an impact on O2 transport than observed lung heterogeneity.

The six panels in **Figure 3** display the estimated (combined and separate) effects of lung and muscle heterogeneities on the O_2 transport and utilization system. The upper-left panel indicates arterial P_{O_2} ($P_{a_{O_2}}$) over a range of exercising muscle $\dot{V}_{MAX}/\dot{Q}$ mismatching (0 to 0.5), expressed as log SD $\dot{V}_{max}$. For each log SD $\dot{V}_{max}$ value, the panel displays $P_{a_{O_2}}$ values for different levels of lung $\dot{V}_A/\dot{Q}$ heterogeneity, from the homogeneous lung (log SD $\dot{Q} = 0$) to

a highly heterogeneous lung ($\log \text{SD}\ \dot{Q} = 2$). Each line represents the outcome at a given level of lung heterogeneity over a range of muscle heterogeneity. This panel shows that muscle heterogeneity has only a small effect on $P_{a_{O_2}}$ at all levels of lung functional heterogeneities. However, as is well known, $\dot{V}_A/\dot{Q}$ inequality has a major impact on arterial oxygenation as shown. Likewise, the upper-right panel shows the effects of muscle heterogeneity on effluent muscle venous P_{O_2} ($P_{v_{O_2}}$). The impact is moderate, and is greater than the effect on $P_{a_{O_2}}$. However, it is quantitatively important only at high levels of tissue heterogeneity, especially in combination with lungs containing little heterogeneity.

The two middle panels of **Figure 3** show the relationships between mitochondrial P_{O_2} ($P_{m_{O_2}}$) and skeletal muscle $\dot{V}_{MAX}/\dot{Q}$ heterogeneity. The left hand panel shows the lowest compartmental values of $P_{m_{O_2}}$ (i.e., when $\dot{V}_{MAX}/\dot{Q}$ is high) and the right hand panel shows the highest compartmental values of $P_{m_{O_2}}$ (i.e., when $\dot{V}_{MAX}/\dot{Q}$ is low). Note that the ordinate scales are very different in these two panels. These panels show that heterogeneity of $\dot{V}_{MAX}/\dot{Q}$ ratios markedly expands the range of $P_{m_{O_2}}$ levels among exercising skeletal muscle compartments. As in the top panels, each line in the two middle panels correspond to different levels of lung heterogeneity from a homogeneous lung ($\log \text{SD}\ \dot{Q} = 0$) to a highly heterogeneous lung ($\log \text{SD}\ \dot{Q} = 2$).

The left middle panel shows that, as expected, the greater the peripheral heterogeneity, the lower the minimum $P_{m_{O_2}}$ values. Moreover, we observe a moderate impact of lung heterogeneity on minimum $P_{m_{O_2}}$, but such impact decreases as skeletal muscle heterogeneity increases. Likewise, the right middle panel shows that skeletal muscle compartments with lowest $\dot{V}_{MAX}/\dot{Q}$ ratios may generate exceedingly high $P_{m_{O_2}}$ estimates that increase with tissue heterogeneity. Homogeneous lungs show the highest $P_{m_{O_2}}$ values for a given level of peripheral tissue heterogeneity.

The lower left panel indicates that muscle heterogeneities have small effects on total muscle $\dot{V}_{O_2}$, especially compared with lung heterogeneities that show a significant impact on muscle $\dot{V}_{O_2}$max. Finally, the lower right panel displays the maximum estimates for compartmental muscle $P_{m_{O_2}}$ (as seen in the middle right panel of the same figure) plotted against the corresponding mean effluent muscle $P_{v_{O_2}}$ (from the top right panel). The individual lines indicate different levels of muscle heterogeneities, from a homogeneous tissue (SDVmax = 0) at the bottom to heterogeneous muscle (SDVmax = 0.5) at the top. In the panel, the dashed straight line corresponds to the identity line. The point of presenting this

relationship is to show that when the dispersion of muscle $\dot{V}_{MAX}$ is 0.2 or greater, some regions of muscle will have mitochondrial P_{O_2} values that exceed P_{O_2} of the effluent muscle venous blood.

3.2. The role of functional heterogeneities, lung and muscle, on O_2 transport and utilization in healthy subjects at altitude

The four panels in **Figure 4** display the effects of altitude on four key outcome variables at maximal exercise – arterial, muscle venous, and mitochondrial P_{O_2} and $\dot{V}_{O_2max}$ itself. Two relationships are shown in each panel – that computed in the absence of either lung or muscle heterogeneity, and that computed allowing for reasonable normal estimates of heterogeneity in each location as listed above in the methods section ($\dot{V}_A/\dot{Q}$ heterogeneity in the lung quantified by a dispersion value (log SD $\dot{Q}$) of 0.5, $\dot{V}_{MAX}/\dot{Q}$ heterogeneity in muscle quantified using an estimate of dispersion (log SD $\dot{V}_{MAX}$) of 0.1, and non-exercising body tissues using typical resting total values of $\dot{V}_{O_2}$ (300 ml/min), $\dot{V}_{CO_2}$ (240 ml/min) and blood flow (5 L/min)). Except for arterial P_{O_2} at sea level and altitudes up to about 10,000ft, the effects of typical levels of heterogeneity are seen to be small, and diminish progressively with increasing altitude.

3.3. Sensitivity of outcomes to mitochondrial respiration and muscle heterogeneity estimates in health

Recall that the three least well established determinants of O_2 flux and partial pressures in the transport/utilization pathway are the $\dot{V}_{MAX}$ and P_{50} of the mitochondrial respiration curve (that links $\dot{V}_{O_2}$ to mitochondrial P_{O_2}) and the extent of muscle heterogeneity. Because of this, we carried out calculations of how variation in their assumed values would affect both $\dot{V}_{O_2}$ and mitochondrial P_{O_2} estimates. In the preceding sections we assumed a value for $\dot{V}_{MAX}$ 20% above measured $\dot{V}_{O_2max}$. In this section, we now use values of $\dot{V}_{O_2max}$ + 10% and $\dot{V}_{O_2max}$ + 30%. For mitochondrial P_{50} (assumed normal value 0.3 mm Hg (Wilson *et al.*, 1977; Gnaiger *et al.*, 1998; Scandurra & Gnaiger, 2010)), we also used values of 0.14 and 0.46 mm Hg. With heterogeneity of $\dot{V}_{MAX}$ estimated at 0.1 (log SD $\dot{V}_{MAX}$), we also used values of 0.2 (moderate heterogeneity) and 0.3 (severe heterogeneity). This yielded 3x3x3 or 27 combinations of these variables. It should also be noted that the values chosen reflect substantial relative differences for each variable.

Figure 5 shows the results of this analysis in a format where predicted $\dot{V}_{O_2max}$ is plotted against the corresponding predicted average muscle mitochondrial P_{O_2} so that the effects can be seen for both of these outcome variables. The top panel shows results when $\dot{V}_{MAX}$ =

$\dot{V}_{O_2max}$ + 10%; the middle panel for $\dot{V}_{MAX}$ = $\dot{V}_{O_2max}$ + 20% and the lower panel for $\dot{V}_{MAX}$ = $\dot{V}_{O_2max}$ + 30%. In each panel, open squares represent P_{50} = 0.14 mm Hg, closed circles a P_{50} of 0.3 mm Hg and open triangles a P_{50} of 0.46 mm Hg. For any one such P_{50}, the three connected points in each case reflect, from left to right, log SD $\dot{V}_{MAX}$ = 0.1 (normal), 0.2 (moderate), and 0.3 (severe heterogeneity).

In terms of predicted $\dot{V}_{O_2max}$, the consequences of these uncertainties are small. The highest $\dot{V}_{O_2max}$ in all three panels is 3415 ml/min, and the lowest is 3192 ml/min. However, in terms of mean mitochondrial P_{O_2} , the effects are greater. $P_{m_{O_2}}$ is systematically higher for the lowest $\dot{V}_{MAX}$ (range of $P_{m_{O_2}}$: 0.8 to 3.7 mm Hg, top panel) to lower panel (highest $\dot{V}_{MAX}$, range of $P_{m_{O_2}}$: 0.3 to 1.9 mm Hg). At any $\dot{V}_{MAX}$, increasing mitochondrial P_{50} results in systematically higher $P_{m_{O_2}}$ values, however, with almost no effect on the relationship between $\dot{V}_{O_2max}$ and $P_{m_{O_2}}$. Finally, increasing $\dot{V}_{MAX}$ heterogeneity raises average $P_{m_{O_2}}$ for any set of $\dot{V}_{MAX}$ and P_{50} values.

3.4. Simulated impact of lung and muscle heterogeneity on $P_{m_{O_2}}$ and muscle $\dot{V}_{O_2}$ in two patients with COPD of different severity: Question 4

As **Table 2** shows, lung heterogeneities had been measured in each patient using the multiple inert gas elimination technique (Blanco *et al.*, 2010). The first patient displays features that would be regarded as reflecting moderate COPD, while the second patient represents end-stage COPD and extremely limited exercise capacity.

Figure 6 displays the impact of functional lung and muscle heterogeneities on the O_2 pathway in the two COPD patients (moderate severity, left panels and end stage severity, right panels). The format indicates the values of both predicted $\dot{V}_{O_2max}$ and $P_{m_{O_2}}$ over a range of values of the same three least certain variables ($\dot{V}_{MAX}$ and P_{50} of the mitochondrial respiration curve and degree of muscle $\dot{V}_{MAX}$ heterogeneity, none of which are known for these patients).

The less affected patient (left three panels) behaves in a fashion very similar to that shown in **Figure 5** for normal subjects (other than for absolute values of peak $\dot{V}_{O_2}$ under all conditions). In particular, mitochondrial P_{O_2} values are in the same range as for normal subjects. Variation in $P_{m_{O_2}}$ across muscle regions is considerable (not shown) with a SD of 10 mm Hg.

For the severely affected patient (right three panels), peak $\dot{V}_{O_2}$ is insensitive to substantial changes in mitochondrial $\dot{V}_{MAX}$, P_{50} or the extent of heterogeneity. Only mitochondrial P_{50} changes will have some effect on mitochondrial P_{O_2} , but it is important to note that the scale of mitochondrial P_{O_2} is very different than normal, and is far lower under all conditions, with little variation throughout the muscle (SD of 1 mm Hg).

4. Discussion

4.1. Summary of major findings

This study has generated the first integrated model of the O_2 pathway that takes into account all the individual components of O_2 transport and utilization considering both exercising and non-exercising tissues at $\dot{V}_{O_2}$max in health and in disease (i.e. COPD), thus allowing for heterogeneity in both lungs and muscle.

The research addresses the separate and combined contributions of functional heterogeneities at pulmonary and at skeletal muscle levels to each of the components of the O_2 pathway. Emphasis is placed on estimating the impact of lung and skeletal muscle $\dot{V}_{MAX}/\dot{Q}$ ratio inequalities on overall muscle $\dot{V}_{O_2}$ and on mitochondrial P_{O_2} at maximal exercise. This was done simulating normal subjects at sea level and altitude, and patients with COPD. The main findings are that, muscle heterogeneity, at a given log SD (**Figure 2**), shows higher potential to affect maximal O_2 availability than does lung $\dot{V}_A/\dot{Q}$ inequality. Moreover, $\dot{V}_{MAX}/\dot{Q}$ heterogeneity results in a wide range of potential mitochondrial P_{O_2} values – a range that could have implications for muscle function as discussed below. These findings stress the relevance of performing further measurements of skeletal muscle heterogeneities in health and disease.

4.2. Implications of functional heterogeneities: lung and skeletal muscle

Whether arterial oxygenation falls as a result of altitude in normal subjects or as a result of heterogeneity in the lungs in patients with lung disease (at sea level), it is clear that O_2 availability to the muscles must fall. This has been appreciated for many years, as has the consequence of such reduced O_2 availability for maximal exercise capacity. The other potentially important consequence of reduced O_2 availability is reduced mitochondrial P_{O_2}. This may have more than one effect on cellular function.

While heterogeneity in the lungs must cause mitochondrial P_{O_2} to fall throughout the muscle (all other factors unchanged), heterogeneity in the muscles will additionally cause mitochondrial P_{O_2} to vary between muscle regions. In those areas with higher than average $\dot{V}_{MAX}$ in relation to blood flow, mitochondrial P_{O_2} is lower than average, but in regions where $\dot{V}_{MAX}$ is low in relation to blood flow, mitochondrial P_{O_2} must rise to levels greater than would be seen in the absence of heterogeneity. The consequences of subnormal mitochondrial P_{O_2} are discussed below. There may be corresponding functional consequences of a high mitochondrial P_{O_2} as well.

A high P_{O_2} may oppose vasodilatation and restrict local perfusion, thus increasing the $\dot{V}_{MAX}/\dot{Q}$ back towards normal and offering an intrinsic mechanism to automatically limit mitochondrial P_{O_2} heterogeneity. A high mitochondrial P_{O_2} will also reduce the capillary to mitochondrial P_{O_2} diffusion gradient, reducing diffusive O_2 transport and again working towards restoring the balance between O_2 supply and demand. Furthermore, the high P_{O_2} may exert genomic effects that may be opposite to those expected when P_{O_2} is below normal (see above). The potential therefore exists for regional regulation of gene expression (and thus for adaptive programs) according to local P_{O_2} . Finally, when mitochondrial P_{O_2} is elevated, the potential exists for increased ROS generation, just as when P_{O_2} is below normal. If so, muscle regions with both very low and very high $\dot{V}_{MAX}/\dot{Q}$ ratios may be at risk of oxidative stress.

4.3 Biological and clinical implications

The multilevel impact of disturbances of cellular oxygenation on cell function is well recognized (Semenza, 2011). Hypoxia- (or hyperoxia-) induced biological alterations may play a significant role on underlying mechanisms in different acute and chronic conditions (Resar *et al.*, 2005). A major conclusion of the present study is that mitochondrial P_{O_2} will vary considerably among muscle regions of different $\dot{V}_{MAX}/\dot{Q}$ ratio. When $\dot{V}_{MAX}/\dot{Q}$ is low, $P_{m_{O_2}}$ is high, and vice versa. This potential variation in $P_{m_{O_2}}$ may have significant biological implications.

First, since a low P_{O_2} facilitates local vasodilatation in muscle (Rowell, 1986), those areas with high $\dot{V}_{MAX}$ in relation to $\dot{Q}$, thus having a low $P_{m_{O_2}}$, may preferentially vasodilate, which means that $\dot{Q}$ may increase locally and that the $\dot{V}_{MAX}/\dot{Q}$ ratio is thus, in part, normalized. In this way, $\dot{V}_{MAX}/\dot{Q}$ heterogeneity may be to some extent self-limited. This corresponds to hypoxic pulmonary vasoconstriction in the lungs, where it has been known for many years that a region with a low $\dot{V}_A/\dot{Q}$ ratio will vasoconstrict, limiting blood flow and tending to push the $\dot{V}_A/\dot{Q}$ ratio back towards normal.

Second, the lower the mitochondrial P_{O_2}, the higher will be the P_{O_2} difference between the muscle microvasculature and the mitochondria, other factors equal. This facilitates the diffusion process, and provides an additional, automatic compensatory mechanism to work in the direction of restoring $\dot{V}_{O_2}$ when blood flow is low. Whether these self-correcting effects are seen in disease remain to be determined.

Third, a low P_{O_2} may have implications for genomic responses. As P_{O_2} falls in regions with high $\dot{V}_{MAX}/\dot{Q}$ ratios, the HIF system may be activated, preferentially in those regions, signaling

adaptive changes to enhance key processes such as glucose transport, glycolysis and angiogenesis. It may also have implications for differential reactive oxygen species (ROS) generation across muscle fibers, since it appears that ROS generation is P_{O_2} dependent (Selivanov *et al.*, 2012). Regions with a low $\dot{V}_{MAX}/\dot{Q}$ and thus a high mitochondrial P_{O_2} may be hyperoxic to the point of inducing regional cellular damage from high ROS levels. These speculative predictions will of course need to be examined experimentally in the future.

4.4. Potential for estimating $P_{m_{O_2}}$ in health and in disease

It may be possible to measure mitochondrial P_{O_2} ($P_{m_{O_2}}$) in the future (Mik, 2013) but this promising approach is not yet generally available. If this, or another, method can be developed into a feasible approach for intact humans, it offers the potential for estimating, at least approximately, the parameters of the in vivo mitochondrial O_2 respiration curve. By varying inspired O_2 concentration over as wide a range as safely possible, paired values of $\dot{V}_{O_2}$ and $P_{m_{O_2}}$ could be measured, and if they were to bracket both the O_2-dependent and O_2-independent regions of the mitochondrial respiration curve, there may be enough information to estimate $\dot{V}_{MAX}$ and P_{50}.

4.5. Limitations of the analysis

Firstly, as in previous work (Wagner, 1993, 1996; Cano *et al.*, 2013), the entire analysis applies to steady state conditions (meaning, that O_2 partial pressures are constant in time, as is $\dot{V}_{O_2}$ itself). Therefore, the analyses should not be extrapolated to transient changes in metabolic rate at the beginning or end of exercise. Additional limitations are that for this modeling approach to apply with accuracy, parameters defining the in vivo mitochondrial respiration curve (again, $\dot{V}_{MAX}$ and P_{50}) are required. While the degree of $\dot{V}_A/\dot{Q}$ heterogeneity in the lungs of individual subjects or patients has been measurable for many years, that in the muscle is not directly accessible by any yet published method. Thus, for the present paper, the estimates used are uncertain, and the quantitative outcomes should not be generalized - they are specific to the particular input variables we used. That is why we elected to run simulations over a range of the most uncertain variables. That said, given that the principal objective of our study was to present the development of an O_2 transport model that encompasses heterogeneity in both lungs and muscle, it seems reasonable to illustrate its prediction capabilities, even if estimates of some input variables are uncertain. With the algorithm now developed, running the simulations with accurate data when available will easily be possible. The quantitative results presented thus show the impact of heterogeneity for the specific cases simulated.

5. Conclusions

The current research includes consideration of functional heterogeneities (lung and muscle), as well as the O_2 consumed by non-exercising tissues, in a previously established integrative O_2 pathway model. It allows application of the modeling approach to patients with chronic diseases such as COPD, and reveals the interplay among lung $\dot{V}_A/\dot{Q}$ heterogeneity and skeletal muscle mismatching on VO_2max. Moreover, skeletal muscle $\dot{V}_{MAX}/\dot{Q}$ ratio inequality creates regions with either very high or very low intracellular PO_2 values with potentially multiple biological consequences, some potentially beneficial and some possibly harmful.

Competing interests

No competing interests.

Author contributions

I. Cano, J. Roca and PD Wagner made substantial contributions to conception and design, and/or acquisition of data, and/or analysis and interpretation of data; I. Cano and PD Wagner constructed, tested and run the algorithms used in the model; I. Cano, J. Roca and PD Wagner participated in drafting the article and revising it critically for important intellectual content and gave final approval of the version to be submitted and any revised version.

Funding

This research has been carried out under the Synergy-COPD research grant, funded by the Seventh Framework Program of the European Commission as a Collaborative Project with contract no.: 270086 (2011–2014), and NIH P01 HL091830.

Tables

TABLE I – Input parameters for the modeling of the oxygen transport system in health at sea level and altitude

Altitude (ft.)	*Barometric pressure (PB), Torr*	*Body temperature (T), ℃*	*Hemoglobin concentration ($[Hb]$), g·dl^{-1}*	*Alveolar ventilation ($\dot{V}$), BTPS, L·min^{-1}*	*Blood flow ($\dot{Q}$), L·min^{-1}*	*Total Lung O_2 diffusing capacity (DL), ml·min^{-1}·Torr^{-1}*	*Total muscle O_2 diffusing capacity (DM), ml·min^{-1}·Torr^{-1}*
0	760	38	14,2	128,3	25,0	50,9	104,6
5000	639	38	14,9	137,1	23,5	60,9	97,1
10000	534	38	15,5	145,9	22,0	70,9	89,6
15000	442	38	16,2	154,6	20,5	80,9	82,1
16000	426	37,9	16,3	156,4	20,2	82,9	80,6
17000	410	37,8	16,5	158,1	19,9	84,9	79,1
18000	394	37,7	16,6	159,9	19,6	86,9	77,6
19000	380	37,6	16,7	161,6	19,3	88,9	76,1
20000	365	37,5	16,9	163,4	19,0	90,9	74,6
21000	351	37,4	17,0	165,2	18,7	92,9	73,1
22000	337	37,3	17,1	166,9	18,4	94,9	71,6
23000	324	37,2	17,2	168,7	18,1	96,9	70,1
24000	311	37,1	17,4	170,4	17,8	98,9	68,6
25000	299	37	17,5	172,2	17,5	100,9	67,1
26000	286	37	17,6	173,9	17,2	102,9	65,6
27000	275	37	17,8	175,7	16,9	104,9	64,1
28000	264	37	17,9	177,4	16,6	106,9	62,6
29000	253	37	18,0	179,2	16,3	108,9	61,1
30000	243	37	18,2	181,0	16,0	110,9	59,6

TABLE II – Input parameters for the modeling of the oxygen transport system in disease (moderate and severe COPD)

Parameter	Moderately limited transport	Severely limited transport
Forced Expired Volume in the 1st second (FEV_1), % predicted post-bronchodilator	66	23
Forced Vital Capacity (FVC), % predicted post-bronchodilator	84	33
FEV_1/FVC	0.60	0.54
Log SD $\dot{Q}$	0.67	0.86
Barometric pressure (PB), Torr	758	765
Fractional Inspired Oxygen (FI_{O_2})	0.2093	0.2093
Hemoglobin concentration ($[Hb]$), g·dl^{-1}	14.4	12.5
Body temperature (T), °C	37.0	36.8
O_2 dissociation curve P_{50} , Torr	26.8	26.8
Resting ventilation ($\dot{V}$), BTPS, L·min^{-1}	7.11	7.44
Resting cardiac output ($\dot{Q}$), L·min^{-1}	3.68	3.20
Resting $\dot{V}O_2$, ml·min^{-1}	235	159
Resting $\dot{V}CO_2$, ml·min^{-1}	174	103
Resting arterial P_{O_2} ($P_{a_{O_2}}$), mm Hg	80	59
Resting arterial P_{CO_2} ($P_{a_{CO_2}}$), mm Hg	35	46
Resting lactate, mmol·L^{-1}	1.47	0.81
Exercise ventilation ($\dot{V}$), BTPS, L·min^{-1}	35.3	8.2
Exercise cardiac output ($\dot{Q}$), L·min^{-1}	7.75	3.98
Exercise $\dot{V}O_2$, ml·min^{-1}	914	355
Exercise arterial P_{O_2} ($P_{a_{O_2}}$), mm Hg	90	59
Exercise arterial P_{CO_2} ($P_{a_{CO_2}}$), mm Hg	31	49
Exercise Lung O_2 diffusing capacity (DL), ml·min^{-1}·Torr^{-1}	100	11
Exercise muscle O_2 diffusing capacity (DM), ml·min^{-1}·Torr^{-1}	26	9
Exercise lactate, mmol·L^{-1}	3.55	2.03

Figures and legends

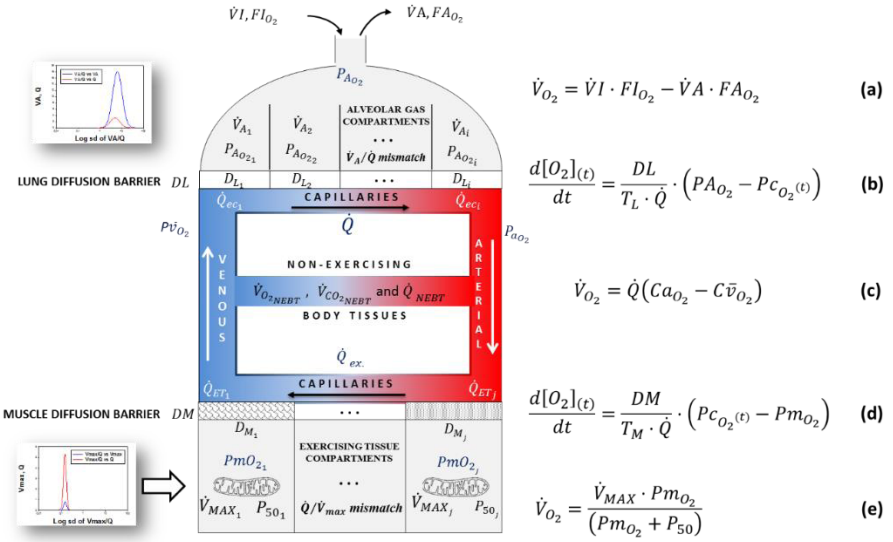

Figure 1: Schematic representation of the oxygen transport and utilization system and the five associated mass conservation equations governing O_2 transport (Eqs. (a)-(d)) and utilization (Eq. (e)).

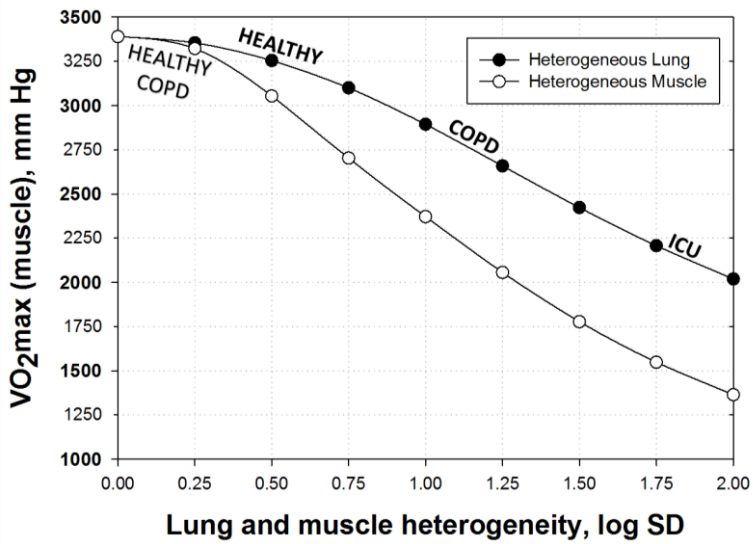

Figure 2: Independent effects of lung $\dot{V}_A/\dot{Q}$ heterogeneity (solid circles) and muscle $\dot{V}_{MAX}/\dot{Q}$ heterogeneity (empty circles) on maximal muscle oxygen uptake ($\dot{V}_{O_2}$max), using input data defining O_2 transport conductances (i.e., ventilation, cardiac output, lung and muscle diffusional conductances, etc.) from normal subjects exercising maximally at sea level in Operation Everest II (Sutton et al., 1988). Healthy subjects show pulmonary log SD $\dot{Q}$ between 0.3 and 0.6 (Wagner *et al.*, 1974), whereas skeletal muscle heterogeneity (log SD $\dot{V}_{MAX}$) presents an average value of 0.10 (Vogiatzis et al, J. Applied Physiol, under review). In patients with moderate to severe COPD, log SD $\dot{Q}$ can present values close to 1.0, but no published data on log SD $\dot{V}_{MAX}$ are available. However, recent studies in patients with COPD (Louvaris et al, in preparation) suggest similar degrees of muscle heterogeneity as in health. Finally, critically ill patients admitted in the Intensive Care Unit (ICU) may show lung heterogeneity values close to 2.0. Again, no information on log SD $\dot{V}_{MAX}$ is available.

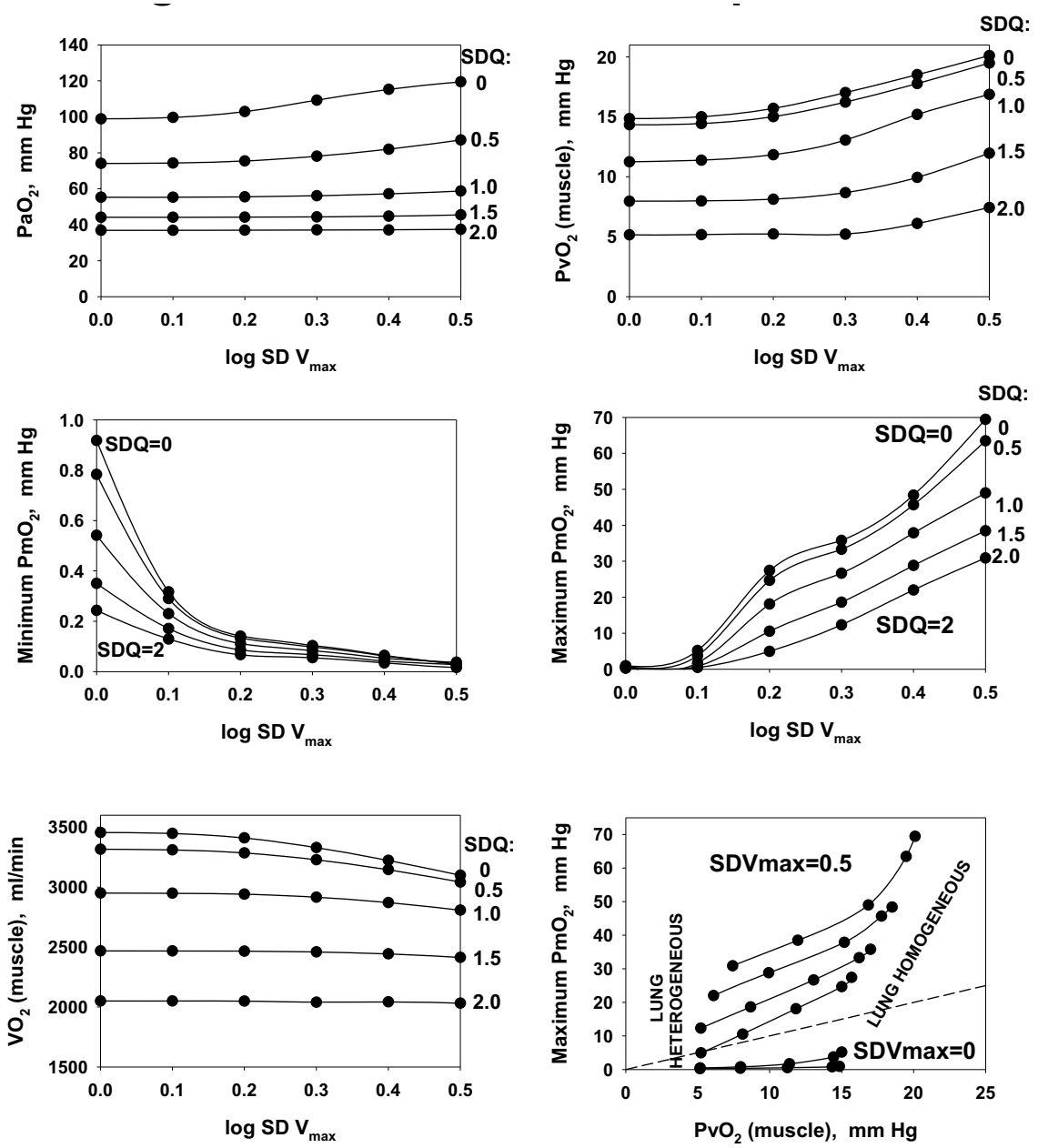

Figure 3: Combined and separated effects of lung and exercising muscle heterogeneities on the O_2 transport pathway: on arterial blood (upper-left panel), venous blood (upper-right panel) and mitochondria (two central panels), maximal muscle oxygen uptake (lower-left panel), and, maximum degree of oxygen unbalance between mitochondrial P_{O_2} of muscle compartments and mean effluent venous ($P_{v_{O_2}}$) oxygen levels (lower-right panel). See text for details.

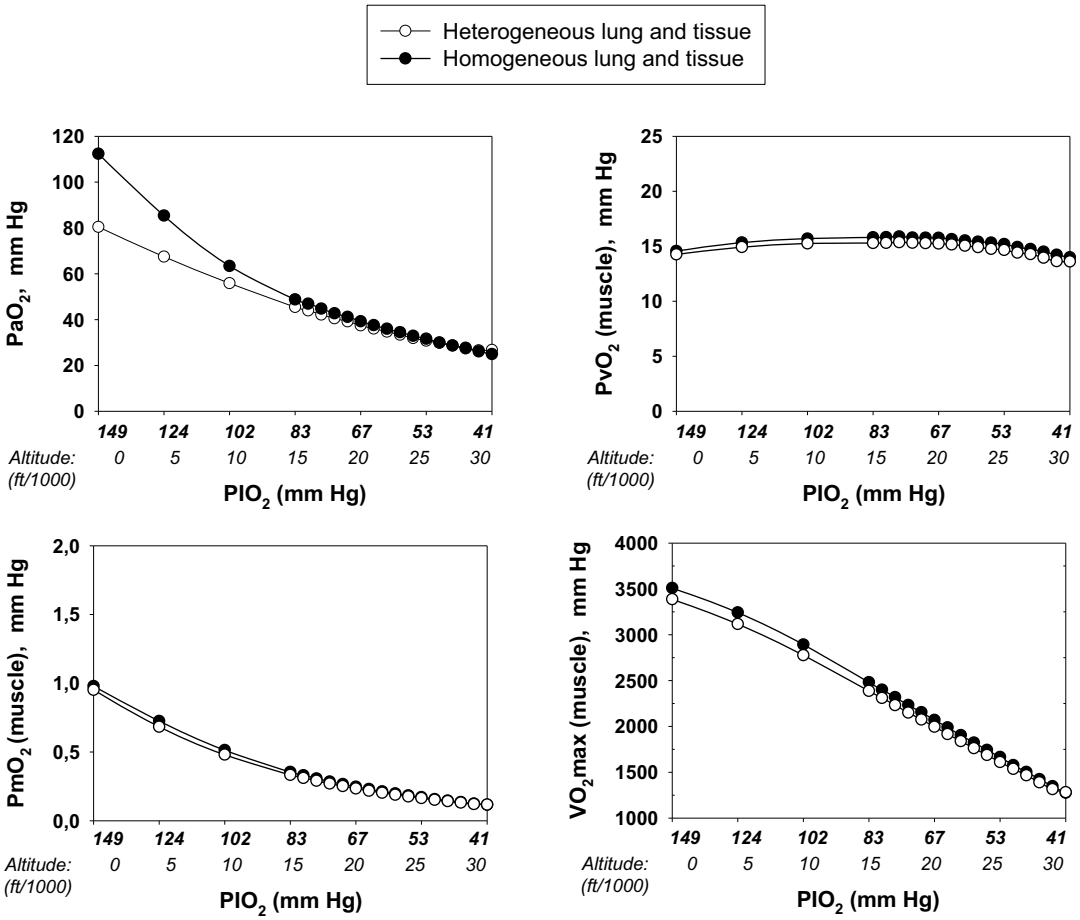

Figure 4: Effects of functional inhomogeneity on arterial P_{O_2} (upper left panel), venous P_{O_2} (upper right panel), mitochondrial P_{O_2} (lower left panel) and $\dot{V}_{O_2}$ (lower right panel) at sea level and altitude. Functional inhomogeneity is expressed as the combined effects of lung ventilation-perfusion inequalities and skeletal muscle perfusion-metabolism mismatching. Mitochondrial respiration parameters were fixed to a $\dot{V}_{MAX}$ of 4,584 ml/min and a P_{50} of 0.3 mm Hg. Filled circles correspond to simulations outputs when considering both homogeneous lung and tissues. Empty circles represent simulation outputs when using reasonable estimates for lung ventilation-perfusion (log SD $\dot{Q}$ of 0.5), tissue perfusion-metabolism (log SD $\dot{V}_{MAX}$ of 0.1), and the metabolic rate of non-exercising tissues (with an assigned $\dot{V}_{O_2}$ of 300 ml/min, a $\dot{V}_{CO_2}$ of 240 ml/min) and assuming that 20% of total blood flow goes to non-exercising tissues. See text for details.

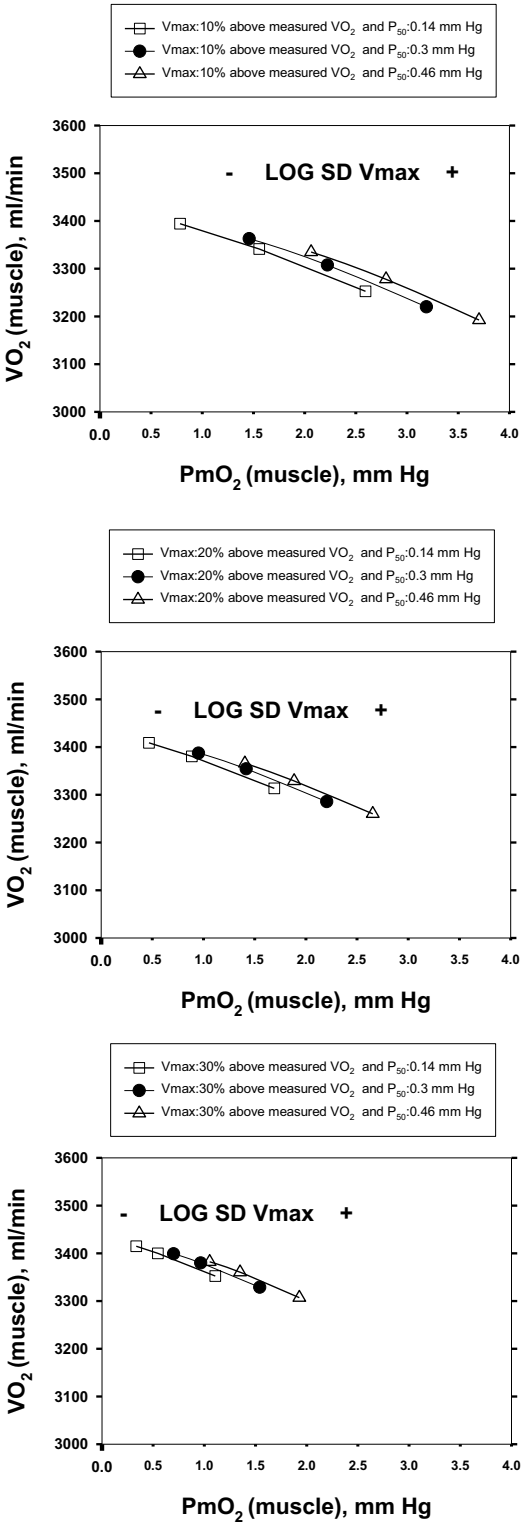

Figure 5: Effects of muscle bioenergetics (mitochondrial respiration $\dot{V}_{MAX}$ and P_{50} parameters) and muscle peripheral heterogeneities on muscle $\dot{V}_{O_2}$ and mitochondrial P_{O_2} ($P_{m_{O_2}}$) in health at sea level. $\dot{V}_{MAX}$ is taken as 10% (upper panels), 20% (middle panels) and 30% (lower panels) greater than measured $\dot{V}_{O_2}$ max. For each $\dot{V}_{MAX}$, three mitochondrial P_{50} values (0.14, 0.3 and 0.46 mm Hg) and three degrees (0.1, 0.2 and 0.3) of muscle perfusion-metabolism inhomogeneity ($\log SD\ \dot{V}_{MAX}$) were evaluated. See text for details.

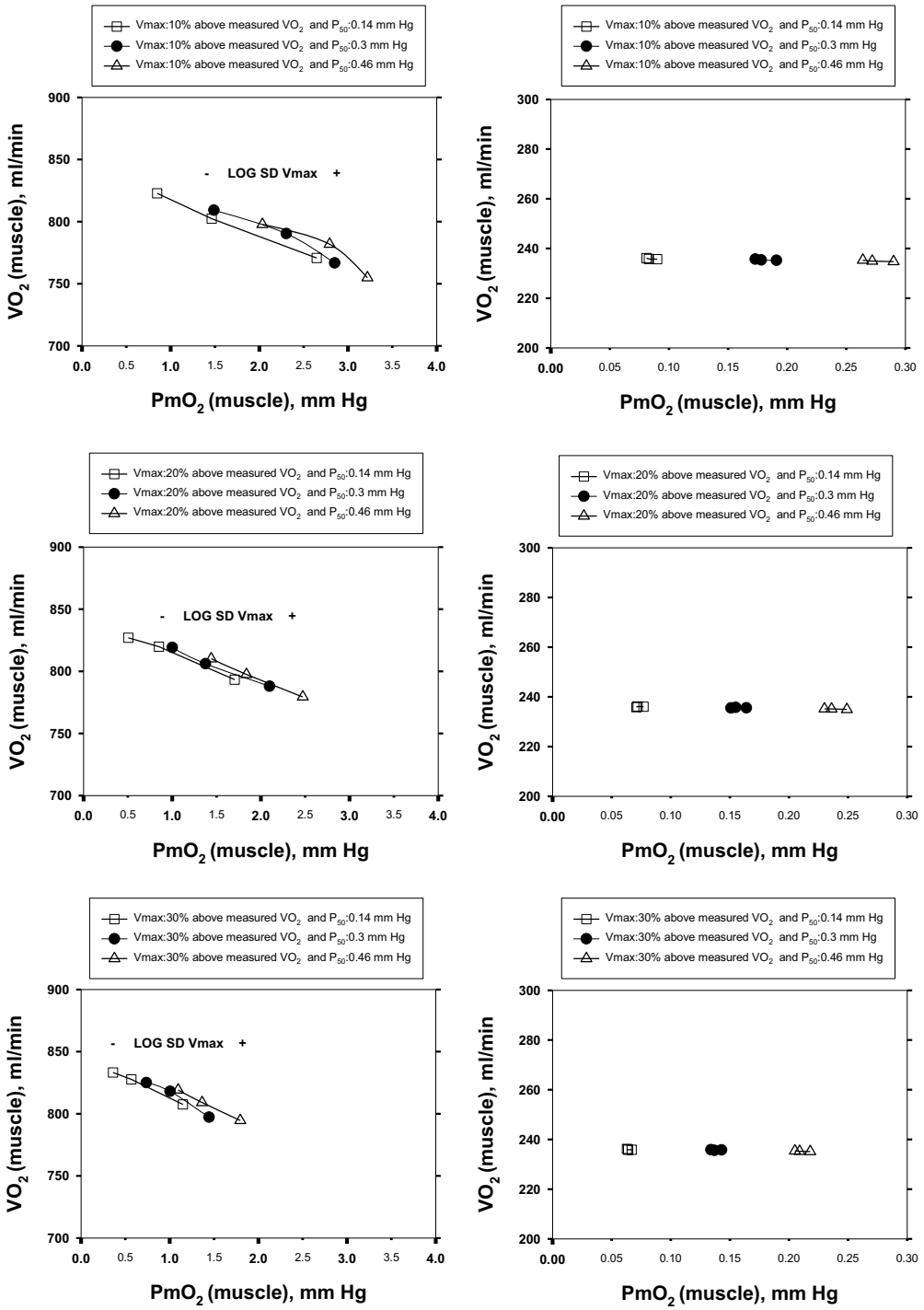

Figure 6: Effects of muscle bioenergetics (mitochondrial respiration $\dot{V}_{MAX}$ and P_{50} parameters) and muscle peripheral heterogeneities on muscle $\dot{V}_{O_2}$ and mitochondrial P_{O_2} ($P_{m_{O_2}}$) for given representatives of mild (left-side panels) and severe (left-side panels) limitation of O_2 transport conditions in chronic obstructive pulmonary disease (COPD). $\dot{V}_{MAX}$ is taken as 10% (upper panels), 20% (middle panels) and 30% (lower panels) greater than measured $\dot{V}_{O_2}$max in the two COPD patients exercising maximally, selected as representatives of both mild and severe O_2 transport conditions. For each $\dot{V}_{MAX}$, three mitochondrial P_{50} values (0.14, 0.3 and 0.46 mm Hg) and three degrees (0.1, 0.2 and 0.3) of muscle perfusion-metabolism inhomogeneity (log SD $\dot{V}_{MAX}$) were evaluated. See text for details.

References

Blanco I, Gimeno E, Munoz PA, Pizarro S, Gistau C, Rodriguez-Roisin R, Roca J & Barberà JA. (2010). Hemodynamic and Gas Exchange Effects of Sildenafil in Patients with Chronic Obstructive Pulmonary Disease and Pulmonary Hypertension. *American journal of respiratory and critical care medicine* **181,** 270-278.

Cano I, Mickael M, Gomez-Cabrero D, Tegnér J, Roca J & Wagner PD. (2013). Importance of mitochondrial in maximal O2 transport and utilization: A theoretical analysis. *Respiratory Physiology & Neurobiology* **189,** 477-483.

Gnaiger E, Lassnig B, Kuznetsov A, Rieger G & Margreiter R. (1998). Mitochondrial oxygen affinity, respiratory flux control and excess capacity of cytochrome c oxidase. *J Exp Biol* **201,** 1129-1139.

Hammond MD & Hempleman SC. (1987). Oxygen diffusing capacity estimates derived from measured VA/Q distributions in man. *Respiration physiology* **69,** 129-147.

Knight DR, Poole DC, Schaffartzik W, Guy HJ, Prediletto R, Hogan MC & Wagner PD. (1992). Relationship between body and leg VO2 during maximal cycle ergometry. *Journal of applied physiology (Bethesda, Md : 1985)* **73,** 1114-1121.

Mik EG. (2013). Measuring Mitochondrial Oxygen Tension: From Basic Principles to Application in Humans. *Anesthesia and analgesia* **117,** 834-846.

Resar JR, Roguin A, Voner J, Nasir K, Hennebry TA, Miller JM, Ingersoll R, Kasch LM & Semenza GL. (2005). Hypoxia-inducible factor 1alpha polymorphism and coronary collaterals in patients with ischemic heart disease. *Chest* **128,** 787-791.

Richardson RS, Haseler LJ, Nygren AT, Bluml S & Frank LR. (2001). Local perfusion and metabolic demand during exercise: a noninvasive MRI method of assessment. *Journal of applied physiology (Bethesda, Md : 1985)* **91,** 1845-1853.

Richardson RS, Leek BT, Gavin TP, Haseler LJ, Mudaliar SRD, Henry R, Mathieu-Costello O & Wagner PD. (2004). Reduced Mechanical Efficiency in Chronic Obstructive Pulmonary Disease but Normal Peak V̇o2 with Small Muscle Mass Exercise. *American journal of respiratory and critical care medicine* **169,** 89-96.

Rowell LB. (1986). *Cardiovascular Adjustments to Hypoxemia. In Human circulation: regulation during physical stress*. Oxford University Press.

Scandurra FM & Gnaiger E. (2010). Cell respiration under hypoxia: facts and artefacts in mitochondrial oxygen kinetics. *Adv Exp Med Biol* **662,** 7-25.

Selivanov VA, Cascante M, Friedman M, Schumaker MF, Trucco M & Votyakova TV. (2012). Multistationary and oscillatory modes of free radicals generation by the mitochondrial respiratory chain revealed by a bifurcation analysis. *PLoS Comput Biol* **8,** e1002700.

Semenza GL. (2011). Oxygen Sensing, Homeostasis, and Disease. *New England Journal of Medicine* **365,** 537-547.

Sutton JR, Reeves JT, Wagner PD, Groves BM, Cymerman A, Malconian MK, Rock PB, Young PM, Walter SD & Houston CS. (1988). Operation Everest II: oxygen transport during exercise at extreme simulated altitude. *J Appl Physiol* **64,** 1309-1321.

Wagner PD. (1993). Algebraic analysis of the determinants of VO2max. *Respiration physiology* **93,** 221-237.

Wagner PD. (1996). A theoretical analysis of factors determining VO2 MAX at sea level and altitude. *Respiration physiology* **106,** 329-343.

Wagner PD. (2008). The multiple inert gas elimination technique (MIGET). *Intensive Care Med* **34,** 994-1001.

Wagner PD, Hedenstierna G & Bylin G. (1987a). Ventilation-perfusion inequality in chronic asthma. *The American review of respiratory disease* **136,** 605-612.

Wagner PD, Laravuso RB, Uhl RR & West JB. (1974). Continuous distributions of ventilation-perfusion ratios in normal subjects breathing air and 100 per cent O2. *The Journal of clinical investigation* **54,** 54-68.

Wagner PD, Sutton JR, Reeves JT, Cymerman A, Groves BM & Malconian MK. (1987b). Operation Everest II: pulmonary gas exchange during a simulated ascent of Mt. Everest. *Journal of applied physiology (Bethesda, Md : 1985)* **63,** 2348-2359.

Welch HG. (1982). Hyperoxia and human performance: a brief review. *Medicine and science in sports and exercise* **14,** 253-262.

West JB. (1969). Ventilation-perfusion inequality and overall gas exchange in computer models of the lung. *Respiration physiology* **7,** 88-110.

Wilson DF, Erecinska M, Drown C & Silver IA. (1977). Effect of oxygen tension on cellular energetics. *American Journal of Physiology - Cell Physiology* **233,** C135-C140.

Manuscript 3:

Oxygen pathway modeling estimates high reactive oxygen species production above the highest permanent human habitation.

Cano I, Selivanov V, Gomez-Cabrero D, Tegnér J, Roca J, Wagner PD, M. Cascante.

Submitted to PLoS One, 2014.

Oxygen pathway modeling estimates high reactive oxygen species production above the highest permanent human habitation

I. Cano [1], V. Selivanov[2], David Gomez-Cabrero[3], Jesper Tegnér[3], J. Roca[1], P. D. Wagner[4], M. Cascante[2,*]

[1]Hospital Clinic, IDIBAPS, CIBERES, Universitat de Barcelona, Barcelona, Catalunya, Spain.

[2]Departament de Bioquimica i Biologia Molecular, Facultat de Biologia, Universitat de Barcelona, and IBUB, Barcelona, Spain.

[3]Unit of Computational Medicine, Department of Medicine, Center for Molecular Medicine, Karolinska Institutet, Karoliska University Hospital, Sweden.

[4]Division of Physiology, Pulmonary and Critical Care Medicine, University of California, San Diego, La Jolla, California

ABSTRACT

The production of reactive oxygen species (ROS) from the inner mitochondrial membrane is one of many fundamental processes governing the balance between health and disease. It is well known that ROS are necessary signaling molecules in gene expression, yet when expressed at high levels, ROS may cause oxidative stress and cell damage. Both hypoxia and hyperoxia may alter ROS production by changing mitochondrial P_{O_2} ($P_{m_{O_2}}$). Because $P_{m_{O_2}}$ depends on the balance between O_2 transport and utilization, we formulated an integrative mathematical model of O_2 transport and utilization in skeletal muscle to predict conditions to cause abnormally high ROS generation. Simulations using data from healthy subjects during maximal exercise at sea level reveal little mitochondrial ROS production. However, altitude triggers high mitochondrial ROS production in muscle regions with high metabolic capacity but limited O_2 delivery. This altitude roughly coincides with the highest location of permanent human habitation. Above 25,000 ft., more than 90% of exercising muscle is predicted to produce abnormally high levels of ROS, corresponding to the “death zone” in mountaineering.

1. Introduction

It is well accepted that cellular hypoxia [1-4] triggers a constellation of biological responses involving transcriptional and post-transcriptional events [5, 6] through activation of cellular oxygen sensors. This includes generation of reactive oxygen species (ROS). Yet, current knowledge on the quantitative relationships between mitochondrial P_{O_2} ($P_{m_{O_2}}$), hypoxia-induced cellular events, and on the release of ROS from the inner mitochondrial membrane, is minimal. For example, how low $P_{m_{O_2}}$ must be to trigger abnormally high ROS generation has not yet been identified. Furthermore, the levels of $P_{m_{O_2}}$ at rest and during exercise are unknown, although myoglobin-associated P_{O_2} has been measured in intact excising humans [7, 8], and is reported to be 3-4 mm Hg, implying that $P_{m_{O_2}}$ is likely even lower. There are promising new approaches being developed to in vivo assessment of $P_{m_{O_2}}$ [9].

Recently, we extended a prior model describing O_2 transport from the air to the mitochondria as an integrated system limiting maximal oxygen uptake $\dot{V}_{O_2MAX}$ [10, 11] to also include the contribution to overall impedance to O_2 flow from the above-zero $P_{m_{O_2}}$ required to drive mitochondrial respiration [12]. This was accomplished by including an equation for the hyperbolic relationship between mitochondrial $P_{O_2}$and mitochondrial $\dot{V}_{O_2}$ as shown by Wilson et al. [13] and confirmed more recently by Gnaiger's group [14, 15]. This has enabled the prediction of $P_{m_{O_2}}$ as a balance between the capacities for muscle O_2 transport and utilization [12, 16]. In addition, we have expanded this model by now allowing for functional heterogeneity in both lungs and muscle [16], which had previously (and reasonably) been taken to be negligible in health. This was done to enable application to disease states. Since mitochondrial ROS generation is affected by cellular oxygenation, this integrative model may afford the opportunity for better understanding the quantitative relationship between O_2 transport, mitochondrial respiration and ROS generation, provided we have an understanding of the relationship between $P_{m_{O_2}}$ and ROS formation.

Recent modeling and experimental studies on mitochondrial ROS production under hypoxia and re-oxygenation [17-19] have proposed an inherent bi-stability of Complex III, i.e. coexistence of two different steady states at the same external conditions: one state corresponding to low ROS production, and a second potentially dangerous state with high ROS production. Temporary deprivation of oxygen could switch the system from low to high ROS production, thus explaining the damaging effects of hypoxia-re-oxygenation. This recently proposed model provides a

conceptual basis for the abnormally high ROS production observed both in hyperoxia [20, 21] and hypoxia [1-4] and has the ability to predict the quantitative relationship between ROS generation and $P_{m_{O_2}}$.

In this paper, we build upon these previous but separate models of O_2 transport as a physiological system and mitochondrial metabolism as a biochemical system, and have linked them through their common variables, $P_{m_{O_2}}$ and $\dot{V}_{O_2}$, establishing one integrated model to predict $P_{m_{O_2}}$ and mitochondrial ROS production. Specifically, we integrate the physiological model of the oxygen pathway predicting $P_{m_{O_2}}$ from the balance between O_2 transport and mitochondrial O_2 utilization [10-12, 16] with the model of electron and proton transport in the mitochondrial respiratory chain, and the ROS production associated with this transport [17-19], thereby predicting the rate of ROS production as a function of $P_{m_{O_2}}$ and $\dot{V}_{O_2}$. The former model is referred to below as the O_2 pathway model, and the latter as the mitochondrial ROS prediction model.

In addition to describing the integrated modeling system, we present estimates of ROS generation in exercising muscle of healthy subjects at different altitudes at and above sea level using O_2 transport data from Operation Everest II [22] and published mitochondrial kinetic data in normal human muscle (discussed in [17]). We found that at sea level, O_2 transport at maximal exercise is sufficient to keep $P_{m_{O_2}}$ high enough that mitochondrial ROS generation is not significantly increased. However, exercise at high altitude is predicted to significantly increasing ROS generation, agreeing with experimental data collected under these conditions [23-25].

2. Materials and methods

2.1. Oxygen pathway model

The modeling of O_2 transport and utilization [10-12] adopted in the current article relies on the concept that maximal mitochondrial O_2 availability is governed by the integrated behavior of all steps of the O_2 transport and utilization system rather than being dominated by any one step. Building on the work of DeJours [43], and Weibel et al [44], it was previously shown [10, 11] how each step (ventilation, diffusion across the alveolar wall, circulation, diffusion from the muscle capillaries to the mitochondria, and finally, oxidative phosphorylation itself) contributes quantitatively to the limits to maximum O_2 uptake ($\dot{V}_{O_2MAX}$). The model is based on the principle of mass conservation at every step, and uses the well-known mass conservation equations for each step as laid out by Weibel et al [45]. Given the oxygen transport properties of the lungs, heart, blood and muscles, and incorporating the (hyperbolic) mitochondrial respiration curve

that relates mitochondrial $\dot{V}_{O_2}$ to mitochondrial P_{O_2} [13-15] the model computes how much O_2 can be supplied to the tissues ($\dot{V}_{O_2}$), and the partial pressures of oxygen at each step (i.e. alveolar ($P_{A_{O_2}}$), arterial ($P_{a_{O_2}}$), venous ($P_{v_{O_2}}$), and mitochondrial ($P_{m_{O_2}}$)). This construct [12] leads to a system of five equations, each describing mass conservation equations governing O_2 transport (Eqs. (1) - (4)) and utilization (Eq. (5)), with the five unknowns also mentioned above.

$$\dot{V}_{O_2} = \dot{V}I \cdot FI_{O_2} - \dot{V}A \cdot FA_{O_2} \quad (1)$$

$$\dot{V}_{O_2} = \dot{V}I \cdot FI_{O_2} - \dot{V}A \cdot FA_{O_2} \quad (2)$$

$$\dot{V}_{O_2} = \dot{Q}\left(Ca_{O_2} - C\bar{v}_{O_2}\right) \quad (3)$$

$$\frac{d[O_2]_{(t)}}{dt} = \frac{DM}{T_M \cdot \dot{Q}} \cdot \left(Pc_{O_2(t)} - Pm_{O_2}\right) \quad (4)$$

$$\dot{V}_{O_2} = \frac{\dot{V}_{MAX} \cdot Pm_{O_2}}{\left(Pm_{O_2} + P_{50}\right)} \quad (5)$$

However, this system ignores heterogeneity of ventilation/perfusion ($\dot{V}_A/\dot{Q}$) ratios in the lung, and heterogeneity of metabolism/perfusion ($\dot{V}_{O_2}/\dot{Q}$) ratios in the muscle. This is laid out in detail in [16], and in the current article, consideration of typical, normal degrees of lung and muscle heterogeneity has been incorporated. The original 5-equation model [12] also failed to take into account that not all of the cardiac output flows to the exercising muscles. Allowance for blood flow to, and O_2 utilization by, non-exercising tissues has accordingly also now been incorporated into the system described in [16] and is used here.

2.2. Parameters of the O2 pathway model

The most complete data set with respect to O_2 pathway conductances during exercise at altitude (ventilation ($\dot{V}A$), cardiac output ($\dot{Q}$), lung (DL) and muscle (DM) diffusional conducances, [Hb]) comes from Operation Everest II [22], but even here, measurements were made only at sea level, and at barometric pressures equivalent to four specific altitudes of 15,000 ft., 20,000 ft., 25,000 ft. and 29,000 ft. Because we wished to simulate the entire altitude domain from sea level to the Everest summit, we used the Operation Everest II data to interpolate parameter values at intervening altitudes. Additional input parameters are required for the analysis. These include: a) maximal muscle mitochondrial metabolic capacity ($\dot{V}_{max}$), b) mitochondrial P_{50} i.e., the P_{O_2} at which mitochondrial respiration is half-maximal, c) dispersion of ventilation/perfusion

ratios in normal lungs, d) dispersion of metabolism/perfusion ratios in muscle, and e) an estimate of total blood flow to non-exercising tissues and their corresponding $\dot{V}_{O_2}$.

For $\dot{V}_{max}$, we chose a value 20% higher than the observed sea level maximal $\dot{V}_{O_2}$ in the Operation Everest II subjects, and this came to 4.58 L/min. The justification is that in healthy fit subjects, $\dot{V}_{O_2}$max is O_2 supply-limited at sea level, since it increases when 100% O_2 is breathed [46, 47]. This demonstrates that mitochondrial metabolic capacity is clearly greater than sea level $\dot{V}_{O_2}$max. For mitochondrial P_{50}, a value of 0.14 mm Hg was chosen. This is the mitochondrial P_{50} value used in the ROS prediction model described below [17-19], and is close to reported values measured in vitro [14, 15]. A representative normal level of ventilation/perfusion heterogeneity (i.e., log SD $\dot{Q}$ = 0.5) was used, since normal subjects display log SD $\dot{Q}$ values of between 0.3 and 0.6 [26], increasing slightly with exercise. Log SD $\dot{Q}$ is the second moment (dispersion) of the perfusion distribution on a logarithmic scale and has been used to quantify $\dot{V}_A/\dot{Q}$ heterogeneity for about 40 years [48-50]. For $\dot{V}_{O_2}/\dot{Q}$ heterogeneity in muscle, there is very limited information. From a new technique based on near-infrared spectroscopy and currently in development, the corresponding dispersion in muscle appears to be about 0.1 (Vogiatzis et al, J. Applied Physiol, under review), and this was used.

Finally, to allow for non-exercising tissue perfusion and metabolism we used typical normal resting values of cardiac output and $\dot{V}_{O_2}$ (specifically, non-exercising total tissue blood flow equal to 20% of maximal sea level cardiac output, and $\dot{V}_{O_2}$ of 300 ml/min).

2.3. Mitochondrial ROS prediction model

The mitochondrial ROS prediction model [17-19] considered in this study accounts for: i) Respiratory complex I that oxidizes NADH and reduces ubiquinone (Q), translocating H+; ii) Respiratory complex II that also reduces Q, oxidizing succinate to fumarate; iii) Respiratory complex III, the net outcome of which is to oxidize ubiquinol, reducing cytochrome c and translocating H+; iv) Respiratory complex IV that oxidizes cytochrome c, reducing molecular oxygen to H_2O and translocating H+; and, v) The H+ gradient utilization for ATP synthesis in respiratory complex V. NADH consumed by complex I is produced in the several reactions of the TCA cycle leading from pyruvate to succinate, and from fumarate to oxaloacetate.

This model consists of a large system of ordinary differential equations that simulate the processes mentioned above based on the general principle of the law of mass action. Simulating the redox (from reduced/oxidized) reactions between the electron carriers constituting complexes I and III, the model takes into account that the carriers occupy fixed positions and have fixed interactions in the space of a respiratory complex. The variables of this model are the

concentrations of redox states of the complex. Each redox state of the complex is a combination of redox states of the electron carriers constituting it. Since a carrier can be in one of the two redox states (reduced or oxidized), the number of variables is 2n, where n is the number of electron carriers fixed in the space of the complex. The model accounts also various forms of the complexes created by binding/dissociation of ubiquinone/ubiquinol. The other respiratory complexes are accounted for in a simplified form, assuming that the electrons that leave complex III ultimately reduce oxygen. Such a reaction is taken to be a hyperbolic function of oxygen concentration and proportional to the concentrations of forms able to donate an electron.

The mechanism of electron transport includes steps where highly active free radicals are formed. These radicals are capable of passing their unpaired high-energy electron directly to oxygen, thus producing superoxide anion radical and then the whole family of ROS such as OH radical and peroxides. The system of equations that constitutes this model is described in [17-19]. Parameter values for the respiratory chain used here were obtained from experimental studies [17] of normal mitochondrial function. The model calculates the levels of free radicals of the electron carriers constituting the respiratory chain (such as semiquinone radical). These radicals, normally formed in the process of electron transport, are responsible for ROS production. These levels are presented here as indicators of ROS production rate.

Overall, the mitochondrial ROS generation model produces two distinct patterns of response to $\mathrm{P_{m_{O_2}}}$ at maximum exercise, as displayed in **Figure 1**. One pattern (HR) reflects above normal high ROS generation and the other (LR) reflects little or normal ROS generation. Briefly, the figure shows the rate of mitochondrial ROS production expressed as concentration of semiquinone radicals (nmol/mg) at Qo site (ubiquinone binding site to complex III at the outer side of the inner mitochondrial membrane) of mitochondrial complex III (y-axis) against time (x-axis) for four different values of $\mathrm{P_{m_{O_2}}}$, indicated in **Figure 1**.

Note that here, $\mathrm{P_{m_{O_2}}}$ is expressed not as absolute values but as multiples of mitochondrial P_{50} (in this case from $0.2 * \mathrm{P_{50}}$ to $10.0 * \mathrm{P_{50}}$). For pattern LR, there is essentially no change in ROS generation, and this corresponds to the two $\mathrm{P_{m_{O_2}}}$ values exceeding the $\mathrm{P_{50}}$ in **Figure 1**. Pattern HR is seen in the two examples where $\mathrm{P_{m_{O_2}}}$ is less than $\mathrm{P_{50}}$, and here a large, almost 10-fold increase in ROS generation occurs. In fact, the switch occurs abruptly when $\mathrm{P_{m_{O_2}}} \sim 2/3 * \mathrm{P_{50}}$. The high sensitivity of mitochondrial ROS production to restrictions of oxygen transport, and thus to low $\mathrm{P_{m_{O_2}}}$, is a consequence of multistationarity, the mechanisms of which are considered in detail in previous publications [17, 18]. Finally, the increase in ROS generation persists after

cessation of exercise, and the lower the $P_{m_{O_2}}$, the longer the persistence time, also shown in **Figure 1**.

The non-linear bi-stability inherent to mitochondrial ROS prediction model [17-19] accounts for the abrupt change of mitochondrial ROS production rate with a change of external (with respect to the respiratory chain) conditions. In principle such a change can be irreversible (in accordance with the phenomenon of bistability investigated in [17-19]), but in the considered case it reverses with a delay. The delay results from slow oxidation of ubiquinol to ubiquinone, which is necessary to activate the Q-cycle in respiratory complex III. The use of $P_{m_{O_2}}$ normalized to P_{50} here reflects the fact that while the model predicts different ROS generation rates at different $P_{m_{O_2}}$ values for a given mitochondrial respiration curve of any particular P_{50}, when $P_{m_{O_2}}$ is the same fraction of P_{50}, ROS generation is the same even if absolute $P_{m_{O_2}}$ and P_{50} are different. For example, if $P_{m_{O_2}} = 0.1$ and $P_{50} = 0.2$, ROS generation would be the same as that computed when $P_{m_{O_2}} = 0.2$ and $P_{50} = 0.4$, because in both cases, $P_{m_{O_2}} / P_{50}$ is the same $(= 0.5)$. This is illustrated in **Figure 2**, panels 1 and 2. In Panel 1, two mitochondrial respiration curves are drawn with the above different absolute P_{50} values (but the same $\dot{V}_{max}$ values). Using the above $P_{m_{O_2}}$ values, $\dot{V}_{O_2}$ in both cases would be the same at $1/3 * \dot{V}_{max}$, shown by the solid circles. Panel 2 replots these data normalizing the x-axis by P_{50} for each case, and normalizing the y-axis by $\dot{V}_{max}$ in each case.

These normalized respiration curves now overlie one another, and the important point is that the relative $P_{m_{O_2}}$ values in the two cases are identical and the relative $\dot{V}_{max}$ values are also identical, as will be ROS generation by the two regions. In a similar fashion, it is important to recognize that different muscle tissue regions may have different numbers of mitochondria and thus different $\dot{V}_{max}$ values even if P_{50} were uniform across regions. The normalization of $\dot{V}_{O_2}$ to $\dot{V}_{max}$ is thus necessary in order to compare different regions. For example, if $\dot{V}_{O_2}$ were the same at 0.2 units in two regions (and P_{50} were also the same in both regions) but $\dot{V}_{max}$ were different at 0.3 and 0.6 units in these two regions (**Figure 2**, panel 3), $\dot{V}_{O_2} / \dot{V}_{max}$ in the first region would be 0.67 but only 0.50 in the second region. When the data are replotted to normalize $P_{m_{O_2}}$ (x-axis) to P_{50} 0 and $\dot{V}_{O_2}$ (y-axis) to $\dot{V}_{max}$ (**Figure 2**, panel 4), the two solid circles now separate. Thus, despite similar absolute $\dot{V}_{O_2}$ values, and the same P_{50}, the second region lies lower on the mitochondrial respiration curve than the first region.

2.4. Integration of the models

Recall that the oxygen pathway model consists of five equations, the solutions to which define the partial pressures of O_2 at each step between the air and the mitochondria as well as the mass flow of O_2 through the system ($\dot{V}_{O_2}max$). Key input variables for this model are mitochondrial $\dot{V}_{max}$ and P_{50} (along with all of the conductances of the O_2 pathway). The key output variable for linkage to the metabolic model is $\dot{V}_{O_2}max$ (as a fraction of $\dot{V}_{max}$). Thus, once the O_2 pathway model has been run for any set of input variables, the metabolic model accepts as inputs from the O_2 pathway model $\dot{V}_{O_2}max$, $\dot{V}_{max}$, and mitochondrial P_{50}, which also then defines mitochondrial P_{O_2} from the hyperbolic mitochondrial respiration curve.

After scaling these variables to harmonize the units between the two models ($\dot{V}_{O_2}$ is in ml/min in the pathway model, but in nanomoles/min/mg mitochondrial protein in the metabolic model) the metabolic model is run, simulating mitochondrial respiration, i.e. the electron flow that reduces the transported oxygen to H2O. The principal outcome of the metabolic model for the present purposes is the rate of generation of ROS at exercise conditions for the given values of $\dot{V}_{O_2}max$, $\dot{V}_{max}$, P_{50} and $P_{m_{O_2}}$.

3. Results

The main outcome of this study is allowing a quantitative analysis of how the physiological O_2 transport pathway [10-12] affects mitochondrial ROS generation in muscle [17-19]. **Figure 3** shows how maximal $\dot{V}_{O_2}$ and mitochondrial P_{O_2} in a homogeneous muscle will fall together with altitude, as computed from the O_2 pathway model.

Figure 3 also displays the degree of ROS generation as a function of mitochondrial P_{O_2} computed from the mitochondrial respiration model. As explained in [17-19], ROS generation abruptly switches from low to high levels when mitochondrial P_{O_2} reaches a critical value of $2/3$ of the P_{50} of the mitochondrial respiration curve – in **Figure 3** at about 0.1 mm Hg since P_{50} is 0.14 mm Hg. In this case, the corresponding altitude is 24,000 ft. above sea level. Thus, open circles (altitudes less than 24,000 ft.) reflect a state of low ROS generation, and closed circles (altitudes greater than 24,000 ft.) reflect a state of high ROS generation. While **Figure 3** shows the outcome for a homogeneous muscle, in reality the muscles will not be perfectly homogeneous, just as no random group of humans will all have exactly the same height or weight. The important type of heterogeneity for O_2 transport in muscle is that of the ratio of mitochondrial metabolic capacity ($\dot{V}_{max}$, reflecting ability to consume O_2) to blood flow ($\dot{Q}$, reflecting O_2 availability). Thus, with heterogeneity, some muscle regions will have lower than average $\dot{V}_{max}/\dot{Q}$ ratio, and other will have a $\dot{V}_{max}/\dot{Q}$ ratio greater than average. Data on the extent of heterogeneity in muscle are

scarce due to lack of methods for its measurement, but recent, unpublished estimates based on near-infrared spectroscopy technology (Vogiatzis et al, J. Applied Physiol, under review) suggest that a small amount of heterogeneity does exist.

When $\dot{V}_{max}/\dot{Q}$ is high (metabolic capacity high in relation to O_2 availability), mitochondrial P_{O_2} will be low, and vice versa as shown in **Figure 4** (simulated for several altitudes from sea level to 30,000 ft.). When expressed as the second moment of the $\dot{V}_{O_2}/\dot{Q}$ distribution, on a log scale, the value is about 0.1. This can be compared to the identically computed and well-established index of ventilation/perfusion ($\dot{V}_A/\dot{Q}$) inequality in the normal lung of 0.3-0.6 [26], which is generally regarded as small. **Figure 4** also shows the range of $\dot{V}_{max}/\dot{Q}$ ratios for a muscle with normal heterogeneity (i.e., dispersion of 0.1) as from about 0.15 to about 0.36, pointing out the large range of mitochondrial P_{O_2} that this seemingly small amount of heterogeneity creates. Thus, muscle regions with a high $\dot{V}_{max}/\dot{Q}$ ratio become susceptible to high ROS generation before those with lower $\dot{V}_{max}/\dot{Q}$ ratio. With the critical switch from low to high ROS production occurring at a $P_{m_{O_2}}$ of about 0.1 mm Hg, **Figure 4** shows that with normal heterogeneity, the muscle regions with highest $\dot{V}_{max}/\dot{Q}$ exhibit high ROS production already at 17,000 ft. altitude, and that at the summit of Mt. Everest (approx. 29,000 ft.), almost 100% of muscle regions will have switched to high ROS production.

Figure 5A shows the consequences of normal muscle $\dot{V}_{max}/\dot{Q}$ heterogeneity for the development of high ROS production in the format of **Figure 3.** The important points are: i) that due to the presence of high $\dot{V}_{max}/\dot{Q}$ regions, high ROS generation is seen (in those regions) already at 17,000 ft., a much lower altitude than for the homogeneous system (24,000 ft.), and ii) that high ROS generation becomes more extensive with further increases in altitude. **Figure 5B** shows the percentage of muscle predicted to have high ROS production over the altitude range from sea level to the Everest summit.

4. Discussion

The results displayed in **Figures 3-5** are specific to the input data used (Tables I and II in the supplementary on-line material). While they take advantage of the most complete data set available on humans exercising over a range in altitude from sea level to the equivalent of the Everest summit, the quantitative outcomes presented in this article would be different if a different data set were used. This should be kept in mind when interpreting the results presented. In addition, some specific, important data are both scarce in the literature and uncertain. The most important of these are the mitochondrial respiration curve characteristics (here defined by two parameters, $\dot{V}_{max}$ and P_{50}), and the extent of heterogeneity in the

distribution of blood flow to muscle regions with different metabolic capacity. However, while the particular results we report depend on the values we took for these functions, the important point is that the integrated model approach coupling physiological elements of O_2 transport with biochemical elements of oxidative phosphorylation stands, no matter what specific data are used to run it. A graphical user interface to parameterize and simulate the integrated model is freely available at https://sourceforge.net/projects/o2ros.

4.1. Biological and clinical implications

It is of interest that our results suggest that ROS generation in exercising normal muscle switches to high levels already at 17,000 ft., or about 5,000 m. This is the altitude above which permanent human habitation does not occur [27], and also the altitude above which humans experience inexorable loss of body mass. It is easy to hypothesize a cause and effect relationship between ROS and these findings, given the generally pro-inflammatory effects of high ROS levels, but whether this is indeed cause and effect or just coincidence remains to be established. In the same vein, the widespread presence of high ROS generation within muscle above 20,000 ft. and almost uniform presence above 25,000 ft. coincides with what is popularly termed the "death zone" in the mountaineering community – altitudes where fatalities are common. Of course, bitter cold, high winds, and hypoxia itself are likely contributors to the high risk of death under these conditions, but it is possible that high ROS production may be playing a role, not just in muscle but perhaps also in critical organs such as the brain. There is a growing body of literature [28-30] suggesting that endogenous ROS at high concentrations are damaging to cells, while at lower levels they are involved in activating important signaling pathways, some of which relate to adaptation to hypoxia (angiogenesis, for example where the promoter region of the critical angiogenic gene VEGF has a binding site for H_2O_2 [31]. They also act as pro-survival molecules regulating kinase-driven pathways [28, 32]. A recent systems analysis of abnormal muscle bioenergetics in patients with Chronic Obstructive Pulmonary Disease (COPD) [33] provides indirect evidence for a central role of cellular hypoxia in explaining abnormal regulation of key metabolic networks regulated by genetic and epigenetic mechanisms. Moreover, there is evidence [34-36] of the role of nitroso-redox disequilibrium explaining systemic effects in several chronic disorders such as COPD, chronic heart failure and type II diabetes. However, current knowledge of mitochondrial dysfunction [37-39] is still incomplete. The centrality of oxygen metabolism in organisms leads to the notion that it is also involved in other complex chronic diseases at essentially every level of organization [5, 40-42].

Potential applications of the integrated transport/metabolic model, which has been presented here only in terms of healthy humans at altitude, are envisioned in systems medicine with

analysis of the potentially greater degree of ROS generation associated with impaired O_2 availability in patients with diseases such as COPD, heart failure, diabetes and peripheral vascular disease. With the necessary input data, this could be done for individual patients to assess the likelihood of high ROS generation in muscle. In addition, the model may allow the prediction of the benefits of exercise programs and pharmacological interventions in these patients. Through its predictions, the current analysis may open new avenues in assessment of the impact of impaired oxygen exchange on increased mitochondrial ROS generation as well as in evaluation of the consequences of oxidative stress on biological functions in different acute and chronic diseases [5, 6]. While prediction of ROS generation may be possible, it is clear that the current integrated model addresses only the relationships between determinants of cellular oxygenation and mitochondrial ROS production. It does not attempt to deal with complexities of the redox system such as the body antioxidant resources that undoubtedly will modulate the biological activity of ROS generated by exercise within muscle, and which will thus affect nitrosative/oxidative cellular damage. Accounting for such elements is well beyond the scope of this article.

5. Conclusions

The integration of the two deterministic modeling approaches considered in this study allows us to establish a quantitative analysis of the relationships between the components of the O_2 pathway [13-15] and mitochondrial ROS generation [17-19]. To this end, the simulations herein using data from exercising normal subjects at sea level and altitude have shown that when $\dot{V}_{O_2}$ is low (less than 40% of mitochondrial oxidative capacity) due to impaired O_2 transport, extremely low $P_{m_{O_2}}$ values will develop, which in turn may be associated with above normal ROS production. This will occur when $P_{m_{O_2}} < 2/3$ of mitochondrial P_{50}. The current investigation may open new avenues for assessing the impact of impaired oxygen transport on increased mitochondrial ROS generation as well as for evaluating the consequences of oxidative stress on biological functions in both acute and in chronic diseases [5,6].

Acknowledgements

This research has been carried out under the Synergy-COPD research grant, funded by the Seventh Framework Program of the European Commission as a Collaborative Project with contract no.: 270086 (2011–2014), AGAUR (2009SGR1308 and 2009SGR911), “ICREA Academia prize” (MC), Spanish Government and the European Union FEDER funds (SAF2011-25726) and NIH P01 HL091830.

Author contributions

IC, PDW, VS, MC, JR, DGC and JT conceived and designed the work, revised critically the content and approved the final version of the manuscript for submission. IC, PDW and VS generated and analyzed the simulations and drafted the article.

References

1. Waypa, G.B., J.D. Marks, R. Guzy, P.T. Mungai, J. Schriewer, D. Dokic, P.T. Schumacker, Hypoxia triggers subcellular compartmental redox signaling in vascular smooth muscle cells. Circ Res, 2010. 106(3): p. 526-35. PMID: 2856085.
2. Bailey, D.M., I.S. Young, J. McEneny, L. Lawrenson, J. Kim, J. Barden, R.S. Richardson, Regulation of free radical outflow from an isolated muscle bed in exercising humans. American Journal of Physiology - Heart and Circulatory Physiology, 2004. 287(4): p. H1689-H1699.
3. Koechlin, C., F. Maltais, D. Saey, A. Michaud, P. LeBlanc, M. Hayot, C. Prefaut, Hypoxaemia enhances peripheral muscle oxidative stress in chronic obstructive pulmonary disease. Thorax, 2005. 60(10): p. 834-41. PMID: 1747208.
4. Cherniack, N.S., Oxygen sensing: applications in humans. Journal of Applied Physiology, 2004. 96(1): p. 352-358.
5. Semenza, G.L., Oxygen Sensing, Homeostasis, and Disease. New England Journal of Medicine, 2011. 365(6): p. 537-547.
6. Schumacker, P.T., Lung cell hypoxia: role of mitochondrial reactive oxygen species signaling in triggering responses. Proc Am Thorac Soc, 2011. 8(6): p. 477-84. PMID: 3359072.
7. Richardson, R.S., E.A. Noyszewski, K.F. Kendrick, J.S. Leigh, P.D. Wagner, Myoglobin O2 desaturation during exercise. Evidence of limited O2 transport. J Clin Invest, 1995. 96(4): p. 1916-1926.
8. Tran, T.K., N. Sailasuta, R. Hurd, T. Jue, Spatial distribution of deoxymyoglobin in human muscle: an index of local tissue oxygenation. NMR Biomed, 1999. 12(1): p. 26-30.
9. Mik, E.G., Measuring Mitochondrial Oxygen Tension: From Basic Principles to Application in Humans. Anesth Analg, 2013. 117(4): p. 834-846.
10. Wagner, P.D., Determinants of maximal oxygen transport and utilization. Annu Rev Physiol, 1996. 58: p. 21-50.
11. Wagner, P.D., Algebraic analysis of the determinants of VO2max. Respir Physiol, 1993. 93(2): p. 221-37.
12. Cano, I., M. Mickael, D. Gomez-Cabrero, J. Tegnér, J. Roca, P.D. Wagner, Importance of mitochondrial in maximal O2 transport and utilization: A theoretical analysis. Respiratory Physiology & Neurobiology, 2013. 189(3): p. 477-483.
13. Wilson, D.F., M. Erecinska, C. Drown, I.A. Silver, Effect of oxygen tension on cellular energetics. American Journal of Physiology - Cell Physiology, 1977. 233(5): p. C135-C140.
14. Gnaiger, E., B. Lassnig, A. Kuznetsov, G. Rieger, R. Margreiter, Mitochondrial oxygen affinity, respiratory flux control and excess capacity of cytochrome c oxidase. J Exp Biol, 1998. 201(Pt 8): p. 1129-39.
15. Scandurra, F.M., E. Gnaiger, Cell respiration under hypoxia: facts and artefacts in mitochondrial oxygen kinetics. Adv Exp Med Biol, 2010. 662: p. 7-25.
16. Cano, I., P.D. Wagner, J. Roca, Effects of Lung and Muscle Heterogeneities on Maximal O2 Transport and Utilization. The Journal of Physiology (submitted), 2014.
17. Selivanov, V.A., T.V. Votyakova, V.N. Pivtoraiko, J. Zeak, T. Sukhomlin, M. Trucco, J. Roca, M. Cascante, Reactive Oxygen Species Production by Forward and Reverse Electron Fluxes in the Mitochondrial Respiratory Chain. PLoS Comput Biol, 2011. 7(3): p. e1001115.
18. Selivanov, V.a., T.V. Votyakova, J.a. Zeak, M. Trucco, J. Roca, M. Cascante, Bistability of mitochondrial respiration underlies paradoxical reactive oxygen species generation induced by anoxia. PLoS computational biology, 2009. 5: p. e1000619.
19. Selivanov, V.A., M. Cascante, M. Friedman, M.F. Schumaker, M. Trucco, T.V. Votyakova, Multistationary and oscillatory modes of free radicals generation by the mitochondrial respiratory

chain revealed by a bifurcation analysis. PLoS Comput Biol, 2012. 8(9): p. e1002700. PMID: 3447950.
20. Berkelhamer, S.K., G.A. Kim, J.E. Radder, S. Wedgwood, L. Czech, R.H. Steinhorn, P.T. Schumacker, Developmental differences in hyperoxia-induced oxidative stress and cellular responses in the murine lung. Free Radic Biol Med, 2013. 61C: p. 51-60.
21. Gore, A., M. Muralidhar, M.G. Espey, K. Degenhardt, L.L. Mantell, Hyperoxia sensing: from molecular mechanisms to significance in disease. J Immunotoxicol, 2010. 7(4): p. 239-54.
22. Sutton, J.R., J.T. Reeves, P.D. Wagner, B.M. Groves, A. Cymerman, M.K. Malconian, P.B. Rock, P.M. Young, S.D. Walter, C.S. Houston, Operation Everest II: oxygen transport during exercise at extreme simulated altitude. J Appl Physiol, 1988. 64(4): p. 1309-21.
23. Sinha, S., U.S. Ray, M. Saha, S.N. Singh, O.S. Tomar, Antioxidant and redox status after maximal aerobic exercise at high altitude in acclimatized lowlanders and native highlanders. Eur J Appl Physiol, 2009. 106(6): p. 807-14.
24. Magalhaes, J., A. Ascensao, G. Viscor, J. Soares, J. Oliveira, F. Marques, J. Duarte, Oxidative stress in humans during and after 4 hours of hypoxia at a simulated altitude of 5500 m. Aviat Space Environ Med, 2004. 75(1): p. 16-22.
25. Joanny, P., J. Steinberg, P. Robach, J.P. Richalet, C. Gortan, B. Gardette, Y. Jammes, Operation Everest III (Comex'97): the effect of simulated sever hypobaric hypoxia on lipid peroxidation and antioxidant defence systems in human blood at rest and after maximal exercise. Resuscitation, 2001. 49(3): p. 307-14.
26. Wagner, P.D., G. Hedenstierna, G. Bylin, Ventilation-perfusion inequality in chronic asthma. Am Rev Respir Dis, 1987. 136(3): p. 605-12.
27. West, J.B., Highest permanent human habitation. High Alt Med Biol, 2002. 3(4): p. 401-7.
28. Gough, D.R., T.G. Cotter, Hydrogen peroxide: a Jekyll and Hyde signalling molecule. Cell Death and Dis, 2011. 2: p. e213.
29. Simon, H.U., A. Haj-Yehia, F. Levi-Schaffer, Role of reactive oxygen species (ROS) in apoptosis induction. Apoptosis, 2000. 5(5): p. 415-418.
30. Kang, M.A., E.Y. So, A.L. Simons, D.R. Spitz, T. Ouchi, DNA damage induces reactive oxygen species generation through the H2AX-Nox1/Rac1 pathway. Cell Death Dis, 2012. 3: p. e249.
31. Oshikawa, J., N. Urao, H.W. Kim, N. Kaplan, M. Razvi, R. McKinney, L.B. Poole, T. Fukai, M. Ushio-Fukai, Extracellular SOD-derived H2O2 promotes VEGF signaling in caveolae/lipid rafts and post-ischemic angiogenesis in mice. PLoS One, 2010. 5(4): p. e10189. PMID: 2858087.
32. Giannoni, E., F. Buricchi, G. Raugei, G. Ramponi, P. Chiarugi, Intracellular reactive oxygen species activate Src tyrosine kinase during cell adhesion and anchorage-dependent cell growth. Mol Cell Biol, 2005. 25(15): p. 6391-403. PMID: 1190365.
33. Turan, N., S. Kalko, A. Stincone, K. Clarke, A. Sabah, K. Howlett, S.J. Curnow, D.A. Rodriguez, M. Cascante, L. O'Neill, S. Egginton, J. Roca, F. Falciani, A Systems Biology Approach Identifies Molecular Networks Defining Skeletal Muscle Abnormalities in Chronic Obstructive Pulmonary Disease. PLoS Comput Biol, 2011. 7(9): p. e1002129.
34. Rodriguez, D.A., S. Kalko, E. Puig-Vilanova, M. Perez-Olabarria, F. Falciani, J. Gea, M. Cascante, E. Barreiro, J. Roca, Muscle and blood redox status after exercise training in severe COPD patients. Free Radic Biol Med, 2012. 52(1): p. 88-94.
35. Hare, J.M., Nitroso–Redox Balance in the Cardiovascular System. New England Journal of Medicine, 2004. 351(20): p. 2112-2114.
36. Singel, D.J., J.S. Stamler, Blood traffic control. Nature, 2004. 430(6997): p. 297-297.
37. Rabinovich, R., R. Bastos, E. Ardite, L. Llinàs, M. Orozco-Levi, J. Gea, J. Vilaró, J.a. Barberà, R. Rodríguez-Roisin, J.C. Fernández-Checa, J. Roca, Mitochondrial dysfunction in COPD patients with low body mass index. The European respiratory journal : official journal of the European Society for Clinical Respiratory Physiology, 2007. 29: p. 643-50.
38. Puente-Maestu, L., J. Perez-Parra, R. Godoy, N. Moreno, A. Tejedor, A. Torres, A. Lazaro, A. Ferreira, A. Agusti, Abnormal transition pore kinetics and cytochrome C release in muscle mitochondria of patients with chronic obstructive pulmonary disease. Am J Respir Cell Mol Biol, 2009. 40(6): p. 746-50.
39. Meyer, A., J. Zoll, A.L. Charles, A. Charloux, F. de Blay, P. Diemunsch, J. Sibilia, F. Piquard, B. Geny, Skeletal muscle mitochondrial dysfunction during chronic obstructive pulmonary disease: central actor and therapeutic target. Exp Physiol, 2013. 98(6): p. 1063-78.
40. Raymond, J., D. Segre, The effect of oxygen on biochemical networks and the evolution of complex life. Science, 2006. 311(5768): p. 1764-7.
41. Baldwin, J.E., H. Krebs, The evolution of metabolic cycles. Nature, 1981. 291(5814): p. 381-2.

42. Koch, L.G., S.L. Britton, Aerobic metabolism underlies complexity and capacity. J Physiol, 2008. 586(1): p. 83-95. PMID: 2375572.
43. Dejours, P., Respiration. 1966.
44. Weibel, E.R., C.R. Taylor, P. Gehr, H. Hoppeler, O. Mathieu, G.M. Maloiy, Design of the mammalian respiratory system. IX. Functional and structural limits for oxygen flow. Respir Physiol, 1981. 44(1): p. 151-64.
45. Weibel, E.R., The Pathway for Oxygen: Structure and Function in the Mammalian Respiratory System1984: Harvard University Press. ISBN: 9780674657915.
46. Welch, H.G., Hyperoxia and human performance: a brief review. Med Sci Sports Exerc, 1982. 14(4): p. 253-62.
47. Wilson, G.D., H.G. Welch, Effects of hyperoxic gas mixtures on exercise tolerance in man. Med Sci Sports, 1975. 7(1): p. 48-52.
48. Briscoe, W.A., A method for dealing with data concerning uneven ventilation of the lung and its effects on blood gas transfer. Journal of Applied Physiology, 1959. 14(3): p. 291-298.
49. Wagner, P.D., R.B. Laravuso, R.R. Uhl, J.B. West, Continuous distributions of ventilation-perfusion ratios in normal subjects breathing air and 100 per cent O2. J Clin Invest, 1974. 54(1): p. 54-68. PMID: 301524.
50. West, J.B., C.T. Dollery, Distribution of blood flow and ventilation-perfusion ratio in the lung, measured with radioactive CO2. Journal of Applied Physiology, 1960. 15(3): p. 405-410.

FIGURES

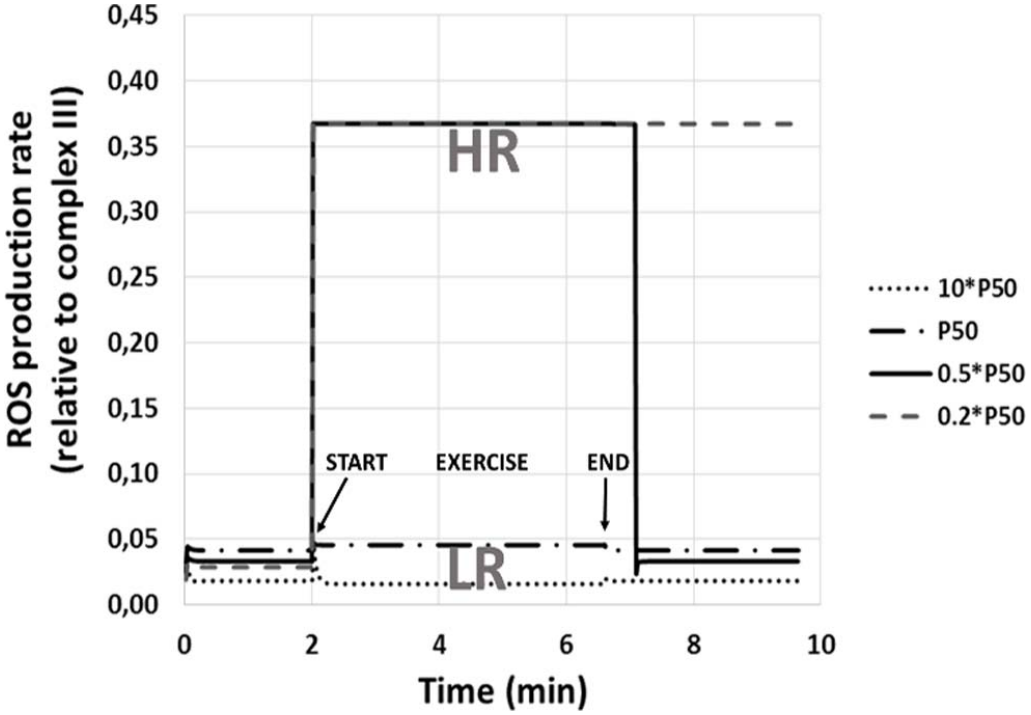

Figure 1. Dynamics of ROS production (expressed as SQo produced, normalized to total complex III abundance (taken as 0.4 nmol/mg mitochondrial protein)) at four steady state concentrations of oxygen (expressed as mitochondrial P_{O_2} relative to P_{50}, the oxygen partial pressure at the half-maximal rate of respiration). Before and after exercise, rest is simulated (no ATP hydrolysis, proton gradient dissipates only due to membrane leak). Between 2 and 6.6 min, exercise is simulated (membrane proton gradient dissipates due to ATP hydrolysis and ATP synthase activity). Overall, ROS production falls into two distinct patterns: one (HR, seen when $P_{m_{O_2}}/P_{50} < 0.67$) reflects high ROS generation and the other (LR, when $P_{m_{O_2}}/P_{50} > 0.67$) reflects little or no ROS generation compared to rest. Note post-exercise persistence of high ROS generation, especially at the lowest $P_{m_{O_2}}$ to P_{50} ratio.

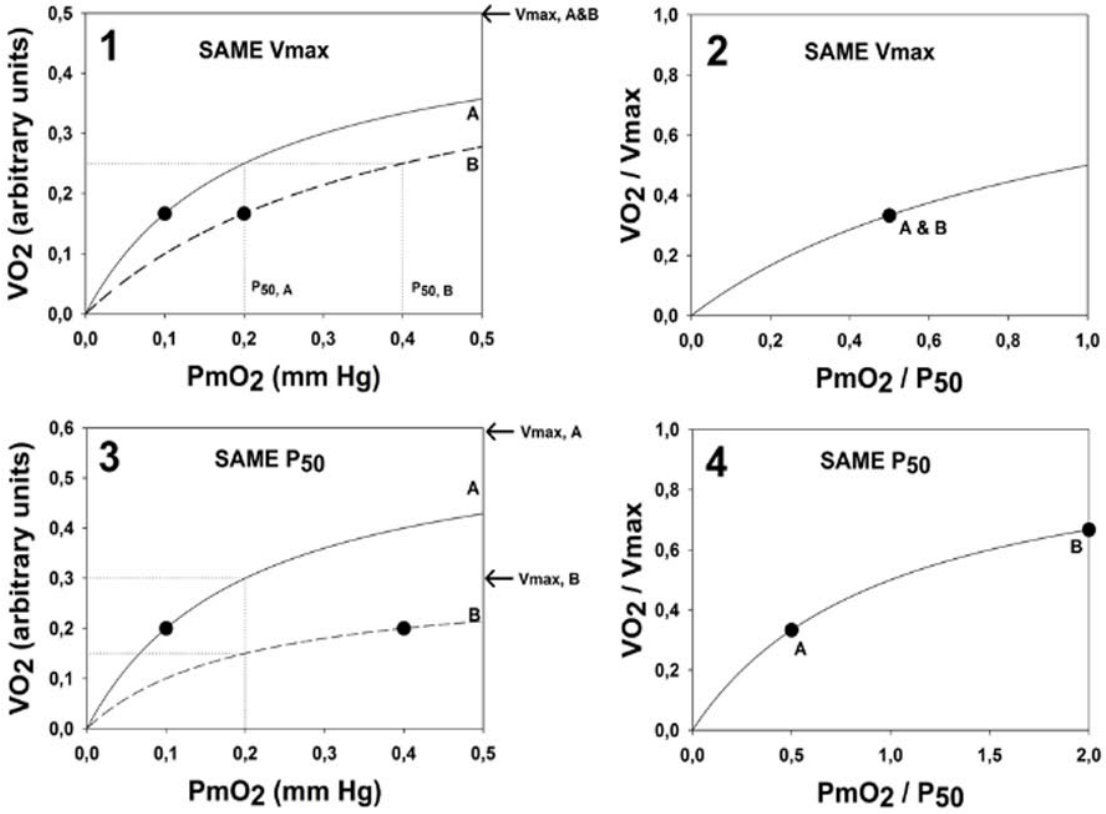

Figure 2. Importance of normalizing both actual $\dot{V}_{O_2}$ to mitochondrial $\dot{V}_{max}$ and actual mitochondrial P_{O_2} ($P_{m_{O_2}}$) to mitochondrial P_{50} when $\dot{V}_{max}$ and/or P_{50} may vary within or between muscles. Panel 1: Example of two muscles (A & B) with the same $\dot{V}_{max}$ but different P_{50} that happen to have the same absolute $\dot{V}_{O_2}$ (closed circles). Although $P_{m_{O_2}}$ is lower in A than B, normalization of both axes (Panel 2) shows that in this case, $P_{m_{O_2}}$ relative to P_{50} is the same, and this means that ROS generation will be the same for A and B. Panel 3: Example of two muscles (A & B) with the same P_{50} but different $\dot{V}_{max}$ that again happen to have the same absolute $\dot{V}_{O_2}$ (closed circles). $P_{m_{O_2}}$ is again lower in A than B, but normalization of both axes (Panel 4) shows that $P_{m_{O_2}}$ relative to P_{50} is lower in A than B, and this means that ROS generation will be high for A and normal for B.

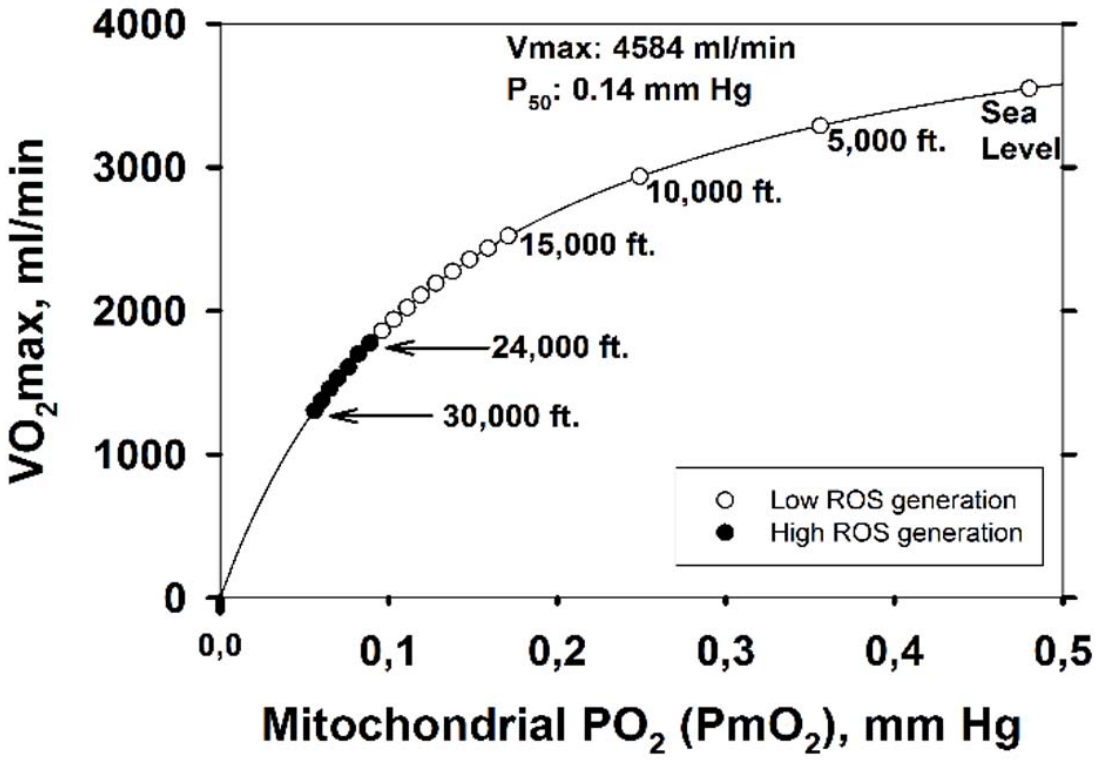

Figure 3. Reduction of maximal $\dot{V}_{O_2}$ and mitochondrial P_{O_2} in a *homogeneous* muscle as a function of altitude, (solid line, computed from the O_2 pathway model) and degree of ROS generation as a function of mitochondrial P_{O_2} computed from the mitochondrial respiration model. Below 24,000 ft, ROS production is low (open circles), but above 24,000 ft, ROS production abruptly increases (closed circles).

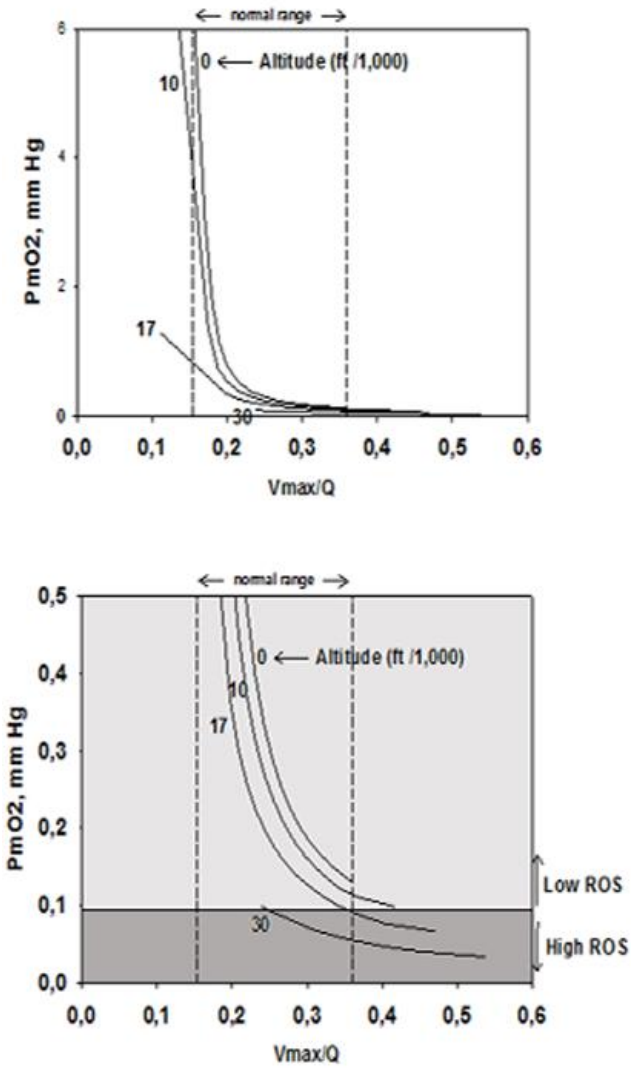

Figure 4. Mitochondrial P_{O_2} ($P_{m_{O_2}}$) as a function of regional ratios of metabolic capacity ($\dot{V}_{max}$) to blood flow ($\dot{Q}$) at four altitudes. The lower $\dot{Q}$ (supply) is in relation to $\dot{V}_{max}$ (demand), the lower is $P_{m_{O_2}}$ at any altitude; also, $P_{m_{O_2}}$ at any $\dot{V}_{max}/\dot{Q}$ ratio falls with increasing altitude. Vertical dashed lines mark the normal range of $\dot{V}_{max}/\dot{Q}$. Both panels show the same data, but the lower panel expands the y-axis in its lower range to show when ROS generation is high (i.e., when $P_{m_{O_2}} < 0.1$ mm Hg). Below 17,000ft, ROS generation remains low, but above this altitude, regions of normal muscle with high $\dot{V}_{max}/\dot{Q}$ ratio generate high ROS levels, until at the Everest summit, almost the entire muscle generates high ROS levels.

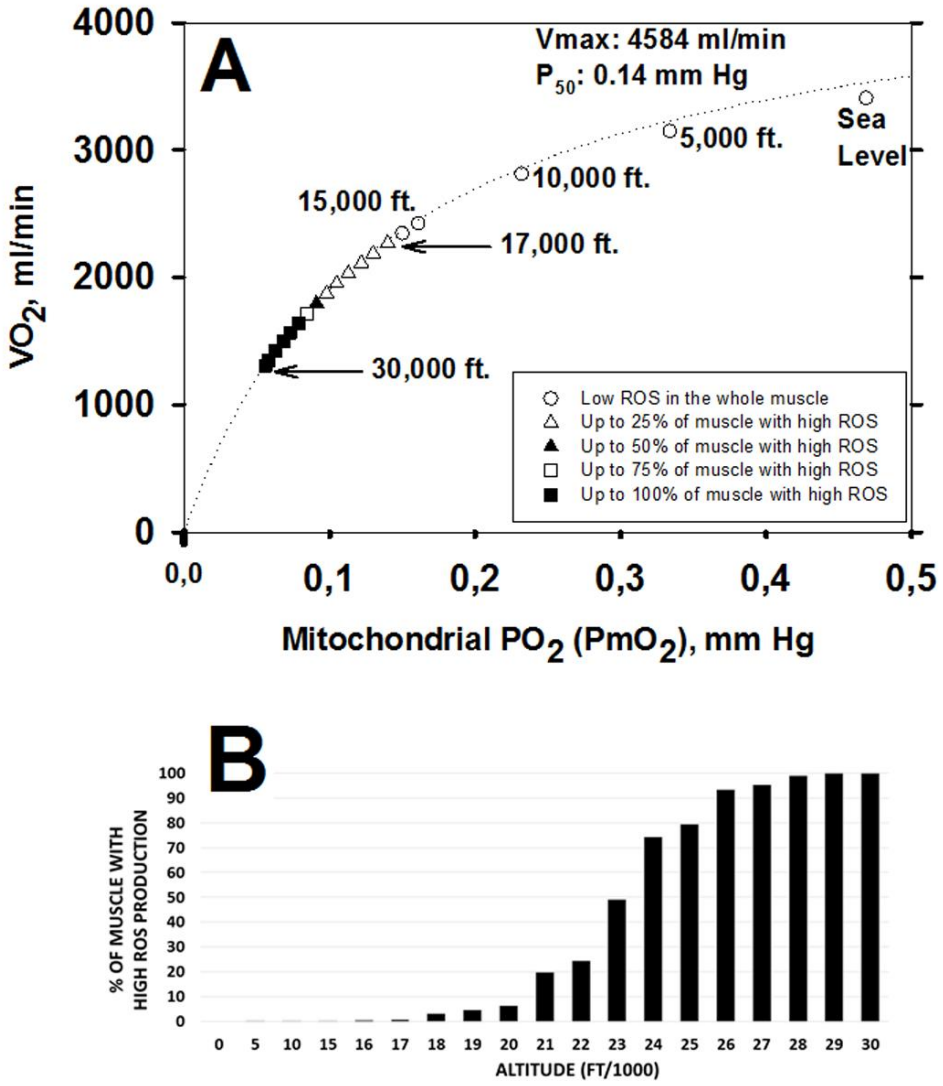

Figure 5. Effect of altitude on ROS generation when considering typical values for lung and muscle heterogeneities. A: Between 0 and 17,000 ft., ROS generation is within the normal range throughout the exercising muscle (open circles). Open triangles indicate that between 17,000 and 22,000 ft., abnormally high levels of ROS are predicted in up to 25% of exercising muscle (in regions with highest metabolic capacity in relation to O_2 transport). The closed triangle (23,000 ft.) indicates high ROS in 25 to 50% of muscle. The open square (24,000 ft.) indicates 50-75% of muscle has high levels of ROS and filled squares (25,000 - 30,000 ft.) show that 75 - 100% of muscle regions express high levels of ROS (see text for more details). B: shows in more detail the percentage of exercising muscle that generates abnormally high levels of ROS at each altitude.

Manuscript 4:

The COPD Knowledge Base: enabling data analysis and computational simulation in translational COPD research.

Cano I, Tényi A, Schueller C, Wolff M, Huertas M, Gomez-Cabrero D, Antczak P, Roca J, Cascante M, Falicani F, Maier D.

Accepted for publication in BMC Journal of Translational Medicine, 2014.

The COPD Knowledge Base: enabling data analysis and computational simulation in translational COPD research

Isaac Cano[1], Ákos Tényi[1], Christine Schueller[2], Martin Wolff[2], M. Mercedes Huertas Migueláñez[3], Philipp Antczak[4], Josep Roca[1], Marta Cascante[1], Francesco Falicani[4], Dieter Maier[2]*

[1] Institut d'investigacions Biomèdiques August Pi i Sunyer, Barcelona, Spain

[2]Biomax Informatics AG, Planegg, Germany

[3]Barcelona Digital, Barcelona, Spain

[4]Computational Systems Research, University of Liverpool, UK

*Corresponding author

Abstract

Background - Previously we generated a chronic obstructive pulmonary disease (COPD) specific knowledge base (www.copdknowledgebase.eu) from clinical and experimental data, text-mining results and public databases. This knowledge base allowed the retrieval of specific molecular networks together with integrated clinical and experimental data. **Results -** The COPDKB has now been extended to integrate over 40 public data sources on functional interaction (e.g. signal transduction, transcriptional regulation, protein-protein interaction, gene–disease association). In addition we integrated COPD-specific expression and co-morbidity networks connecting over 6 000 genes/proteins with physiological parameters and disease states. Three mathematical models describing different aspects of systemic effects of COPD were connected to clinical and experimental data. We have completely redesigned the technical architecture of the user interface and now provide html and web browser-based access and form-based searches. A network search enables the use of interconnecting information and the generation of disease-specific sub-networks from general knowledge. Integration with the Synergy-COPD Simulation Environment enables multi-scale integrated simulation of individual computational models while integration with a Clinical Decision Support System allows delivery into clinical practice. **Conclusions -** The COPD Knowledge Base is the only publicly available knowledge resource dedicated to COPD and combining genetic information with molecular, physiological and clinical data as well as mathematical modelling. Its integrated analysis functions provide overviews about clinical trends and connections while its semantically mapped content enables complex analysis approaches. We plan to further extend the COPDKB by offering it as a repository to publish and semantically integrate data from relevant clinical trials. The COPDKB is freely available after registration at www.copdknowledgebase.eu.

Background

We previously reported the public availability of a chronic obstructive pulmonary disease (COPD) specific knowledge base [1]. This COPDKB semantically integrated existing COPD related knowledge such as genotype - phenotype relations or signal transduction pathways into structured networks that were connected with clinical and experimental data. To this end an object-oriented knowledge model was generated which contained concepts such as “gene”, “disease” or “organ” and their associations such as “causes”, “damages”. We established a general human molecular knowledge network of over 3.6 million connections (e.g. gene–disease associations, protein–protein interactions) with disease-specific signal transduction (54 pathways) and metabolite (122) information manually curated from the literature. Initial search, retrieval and R-plugin -based data-mining methods integrated into the COPDKB enabled the retrieval of disease- or case-specific sub-networks e.g. lung specific by expert users for data analysis and model generation. To this end, a thick Java client provided a wizard based user interface to create natural language like queries such as

“Object to find is a Patient which simultaneously is annotated by Patient diagnostic data which has GOLD attribute greater than 2 and is annotated by Patient Anthropometrics which has BMI-BT attribute less than 18 and never is diagnosed with a NCI Thesaurus entry which is inferred by ontology entry which has name like `*cancer*'”, which would retrieve all patients diagnosed with COPD severity grade above 2 but no cancer which have low body mass index. In addition graph based navigation allowed single step network expansions to e.g. navigate from a group of patients to the diseases they are diagnosed with and from there to the genes associated with these diseases. However, validation with user groups showed that to enable application by clinical researchers, a significant simplification of the user interface was required.

To extend the applicability of the COPDKB as a central part of a biomedical research platform we identified several aims:

1. Update existing and integrate further COPD-specific knowledge and semantically map it to clinical, physiological and molecular data of COPD patients to generate a full repository of COPD-associated features.
2. Extend the capability of knowledge representation to include non-SBML-based mathematical models and integrate COPD-specific computational models. Semantically connect models of different types (e.g. ODE, probabilistic) with each other as well as existing relevant data.
3. Generate an intuitive browser-based user interface for clinical and biomedical researchers.
4. Connect the aggregated COPD-specific knowledge to a clinical decision support system (CDSS), which provides translation into clinical practice.

Methods

The requirement specification used elicitation methods such as user observations, focus groups, interviews and workshops to establish the use cases and workflows, which were refined based on a prototyping approach applying agile development methods. The architecture design approach followed the ISO/IEC 42010:2007 standard. Implementation of the user interface framework is based on the open source Foswiki framework (www.foswiki.org) for which a plugin was developed to connect the BioXM™ Knowledge Management Environment. While details of the technical architecture of BioXM have been reported elsewhere [2] we briefly summarise it here to aid understanding. As depicted in **Figure 2** BioXM is implemented as a platform-independent Java client–server application with modular architecture and a relational database management system backend. The Foswiki plugin calls a dedicated servlet deployed in an Apache Tomcat servlet container. The servlet connects to different BioXM application server programming interfaces (APIs) to execute searches and retrieve pre-defined reports through the wiki plugin into an html user interface which is accessible by any modern web-browser. A BioXM SOAP web service is used to interoperate with external applications such as the Clinical Decision Support System (CDSS) and Simulation Environment (SE). Data analyses methods are based on R scripts, which the BioXM R-plugin calls and presents the results directly in the user interface. Based on this plugin, content displayed in the browser can be dynamically generated from the knowledge base repository. The resulting user interface was iteratively validated and refined by focus groups of biomedical researchers within the Synergy-COPD projects as well as biohealth research students during two subsequent summer schools of the Erasmus Mundus BioHealth Computing program.

Data integration and semantic mapping was performed as described previously [1]. Briefly summarized, semantic mapping templates are generated manually between the conceptual data model of individual resources and the disease-specific knowledge model. Integration of data updates are subsequently performed automatically.

Manual curation of disease-specific knowledge was generated by extracting from expert-specified publications and the results were enriched by expert panel discussions.

Results

Overview of the knowledge base

The COPDKB now provides interoperability and integration between multiple data sources and tools commonly used in biomedical research. It also extends to include new tools such as a multi-scale Simulation Environment [3] that enables the execution of disease-specific simulations based on the integration of multiple sub-models. The COPDKB is based on the concept of “knowledge

as network" and bridges multiple sources and scales of knowledge by abstracting commonly used concepts to communicate disease-specific knowledge into objects and their relations. Structuring explicit and implicit knowledge into these formal concepts enables the use of existing, well-defined vocabularies (e.g. GO[4], ICD10 [5]) and standards (e.g. SBML[6], HL7[7]) to represent molecular, biochemical and clinical processes.

One of the challenges for the use of computation models in biomedical research is the integration of models at different scales as well as the mapping to corresponding clinical, physiological or molecular data. We defined standard operating procedures for model documentation and developed a realisation for the concept of composite use of orthogonal ontologies [8] to create semantic descriptions for models, model parameters and clinical parameters. The concept of combinatorial ontology use. Traditionally, ontologies are created with the intention to establish well defined, highly detailed concepts that capture the full semantic meaning of complex facts such as "positive regulation by symbiont of defense-related host calcium-dependent protein kinase pathway (GO:0052102)". In this way such a fact can be expressed by assigning a single ontological term. However, due to the complexity and expressivity of descriptions for biomedical functions and processes especially in physiology often no single ontological concept will fully describe the semantic meaning. Therefore a combinatorial description which combines multiple concepts has to be created semi-automatically e.g. by matching a free text description such as "partial arterial blood pressure" to terms in existing ontologies and then selecting the appropriate concepts from several, ideally orthogonal i.e. non-overlapping, ontologies, to generate an overall complete representation such as "MESH:D010313 Partial Pressure; PubChem:977 Oxygen; FMA:83066 Portion of arterial blood". Our realisation of this concept included standards for the definition of spatio-temporal compartments to allow ontology-based model–model and model–data connection. As a rule concepts should be selected from within a single ontology but if this does not create a full semantic description concepts from different ontologies can be combined. New inference methods are required to make use of such combinatorial descriptions and we decided to implement a network similarity search approach, which treats individual descriptors as objects in a network and uses within-ontology as well as between-ontology relations to infer object equivalence. Specifically, our algorithm treats the collection of descriptors as a specific network (*semantic_descriptorA*) and searches all other existing descriptor collections (*semantic_descriptorX* to *semantic_descriptorY*) for "similar" networks. A *semantic_descriptor* is more similar to the input the more a) shared nodes (ontology entries); b) identical edges (connections between two ontology entries); c) similar nodes (ontology entries connected to the identical node by intra- and inter-ontology relationship, i.e., ontological inference) and d) similar edges (alternative edge classes connecting identical or similar nodes) are found. A similarity score is calculated by summing individual node/edge scores multiplied by the coverage, i.e., total score

= Sum(individual scores) * coverage. Individual scores are defined as "1" for identical matches and scores for similar nodes/edges are derived by dividing 1 by the number of required steps to reach the "similar" object, i.e., a distance-based measure with diminishing contribution. The coverage is calculated as a fraction of objects in the input *semantic_descriptor* actually recovered in the search targets.

It is therefore possible to deduce, for example, a 98% similarity between the above described model parameter and a clinical parameter described as "NCI: C25378 Partial; NCI: C25195 Pressure; PubChem:977 Oxygen; FMA:45623 Systemic arterial system" (see **Figure 1**). The proposed mappings are verified manually and, if found true, are fixed, enabling the parameterisation of computational models based on personalised data, the integrative simulation of multi-scale models and the subsequent validation of model predictions against individual clinical data.

In addition to the semantic description of different types of knowledge and data, we therefore generated a technical integration between the three compounds required for integrative simulation and clinical decision support, the COPDKB, the Simulation Environment (SE, [3]) and Clinical Decision Support System (CDSS). We generated an architecture meta-model consisting of the following concepts: software components, graphical user interface (GUI), application programming interface (API), data types and information flow. **Figure 3** shows an integrative UML-type diagram of the organisational, infrastructural and informational architecture views depicting the involved software components, their APIs and the information flows between them. The user interaction was designed within the individual software applications to optimise the use-case and user-group-dependent issues. Therefore the COPDKB provides the primary access point to integrate, curate, search and retrieve COPD-related knowledge; the SE interface is designed to enable the explorative execution and personalisation of integrated, COPD-related computational models; and the CDSS ideally becomes unobtrusively integrated into the user interfaces of existing clinical information and management systems to extend the functionality of accepted clinical practice user interfaces to provide disease-specific, individualised support.

Resources included

We extended the disease-specific structured knowledge network significantly with several new resources (see **Table 1 - Resources integrated into the COPDKB** for an overview). Criteria for inclusion of new resources were the major aims of the Synergy-COPD project: a) to analyse systemic, especially skeletal muscle related mechanisms involved in COPD b) to analyse co-morbidity related COPD heterogeneity and corresponding molecular mechanisms and finally c) to aid the generation of clinical decision support for diagnosis and therapy. To this end we applied

literature mining, integration of existing structured databases, clinical studies and ontologies as follows:

1) Additional COPD-associated knowledge was curated from the literature. Within the Synergy-COPD project a main focus was on the understanding for epigenetic regulation of muscle phenotypes and development [9] as well as disease co-morbidities derived from OMIM gene–disease associations [10] and patient records [11].
2) The general knowledge on human regulatory processes was extended by integration of miRNA regulation information from miRBase [12] and transcriptional regulation information from ITFP [13] .
3) Regarding clinical COPD data, we integrated a second major study on COPD, PAC-COPD [14], which focuses on the phenotypic heterogeneity and the extent to which this heterogeneity is related to clinical development of COPD.
4) We extended the range of ontologies integrated into the COPDKB to improve the coverage of medical terms, diagnosis and processes. To this end we integrated the Medical Subject Headings (MeSH, [15]), the International Classification of Diseases with Clinical Modifications, Ninth and Tenth Revision (ICD9-CM, ICD-10-CM) [16] and SNOMED [17]. We used the UMLS Metathesaurus [18] to derive mappings between the different medical vocabularies and managed to relate over 150 000 concepts. These mappings allowed us to integrate a number of different gene–disease association resources which had used different disease vocabularies e.g. OMIM or ICD9.
5) Finally the COPDKB was extended significantly by results derived from the Synergy-COPD project.

We updated the expression-based association network derived from the BioBridge clinical study [19] with a new version now integrating gene expression data with physiological attributes such as VO_2max, protein modifications and metabolite measurements providing a COPD-training-specific network. A further three gene-expression-based association networks specific to angiogenesis in young and elderly adults as well as a mouse model on inactivity effects on muscle were made available (personal communication FF).

In addition to the general co-morbidity network mentioned above, two COPD-specific co-morbidity networks were generated within the project based on US Medicare and Swedish health system patient records totalling 13 million patients over 3 years [11] and 5 million patients over 9 years (personal communication DGC), respectively . To normalise health-system-specific differences in disease coding, a disease grouping was developed by clinical experts and integrated into the COPDKB. Similar to the disease grouping, we needed to bridge and unify signal transduction pathway, transcriptional regulation and metabolism information integrated from databases such as KEGG [20] and Reactome [21] as well as from COPD-specific literature mining

efforts reported earlier [1]. To this end we generated a Jaccards index-based clustering based on the overlap of pathway participants. At a conservative cut off of 0% FDR, this resulted in 13 groups summarising 421 individual pathways (out of 1367 total). Finally, we integrated computational models describing different cells, tissues, organs and physiological processes involved in COPD and its systemic effects. Three of these form the core of a COPD disease model, specifically a lung air and blood flow model [22] an oxygen transport model [23–25] and a muscle cell bioenergetics and ROS production model [26, 27].

Overall the COPDKB now provides access to almost 850 000 nodes, from genes, proteins and metabolites to cells, tissues and organs. 9.5 million associations between these nodes can be mined to derive COPD-specific hypotheses and data.

Tools for mining

The simplest way to work with the updated COPDKB is by accessing its new, HyperText Markup Language (HTML) and browser-based user interface (see supplemental file S1 for a detailed description and screenshots). It provides individual sections for disease-specific public knowledge, analysis results, mathematical and network models, as well as clinical data.

The browsing functions in each of these sections allow users to navigate through specific sub-sections e.g. the list of all COPD-associated genes or pathways.

All integrated information can be exported and can be filtered by keyword or numerical value using the column selector (e.g. “gene function: DNA binding” or “expression value: >1 AND < 100”). Cross-navigation between semantically mapped or associated data types is possible by following the “Change type” buttons, for example, to jump from a list of genes to the diseases associated with them. The “Data matrix” button allows users to show actual data associated to any displayed entity (if the user has access to those data, see above). On such a data matrix the “Statistics” button allows access to a simple box-plot overview statistic (mean, STDEV, min, max, quartiles) as well as t-test-based comparison of two groups (e.g. FEV1 for high/low BMI COPD patients).

In addition to the simple browse and filter access, we implemented a set of form-based searches, which allow more direct access to information and are continuously expanded based on user feedback. Currently the search form for patient selection is based on all clinical parameters such as BMI or dyspnoea Borg scale, allowing minimum and maximum threshold values to be set (**Figure 4**). Other search forms allow molecular data (e.g. metabolite or protein measurements) to be retrieved.

Two interactive data-mining methods, the network search and network ranking, are currently available only from the Java-based expert user interface. These expert-generated results are then made available in the standard user interface in the same way as other data. The network search

is a variant of the breadth-first-search [28], a graph search algorithm that begins at the root node and explores all the neighbouring nodes, which is iteratively repeated for each neighbour until a target node is reached. Within the COPDKB the path between nodes (the "associations") receives user-defined penalty scores and only the alternative with the lowest score or all alternatives below a certain threshold are retained. Different association types can carry different penalty scores. For example, a "high quality" protein–protein interaction (PPI) derived from co-immunoprecipitation might carry a penalty score of 1 while a "low quality" PPI detected by two-hybrid experiments might have a score of 3. Based on the overall penalty score, shorter and more "high quality" paths are preferred. The network ranking method developed within Synergy-COPD takes the result of a network search and assigns additional quality values to each of the nodes; these quality values can represent complex information such as "number of associated diseases" or "variability in muscle expression", the later derived from the analysis of over 4000 muscle-specific expression data sets available in GEO [29].

Finally the "network similarity" search is available directly from the standard COPDKB user interface. It compares different networks, e.g. signal transduction pathways or semantic descriptors of model parameters, based on the occurrence of identical or "similar" nodes and associations. In this context similarity is defined as proximity within an ontology. Based on this search method, a list of clinical and model parameters, for example, can be ranked according to their semantic similarity.

Major uses in Synergy-COPD

So far the major use for the COPDKB has been as the central collaboration and biomedical research platform within the Synergy-COPD project. As Systems Medicine is an inherently interdisciplinary process, it is extremely important to enable the generation of a common language between experts from different disciplines. The COPDKB has been used to map between knowledge and data from clinical researchers, computer scientists and mathematicians using the semantic description concept and the network similarity search. Clinical parameters from two different clinical studies have been unified and integrated with three computational models and eight association networks. While the COPDKB currently provides only simple analysis features it has been extensively used to support complex analysis workflows. Integrative network association analysis on combined clinical and molecular (expression, metabolic, protein) data was enabled by the corresponding data mapping and integration in the COPDKB [19]. The connection between data analysis results and the existing computational models was derived from network searches which took the highly ranked genes/proteins/metabolites/clinical parameters from the data analysis and searched for connecting paths to the described model parameters based on, in case of the bioenergetics model [26, 27], mappings to reference genes/proteins/metabolites.

Another important type of information provided by the COPDKB were the multiple mapped and integrated gene–disease and gene–gene associations. These were mainly used to provide molecular connections and mechanisms between different diseases derived, for example, from co-morbidity analysis. As described separately, the COPDKB also forms the knowledge backbone for the Simulation Environment. It provides the mappings between different models that are required by the SE for integrative multi-scale model execution and it subsequently holds the simulation results and maps them back to corresponding clinical data for validation. The final major use case for the COPDKB is to act as a fact repository for the Clinical Decision Support System (CDSS). The COPDKB provides co-morbidity and drug–drug interaction information to the CDSS, which subsequently generates alerts on possible disease co-occurrences or adverse drug interactions.

A final important use case turned out to be using the COPDKB as an educational tool to introduce non-clinicians to the issues and challenges of COPD-related Systems Medicine. Within the Erasmus Mundus BioHealth Computing program, the COPDKB was the initial access point for all students to learn about the different aspects of Systems Medicine, from clinical question to available knowledge and data, to analysis methods and predictive mathematical models. The feedback provided by these focus groups in turn greatly helped to improve the COPDKB user interface and shape further requirements.

Discussion

Within biomedical research, we increasingly rely on computational support to keep track of our understanding of complex systems such as ecosystems or the human body and its malfunctions. So far, within Systems Medicine only a few examples of computational disease knowledge resources are available (e.g. [30]) and the COPDKB is to our knowledge the only such resource regarding COPD. Moreover, by integrating the COPDKB tightly with a Simulation Environment, it extends from a dynamic, but still lexicon-type reference resource, into a truly predictive and individual tool. Due to the integration with a Clinical Decision Support System, it is able to deliver these individualised predictions directly into clinical practice.

However, several caveats remain. Although many of the available relevant structured public knowledge resources have been integrated, the majority of disease knowledge still remains hidden in the literature. Text-mining methods and manual curation provide some inroads into this wealth, but are far from sufficient to generate a truly complete picture of our current knowledge. Another limitation is the quality and context specificity of the integrated knowledge. Many resources do not extract these measures and therefore they remain hidden in the original literature. Detailed knowledge structuring efforts, such as developing a mathematical model of a certain process, still

require major manual literature-review efforts; the COPDKB only provides a rough framework and an indication where to start and which pathways to follow.
Regarding a full biomedical research platform, the COPDKB currently still lacks accessibility of the integrated data-analysis and data-mining methods for non-expert users. The majority of available knowledge is on the molecular level and only a small part of it is specific to COPD.

Conclusions

The COPDKB provides a step in our development of a biomedical research platform for System Medicine as well as the most comprehensive COPD-specific knowledge base. The COPDKB proved a valuable tool for the analysis and computational modelling of COPD although several gaps and weaknesses still remain, some inherent to the platform itself, some generic from the way we still communicate knowledge. Future developments will focus on three aspects: improving the quality of the disease-specific knowledge, extending the integrated COPD-related clinical data sources and bringing the validated data analysis workflows into the reach of non-bioinformaticians.

Competing interests

DM, CS and MW are employed at Biomax Informatics AG and will therefore be affected by any effect of this publication on the commercial version of the BioXM™ Knowledge Management Environment on which the COPDKB is based. IC, AT, MH, DGC, PA, JR, MC and FF are employed at academic institutes and will therefore be affected by any effect of this publication on their publication records.

Authors' contributions

IC conceived, implemented and validated the initial UI and co-drafted the manuscript. AT implemented the prioritisation strategy. CS specified the HL7 vMR support and implemented the medical ontology mapping. MW designed and implemented the technical UI framework. MH co-developed the COPDKB–SE integration architecture and implemented the integration interface. FF, PA and DGC co-developed the data analysis and prioritisation strategy. In addition DGC provided the COPD-specific co-morbidity networks and PA implemented the pathway clustering method. JR conceived the integrative biomedical research platform and co-defined the user interface specification. MC provided input to the semantic mapping of mathematical models and the prioritisation validation. DM conceived, designed and specified the COPDKB, co-developed

the architecture design and drafted the manuscript. All authors read and approved the final manuscript.

Acknowledgements

We would like to thank Claudia Vargas, Eleonora Minina, Igor Marin de Mas and Jörg Menche who provided the disease grouping, proteolysis to COPD, bioenergetics-model-to-enzyme mapping and parts of the co-morbidity networks, respectively. This research was supported by the Synergy-COPD European project (FP7-ICT-270086).

References

1. Maier D, Kalus W, Wolff M, Kalko SG, Roca J, Marin de Mas I, Turan N, Cascante M, Falciani F, Hernandez M, Villà-Freixa J, Losko S: **Knowledge management for systems biology a general and visually driven framework applied to translational medicine**. *BMC Syst Biol* 2011, **5**:38.
2. Losko S, Heumann K: **Semantic data integration and knowledge management to represent biological network associations**. *Methods Mol Biol Clifton NJ* 2009, **563**:241–258.
3. Huertas Migueláñez MM, Cecaroni L: **A simulation and integration environment for heterogeneous physiology-models**. *IEEE 15th Int Conf E-Health Netw Appl Serv Heal 2013* 2013.
4. Ashburner M, Ball CA, Blake JA, Botstein D, Butler H, Cherry JM, Davis AP, Dolinski K, Dwight SS, Eppig JT, Harris MA, Hill DP, Issel-Tarver L, Kasarskis A, Lewis S, Matese JC, Richardson JE, Ringwald M, Rubin GM, Sherlock G: **Gene ontology: tool for the unification of biology. The Gene Ontology Consortium**. *Nat Genet* 2000, **25**:25–9.
5. **The international conference for the tenth revision of the International Classification of Diseases. Strengthening of Epidemiological and Statistical Services Unit. World Health Organization, Geneva**. *World Health Stat Q Rapp Trimest Stat Sanit Mond* 1990, **43**:204–245.
6. Hucka M, Finney A, Sauro HM, Bolouri H, Doyle JC, Kitano H, Arkin AP, Bornstein BJ, Bray D, Cornish-Bowden A, Cuellar AA, Dronov S, Gilles ED, Ginkel M, Gor V, Goryanin II, Hedley WJ, Hodgman TC, Hofmeyr J-H, Hunter PJ, Juty NS, Kasberger JL, Kremling A, Kummer U, Le Novère N, Loew LM, Lucio D, Mendes P, Minch E, Mjolsness ED, et al.: **The systems biology markup language (SBML): a medium for representation and exchange of biochemical network models**. *Bioinforma Oxf Engl* 2003, **19**:524–31.
7. **Health Level Seven International - Homepage** [http://www.hl7.org/index.cfm?ref=nav]
8. Barreiro E, Sznajder JI: **Epigenetic regulation of muscle phenotype and adaptation: a potential role in COPD muscle dysfunction**. *J Appl Physiol Bethesda Md 1985* 2013, **114**:1263–1272.
9. Goh K-I, Cusick ME, Valle D, Childs B, Vidal M, Barabási A-L: **The human disease network**. *Proc Natl Acad Sci* 2007, **104**:8685 –8690.
10. Hidalgo CA, Blumm N, Barabasi A-L, Christakis NA: **A dynamic network approach for the study of human phenotypes**. *PLoS Comput Biol* 2009, **5**:e1000353.
11. Griffiths-Jones S, Grocock RJ, van Dongen S, Bateman A, Enright AJ: **miRBase: microRNA sequences, targets and gene nomenclature**. *Nucleic Acids Res* 2006, **34**(Database issue):D140–144.
12. Zheng G, Tu K, Yang Q, Xiong Y, Wei C, Xie L, Zhu Y, Li Y: **ITFP: an integrated platform of mammalian transcription factors**. *Bioinformatics* 2008, **24**:2416 –2417.

13. Garcia-Aymerich J, Gómez FP, Antó JM: **Phenotypic characterization and course of chronic obstructive pulmonary disease in the PAC-COPD Study: design and methods**. *Arch Bronconeumol* 2009, **45**:4–11.
14. Rogers FB: **Medical subject headings**. *Bull Med Libr Assoc* 1963, **51**:114–116.
15. SLEE VN: **The International Classification of Diseases: Ninth Revision (ICD-9)**. *Ann Intern Med* 1978, **88**:424–426.
16. Wang AY, Barrett JW, Bentley T, Markwell D, Price C, Spackman KA, Stearns MQ: **Mapping between SNOMED RT and Clinical terms version 3: a key component of the SNOMED CT development process**. *Proc AMIA Annu Symp AMIA Symp* 2001:741–745.
17. Lindberg C: **The Unified Medical Language System (UMLS) of the National Library of Medicine**. *J Am Med Rec Assoc* 1990, **61**:40–42.
18. Turan N, Kalko S, Stincone A, Clarke K, Sabah A, Howlett K, Curnow SJ, Rodriguez DA, Cascante M, O'Neill L, Egginton S, Roca J, Falciani F: **A systems biology approach identifies molecular networks defining skeletal muscle abnormalities in chronic obstructive pulmonary disease**. *PLoS Comput Biol* 2011, **7**:e1002129.
19. Kanehisa M, Goto S: **KEGG: kyoto encyclopedia of genes and genomes**. *Nucleic Acids Res* 2000, **28**:27–30.
20. Joshi-Tope G, Gillespie M, Vastrik I, D'Eustachio P, Schmidt E, de Bono B, Jassal B, Gopinath GR, Wu GR, Matthews L, Lewis S, Birney E, Stein L: **Reactome: a knowledgebase of biological pathways**. *Nucleic Acids Res* 2005, **33**(Database issue):D428–32.
21. Swan AJ, Clark AR, Tawhai MH: **A computational model of the topographic distribution of ventilation in healthy human lungs**. *J Theor Biol* 2012, **300**:222–231.
22. Wagner PD: **Algebraic analysis of the determinants of VO2,max**. *Respir Physiol* 1993, **93**:221–237.
23. Wagner PD: **Determinants of maximal oxygen transport and utilization**. *Annu Rev Physiol* 1996, **58**:21–50.
24. Cano I, Mickael M, Gomez-Cabrero D, Tegnér J, Roca J, Wagner PD: **Importance of mitochondrial P(O2) in maximal O2 transport and utilization: a theoretical analysis**. *Respir Physiol Neurobiol* 2013, **189**:477–483.
25. Selivanov VA, Cascante M, Friedman M, Schumaker MF, Trucco M, Votyakova TV: **Multistationary and oscillatory modes of free radicals generation by the mitochondrial respiratory chain revealed by a bifurcation analysis**. *PLoS Comput Biol* 2012, **8**:e1002700.
26. Selivanov VA, Votyakova TV, Pivtoraiko VN, Zeak J, Sukhomlin T, Trucco M, Roca J, Cascante M: **Reactive oxygen species production by forward and reverse electron fluxes in the mitochondrial respiratory chain**. *PLoS Comput Biol* 2011, **7**:e1001115.
27. Moore EF: **The shortest path through a maze**. In *Proc Int Symp Theory Switch*. Harvard University Press; 1959:285–292.
28. Edgar R, Domrachev M, Lash AE: **Gene Expression Omnibus: NCBI gene expression and hybridization array data repository**. *Nucleic Acids Res* 2002, **30**:207–10.
29. Fujita KA, Ostaszewski M, Matsuoka Y, Ghosh S, Glaab E, Trefois C, Crespo I, Perumal TM, Jurkowski W, Antony PMA, Diederich N, Buttini M, Kodama A, Satagopam VP, Eifes S, Del Sol A, Schneider R, Kitano H, Balling R: **Integrating pathways of Parkinson's disease in a molecular interaction map**. *Mol Neurobiol* 2014, **49**:88–102.

The 2011 and 2013 versions of ICD-9-CM and ICD-10-CM respectively were retrieved from the Centres for Disease Control and Prevention at:

- http://www.cdc.gov/nchs/icd/icd9cm.htm
- http://www.cdc.gov/nchs/icd/icd10cm.htm

Figures

Figure 1 - Semantic network similarity

"Equivalent" meaning of different parameters is determined by the overlap of their corresponding semantic descriptors, taking into account transitive relations within and between ontologies.

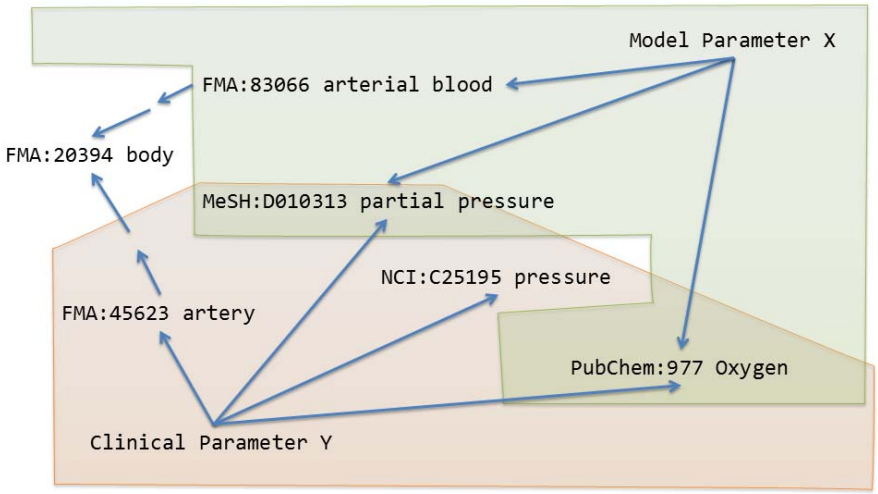

Figure 2 - BioXM technical structure

The modular BioXM architecture decouples tasks such as authorisation and access control from data management, search and reporting. The dynamic semantic knowledge model defines which objects and associations can be represented and analysed. Selecting from multiple "App" functions a highly specific browser-based user interface can be generated within the Foswiki open source framework.

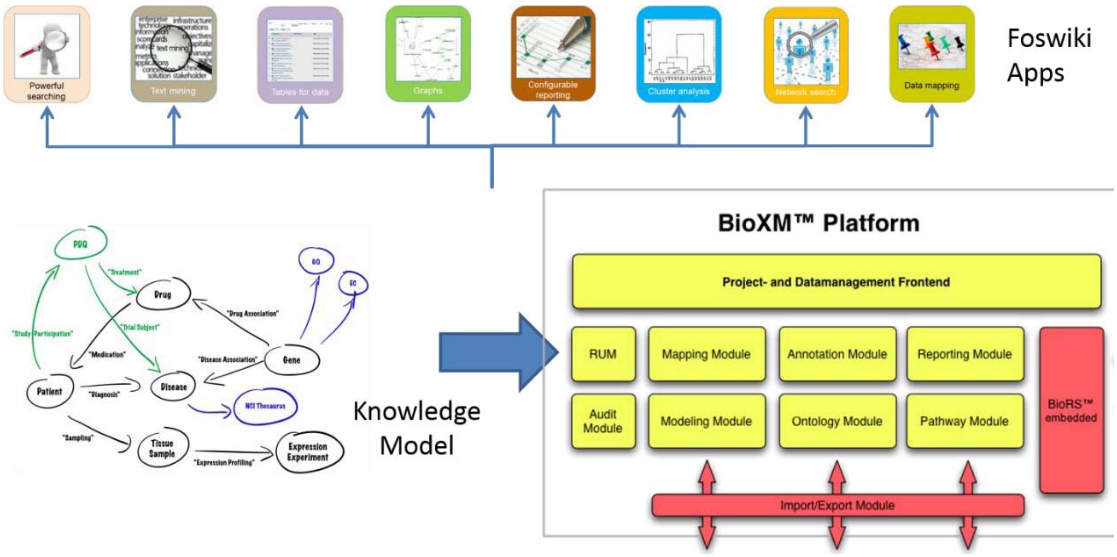

Figure 3 - Software architecture

Integrative UML-like diagram representing the organisational, infrastructural and informational view of the software architecture. All modules communicate based on WebServices. The COPDKB provides information of type model, model parameters, parameter values (summarised as "simulation knowledge") and experimental data to the SE. The SE feeds back simulation results. With the CDSS the COPDKB exchanges requests for information on knowledge about co-morbidities and drug-interactions and provides corresponding search results. COPDKB = COPD Knowledge Base, SE = Simulation Environment, CDSS = Clinical Decision Support System, API = Application Programming Interface.

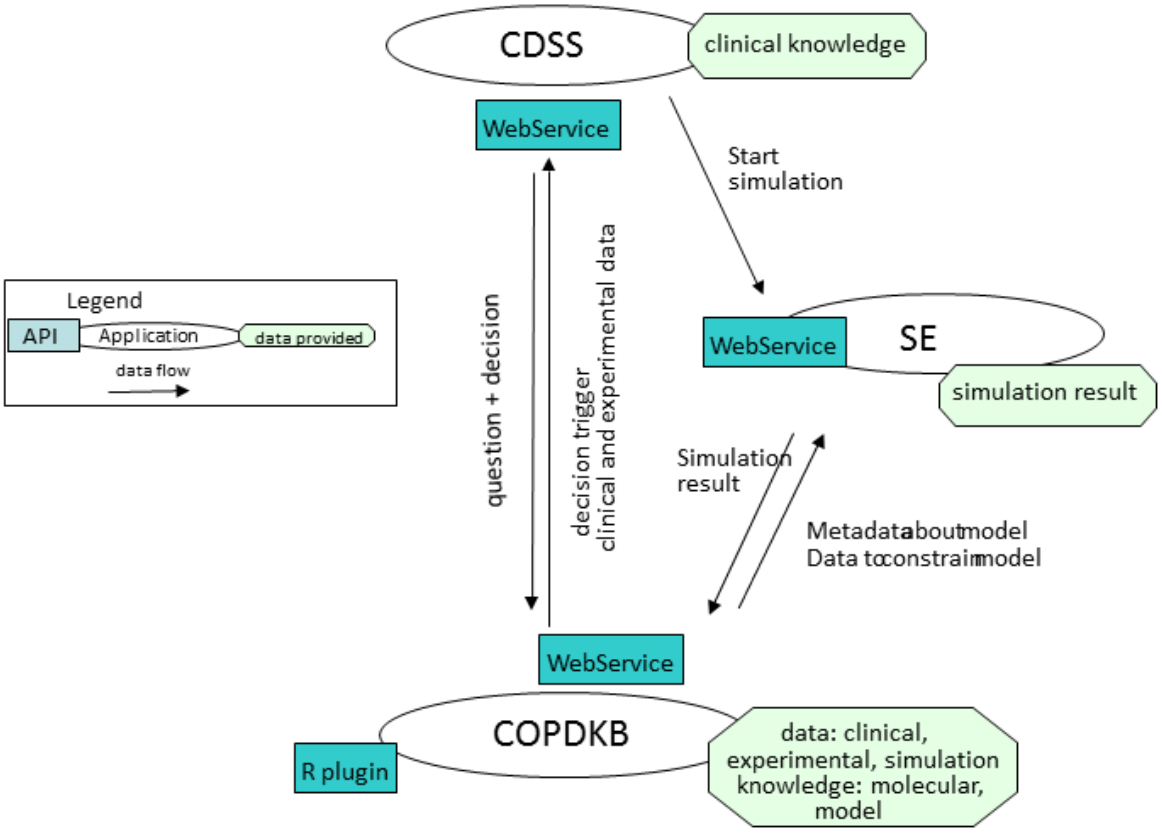

Figure 4 - Search form

Search forms provide pre-defined selections of parameters for which thresholds can be set to retrieve data. Here the body mass index was selected to retrieve patients with corresponding values.

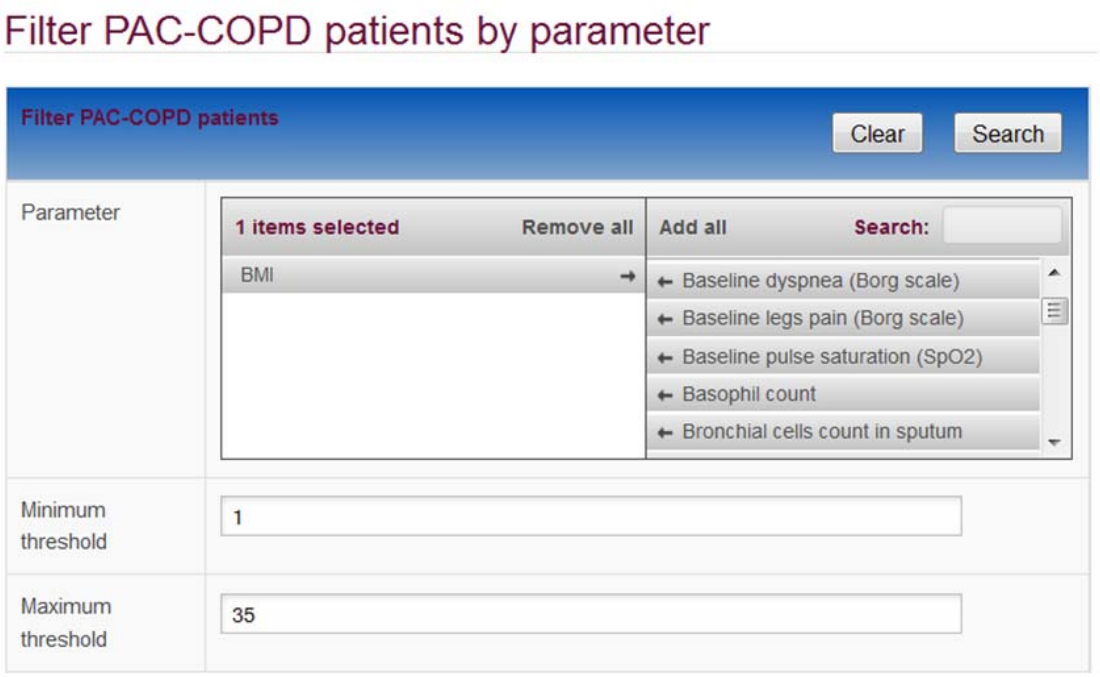

Tables

Table 1 - Resources integrated into the COPDKB

Data sources added since the first release of the COPDKB

Resource	Information type	Number of nodes	Number of associations
BioBridge omics network 2012	BioBridge 8w training extended by protein and metabolite measurements	4878	11448
Co-morbidity network	Co-morbidity network from OMIM gene–disease associations as well as Medicare and Swedish health system patient data	8 435	3 973 126
COPD literature mining	GWAS and epigenetic gene– disease associations	18	20
Disease grouping	Expert-based manual grouping of diseases	493 diseases	27 groups
Human angiogenesis young, old	Public, angiogenesis-related expression data	3691	3782
ICD 9	International classification of disease, ninth revision	13 222	
ICD 10	International classification of disease, tenth revision	12 416	
ITFP	Transcription factors and targets	2 143 TF, 6 710 targets	74 907
MeSH	Medical subject headings	24 767	
miRbase	micro RNA	2024 human miRNA	
miRTarBase	microRNA targets	12 194 human targets	38 311
Mouse inactivity-induced muscle wasting	Public mouse, inactivity-induced muscle wasting data gene expression GSE25908,	15 287	154 597
PAC-COPD	Clinical study	342 patients, 260 clinical attributes	
Pathway network	Jaccard index based clustering of pathways from KEGG, Reactome and the BioBridge COPD text mining	1138 pathways	1815 associations
SNOMED-CT	Systematized Nomenclature of Medicine — Clinical Terms	296 519	

Manuscript 5:

A Multi-tier ICT Framework to Deploy Integrated Care Services.

Cano I, Alonso A, Hernandez C, Burgos F, Martinez-Roldan J, Roca J.

Submitted to BMC Medical Informatics and Decision Making, 2014.

Software article

A multi-tier ICT framework to deploy integrated care services

Isaac Cano[1], MSc; Albert Alonso[1], MD, PhD; Carmen Hernandez[1], RN, MSc ; Felip Burgos[1], RN, PhD; Juan I Martinez-Roldan[2], MD; Josep Roca[1], MD, PhD

[1]Hospital Clinic, IDIBAPS, CIBERES, Universitat de Barcelona, C/Villarroel 170, 08036, Barcelona, Spain.
[2]Linkcare Health Services, C/ Roger de Llúria 50, Sobreático A, 08009 Barcelona, Spain.

ABSTRACT

Background – Integrated Care Services (ICS) supported by Information and Communication Technologies (ICT) enhance health outcomes in a cost-effective manner, but deployment of ICS in areas involving heterogeneous healthcare providers is still a challenge. Change management and ICT strategies constitute two pivotal factors modulating success of deployment of ICS. The current manuscript reports on the ICT developments carried out to support the deployment of four ICS as part of the EU project NEXES.

Results – The Linkcare® platform facilitated patient-centered management through shared-care plans across healthcare tiers. It provided collaborative tools underpinning organizational interoperability among actors: professionals and patients/caregivers. Moreover, it offered integration with provider-specific electronic health records via interoperability middlewares or using regional health information exchange tools. NEXES demonstrated effectiveness, complementariness and high potential for cost-containment in the four ICS assessed: Wellness and Rehabilitation (n= 282); Enhanced Care (n=1,037); Home Hospitalization and Early Discharge (n=2,404); and, Support to remote diagnosis (n=8,047).

Conclusions - Linkcare® covered the technological requirements of the project providing key ICT functionalities to support ICS for chronic conditions. Moreover, the flexibility of the ICT platform ensures readiness to support various regional deployment strategies.

Key words: *Chronic care, Clinical Decision Support Systems, Care coordination, eHealth, Integrated Health Care Systems*

1. Background

Health systems worldwide are facing a profound evolution driven by three major forces that are converging in terms of their impact on health information systems. Firstly, the epidemics of non-communicable diseases [1-3] is prompting both conceptual and organizational changes in the way we approach delivery of care for chronic patients. A second vector of change is the need to ensure financial sustainability of healthcare systems by generating efficiencies that ideally should lead to containment of overall healthcare costs without precluding the necessary innovations [1]. Last, but not least, Systems Medicine [4] is proposing an innovative approach to our understanding of disease mechanisms that is contributing to build-up personalized medicine [5] with important implications on future strategies for patient management.

A commonality of these three driving forces is the need for efficient and intensive use of Information and Communication Technologies (ICT) to support novel Integrated Care Services (ICSs) for chronic patients [6]. However, conventional Health Information Systems (HIS) only very rarely incorporate the required process logic to support ICSs management [7]. Conventional care relies on the management of clinical episodes with a disease-oriented approach, whereas in ICSs continuity of care with a patient-centered approach are key principles. Most importantly, integrated care requires organizational interoperability among healthcare providers and with social support.

We acknowledge that examples of successfully addressing the technological requirements associated with the deployment of ICSs within a given health information network do exist [8, 9]. However, this issue remains a major challenge in those healthcare sectors with heterogeneous providers each one using proprietary HISs. Moreover, there is a need for new paradigms bridging traditional Electronic Heath Records (EHR) and informal care through patient's personal health records.

The development of the Integrated Care Shared Knowledge platform (Linkcare®) reported here was part of the NEXES project [10]. NEXES aimed at assessing the deployment of four different ICSs covering the entire spectrum of severity of chronic patients. The project was conducted in three European sites: Barcelona (Catalonia); Trondheim (Norway) and Athens (Greece). The hypothesis behind the study was that a comprehensive ICT platform fulfilling the requirements of ICS plays a significant role for the successful deployment of the novel services.

Each of the sequential building blocks of a given ICS (i.e. case identification, case evaluation, work plan definition, follow-up and event handling, and discharge) typically involves the participation of a limited number of actors. If properly designed, each of these blocks should render outcomes that are relevant for execution of the next phase. Identification of tasks and allocation of them to the different actors was described using the BPMN (Business Process Modeling Notation) [11] formalism. Despite the descriptive part of the BPMN for each ICS can

be generalized to all settings, the design needs to be contextualized to optimize performance. The BPMN formalism was used to create the process logic of the ICS and to formalize the Linkcare® core functional requirements. This is to be complemented by other non-functional requirements, including interoperability with existing proprietary Health Information Systems (HIS) and privacy and security controls.

The current study reports on the technological developments carried out to support the process logic of ICS in a care coordination scenario. The manuscript describes: (i) the processes followed to develop the logics of the clinical processes and the associated ICT support; and, (ii) a summary of the ICS outcomes endorsing the adequacy of the technological setting. Further developments of the Linkcare® platform were carried out beyond the project, as part of the process of regional deployment in Catalonia. The characteristics of ICS and its practical implementation and assessment in NEXES have been extensively reported elsewhere [12].

2. Implementation

We adopted Enterprise Application Integration (EAI) software architectural principles [13] since they provide a common basic set of ICT solutions for integration at site level with potential for scalability. This option allowed integration with external legacy systems using interoperability middlewares for extending the core module with third-party functionalities. Overall, Linkcare® acts as a common facade, on top of existing Health Information Exchange (HIE) systems, with functionalities that facilitate organizational interoperability between professionals participating in ICSs management and execution. The European legislation on health data transfer and security [14-17], as well as the specifics of its real application at site level were analyzed and compared with particular emphasis on the impact of ICSs deployment. Moreover, the international regulations on medical devices [18-20] were also considered in the design of Linkcare®. Crucial to the success in adopting the proposed ICT solution was the goodness of fit between technology and work practices of the end users [21]. To this end, at different time points in the process of implementing the current Linkcare® platform, different evaluation methods and tools were applied with specific purposes following the iterative approach described by Catwell et al. [21]. Since early development phases, we introduced specific tools of formative evaluation to verify assumptions, generate understanding and reveal incidences in order to minimize future problems, namely: misunderstanding of specifications, rejections by end-users, etc. To this end, the Method for the ASsessment of Telemedicine applications (MAST) was used for iteratively evaluating the technological developments. Moreover, when the Linkcare® platform was operational, we incorporated tools of summative evaluation to assess outputs.

Linkcare® acts as a common interface exposing only the relevant information and interfaces of the underlying applications to the end-user. To this end, the system uses a component-based three-

tier architecture as depicted in **Figure 1**. The three-tier architecture consists of the following presentation, logic and data tiers.

Presentation tier

The presentation tier is composed of (i) a set of separate web portals for ICS management and execution (professionals portal), for team management, for call center operators (automatic call identification and call event processing), for patient self-management (self-explorations, educational material and event posting), the ICS Editor, and for system maintenance; and (ii) an Android application [22] to allow self-explorations and remote measurements using wireless medical device.

Logic tier

The logic tier dispatches through a SOAP web service bus all user-interface transaction requests. This allows easily embedding Linkcare® into existing corporate systems (in-place HIE if available) and provide a mean to facilitate privacy-preserving health data mining. All web service requests are properly recorded for data access tracking purposes and audit. The SOAP web services are divided into five main categories (see Multimedia Appendix 2 for a comprehensive technical specification of the currently available web services). *System Services* are designed to provide system parameters, such as language lists, multilingual descriptions, roles, source references, etc. *Session services* are used for session persistence acknowledgement. *Center services* provide organization information of a particular center, such as center-associated users, users and user's roles. Centers can be associated to other centers, and grant them access or administrative relations. So users who belong to different organizations can access the shared clinical data. *Library services* allow access to the resource library. The main library resources are the ICS templates, the work plan templates and the ICS available tasks. Finally, *Clinical Data Bank Services* anonymously store and exchange clinical information of cases. Linkcare® maintains a list of case identifiers that point to one or more health care information systems to retrieve the personal data. However, the personal data itself is not stored in Linkcare®, and each user access to such data is retrieved from the related source in real time, passing the user's credentials for that particular source.

Data tier

Finally, the data tier anonymously records all task and event execution information in a local or cloud database management system. Interoperability with clinical data is ensured by supporting different sets of terminology (i.e. International Classification of Diseases, ICD-9CM; SNOMED) and the HL7 2.5/3 standard for exchanging information between medical applications. A detail description of the system software and hardware requirements is provided in Multimedia Appendix 1.

3. Results and discussion

The core technological output of NEXES [10] was an open source Integrated Care Shared Knowledge platform (Linkcare®) released under a Creative Commons license, based on (i) patient-centered management via agreed ICSs, and (ii) technical support for coordination of healthcare professionals, considering ICSs as the archetypal coordination model. To this end, basic functionalities of the Linkcare® platform (**Figure 2**) include: ICSs management with web-based and user-friendly portals for healthcare professionals (**Figure 3, upper panel**) and patients (**Figure 3, lower panel**), integration with provider-specific EHR, interoperability with remote monitoring devices (by means of the Linkcare Mobility Android App [22]), integration with clinical decision support systems, incorporation of support center functionalities and delivery of educational resources. It is of note that integration at site level should be provided by the local systems integrator using, if available, local or regional Health Information Exchange. In the following sections, we take a generic ICS to describe the user roles, how an already existing generic ICS is managed and executed and what are the functionalities and software architecture principles Linkcare®.

3.1. Linkcare® user roles

Linkcare® considers a miscellaneous set of roles belonging to the following three main categories: *i) Patient/Caregiver* - this category identifies the primary recipient of the services. Within a given ICS tasks can be assigned to both patients and/or caregivers; *ii) Health & social care professional* - this role category encompasses the set of professionals that are members of the teamwork for a given patient and ICS. It is of note the importance of the *Case Manager* role as the professional holding responsibility, for a given ICS and patient, on team performance and program execution; and *iii) Assistant roles* - this category includes clerical workers and call center operators having access to a reduced set of assistant-specific user and patient data views. Additionally, ICT related roles (system administrator, operator manager, etc.) are also supported by the Linkcare® platform.

3.2. Incorporating a new ICS template: The ICS editor

The internal relational entities (depicted in **Figure 4**) and software architecture of Linkcare® support the process control logic of ICSs depicted in **Figure 5**, which core elements can be customized with the *ICS editor,* a suite of tools to graphically manage the following main four ICS components: *i) Linkcare® users* - this interface allows to register new professionals, and to manage healthcare teams already participating in any ICS supported by the Linkcare® platform. Users are required to indicate their ID and contact information, preferred working language, username and password and working hours. The user roles during the management and execution of the ICS will also be specified at this stage. Most of this information can be extracted from local authentication servers; *ii) ICS template* - ICS templates serve as a reference framework being later

customized to patient-specific conditions and the local characteristics of the healthcare provider. An ICS template is composed of a set of admission and discharge forms, templates for reporting admission, follow-up and discharge reports, as well as a predefined work plan; *iii) Electronic forms* - this interface allows to incorporate new forms (electronic questionnaires and checklists) to the library of forms or to manage already existing ones. At edit mode, each question can be stated in several languages and formulas can be incorporated into the questionnaire. The library of forms allows to share and reuse questionnaires and checklists *(see examples in Multimedia Appendix 1)*. Besides electronic forms, Linkcare® also allow professionals to customize report templates. Normalization of data collection via electronic forms using standard terminologies, and report templates empowers the ability of Linkcare® for privacy-preserving health data mining; and *iv) ICS tasks* - ICS templates have an associated work plan template, which is a set of tasks or interventions (e.g. questionnaires, vendor-specific remote monitoring of vital signs, audio and video conferences, etc.) scheduled to be executed during a predefined period of time, or always available (patient's optional tasks). Work plan templates can be customized to patient-specific needs selecting tasks from the ICS library of available resources.

3.3. ICS management and execution

Once the agreed ICS is incorporated into the Linkcare® platform, healthcare professionals can start the management and execution of the ICS. Depending on their role in the given ICS, professionals will have different access and operational rights.

The general functional workflow for ICS planning and execution, depicted in **Figure 5**, expands the ICS *Work plan definition* stage, into two functions: *Work plan customization* and *Task assignment*, allowing to better differentiate between the customization of the work plan template to patient-specific conditions and the planned management of both tasks and healthcare workforce. The technological implications of these stages and their functional workflow are described in detail below.

3.3.1. Case identification

This first step allows labeling a new case as eligible for enrolment into the Linkcare® platform, still with no selection of a specific ICS, which will be performed by the same or another healthcare professional during case evaluation. Patient information stored in external provider-specific EHR can be retrieved at this stage to ease case identification.

3.3.2. Case evaluation

In this step, professionals gathers information from patients with a twofold aim. Firstly, patient's inclusion into a given ICS template and, secondly, comprehensive assessment of the case to facilitate the work plan definition. Patient inclusion is associated to eligibility established through well-standardized forms. In addition, healthcare professionals can have access to the history of previous disease episodes stored in the corporate EHR and the history of previous and current

ICS admissions to support case evaluation, ultimately leading to the next stage for Work plan definition or discarding the case if not eligible.

3.3.3. Work plan definition

The work plan can be built from scratch or based upon an ICS-specific predefined work plan. As mentioned above, we distinguish the following two sub-stages: *i) Work plan customization - t*his stage allows the selection of specific tasks to personalize the predefined work plan to patient-specific conditions and needs. The library of tasks available, designed and evaluated in NEXES [10], included: informative documents supporting diagnosis, treatment and ICS management, electronic forms, tasks associated to the support center (i.e. phone calls, SMS messaging, videoconferencing, etc..) and patient remote monitoring using either electronic questionnaires or wireless sensors of vital signs; and *ii) Task Assignment - i*t corresponds to scheduling and allocation of tasks to the individual professionals of the team (e.g. healthcare professional, patient, social worker, etc.) taking into account the agenda of individual members of the care team. Otherwise, ICS optional tasks have a predefined task leader and can be performed anytime.

3.3.4. Follow-up & events handling

This stage corresponds to the running and management of a given ICS in a particular patient until its termination. In addition, this step encompasses event management. Events are generated by the patient (case) or by professionals (issuer agent) and registered to the system by healthcare professionals (poster agent) to request a service or advice to another professional or team (assigned agent). Events can be also generated because of the findings reported in a task. A specific event called Second Opinion allows requesting collaboration with other Linkcare® users. During the execution of the ICS work plan, follow-up reports can be generated and delivered to be stored in an external EHR. The continuous patient's assessment during this phase may lead to changes in the working plan triggered by unexpected events.

Patient self-management is a crucial part of ICSs. Accordingly, Linkcare® supports patients' empowerment with a web-based patient gateway, which allows patients access to their optional and scheduled tasks, to review their follow-up, to check educational information, to share documents of their choice with its case manager and the remote monitoring of patients' vital signs.

3.3.5. Discharge

Once the assigned ICS working plan is completed, the patient can be discharged or re-evaluated to be included in a different ICS. The ICS execution can also be terminated by patient's voluntary decision or by a change in the personal or health conditions that would make him/her no longer eligible. Ultimately, patient discharge reports are generated and sent to the corresponding EHR.

3.4. System usage and performance

The current Linkcare® platform successfully supported the deployment of the four ICSs, as described in detail elsewhere [12] and in the Multimedia Appendix 3 (Lessons Learnt in the

Validation Trials and Supporting Investigations), with full technical integration at site level (i.e. integration with the corporate EHR of the Hospital Clinic). Main features of Linkcare® are highlighted in **Table 1**.

A total of four major ICSs, designed and evaluated in the NEXES project [10], were created, managed and executed with the support of Linkcare®: *i)* Wellness and Rehabilitation (W&R), composed of one-year follow-up with ICT support after endurance training aiming at generating sustainability of training effects and fostering healthier lifestyles in clinically stable patients (entered, n=337, completed, n=154); *ii)* Enhanced Care (EC) for frail chronic patients targeting to reduce hospital admissions (n=1.541 and 1,340); *iii)* Home Hospitalization and Early Discharge (HH/ED) targeting tertiary bed savings and early readmissions avoidance (n=4.534 and 2.404); and, *iv)* Support to remote diagnosis (Support) for the remote quality assessment of spirometry testing (n=8,139 all completed). The four major ICSs were assessed in two European sites: Barcelona (ES), 540.000 inhabitants, driven by a tertiary hospital (11.128 patients) and Athens (GR), pilot studies conducted by a tertiary hospital (388 patients). During the project lifetime [10], in the Barcelona site, the assessment of the four ICSs ran in parallel with significant organizational changes promoting transfer of hospital-based specialized care to extramural community care. These ICSs should not be envisaged as silos. Instead, their adequate articulation in a given patient allows appropriate coverage of the complexities faced in chronic care [12]. Effectiveness, complementariness, transferability and cost-containment of the four ICS were proven in Barcelona and GR [12]. The project also identified strategies to foster EU deployment of the model of care.

3.5. Technological achievements and challenges for large-scale deployment

The current study describes the characteristics of the modular open-source ICT platform conceived to cover the requirements for deployment of the NEXES' field studies [10]. The platform (Linkcare®) has been operational during the project lifetime in one of Barcelona's Health Care Districts accounting for 540.000 inhabitants, showing potential for further deployment at regional level. Overall, Linkcare® incorporates *integrated care clinical process logics* allowing patient-centered management with high potential for both patient-specific and provider-specific customization. Ultimately, only the core of the platform encoding ICS-specific process logic is required for deployment. Either the presentation or the data tiers can be accommodated to site-specific requirements.

Linkcare® has adopted a Health Information Sharing (HI-Sharing) approach that allows sharing data over complex processes without having to make changes to the corporate HIS or EHR data structures. In this sense, all patient information gathered and managed by the Linkcare® platform is reused, if possible, from existing EHRs. Otherwise, new data entered to the system (e.g. patient

remote monitoring measurements, patient answers to questionnaires, etc.) can be then delivered to the corresponding EHR. Within this scenario, Linkcare® acts as a common interface for electronic health information that is properly integrated based on the agreed ICS workflow.

Key aspects of Linkcare® have been evolving beyond NEXES and the preparatory strategies for regional deployment have been formulated. The open and modular nature of the Linkcare® platform should facilitate its extensive deployment following the scheme depicted in **Figure 6** and the implementation strategy developed within NEXES for the transfer from a HIE setting to a HI-Sharing in Norway (see Annex I from the Multimedia Appendix 3). As depicted in **Figure 6**, the Integrated Care Shared Knowledge platform (Linkcare®) presented here will support the execution of complex integrated care processes while keeping messaging responsibility on regional Health Information Exchange (the WIFIS project in Catalonia). Currently supported processes have defined a set of reference HL7 messages, which will be extended with the new set of messages that will ensure organizational interoperability between the different healthcare tiers supporting the execution of the each one of ICSs considered for regional deployment. Moreover, patients will access their personalized work plan to perform their tasks throughout the Catalan patient gateway (i.e. Personal Health Folder). In addition to the Personal Health Folder, the Catalan shared electronic health record (HC3), which currently acts as a common digital document repository but will capitalize Health Information Exchange across health sectors, are the two key bridging tools for technical interoperability between the different Catalan Health Sectors.

3.6. Technological lessons

The experience gathered in the other two NEXES sites, Athens and Trondheim, was extremely useful to identify those conditions wherein the implementation of Linkcare® may show different types of limitations.

In Norway, NEXES was deployed in the Central Norwegian Region Health Area (CNRHA) as part of the preparatory phase of the Coordination Reform [23, 24]. Since the very beginning of the project [10], however, it became apparent that the Norwegian legal frame on health data transfer precluded the use of the current Linkcare® platform for deployment of the ICSs. Instead, an alternative nationwide platform based on exchange of electronic messaging among providers (HIE) was used. During the project lifetime, it has been shown that technological support of ICSs based on a pure HIE approach constitutes a clear limitation for the deployment of integrated care being a significant explanatory factor of the lack of effectiveness of the interventions on the Norwegian site in W&R and EC.

In Greece, a core initial version of Linkcare® was used to support the NEXES field studies as an standalone application because of the lack of a fully operational HIS in place, at least until 2011. The project in Athens was developed by qualified and motivated early adopters of ICSs and it

provided valuable information for deployment of chronic care in a highly fragmented health system.

3.7. Future developments

Linkcare® can be used for not only patient management, but also it can also have a role as knowledge sharing tool across healthcare sectors. Most importantly, it can evolve as a platform bridging healthcare sectors with informal care (i.e. life style management or case finding programs run by informal careers) [25, 26] through integration of the personal health folder already assessed in NEXES, as part of the Wellness and Rehabilitation ICS [27]. Moreover, Linkcare® also shows possibilities as a tool bridging formal healthcare with bioscience research [28]. All this potential leads to new exciting challenges that will need to be faced to successfully pave the way for the development of the future 4P (Predictive, Preventive, Personalized and Participatory) medicine for patients with chronic conditions.

4. Conclusions

The Integrated Care Shared Knowledge platform (Linkcare®) successfully provided technical support, considering ICSs as the archetypal coordination model, for the management of the four complex ICS assessed in NEXES [12]. Linkcare® builds on top of Health Information Exchange to facilitate large-scale deployment of integrated care because it facilitates the transfer of complexity from specialized care to the community and to patients' home.

5. Availability and requirements

- **Project name**: Linkcare API
- **Project home page**: http://wiki.linkcare.cat
- **Operating system(s)**: Platform independent
- **Programming language**: Any SOAP compliant client
- **Other requirements**: SaaS subscription
- **License**: CREATIVE COMMONS
- **Any restrictions to use by non-academics**: commercial license needed for commercial distribution

6. Ethics

This research has been carried out within an appropriate ethical framework, the ethical approval has been granted for the correct execution of the NEXES project from the Ethics Committee for Clinical Research from Hospital Clínic de Barcelona. Registry 2012/7651, and informed consents to participate in the study have been properly obtained from participants.

7. List of abbreviations

BPMN:	business process modelling notation
CDSS	Clinical decision support systems
EAI	enterprise application integration
EHR:	electronic health record
EU:	European Union
HIE	Health information exchange
HIS:	health information system
ICS:	integrated care service
ICT:	information and communication technologies
MAST	method for the assessment of telemedicine applications
SOAP	simple object access protocol

8. Competing Interests

Juan I Martinez-Roldan is the CEO of Linkcare HS. AA, CH, FB, JIM and JR have financial competing interests.

9. Authors' contributions

AA, CH, FB and JR made substantial contributions to conception and design of the four Integrated Care Services (ICSs) and consequent functional and non-functional requirements to be considered when designing and developing the Integrated Care Share Knowledge Platform (Linkcare®). IC, AA, CH, FB, JIMR and JR assist to construct, test and deploy the Linkcare® platform. IC, AA, JI MR and JR participated in drafting the article and revising it critically for important intellectual content and gave final approval of the version to be submitted and any revised version.

10. Acknowledgements

The study have been funded by the NEXES European project (CIP-ICT-PSP-2007-225025) and the PITES national project (PI09/90634 and PI12/01241).

Special thanks to the NEXES consortium:

Hospital Clinic de Barcelona – Institut d'investigacions Biomèdiques August Pi i Sunyer (IDIBAPS), Barcelona, Catalonia: Josep Roca (Project Coordinator), Albert Alonso, Anael Barberán, Felip Burgos, Isaac Cano and Carme Hernàndez.

Central Norway Regional Health Authority (CNRHA), Trondheim, Norway: Anders Grimsmo, Arild Pedersen and Sigmund Simonsen.

Trondheim City Council, Trondheim, Norway: Helge Gåresen, Klara Borgen.

Saint Olav's Hospital HF, Trondheim, Norway: Stian Saur.

1st YPE of Attica – Sotiria Hospital, Athens, Greece: Theodore Vontetsianos, Alexis Milsis and Thodoris Katsaras.

1st Department of Respiratory Medicine, National and Kapodistrian University of Athens, Athens, Greece: Ioannis Vogiatzis

Santair SA, Athens, Greece: George Vidalis.

Linkcare HS, Barcelona, Catalonia: Joan Ignasi Martínez (JIM) Roldán.

Stiftelsen Sintef, Trondheim, Norway: Babak Farshchian, Joe Gorman, Leendert Wienhofen

Intracom Telecom, Athens, Greece: Ilias Lamprinos

Fundació TicSalut, Barcelona, Catalonia: Josep Manyach and Montse Meya.

TXT e-solutions, Milano, Italy: Salvatore Virtuoso

Telefónica I+D, Barcelona, Catalonia: Jordi Rovira

11. Multimedia Appendix 1
Linkcare® technical requirements and list of currently available forms.

12. Multimedia Appendix 2
Linkcare® web services technical specification.

13. Multimedia Appendix 3
Lessons Learnt in the Validation Trials and Supporting Investigations.

References
1. WHO, *2008-2013 Action Plan for the Global Strategy for the Prevention and Control of Noncommunicable Diseases, ISBN: 9789241597418, URL:http://www.who.int/nmh/Actionplan-PC-NCD-2008.pdf. Accessed: 2013-08-20. (Archived by WebCite® at http://www.webcitation.org/6J0XGnHcJ)*.
2. WHO, *World Health Statistics 2010. URL:http://www.who.int/whosis/whostat/EN_WHS10_Full.pdf. Accessed: 2013-08-20. (Archived by WebCite® at http://www.webcitation.org/6J0XngNEO)*.
3. EU, C., *Innovative approaches for chronic diseases in public health and healthcare systems. Council of the EU 3053rd Employment, social policy health and consumer affairs.*, 2010.
4. Auffray, C., Z. Chen, L. Hood, *Systems medicine: the future of medical genomics and healthcare.* Genome Med, 2009. **1**: p. 2. PMID: 19348689.
5. Auffray, C., D. Charron, L. Hood, *Predictive, preventive, personalized and participatory medicine: back to the future.* Genome Medicine, 2010. **2**(8): p. 57. PMID: 20804580.

6. Organization, W.H., *How Can Telehealth Help in the Provision of Integrated Care?*2010: World Health Organization.
7. WHO, *Innovative Care for Chronic Conditions: Building Blocks for Action. Geneva: World Health Organization (WHO/MNC/CCH/02.01). URL:http://www.who.int/chp/knowledge/publications/icccreport/en/. Accessed: 2013-08-20. (Archived by WebCite® at http://www.webcitation.org/6J0iTPMcg).* Geneva: World Health Organization, 2002.
8. Chen, C., T. Garrido, D. Chock, G. Okawa, L. Liang, *The Kaiser Permanente Electronic Health Record: transforming and streamlining modalities of care.* Health Aff (Millwood), 2009. **28**(2): p. 323-33. PMID: 19275987.
9. Saleem, J.J., M.E. Flanagan, N.R. Wilck, J. Demetriades, B.N. Doebbeling, *The next-generation electronic health record: perspectives of key leaders from the US Department of Veterans Affairs.* J Am Med Inform Assoc, 2013. **20**(e1): p. e175-7. PMID: 3715365.
10. NEXES, *Supporting Healthier and Independent Living for Chronic Patients and Elderly.* CIP-ICT-PSP-225025, 2008-2013.
11. Allweyer, T., *BPMN 2.0: Introduction to the Standard for Business Process Modeling.* 2010: Books on Demand GmbH. ISBN: 9783839149850.
12. Hernandez, C., J. Garcia-Aymerich, A. Alonso, A. Grimsmo, T. Vontetsianos, F. Garcia-Cuyas, A. Garcia-Altes, I. Vogiatzis, H. Garåsen, L. Pellise, L. Wienhofen, I. Cano, M. Meya, M. Moharra, J. Martinez, J. Escarrabill, J. Roca, *Lessons Learnt from the Deployment of Integrated Care Services for Chronic Patients in the NEXES Project: Barriers and Site Strategies.* Submitted to IJIC., 2014.
13. Linthicum, D.S., *Enterprise Application Integration*2000: Addison-Wesley. ISBN: 9780201615838.
14. Parliament, E., *Directive 95/46/EC of the European Parliament and of the Council of 24 October 1995 on the protection of individuals with regard to the processing of personal data and on the free movement of such data, Off. J.L. 281 (Nov. 23, 1995)("Data Protection Directive").* 1995
15. Parliament, E., *Directive 2002/58/EC of the European Parliament and of the Council of 12 July 2002 concerning the processing of personal data and the protection of privacy in the electronic communications sector, Off. J.L. 201, 31.7.2002, at 37. (Directive on Privacy and Electronic Communications).* 2002.
16. Quinn, P., P. De Hert, *The Patients' Rights Directive (2011/24/EU) – Providing (some) rights to EU residents seeking healthcare in other Member States.* Computer Law & Security Review, 2011. **27**(5): p. 497-502.

17. SMART, *Study on the Legal Framework for Interoperable eHealth in Europe* URL:http://www.ehealthnews.eu/images/stories/pdf/ehealth-legal-fmwk-final-report.pdf. Accessed: 2013-08-20. (Archived by WebCite® at http://www.webcitation.org/6J0kRlL0R), 2009.
18. Cheng, M., W.H. Organization, *Medical Device Regulations: Global Overview and Guiding Principles*2003: World Health Organization. ISBN: 9789241546188.
19. Eccleston, R.C., *A model regulatory program for medical devices: an international guide*2001: Pan American Health Organization. ISBN: 9789275123454.
20. Cheng, M., *A guide for the development of medical device regulations*2002: Pan American Health Organization. ISBN: 9789275123720.
21. Catwell, L., A. Sheikh, *Evaluating eHealth Interventions: The Need for Continuous Systemic Evaluation.* PLoS Med, 2009. **6**(8): p. e1000126. PMID: 19688038.
22. *Linkcare Mobility App. URL:https://play.google.com/store/apps/details?id=net.genaker.linkcare. Accessed: 2013-08-20. (Archived by WebCite® at http://www.webcitation.org/6J0YJZwJH)*. 2013.
23. Heimly, V., J. Hygen, *The Norwegian Coordination Reform and the Role of Electronic Collaboration.* Electronic Journal of Health Informatics, 2011. **6**(4).
24. *The Coordination Reform. Norwegian Ministry of Care and Health Services. Summary in English. URL:http://www.regjeringen.no/upload/HOD/Samhandling%20engelsk_PDFS.pdf. Accessed: 2013-08-20. (Archived by WebCite® at http://www.webcitation.org/6J0lPseWQ).* Report 47 to the storting, 2008-09.
25. Burgos, F., C. Disdier, E.L. de Santamaria, B. Galdiz, N. Roger, M.L. Rivera, R. Hervas, E. Duran-Tauleria, J. Garcia-Aymerich, J. Roca, *Telemedicine enhances quality of forced spirometry in primary care.* Eur Respir J, 2012. **39**(6): p. 1313-8. PMID: 22075488.
26. Castillo, D., R. Guayta, J. Giner, F. Burgos, C. Capdevila, J.B. Soriano, M. Barau, P. Casan, *COPD case finding by spirometry in high-risk customers of urban community pharmacies: a pilot study.* Respir Med, 2009. **103**(6): p. 839-45. PMID: 19200706.
27. Barberan-Garcia A, V.I., Golberg HS, Vilaró J, Rodriguez DA, Garåsen HM, Troosters T, Garcia-Aymerich J, Roca J and NEXES consortium, *Effects and barriers to deployment of telehealth wellness programs for chronic patients across 3 European countries.* Respir Med, 2014. **108**(4): p. 9.
28. Jensen, P.B., L.J. Jensen, S. Brunak, *Mining electronic health records: towards better research applications and clinical care.* Nat Rev Genet, 2012. **13**(6): p. 395-405.

Tables

Table 1. Ten principal features of the Integrated Care Shared Knowledge platform (Linkcare®).

1. Supports the clinical process logics of Integrated Care Services
2. Highly customizable to both patient and site characteristics
3. Technical interoperability with Electronic Health Records across healthcare tiers, directly or via in-place Health Information Exchange
4. The implementation does not require replacement of pre-existing proprietary Electronic Health Records
5. Key technical elements for organizational Interoperability at a health system level
6. Open source
7. Three-tier architecture
8. Integration with Clinical Decision Support Systems
9. Compliant with knowledge management tools
10. Potential for bridging with informal care and biomedical research

Figures

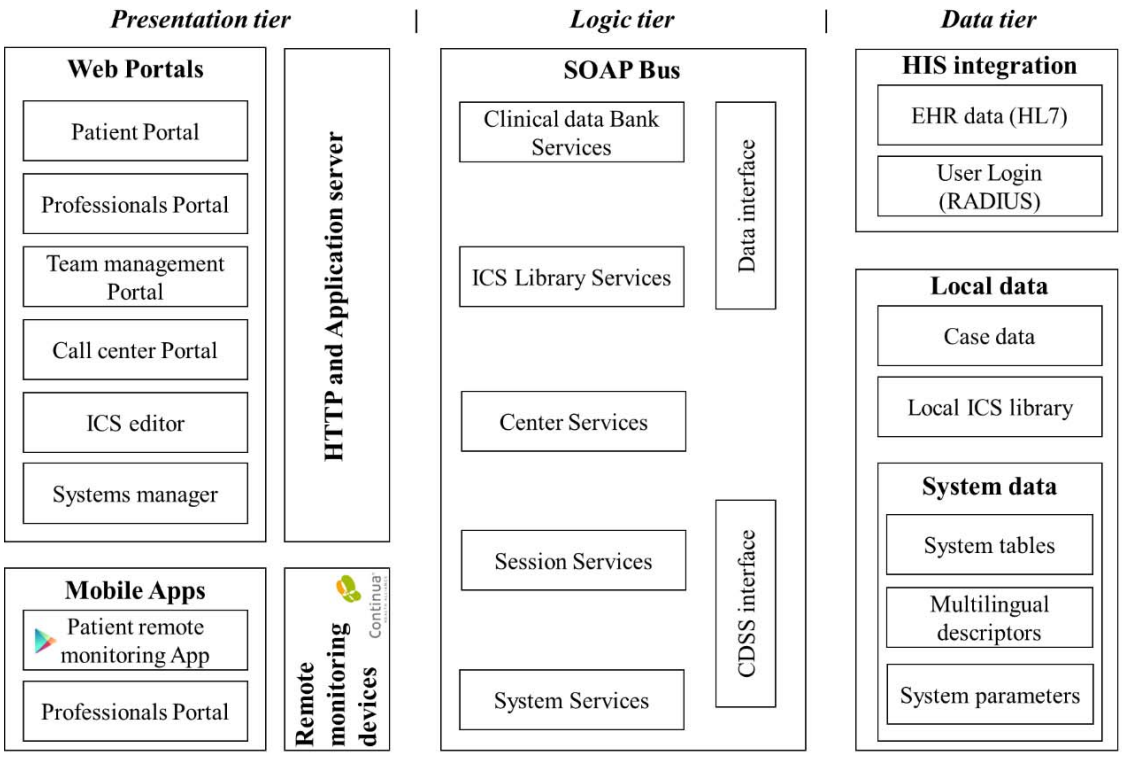

Figure 1. Three-tier architecture of the Linkcare® platform. This multitier architecture allows separating the presentation or graphical user interface, business or application and data management logics, which permits the option of modifying or adding a specific layer, without reworking the entire application, in response to changes in requirements or technology.

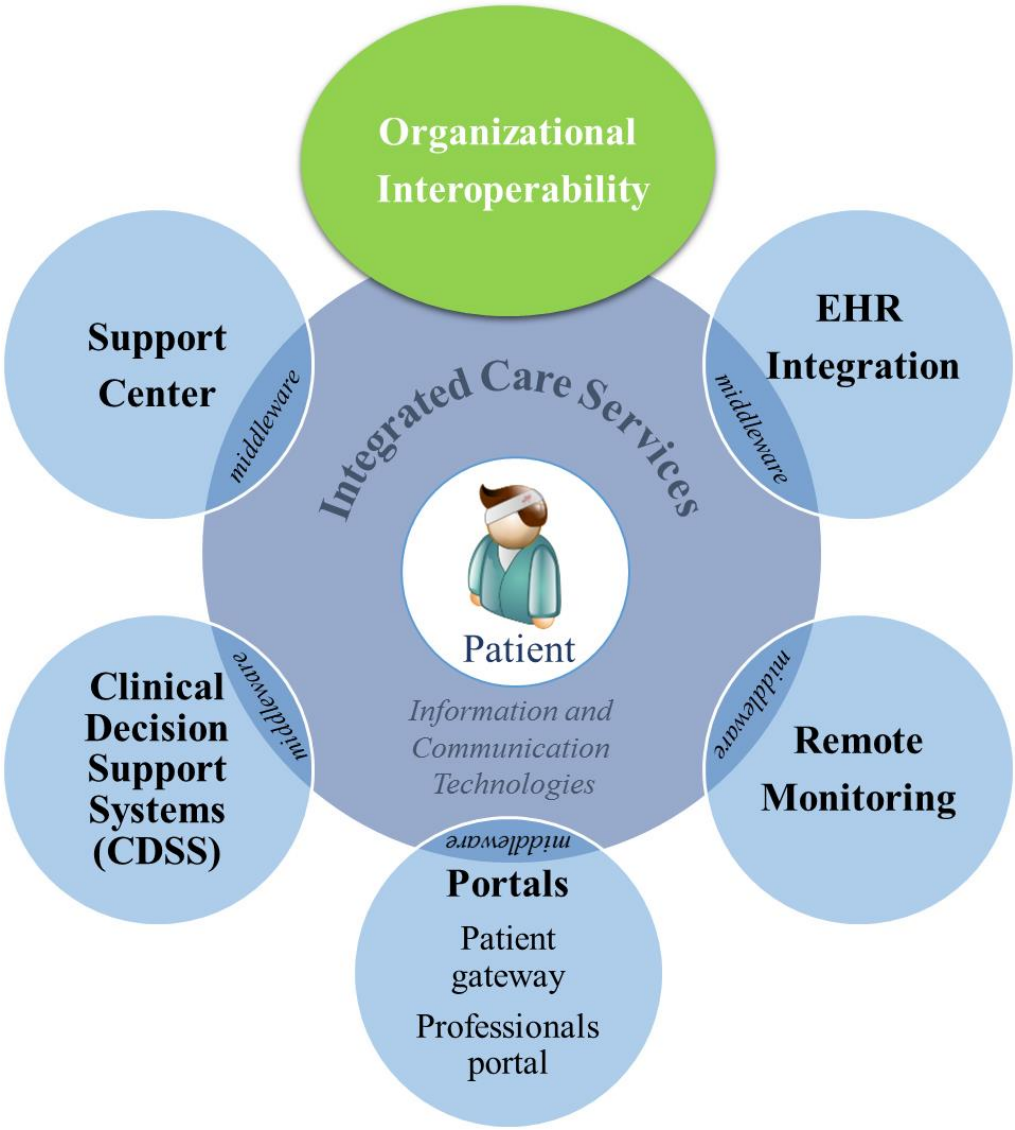

Figure 2. Based on patient-centered ICSs, the Linkcare® platform provides key technical elements for organizational interoperability between healthcare professionals from various tiers of care and enhances accessibility and proactivity of both patients and caregivers. This is thanks to specific functionalities attached to the Linkcare® platform via interoperability middlewares. These functionalities facilitate access via the support center and portals. The traditional call center functionalities are enriched with novel patient gateways and portals for healthcare professionals. Other interesting features are patient empowerment for self-management of his/her condition with remote monitoring, integration with site-level Electronic Health Records (EHR) and automated clinical decision support.

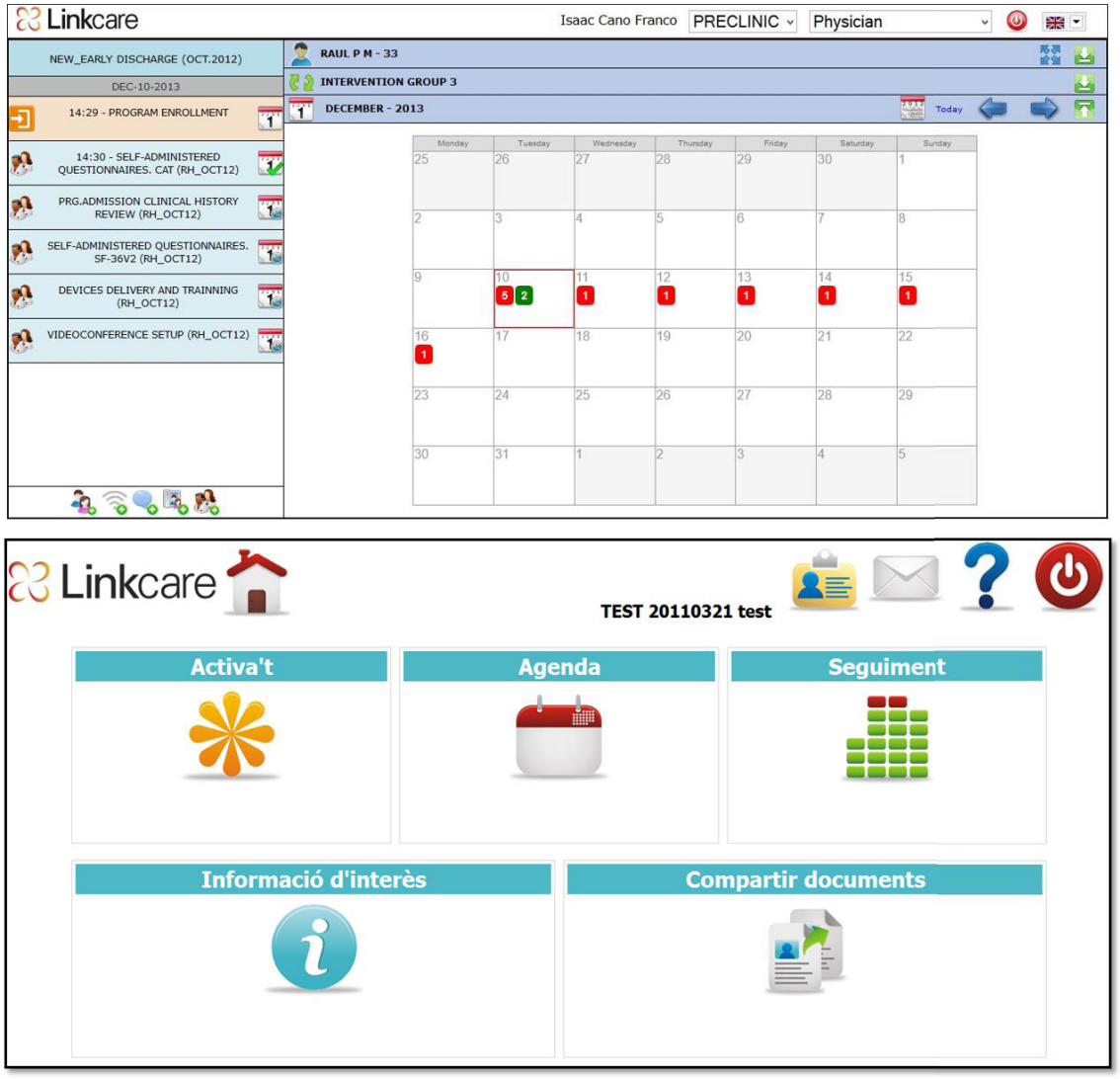

Figure 3. The upper panel shows the Linkcare® web-based user interface for healthcare professionals, which provides an overview of the patient information, a calendar view of the patient's work plan status and a set of tools for work plan follow-up and personalization. The lower panel shows the home page of the Linkcare® patient gateway used to support the wellness and rehabilitation ICS evaluated in the NEXES project. From this home page, patients can access to their optional ("ACTIVA'T") and scheduled ("AGENDA") interventions, patients can easily review their follow-up ("SEGUIMENT"), check educational information ("INFORMACIÓ D'INTERÈS") and finally send patient's documents of their choice to professionals ("COMPARTIR DOCUMENTS").

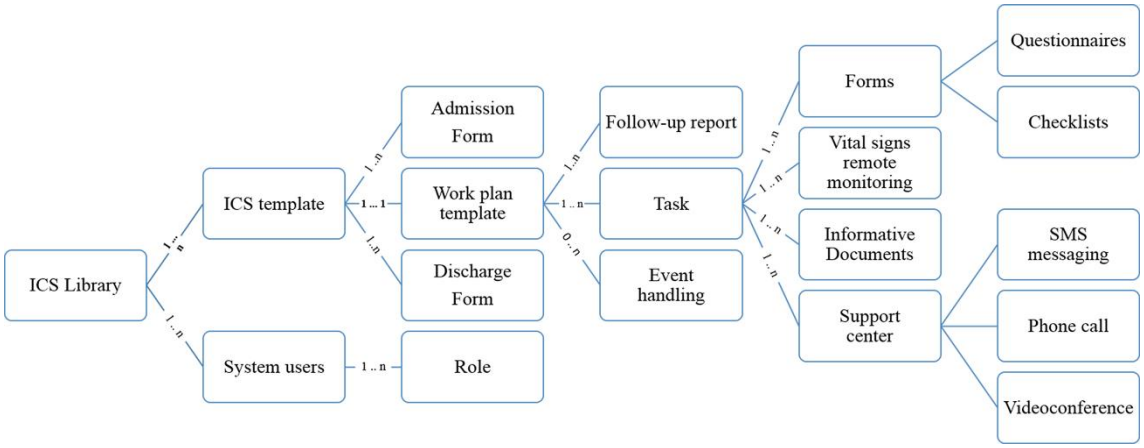

Figure 4. Linkcare® relational entities that support the creation and edition of ICSs. The Library of ICSs contains the set of available ICS templates and the system users potentially having a role in ICS management and execution. ICS templates are composed of admission and discharge form templates and a customizable work plan, which is used as the reference guide for the scheduling of tasks and the generation of follow-up reports. Finally, event handling is provided during the execution of the patient-specific work plan.

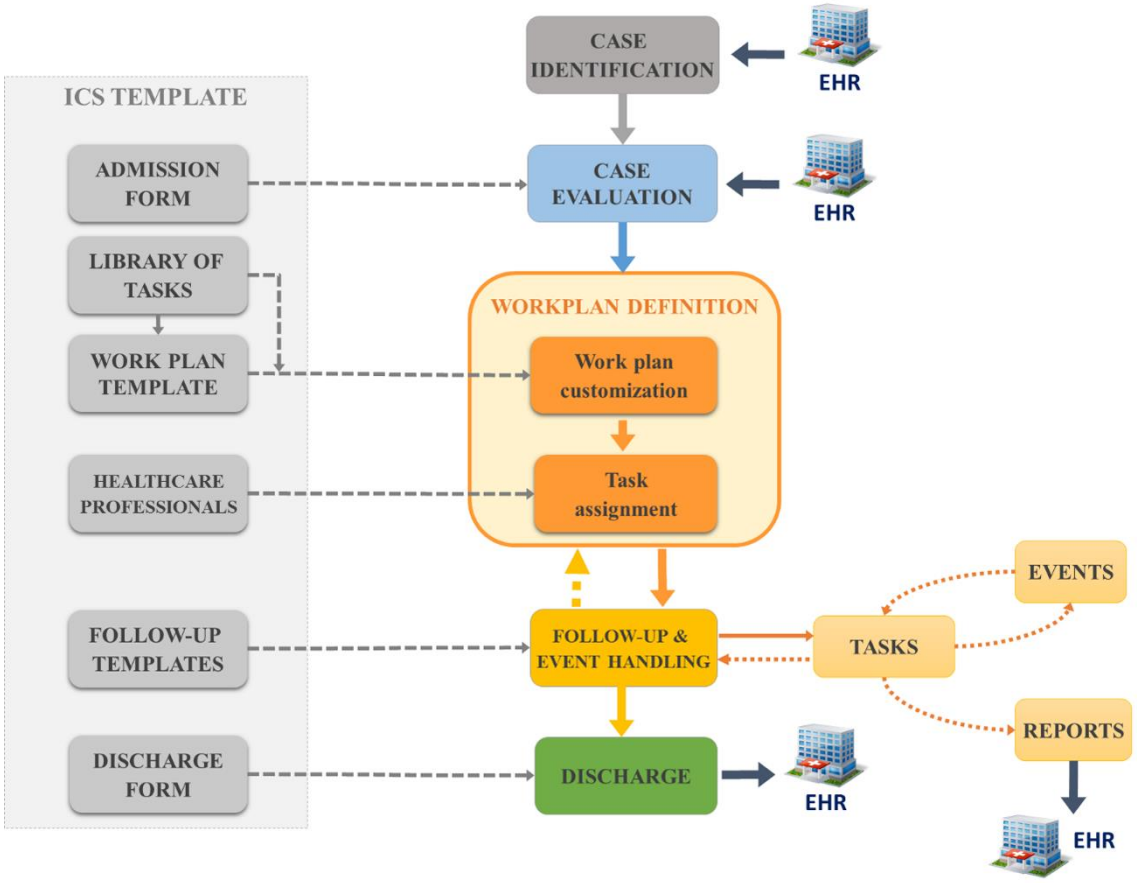

Figure 5. Linkcare® workflow for ICS management and execution. The corresponding ICS template is used as a library of resources for the correct customization and execution of the ICS workflow. Integration with corporate EHR allows instant access to required patient information for case identification and evaluation, avoid data duplicity and preserve the current corporate clinical data chain of custody. Follow-up and discharge reports can also be sent to the corporate EHR to keep trace of the ICS execution as part of the patient clinical episodes.

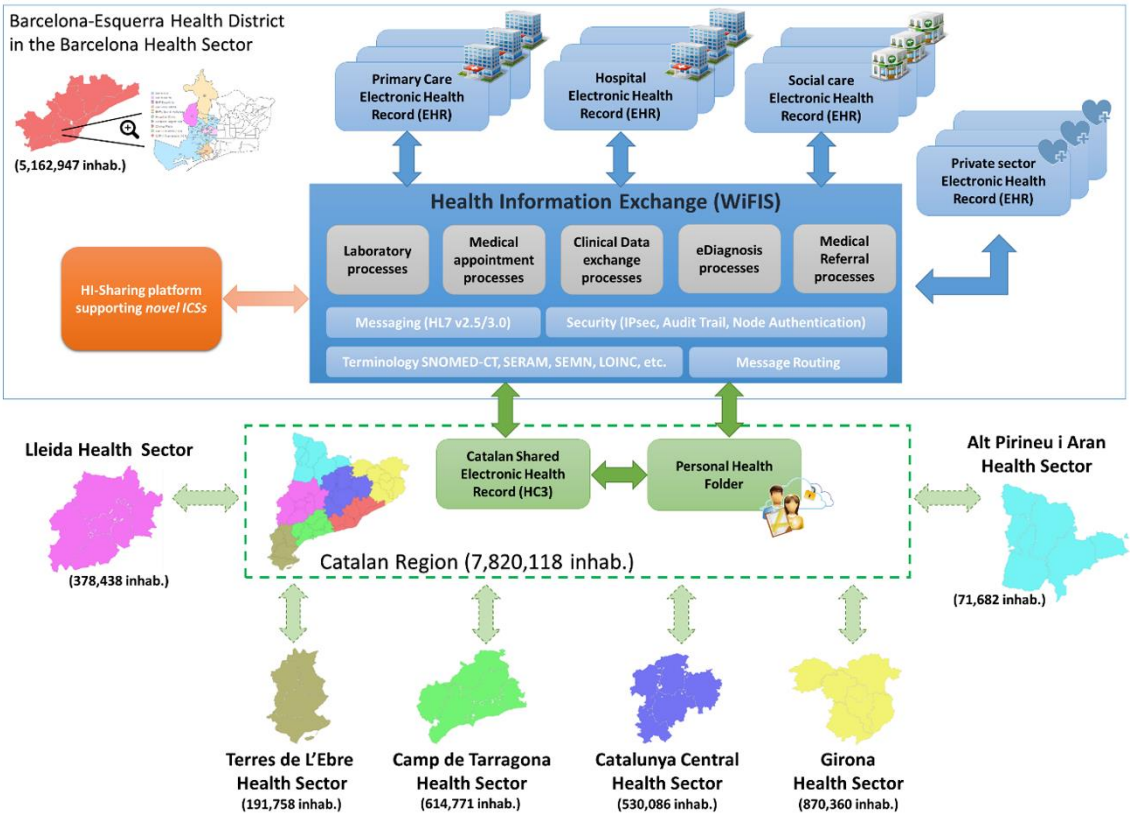

Figure 6. Interoperability framework for the regional deployment of the current HI-Sharing platform (Linkcare® - orange box) in a Catalan Health district and/or sector level. The Catalan Region has seven different healthcare sectors depicted in the figure. The sectorial HIE framework (i.e. the Catalan WiFIS standard) integrate basic highly standardized processes, namely: medical appointments, clinical data exchange, medical referral, etc., among healthcare providers with heterogeneous proprietary systems. In this scenario, the deployment of novel ICSs will be supported by the HI-Sharing platform (Linkcare®) described in the current study. At regional level, the Catalan Shared Electronic Health Record (HC3) currently acts as the common repository for health data exchange. However, it could also perform sectorial message routing and message delivery control. Finally, citizens can access their health related data via a Personal Health Folder (PHF) connected to the HC3. The PHF can also act as the citizen entry point for some of the supported processes (e.g. Medical appointments, participation in ICSs, etc.) and informal health data sources (e.g. mobile health applications, community medical devices, etc.). The NEXES project has shown a high potential of the PHF to support patient's empowerment for self-management and healthier life styles [27].

Manuscript 6:

Biomedical Research in a Digital Health Framework.

Cano I, Lluch-Ariet M, Gomez-Cabrero D, Maier D, Kalko S. G, Cascante M, Tégner J, Miralles F, Herrera D, Roca J and the Synergy-COPD consortium.

Accepted for publication in BMC Journal of Translational Medicine, 2014.

Biomedical Research in a Digital Health Framework

I. Cano[1*], M. Lluch-Ariet[2], D. Gomez-Cabrero[3], Dieter Maier[4], S. G. Kalko[1], Marta Cascante[1], J. Tégner[3], F. Miralles[2], D. Herrera[5], J. Roca[1] and the Synergy-COPD consortium

Affiliations

[1] IDIBAPS-Hospital Clínic, CIBERES, Universitat de Barcelona, 08036, Barcelona, Catalunya, Spain.

[2] Department of eHealth, Barcelona Digital, Roc Boronat 117, 08017 Barcelona, Catalunya, Spain.

[3] Unit of Computational Medicine, Department of Medicine, Center for Molecular Medicine, Karolinska Institutet, Karolinska University Hospital, Stockholm, Sweden.

[4] Biomax Informatics AG, Robert-Koch-Str. 2, Planegg, Germany.

[5] Almirall R&D, Laureà Miró 408-410, 08980 Sant Feliu de Llobregat, Barcelona.

Correspondence

* Isaac Cano, MSc, IDIBAPS Research Institute, C/Villarroel 170, 08036, Barcelona, Spain. Phone: 34 932 275 747, Fax: 34 932 275 455, Email: iscano@clinic.ub.es

Running Title

The Digital Health Framework

Abstract

This article describes a Digital Health Framework (DHF), benefitting from the lessons learnt during the three-year life span of the FP7 Synergy-COPD project. The DHF aims to embrace the emerging requirements – data and tools – of applying systems medicine into healthcare with a three-tier strategy articulating formal healthcare, informal care and biomedical research. Accordingly, it has been constructed based on three key building blocks, namely, novel integrated care services with the support of information and communication technologies, a personal health folder (PHF) and a biomedical research environment (DHF-research). Details on the functional requirements and necessary components of the DHF-research are extensively presented. Finally, the specifics of the building blocks strategy for deployment of the DHF, as well as the steps toward adoption are analyzed. The proposed architectural solutions and implementation steps constitute a pivotal strategy to foster and enable 4P medicine (Predictive, Preventive, Personalized and Participatory) in practice and should provide a head start to any community and institution currently considering to implement a biomedical research platform.

Key words: *Biomedical Research, Chronic care, Clinical Decision Support Systems, Integrated Health Care Systems, Patient Decision Support Systems, Personal Health Folder*

1. Background

The seminal purpose of the systems medicine design [1] conceived for the Synergy-COPD project [2] was to generate knowledge on underlying mechanisms explaining heterogeneities observed in chronic obstructive pulmonary disease (COPD) patients. The ultimate aim of the project was to use such knowledge to refine patient's stratification, prognosis and treatment response, which then should lead to efficient preventive strategies aiming at modulating disease progress while reducing the burden of COPD on healthcare.

It is well accepted that predictive medicine is opening entirely new and fascinating scenarios for the interplay between clinical practice and biomedical research. However, at the same time, it is generating novel requirements with impact on adoption. Firstly, the need for multilevel integration of heterogeneous patient information (**Figure 1**), namely: socio-economical, life-style, behavioral, clinical, physiological, cellular and "omics" data [3] and their use for the design of a personalized digital patient from virtual physiological models. Secondly, the need to extend current trends on open data from the biomedical community [4] to the clinical practice and the whole society, by engaging citizens and solving privacy and regulatory constraints, Finally, the need for highly applicable user-profiled functionalities for data management and knowledge generation. Accordingly, innovative and robust Information and Communication Technologies

(ICT) will be needed as supporting tools to overcome well-identified current functional limitations [5].

The concept of **Digital Health Framework** (DHF) (**Figure 2**) emerged from the Synergy-COPD project to foster adoption of predictive medicine. The DHF consists of the articulation of open and modular ICT components supporting organizational interoperability, and appropriate functionalities, among three main areas, namely: i) informal care, ii) formal care, and, iii) biomedical research. Briefly, informal care includes any aspect with impact on health (e.g. life style, environmental and behavioral aspects, etc.) occurring in the community, whereas formal care refers to any interaction with health professionals at different levels of the healthcare system. Biomedical research refers to all research levels from bench to clinical and to public health. In our hands, to materialize such an ambitious vision, a building block approach is considered necessary. Moreover, the progress from the initial proof-of-concept to pilot implementation and to extensive deployment shall be planned following a stepwise strategy.

The first building-block was the design and initial deployment of an open source **Integrated Care Shared Knowledge Platform** supporting Integrated Care Services (ICS) for chronic patients [6], initiated at the EU project NEXES [7]. During the life span of NEXES, a **Personal Health Folder (PHF)** was successfully piloted [8], as a supporting tool to achieve long-term sustainability of training-induced effects and promote active life styles in COPD patients. The PHF constitutes the second building block currently being implemented in a health district (Barcelona-Esquerra, 540.000 inhabitants) in Barcelona as a tool to integrate informal and formal care in community-based ICS for frail chronic patients [9]. Moreover, the **Clinical Decision Support Systems (CDSS)** generated during the Synergy-COPD lifetime (described in the "Clinical Decision Support Systems (CDSS) for preventive management of COPD patients" chapter of the current monograph) has been integrated into the platform supporting ICS [6]. Consequently, the interplay between the first two building blocks (informal and formal care) is operational in a controlled deployment scenario and is currently evolving toward maturity. We shall keep in mind, however, that active citizens/patients together with a prepared multidisciplinary health workforce will be the real key drivers of the transition from current healthcare practice to full deployment of predictive medicine for chronic patients.

The current report focuses on the third building block of the DHF, tackling biomedical research (DHF-research). The manuscript analyses architectural design, functionalities and implementation strategies of interoperability between healthcare and biomedical research.

2. Progress from this paper

We report on the key elements needed for the design of the DHF-research, showing interoperability with the open Integrated Care Shared Knowledge Platform already operational in the Barcelona-Esquerra health district. From the methodological standpoint, the manuscript performs a systematic description of the DHF-research architecture and functionalities based on the lessons learnt in Synergy-COPD indicating the contributions beyond the current state of the art. The expected outcome of the manuscript is to generate a proof-of-concept of the DHF-research component as well as to propose strategies for its assessment and future implementation.

3. The DHF principles: lessons learned from the Synergy-COPD project.

3.1. *Main actors of the DHF*

Table 1 describes the profiles of typical actors in the DHF: biomedical research actors (Clinical and Basic scientists), healthcare actors (specialized and primary care), and three patient profiles corresponding to three possible COPD status (moderate COPD, complex COPD and COPD with comorbid conditions). Furthermore, the three patient profiles represent different levels of stratification and personalized therapeutic strategies guided by CDSS. The CDSS is embedded into the Integrated Care Shared Knowledge Platform [6] which, in turn, make summary PHF information available to the clinician. In all three cases, the PHF-PDSS facilitates bidirectional interactions between patients and health professionals toward improving adherence to treatment, patient empowerment of his/her health status and interfacing with informal and social care [8]. Finally, the professionals with **research roles** will be using the **biomedical research platform (DHF-research)**, which has as data sources clinical information (through the Integrated Care Shared Knowledge Platform) as well as heterogeneous public and corporate sources of biomedical research data and the necessary tools to manage and process these data.

Overall, an integrated care scenario provides support to organizational and technical interoperability between informal care and healthcare systems, which in turn feeds the DHF-research with controlled and standardized clinical information for off-line research purposes. As an example, the Synergy-COPD project identified that oxidative stress may play a central role in COPD-complex and COPD-co-morb such that research professionals (with translational clinical and basic background) cooperate using the DHF-research to further explore other poorly known mechanisms and to generate combined biomarkers to assess novel therapeutic strategies in the clinical scenario. The DHF-research should be shaped to provide user-profiled functionalities such that research professionals with different profiles can make use of it, ultimately leading to the generation of novel rules that should feed in-place CDSS and PDSS.

3.2. *Functional principles*

Based on the storyboard presented in the previous section we identified three key functional principles for the correct adoption of the DHF-research, namely: *(i)* data standardization strategies and open data policies, toward technical, syntactic and semantic interoperability between clinical data systems and biomedical research platforms, taking into account the privacy challenges of biomedical data sharing; *(ii)* profile-specific visual data mining functionalities covering the disparate needs and backgrounds of the DHF actors; and finally *(iii)* profile-specific environments supporting multi-scale predictive modelling and several forms of complex data analytics.

3.3. *Architectural principles*

The DHF-research architecture considers specific components to cover the need for organizational interoperability between research professionals working together over the same hypothesis and study design, as identified during the execution of Synergy-COPD. Moreover, general architectural principles are considered toward an open source solution with a rich set of functionalities empowering knowledge sharing, data querying and data analytics by means of a distributed, multi-layer, service oriented and ontology-driven architecture.

3.4. *Ethical and legal issues*

The evolving European legislation on health data transfer and security [10-13] was analyzed and taken into account for the design of each of the three components of the DHF (**Figure 2**) and facilitate the empowerment of patients to open their personal clinical data and derived studies to the scientific community.

3.5. *Deployment strategies and assessment*

The three building blocks of the DHF (**Figure 2**) have independent deployment strategies all of them with a stepwise approach. The DHF-research is in an early phase of the design of the proof-of-concept generated from the lessons learnt in the Synergy-COPD project. Steps for a proper validation and identification of strategies for deployment were defined in the study.

4. Description of the components and functionalities of the DHF-research

The Synergy-COPD project prompted the identification of three pivotal layers of the DHF-research, depicted in **Figure 3**, to support the research functionalities presented in subsection **3.1**: *i)* a semi-automatic data mapping, consistency, and standardization layer; *ii)* an integrative knowledge management layer to gather and integrate clinical and biomedical knowledge coming from various healthcare electronic health systems and research information systems, as well as public databases; and, *iii)* to build on top of the knowledge management layer, a qualitative and

quantitative data exploitation layer with profile-specific visual data mining user-profiled interfaces.

In the standardization layer displayed at the bottom of **Figure 3**, mapping, consistency, and standardization of clinical data will primarily rely on in-place health information exchange (HIE) infrastructures, where standard terminology (e.g. SNOMED-CT, SERAM, SEMN, LOINC, etc.), message encoding (e.g. HL7 2.x / 3.x, MLHIM, openEHR, ISO 13606, etc.), message routing and Security (e.g. IPSec, Audit trail, Node authentication, etc.) will be used. Moreover, the HIE infrastructure will provide the required technical and syntactic interoperability to support the information exchange requirements inherent to the logics of integrated care processes. Specifically, the DHF considers the use of an open source Integrated Care Shared Knowledge Platform designed to support the execution of ICS [6], which allows to normalize the process logics of ICS to a common legacy schema or data model. Similarly, standardization of biomedical research data and metadata (ISA-Tab [14], MIAME, etc.) is a required task before its connection to the knowledge management layer. This step will not be required for those public biomedical research data sources already standardized (e.g. Ensembl, Uniprot and KEGG). The ICS Knowledge Platform also considers integration with personal health folders, so that valuable data generated outside the boundaries of formal healthcare institutions, such as self-management questionnaires and applications, genomic and biomedical data, will be gathered and effectively incorporated into the formal care arena in the context of an integrated care service prescribing interactions with patients via the personal health folder. Ultimately, data normalization and curation is the responsibility of each data source before interfacing with the knowledge management system. However, each data source should agree with the knowledge management layer how to effectively ensure data normalization. Finally, each data source should make use of their specific front-end interfacing to effectively support the normalization and curation of already existing data, or to support the normalization of the data right at the data source (e.g. questionnaires, lab tests, etc.).

Once all input data sources are properly encoded to a reduced set of common vocabularies and metadata schemas, and the exploitation rights granted, a knowledge management layer (as depicted in the middle of **Figure 3**) should allow the investigator to first integrate [15] and then to manage all of the above DHF-research information assets with easy to use and agile knowledge management graphical user web interfaces. The proprietary knowledge management solution assessed during the execution of the Synergy-COPD project [16] was based on the concept of knowledge as network by abstracting commonly used concepts and knowledge into objects and their relations. In addition, it bridged multiple sources and scales of knowledge and various deterministic and probabilistic models with a systems biology approach. Structuring explicit and implicit knowledge into these formal concepts enabled the use of existing well-defined

vocabularies (e.g. GO, ICD10) and standards (e.g. SBML, HL7) to couple true semantic integration (i.e. the mapping of equivalent meaning and objects) across all information types relevant in translational research with a flexible and extensible data model, ensuring robustness against structural changes in services and data, transparent usage, and low set-up and maintenance requirements. This knowledge management layer may also facilitate non-technological aspects of human and cultural dimensions to effectively enable information and knowledge sharing.

Finally, this leads to the exploitation layer as displayed in the upper side of **Figure 3** wherein potential use of profile-specific visual data exploitation portals are considered to support agile data querying at first and facilitating posterior data analytics. The latter will include a simulation environment capable of facilitating the user-friendly simulation of multi-scale predictive models, from common descriptive analytics to complex modelling approaches.

The user-profiled portals ought to be primarily used by the two research actors of the DHF, the clinical and the basic scientist (**Table1**), allowing them, for example, to mine registered information to gain insight into mechanisms leading from health to disease transition and to study disease natural evolution, as well as interactions among diseases. Initial search, retrieval and R-plugin based data mining methods integrated into the Synergy-COPD knowledge base (described in "*The Synergy-COPD Knowledge Base: a data exploitation approach*" chapter of the current monograph) enabled the retrieval of disease or case specific sub-networks by expert users but the validation showed that to enable application by clinical researchers a simplification of the user interface was required. To this end, the DHF-research considers the use of agile data querying interfaces such as those powered by the BioMart [17, 18] platform, used in the international cancer genome consortium (ICGC) Data Portal [19]. However, connectors to the R programming language should be available to accommodate for the needs of basic researchers having a bioinformatics profile. In addition, standard data analytic tools commonly used by clinical researchers should be made available within the exploitation layer. Moreover, such user-profiled portals may include links to new tools such as the Synergy-COPD multi-scale simulation environment (described in the "*Simulation Environment and Graphical Visual Application: a COPD use-case*" chapter of the current monograph), designed to enable the explorative execution of computational models. Ultimately, this data exploitation process should enable the translation of novel biomedical research outcomes into real clinical practice via generation of rules feeding novel CDSS. The latter (CDSS) should be embedded into novel clinical processes defined in terms of integrated care services, so closing the DHF continuous improvement circle.

5. Contributions of the DHF-research beyond the current state of the art

We performed a thorough review of available ICT platforms that have been designed to support biomedical research with a systems approach [20-24]. Unfortunately, the reported information is fragmented and often insufficient to display a complete picture of each translational research platform. We review here the main characteristics of five state of the art initiatives considering the above DHF-research functional layers, namely: data standardization, knowledge management and data exploitation.

Standardization layer - All five systems [20-25] support integration of data encoded using standard terminologies for clinical data entities (e.g. ICD9-CM, SNOMED, LOINC, etc.), but such an extensive use of standard terminologies is more difficult to accomplish in the context of basic biomedical research data adding extra efforts for the appropriate integration of data from different omics levels (e.g. Ensemble database, based on the BioMart project [17, 18]).
A completely differentiating issue is the potential to interoperate with in-place clinical information, as such a functionality was only reported in STRIDE [20] that showed interoperability through a Health Information Exchange (HIE) platform via HL7 RIM messaging. It is of note that none of the five systems analysed [20-24] showed potential to interoperate with chronic care clinical information as described above.
Knowledge management layer – All platforms [20-24] have reported the use of multiple standard terminologies for semantic integration of data from various sources, but none of them describes a complete set of tools for inference analyses as reported in detail in the "*The Synergy-COPD Knowledge Base: a data exploitation approach*" chapter of the current monograph. There is also a clear need to extend the Open Access framework into the clinical and personal perspective.

Exploitation layer – All state of the art translational research platforms offer comprehensive sets of data mining and exploitation tools through unique user portals targeting all types of researchers roles, which necessarily limits acceptability and usability of the system that otherwise could greatly improve with a user-profiled approach. Moreover, current data exploration and data querying tools (such as the i2b2 [22] query tool) show potential to evolve toward more dynamic and agile data exploration capabilities.

The review clearly identified the need for expanding the spectrum of users that should be achievable through a proper user-profiled orientation aiming at enhancing current user interfaces. An open source architecture with a service-oriented approach seems most adequate to build-up innovative business models allowing the continuous developments of enhanced functionalities based on sustainable costs-benefit ratios. Open Data schemas for all kind of data that the DHF integrates, the active role of patients and their empowerment to grant access to their own data, become crucial.

6. Discussion

6.1. *Contributions to a biomedical research scenario for predictive medicine*

The convergence of two major driving forces: *i)* current re-shaping of health systems seeking efficiencies through the alignment with the needs generated by chronic conditions, as discussed in detail in the "*Synergy-COPD: a multidisciplinary approach for understanding and managing a chronic non-communicable disease*" chapter of the current monograph and in [1]), and, *ii)* rapidly evolving perspectives of biomedical knowledge [26] is fostering the transition towards a mature 4P medicine scenario for chronic patients. To the best of our knowledge, Synergy-COPD has provided one of the first relevant technological and biomedical contributions to this transition, using COPD and the analysis of co-morbidities as a use case. But most importantly, the project has identified important gaps, crucial unmet needs and strategic proposals that should help to consolidate the emerging scenario, specifically in the COPD case and in general to other disease areas. In this context, the conceptualization of the components of the DHF-research, as well as the proposals for its effective deployment together with the articulation of biomedical research with both formal and informal care, constitute one of the most significant outcomes of the project.

The deployment of the concepts described in the current report should allow an efficient bidirectional articulation between biomedical research and both healthcare and environmental factors with impact on disease development and activity. By doing so, we can reasonably speculate that preventive strategies modulating the transition from health to disease, as well as disease progress, will be effectively implemented and adopted as part of the future conventional health promotion and healthcare scenario. Finally, it is expected that such future healthcare scenario may influence business innovation in pharmacological industry and healthcare business models by overcoming current fragmentation among informal care, healthcare and biomedical research, which shall have a high impact in shortening time to market for both drug development and drug repositioning. It may also help to foster novel synergies between pharmacological and non-pharmacological therapies.

6.2. *Challenges for deployment of the DHF*

The complexities of the deployment of the three-tier DHF, involving multiple interoperability levels (e.g. technological, organizational-cultural, etc.) and actors, are acknowledged.

Informal Care - Previous experiences using Personal Health Systems [27] in general and with the PHF-PDSS [8] in particular have shown the potential of this tool serving three main purposes: *i)* empowering citizens and patients toward an active role in disease prevention and management, *ii)* favoring collection of structured information on environmental, sociological and behavioral factors influencing health status, as well as informal care interventions, and, *iii)* contributing to

organizational interoperability at health system level. However, practicalities limiting the extensive deployment and adoption of the PHF-PDSS have not been fully solved yet, but all of them seem actionable. These limiting factors encompass a wide spectrum of aspects, namely: technological approaches securing subject identification and data privacy, legal classification of the supporting systems as medical or non-medical devices, design of user-friendly interfaces and business models generating incentives for adoption, and also the interfacing between PHF-PDSS (informal care) and electronic health records (formal healthcare). It is of note, however, that all the above limiting factors are being addressed in several EU regions because the PHF-PDSS is becoming a pivotal component in the reshaping of the health system to face the challenge of chronic conditions.

Formal care – There is increasing evidence that deployment of articulated integrated care services (ICS) covering the entire spectrum of patient severity is a good strategy to enhance health outcomes with cost containment [28]. Different open ICT-platforms and strategies have been proposed to efficiently support the extensive deployment of ICS [28]. Implicit with those strategies are the integration of information collected through the PHF-PDSS (articulation with informal care) and clinical data normalization aiming at facilitating information sharing across healthcare tiers and among territories. **Figure 3** in the current manuscript proposes such open ICT-platforms as a realistic option to integrate citizen information generated in either an informal or a formal care scenario, into biomedical research platforms (DHF-research). We acknowledge, however, that extensive deployment of those systems is still under development. A complementary approach to the proposal indicated in **Figure 3** to facilitate short-term data integration into DHF-research could be the setting of highly curated clinical datasets specifically used for research purposes.

Biomedical research – The deployment of DHF-research proposals displayed in **Figure 3** require stepwise implementation strategies wherein two key aspects clearly emerge as main short-term priorities. Firstly, ICT developments aiming at generating user-friendly portals for clinicians devoted to translational research. A second element is the convergence of on-going developments in the area of knowledge management giving particular priority to the assessment of inter-molecular (proteins, genes, or metabolites) interactions (physical or functional), transcriptional regulation and gene-disease association, that should foster the bridging between omics-generated knowledge and the clinical arena. Finally yet importantly, progresses in this area will be strongly associated to strategies fostering convergence of on-going ICT developments including both open and proprietary approaches. Finally, a relevant area is the design of innovative business models providing sustainability of biomedical research platforms beyond specific research and/or infrastructure projects that triggered the initial settings.

For all three DHF tiers, both legal and ethical aspects ensuring privacy and security of data transfer and management delineate a crucial area to be properly handled. Both data anonymization and encryption strategies have experienced a significant progress contributing to partially solving the problem. However, they show clear limitations in areas such as the management of genetic information wherein data anonymization is a challenge. In addition, the use of data for purposes other than the original data collection aims may generate limitations and activating communities of data donators for scientific purposes with a wider view than current practices is required. Clearly, evolving both legal frames and citizen cultural attitudes will be crucial to achieve a balance between social acceptance of anonymized data sharing together with reasonable levels of security and privacy of data transfer and management.

6.3. *Developments beyond the project lifetime*

We fully acknowledge that the current manuscript only displays basic lessons learnt during the Synergy-COPD project life span. Next immediate steps to be taken before the end of the project are twofold. First, to establish a focus group, including all actors, for the qualitative assessment of the current DHF proposal. The aim of the focus group should be to perform a qualitative assessment of the DHF fitness to transfer the biomedical research use case of Synergy-COPD to more general clinical research needs. Second, to generate structured interactions with well-known international experts in the three tiers of the DHF to prioritize specific steps of the deployment strategy, and, to plan collaborative interactions with selected on-going projects addressing similar aims.

7. Conclusions

The DHF is presented as a comprehensive and coherent ICT strategy supporting emerging requirements of applied systems medicine with novel interactions between informal care, formal healthcare and biomedical research. The current manuscript proposed ICT solutions for the three DHF tiers, extending more its biomedical research component, and stepwise strategies for effective deployment of the concept that should foster implementation of 4P medicine.

8. Competing interests

The authors declare that they have no competing interests.

9. Author's contributions

I. Cano1, M. Lluch-Ariet, D. Gomez-Cabrero, Dieter Maier, S. G. Kalko1, Marta Cascante, J. Tégner, F. Miralles and J. Roca made substantial contributions to conception and design of the Digital Health Framework; I. Cano, M. Lluch-Ariet, Dieter Maier and J. Roca participated in drafting the article; I. Cano1, M. Lluch-Ariet, D. Gomez-Cabrero, Dieter Maier, S. G. Kalko1,

Marta Cascante, J. Tégner, F. Miralles, D. Herrera, J. Roca and the Synergy-COPD consortium revised the article critically for important intellectual content and gave final approval of the version to be submitted and any revised version.

10. Acknowledgements

This research has been carried out under the Synergy-COPD research grant, funded by the Seventh Framework Program of the European Commission as a Collaborative Project with contract no.: 270086 (2011–2014).

11. References

1. Bousquet J, Anto J, Sterk P, Adcock I, Chung K, Roca J, Agusti A, Brightling C, Cambon-Thomsen A, Cesario A, et al: **Systems medicine and integrated care to combat chronic noncommunicable diseases.** *Genome medicine* 2011, **3:**43.
2. Synergy-COPD: **Modelling and simulation environment for systems medicine: Chronic obstructive pulmonary disease (COPD) as a use case.** *FP7-ICT-270086* 2011-2013.
3. Barabasi AL: **Network medicine--from obesity to the "diseasome".** *N Engl J Med* 2007, **357:**404-407.
4. E. C: **Global genomic data-sharing effort kicks off. Nature News. 06 March 2014.** *URL:http://wwwnaturecom/news/global-genomic-data-sharing-effort-kicks-off-114826 Accessed: 2014-03-18 (Archived by WebCite® at http://wwwwebcitationorg/6OAELb42a)* 2014.
5. Cases M, Furlong LI, Albanell J, Altman RB, Bellazzi R, Boyer S, Brand A, Brookes AJ, Brunak S, Clark TW, et al: **Improving data and knowledge management to better integrate health care and research.** *J Intern Med* 2013, **274:**321-328.
6. Cano I, Alonso A, Hernandez C, Burgos F, Martinez-Roldan J, Roca J: **A Multi-tier ICT Framework to Deploy Integrated Care Services.** *submitted to JAMIA* 2014.
7. NEXES: **Supporting Healthier and Independent Living for Chronic Patients and Elderly.** *CIP-ICT-PSP-225025* 2008-2013.
8. Barberan-Garcia A VI, Golberg HS, Vilaró J, Rodriguez DA, Garåsen HM, Troosters T, Garcia-Aymerich J, Roca J and NEXES consortium: **Effects and barriers to deployment of telehealth wellness programs for chronic patients across 3 European countries.** *Respiratory medicine* 2014, **108:**9.
9. Isaac Cano ML-A, Carme Hernandez, et al.: **Community-based Integrated Care Service (ICS) for frail chronic patients: design, assessment and adoption.** *To be submitted* 2014.
10. Parliament E: **Directive 95/46/EC of the European Parliament and of the Council of 24 October 1995 on the protection of individuals with regard to the processing of personal data and on the free movement of such data, Off. J.L. 281 (Nov. 23, 1995)("Data Protection Directive").** 1995
11. Parliament E: **Directive 2002/58/EC of the European Parliament and of the Council of 12 July 2002 concerning the processing of personal data and the protection of privacy in the electronic communications sector, Off. J.L. 201, 31.7.2002, at 37. (Directive on Privacy and Electronic Communications).** 2002.
12. Quinn P, De Hert P: **The Patients' Rights Directive (2011/24/EU) – Providing (some) rights to EU residents seeking healthcare in other Member States.** *Computer Law & Security Review* 2011, **27:**497-502.
13. SMART: **Study on the Legal Framework for Interoperable eHealth in Europe** *URL:http://wwwehealthnewseu/images/stories/pdf/ehealth-legal-fmwk-final-reportpdf Accessed: 2013-08-20 (Archived by WebCite® at http://wwwwebcitationorg/6J0kRlL0R)* 2009.

14. Sansone SA, Rocca-Serra P, Field D, Maguire E, Taylor C, Hofmann O, Fang H, Neumann S, Tong W, Amaral-Zettler L, et al: **Toward interoperable bioscience data.** *Nat Genet* 2012, **44:**121-126.
15. A. Seoane J, Aguiar-Pulido V, R. Munteanu C, Rivero D, R. Rabunal J, Dorado J, Pazos A: **Biomedical Data Integration in Computational Drug Design and Bioinformatics.** *Current Computer - Aided Drug Design* 2013, **9:**108-117.
16. Maier D, Kalus W, Wolff M, Kalko SG, Roca J, Marin de Mas I, Turan N, Cascante M, Falciani F, Hernandez M, et al: **Knowledge management for Systems Biology a general and visually driven framework applied to translational medicine.** *BMC systems biology* 2011, **5:**38.
17. Baker M: **Quantitative data: learning to share.** *Nat Meth* 2012, **9:**39-41.
18. Kasprzyk A: **BioMart: driving a paradigm change in biological data management.** *Database : the journal of biological databases and curation* 2011, **2011:**bar049.
19. ICGC: **International Cancer Genome Consortium Data portal.** *URL:http://dccicgcorg/ Accessed: 2014-02-18 (Archived by WebCite® at http://wwwwebcitationorg/6NThL0dwg)*.
20. STRIDE: **Stanford Translational Research Integrated Database Environment.** *URL:https://clinicalinformaticsstanfordedu/ research/stridehtml Accessed: 2014-02-18 (Archived by WebCite® at http://wwwwebcitationorg/6NTSpBql3)*.
21. BTRIS: **The Biomedical Translational Research Information System.** *URL:http://btrisnihgov/ Accessed: 2014-02-18 (Archived by WebCite® at http://wwwwebcitationorg/6NTT5HIbm)*.
22. i2b2: **Informatics for Integrating Biology and the Bedside.** *URL:https://wwwi2b2org/ Accessed: 2014-02-18 (Archived by WebCite® at http://wwwwebcitationorg/6NTU2Gh6w)*.
23. tranSMART: **knowledge management platform.** *URL:http://transmartfoundationorg/ Accessed: 2014-02-18 (Archived by WebCite® at http://wwwwebcitationorg/6NTThyMAp)*.
24. Oracle: **Health Sciences Translational Research Center.** *URL:http://wwworaclecom/us/products/applications/health-sciences/translational-research/indexhtml Accessed: 2014-02-18 (Archived by WebCite® at http://wwwwebcitationorg/6NTULYEYt)*.
25. Abugessaisa I, Gomez-Cabrero D, Snir O, Lindblad S, Klareskog L, Malmstrom V, Tegner J: **Implementation of the CDC translational informatics platform - from genetic variants to the national Swedish Rheumatology Quality Register.** *Journal of Translational Medicine* 2013, **11:**85.
26. Hood L, Auffray C: **Participatory medicine: a driving force for revolutionizing healthcare.** *Genome medicine* 2013, **5:**110.
27. Doris Schartinger SG, Barbara Heller-Schuh, Effie Amanatidou, Günter Schreir, Ian Miles, Laura, Pombo-Juárez, Özcan Saritas, Peter Kastner & Totti Könnölä: **Personal Health System - State of the Art. February 2013. Deliverable D1.1 of the PHS Foresight project (Grant Agreement No: 305801).** *URL:http://wwwphsforesighteu/wp-content/uploads/2013/03/PHS_D11_Report_20130228pdf Accessed: 2014-03-18 (Archived by WebCite® at http://wwwwebcitationorg/6OAEWkyxS)* 2013.
28. Roca J GH, Grimsmo A, Meya M, Alonso A, Gorman J, et al. : **NEXES: Supporting Healthier and Independent Living for Chronic Patients and Elderly: Final report.** *URL:http://wwwnexeshealtheu/media/pdf/nexes_final_reportpdf Accessed: 2014-03-14 (Archived by WebCite® at http://wwwwebcitationorg/6O412APYq)* 2013.

12. Figures

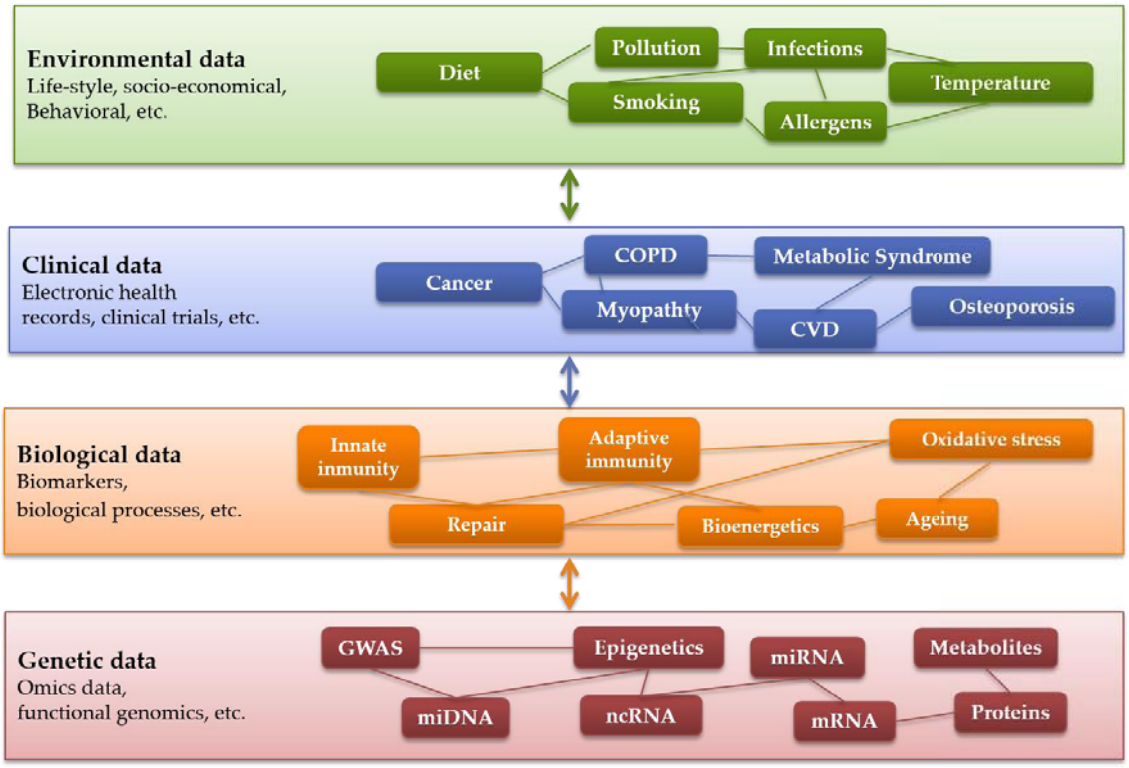

Figure 1: *The holistic approach intrinsic to system medicine of non-communicable diseases (NCDs) prompts the need for multilevel integration of heterogeneous patient information generated by different data sources, namely: environmental, clinical and biological data.*

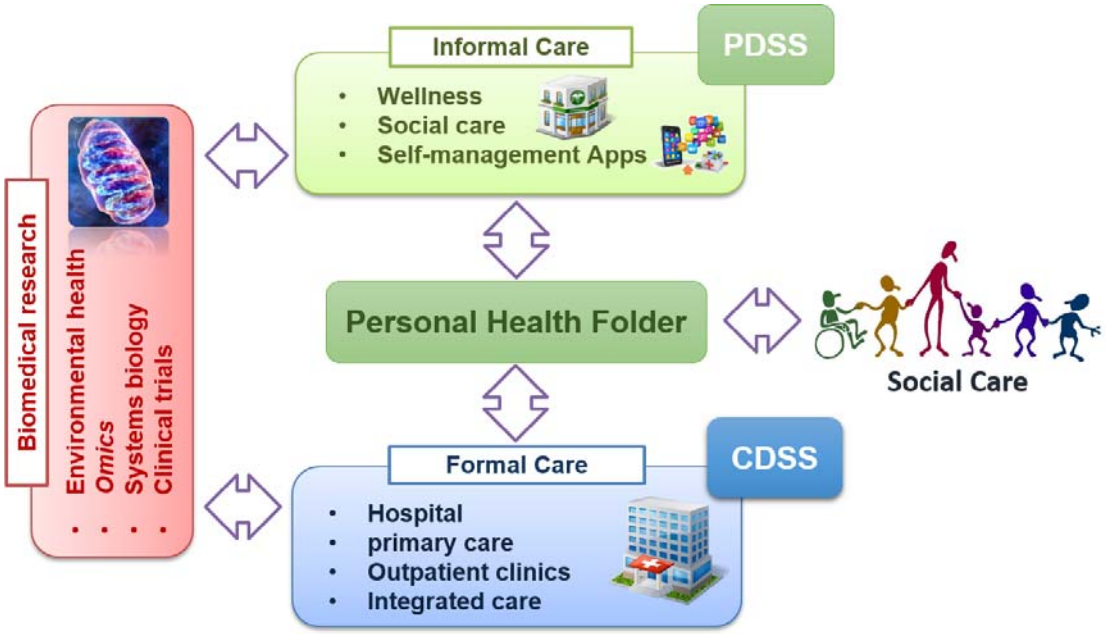

Figure 2: The concept of Digital Health Framework covers the different areas wherein information can be obtained and actions are taken: *i)* informal care, *ii)* formal care, and, *iii)* biomedical research. In this scenario, a personal health folder incorporating patient decision support systems (PDSS) might facilitate the incorporation of data coming from informal care into formal healthcare. In addition, biomedical research, referring to all research levels from clinical to basic research, should be shaped to provide user-profiled functionalities such that research professionals with different profiles can make use of clinical and biomedical knowledge from formal healthcare and heterogeneous biomedical research data sources, ultimately leading to the generation of novel rules that should feed in-place clinical decision support systems (CDSS).

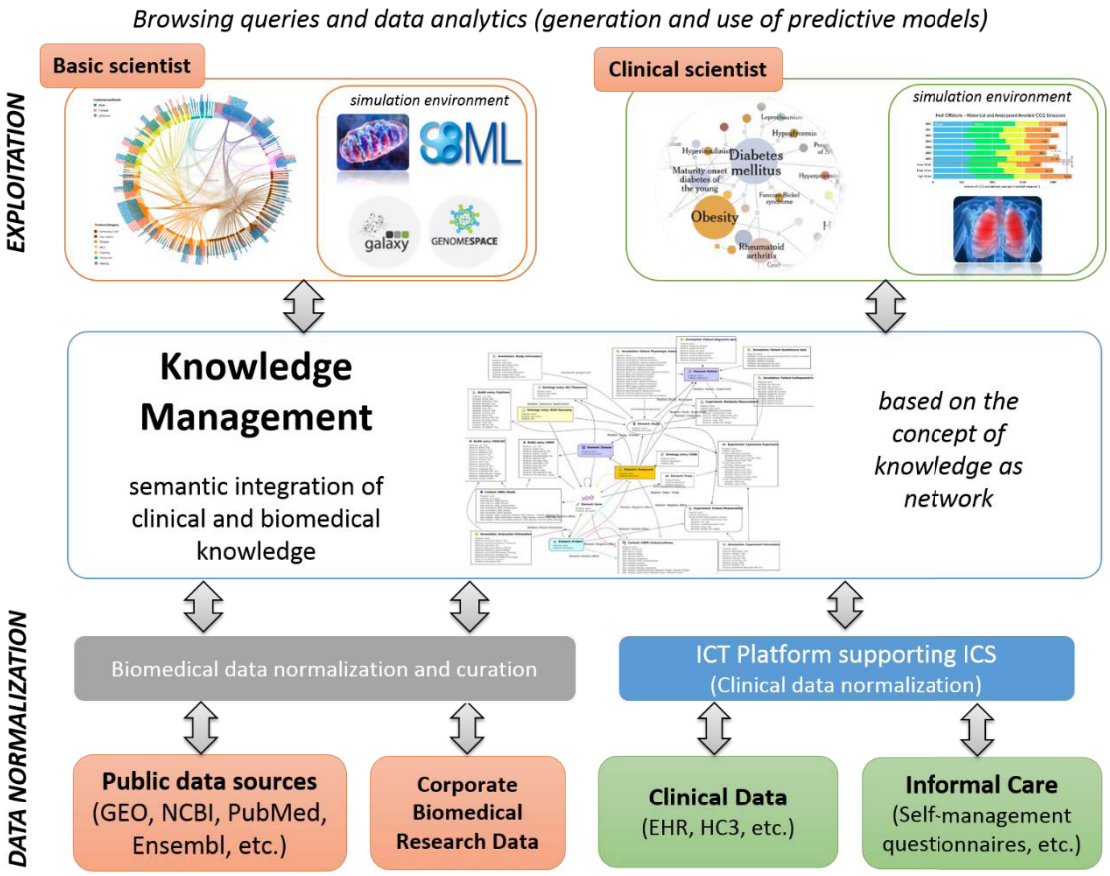

Figure 3: DHF-research components and functionalities include semi-automatic data standardization approaches, data integration and knowledge management, profile-specific visual data mining portals and user-profiled simulation environments (see text for further details).

13. Tables

Table 1. Description of Actors and Roles in the Digital Health Framework

Actors		Roles	Complexity	ICT support
Patient	COPD-moderate	Self-management	PC	PHF-PDSS
	COPD-complex		PC&Specialist	
	COPD-co-morb			
Primary Care		Clinical	Primary Care	CDSS
Specialized Care			Secondary Care	
Clinical Scientist		Research	Academic	DHF-research
Basic Scientist				

COPD-moderate, patient with moderate functional impairment and low activity disease; **COPD-complex,** patient with moderate to severe functional impairment with active disease both at pulmonary and systemic levels (skeletal muscle dysfunction/wasting); **COPD-co-morb**, patient with moderate functional impairment, high activity disease and co-morbid conditions (metabolic syndrome and cardiac failure);**PC**, Primary Care professionals (doctor & nurse); **Specialized Care,** Specialized Care (doctor&nurse); **Clinical Scientist,** Translational research with clinical focus; **Basic Scientist**, Translational research with focus on basic sciences; **PHF-PDSS**, personal health folder including Patient Decision Support Systems; **CDSS**, Clinical Decision Support Systems; **DHF-research**, Digital Health Framework-Biomedical research platform.

Main findings

The main findings of this PhD thesis can be allocated within the following three principal research objectives.

Quantitative analysis of cellular oxygenation and mitochondrial ROS generation relationships – this study generated the first deterministic integrated computational model, freely available at https://sourceforge.net/projects/o2ros, combining the physiological determinants of the O_2 pathway and biochemical modulators of mitochondrial respiration and ROS generation. It provided the basis for a quantitative assessment of the relationships between determinants of tissue oxygenation and mitochondrial ROS production.

Specifically, we showed that mitochondrial PO_2 (PmO_2) likely plays only a small role in total O_2 flux resistance (**Manuscript 1**). The model indicates that the ratio between O_2 transport capacity and mitochondrial O_2 utilization determines mitochondrial PO_2 (PmO_2). The phenomenon might be highly relevant after high intensity resistance training in COPD patients with limitation of O_2 transport due to the pulmonary disease. Other physiological determinants of the O_2 pathway were deeply analyzed, such as lung and peripheral heterogeneities. In this respect, *in silico* estimations showed that a given degree of heterogeneity in the skeletal muscle reduces overall O_2 transfer more than does lung heterogeneity. But since the observed functional lung heterogeneity is greater than in muscle, the former has a greater impact on overall O_2 transport (**Manuscript 2**). In addition, muscle heterogeneity showed to increase the range of skeletal muscle PmO_2 values, and in regions with a low ratio of metabolic capacity to blood flow, PmO_2 could exceed that of mixed tissue venous blood. Unfortunately, assessment of skeletal muscle functional heterogeneities is highly limited due to technological constraints.

Ultimately, this PhD thesis developed a multi-scale integrated model to predict conditions under which PmO_2 might fall enough to cause abnormally high reactive oxygen species (ROS) generation. Simulations using data from healthy subjects during maximal exercise revealed that altitude triggers high mitochondrial ROS production in skeletal muscle regions with high metabolic capacity, but limited O_2 delivery, already evident at approx. 17,000 ft. above sea level (**Manuscript 3**). This is the altitude above which permanent human habitation does not occur [124], and also the altitude above which humans experience inexorable loss of body mass. It is easy to hypothesize a cause and effect relationship between ROS and these findings, given the biological effects of high ROS

levels, but whether this is indeed cause and effect or just coincidence remains to be established.

Although the integrated model seems to provide reasonable results for healthy subjects, it may require obvious enhancement of parameter estimation for its application to disease, as discussed below. This could be done through two complementary strategies: *i)* the interplay with semi-quantitative probabilistic modeling (Bayesian [97] and Thomas [91] networks), as approached in the Synergy-COPD project; and, *ii)* experimental studies.

Technological support for deployment of patient-centered care – the ultimate goal of the modeling approaches explored in **Objective 1** was to contribute, together with other studies carried out in Synergy-COPD, to the generation of biomedical knowledge to enhance patient stratification. This ambitious aim requires exploring applicable strategies to foster the transfer of such biomedical research achievements into the clinical practice, for example in the form of novel systems medicine approaches applicable to integrated care of chronic conditions.

With respect to deployment of integrated care, an open and modular platform, conceived to provide the common basic set of tools and technologies to support the implementation of innovative integrated care services (ICS) for chronic patients, has been generated (**Manuscript 5**). The platform has effectively covered the four ICS assessed within the NEXES European project (2008-2013, www.nexeshealth.eu) in one of Barcelona's Health Care Districts accounting for 540.000 inhabitants, and has shown potential for further deployment at regional level.

To empower the regional deployment of the ICS-ICT approach presented in this PhD thesis, a recent strategic alliance between BDigital Technological Centre and Hospital Clínic, named Barcelona Virtual Health Practice (BCN-VHP), aims to contribute to the regional deployment initiatives undertaken by TIC-SALUT (Catalan Department of Health).

With respect to explore applicable strategies for the articulation between integrated care (i.e. formal healthcare), informal care and biomedical research, it was articulated the concept of the Digital Health Framework (DHF) (**Manuscript 6**). DHF provides an operational approach to link innovative systems-oriented biomedical research with the new healthcare scenario. We have reported on attitudes (pro-. and con-) and on specific proposals regarding ongoing changes toward 4P medicine in an integrated care scenario. Moreover, we have identified leadership among key members of the regional

translational research community that will generate additional contribution during the process of deployment of the DHF beyond this PhD.

A systems medicine approach to knowledge management in translational research – the DHF, as an operational setting, should provide four major elements: *i)* to facilitate inclusion of modeling covariates covering non-biological dimensions (behavioral, environmental, social, life style factors, etc.) with important implications on health risk assessment; *ii)* to introduce a dynamic assessment of risk assessment and stratification; *iii)* to provide interoperability among actors at system level including informal care (considering the emerging role of personal health folders and mobile applications) and healthcare; and, *iv)* to cover the requirements of a systems-oriented biomedical research platform including appropriate user-profiled interfaces, as a comprehensive strategy to enforce the transition toward 4P medicine.

While an ICS-ICT articulation of the formal and informal healthcare tiers of the DHF has been presented in **Manuscript 5**, the DHF biomedical research component (DHF-research) required three different areas for action with likely well-differentiated strategies.

Firstly, **data normalization and transfer,** which involves important aspects such as standards, technical interoperability, as well as the need to address ethical and legal constraints. A second area for action includes all aspects associated with **user-friendly profiled interfaces**. Finally, a third key area for action is **knowledge management,** involving issues like the interplay between open source and proprietary solutions, general vs. case-specific knowledge base approaches, the role of knowledge management in the interplay between network modeling and deterministic modeling, etc. In this respect, under the umbrella of the Synergy-COPD project, we developed a COPD-specific knowledge management environment (**Manuscript 4**), open to the biomedical research community at www.copdknowledgebase.eu, which proved a valuable tool for the analysis and computational modeling of COPD.

It is acknowledged that several gaps and weaknesses remain. Some of them are associated to specificities of our environment; whereas other limiting factors are generic and associated to the way we communicate knowledge. Future developments will focus on improvement of the quality of disease-specific knowledge, and enhancement of usability of the user-interfaces to speed-up data access, bringing validated data analysis workflows into the reach of non-bioinformaticians.

Assessing the model of the oxygen pathway and mitochondrial ROS generation in health and in disease

Under the scope of this PhD thesis, three different approaches were undertaken to indirectly assess the adequacy of the integrated model for the *quantitative analysis of the interplay between the O_2 pathway and mitochondrial ROS generation in the skeletal muscle*. We first analyzed the relationships between estimated mitochondrial ROS generation and permanent human habitation at high altitude, a well-identified biological phenomenon. Such a relationship in health was explored in the **Manuscript 3** of the current PhD thesis. In addition, the following analyses were undertaken to explore COPD conditions:

- Assessment of the dissociation between cellular hypoxia (and ROS generation) and FEV_1 using two independent datasets [88, 89];
- Assessment of the association between estimated ROS levels and measured nitroso-redox unbalance in arterial blood, and in skeletal muscle before and after endurance training in healthy subjects and in COPD patients using the BioBridge dataset [89].

Dissociation between cellular hypoxia (and ROS generation) and FEV_1

To assess the effect of estimated aerobic capacity in overall O_2 pathway performance and its relation with classical GOLD staging (FEV_1), a sensitivity analysis over the mitochondrial respiration capacity (Vmax) was carried out in a group of COPD patients with mild to severe disease [88]. The central messages of this analysis, depicted in **Figure 6**, were: *i)* PmO_2 at maximal exercise is determined by the O_2 transport to mitochondrial O_2 utilization capacity ratio (as reported in **Manuscripts 1-3**), such that the lower the maximum O_2 transport potential for a given mitochondrial capacity, the lower PmO_2; *ii)* tissue oxygenation levels were not related with FEV_1; and, *iii)* low PmO_2 values associated with abnormally high mitochondrial ROS production at peak exercise were predicted to occur in these patients.

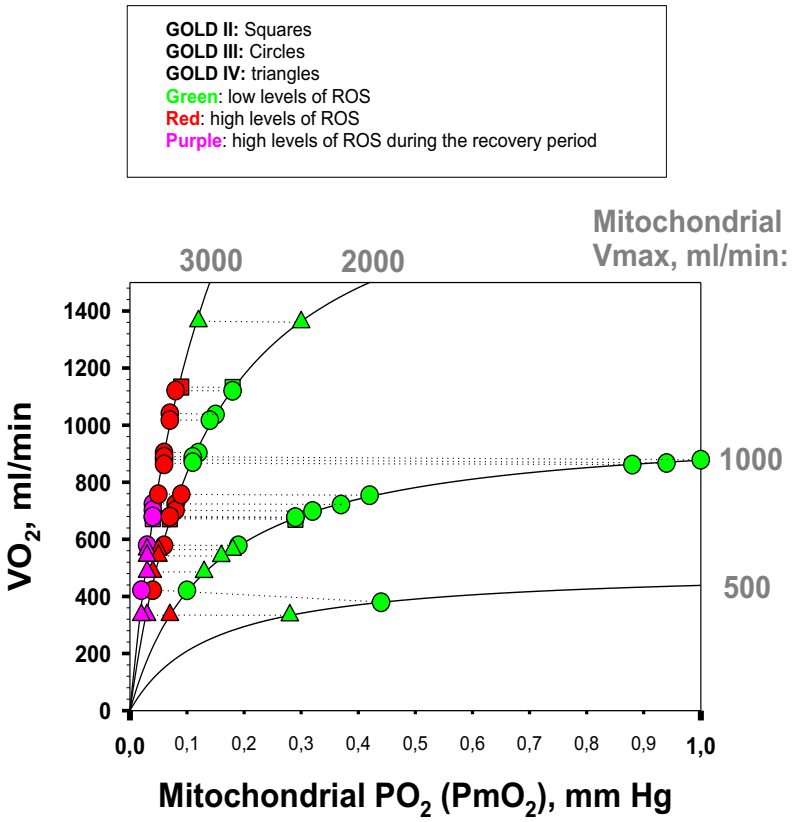

***Figure 6**: Relationships between measured maximum O_2 transport (VO_2), y-axis; and, estimated cellular oxygenation (PmO_2), x-axis, in COPD patients. The different symbols correspond to classical GOLD stages: squares, GOLD II; circles GOLD III; and, triangles, GOLD IV. The symbols connected with discontinuous lines correspond to the same patient (same VO_2) with estimated PmO_2 values corresponding to different mitochondrial oxidative capacities (Vmax values and VO_2/Vmax ratios). For a given patient, the lower the VO_2/Vmax ratio, the lower was the estimated overall exercising tissue PmO_2. The colors correspond to the levels of mitochondrial ROS generation: green, mitochondrial ROS levels similar to those seen in healthy subjects; red, abnormally high mitochondrial ROS levels; and, violet, high ROS levels that persist after exercise withdrawal. The lower the PmO_2, the higher were mitochondrial ROS levels.*

Complementarily to the previous analysis, an analysis of the relationships between measured maximum (peak) oxygen uptake vs. the estimated skeletal muscle mitochondrial O_2 partial pressure (PmO_2) and mitochondrial ROS production was done using data from BioBridge [89] (see **ANNEX I**) in order to explore the relationships between tissue events (cellular hypoxia and abnormal mitochondrial ROS generation) and lung mechanics expressed as FEV_1 percent predicted.

The results of the analysis are depicted in **Figure 7** wherein we confirmed dissociation between lung mechanics (classical GOLD staging based on FEV_1) and cellular hypoxia (abnormal ROS production) in COPD patients, further suggesting the need for assessing aerobic capacity in the clinical scenario.

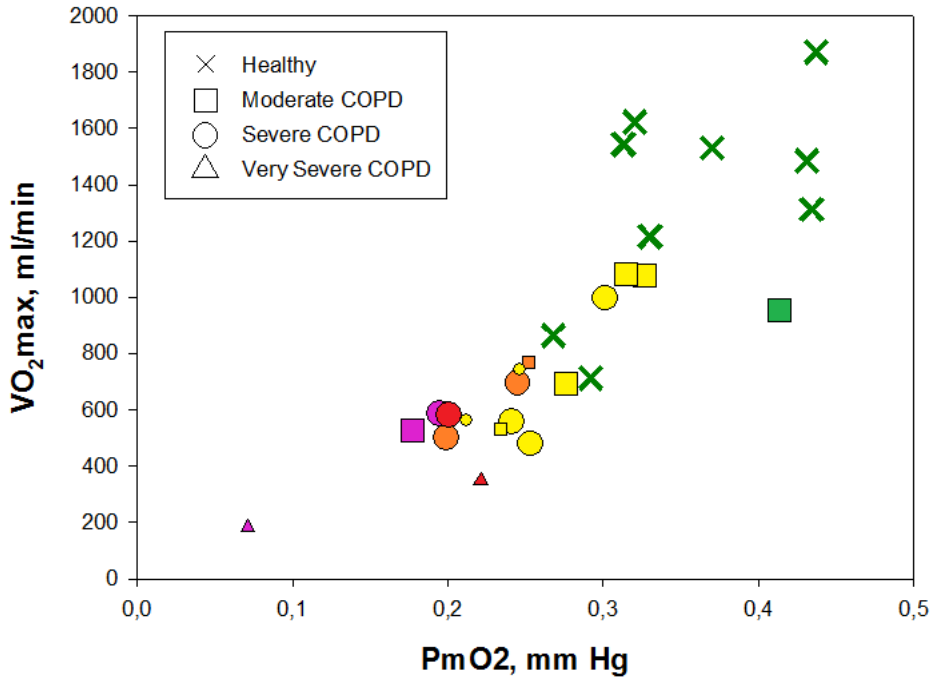

Figure 7: *Relationships between estimated average muscle maximum O_2 transport (VO_2), y-axis; and, estimated average muscle cellular oxygenation (PmO_2), x-axis, in COPD patients and healthy subjects. The different symbols correspond to classical GOLD stages: squares, GOLD II; circles GOLD III; and, triangles, GOLD IV. The colors correspond to the percent of exercising muscle estimated to generate abnormally high mitochondrial ROS generation: green (0%), yellow (0% - 24.9%), orange (25% - 49.9%), red (50% - 74.9%), and violet (75% - 100%). The symbol size correspond to the subject measured body mass index (BMI): big symbols indicate subjects with normal BMI (>21 kg/m^2) while small symbols indicate subjects with low BMI (≤ 21 kg/m^2).*

Assessment of the association between ROS production and measured nitroso-redox unbalance before and after endurance training in healthy subjects and in COPD

This assessment of the association between ROS production and measured nitroso-redox unbalance before and after endurance training in healthy subjects and in COPD patients was done using data from BioBridge [89] (see **ANNEX I**). **Figure 8** displays the results of measured peak oxygen uptake, estimated mitochondrial oxygenation (PmO_2) and estimated percentage of skeletal muscle with abnormally high ROS levels for the three groups of subjects: healthy individuals (C), COPD with preserved BMI (N) and COPD patients with low BMI (L). The figure indicates that healthy subjects pre-training showed higher both measured VO_2 peak and estimated tissue oxygenation (PmO_2) than COPD patients with no abnormally high mitochondrial ROS levels. In contrast, COPD patients pre-training presented high ROS levels. In healthy subjects, endurance training induced physiological effects (ΔVO_2 peak) without estimating abnormally high ROS levels. It is of note that COPD patients also enhanced VO_2 peak after training, but

training-induced responses were heterogeneous at all levels [80, 81], as reported in the figure, for estimated mitochondrial ROS production.

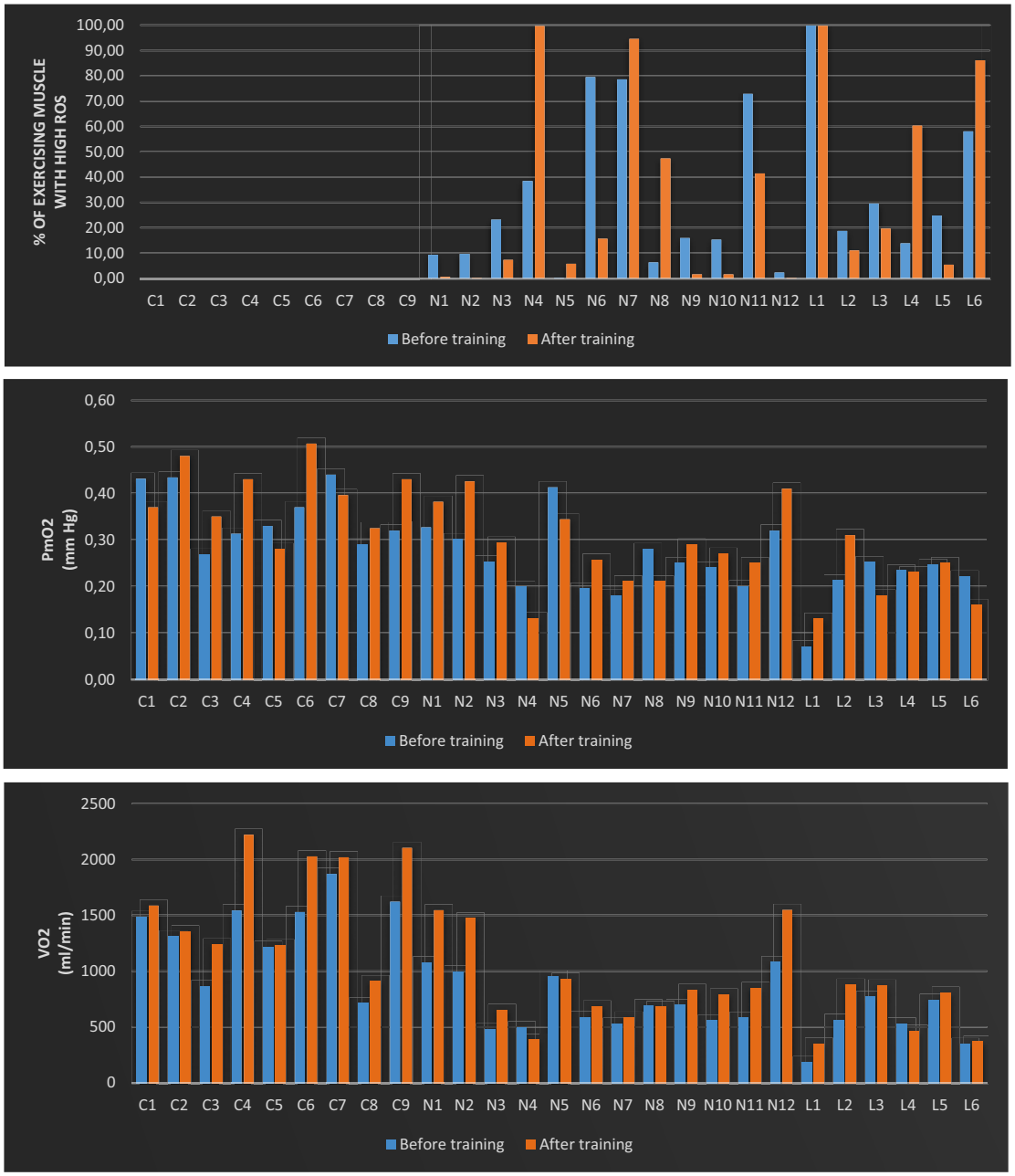

***Figure 8**: Estimated percent of exercising muscle predicted to generate abnormally high mitochondrial ROS generation (upper panel), estimated overall exercising muscle oxygenation (middle panel), and estimations for overall VO_2max (lower panel). Simulation results for healthy subjects (C1-C9), COPD patients with normal body mass index (BMI) (N1-N12), and COPD patients with low BMI (L1-L6 both before and after a training period of 8 weeks.*

Figure 9 depicts the analysis (pre-, post-training, post- minus pre- training difference) of the comparisons between estimated mitochondrial ROS generation and several

measured redox variables, in arterial blood and skeletal muscle, in the BioBridge dataset [89]. As displayed in the figure, no significant associations with physiological meaning were observed in the analyses.

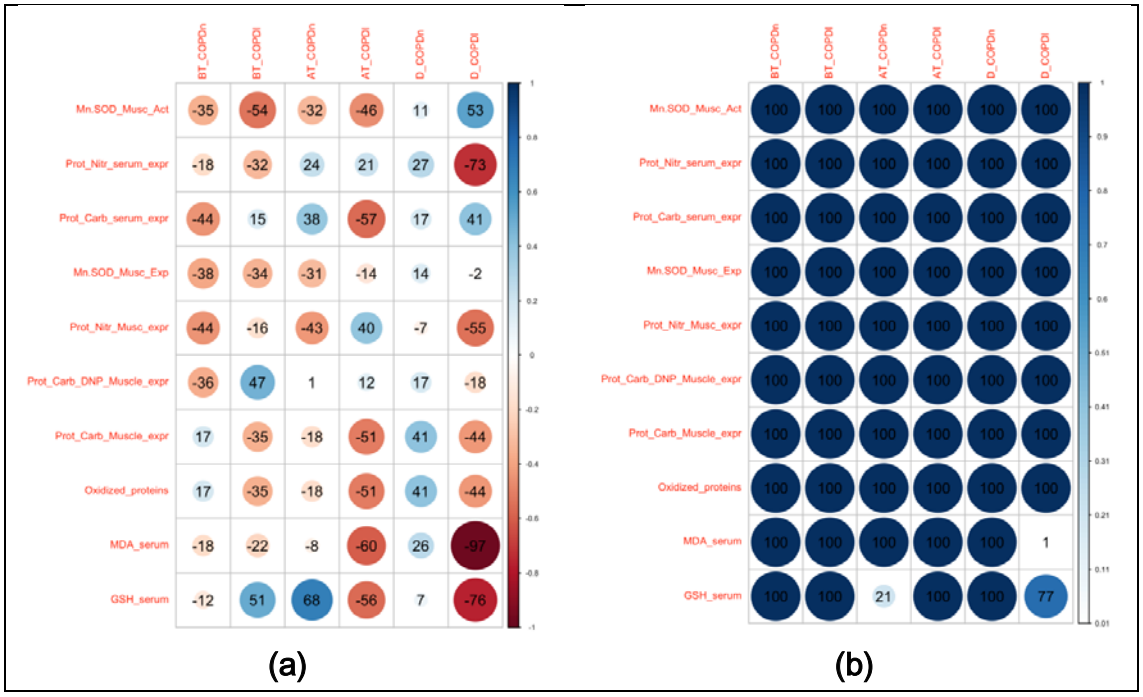

***Figure 9**: Left-hand panel (a) shows that % of skeletal muscle (i.e. Vmax) producing high levels of ROS production for different disease groups (COPDN and COPDL denote COPD patients with normal and low Fat Free Mass Index respectively) and conditions (BT (Before training), AT (After training and D (After minus Before Training Difference)) is correlated with clinical measurements. In each comparison, the Pearson Correlation was computed, and the coefficient is provided in a percentage style. In the right-hand panel (b) Bonferroni-Adjusted P-values (in a percentage style) are shown. The MDA_Serum vs. %Vmax explained by ROS is the only bivariate that significantly correlates when the difference after and before training is considered (adjusted p-value <0.05).*

Future developments

The lack of significant associations with physiological meaning observed in the analyses of the association between ROS production and measured nitroso-redox unbalance after endurance training in healthy subjects and in COPD patients can have two potential explanations: *i)* one possibility takes into account that the integrated model estimates the rate of mitochondrial ROS production, expressed as concentration of semiquinone radicals (nmol/mg) at Qo site (ubiquinone binding site to complex III at the outer side of the inner mitochondrial membrane) of mitochondrial complex III, whereas the analyses assess its association with oxidative stress conditions that are the end result of ROS levels plus the balance between the generation of ROS with their elimination by the

scavenging system; and/or, *ii)* the lack of correlation comes from the need for an enhanced model parameter estimation with respect mitochondrial function under disease conditions.

Overall, future developments should address the two aspects: *i)* to incorporate the complete mitochondrial oxidation-reduction (redox) system to face the need for oxidative stress estimations; and, *ii)* to consider a better parameterization of COPD-like mitochondrial bioenergetics [60]. To this end, as alluded to above, Synergy-COPD explored the use of semi-quantitative approaches based on the Thomas formalism [91], to contribute to enhanced parameter estimation for mitochondrial function in the integrated model. In addition, future respiratory assays to measure mitochondrial metabolic rates with a closed-chamber respirometry system should be planned [125, 126].

Challenges for regional deployment of ICS-ICT

This PhD thesis presented an ICT platform that incorporates integrated care clinical process logics allowing patient-centered management with high potential for both patient-specific and provider-specific customization (**Manuscript 5**). This ICS-ICT platform covered the requirements for deployment of the NEXES' field studies [12], being operational during the project lifetime in one of Barcelona's Health Care District accounting for 540.000 inhabitants, and showing potential for further deployment at regional level.

However, characterization of the driving forces at site level and identification of dominant barriers for the change are pivotal elements to be taken into account in the process of site adaption of the deployment strategies. To this end, factors that may be limiting transferability of a given ICS should be considered in the planning of the deployment phase. Moreover, the overall strategy for deployment should be based on a building blocks approach focusing on short-term outcomes that generate continuous feedback and iterations, which may help to refine the following key challenges of the deployment process: technological aspects, organizational setting, ethical & regulatory issues, and business models. However, only the technological challenges for regional deployment of ICS-ICT are under the scope of this PhD thesis.

Technological challenges – key technological aspects of any ICS-ICT solution to scale-up to multi-provider interoperability must address the need for the secure, reliable and systematic exchange of health information across different healthcare providers while

supporting shared ICS processes. Moreover, in those regions were initiatives for health information exchange are in-place, the ICS-ICT solution should be articulated correspondingly (with proper integration of the presentation and data tiers), while in regions were sectorial platforms for health information exchange do not exist, the ICS-ICT solution can also provide technological support for health information exchange.

For the extensive deployment of the NEXES ICS-ICT experience as enabler of ICS deployment in the Catalan health region, we have to take into account that both the technological challenges of the ICS-ICT platform and the regional ecosystem for health information exchange have evolved beyond NEXES. Current technological challenges for a successful regional deployment of the NEXES ICS-ICT experience include the need to incorporate ICS process logics on top of the regional health information exchange project (WiFIS). WiFIS aims to standardize and integrate all processes between health institutions providing reference message encoding (i.e. HL7 v2.5/3.0), message routing, terminology (i.e. SNOMED-CT, SERAM , LOINC, etc.) and security (i.e. IPsec, audit trail, node authentication, etc.) within a specific regional health sector and between them. This means that only the core ICS process logics of the ICS-ICT platform ought to be incorporation to the current set of supported shared processes (laboratory, medical appointment, clinical data exchange, medical referral and e-Diagnosis processes).

Additional technological challenges account for the enrichment of the ICS-ICT personal health folder assessed in NEXES [108], evolving to mobile applications that make use of MobileID solutions to ease citizen's access to their personal health folder. Such mobile applications properly accredited in the regional patient gateway and articulated with the regional shared electronic health record, may cover a twofold aim: *i)* articulation of non-clinical and clinical information; and, *ii)* empower patients for self-management.

Worth to mention that the above regional deployment of the ICS-ICT initiated in the Integrated Healthcare sector of Hospital Clinic (AISBE, 540.000 inhabitants) during the NEXES experience, its being further extended to the entire region driven by two pivotal initiatives activated during fall 2013: a COPD case finding program using forced spirometry, and a community-based ICS-ICT approach for Long Term Oxygen Therapy (LTOT) being developed within the frame of the ACT project (Advancing Coordinated Care and Telehealth) in Catalonia. The two initiatives represent important political commitments that will be deployed during 2014 in AISBE and extended to the entire region during the period 2015-17. These initiatives will be partly carried out under the umbrella of a recent strategic alliance between BDigital and Hospital Clinic named Barcelona Virtual Health Practice (BCN_VHP) that aims to contribute to the regional

deployment initiatives undertaken by TIC-SALUT (Catalan Department of Health). In this scenario, Linkcare Health Services SL is also contributing.

Next steps for development of the DHF for biomedical research

This PhD thesis identified that deployment of 4P medicine involving implementation of sound strategies for patient health-risk assessment and stratification generate two key requirements. Firstly, articulation between informal care and healthcare, as discussed in the previous section, allowing incorporation of non-clinical information into patient management; that is, data on patient adherence profile, lifestyle (physical activity, nutritional habits, addictions, etc.), social support needs and environmental and societal factors that have a well-accepted impact on health status and survival.

A second major requirement is the articulation of this scenario with systems-oriented biomedical research platforms ensuring continuous cross-fertilization between research and patient care. This ideal setting would cover both incorporation of non-biomedical data into predictive modeling and would provide dynamic modeling approaches that should facilitate the way toward truly personalized medicine. Such a proposal has been described in this PhD thesis under the concept of Digital Health Framework (DHF).

The DHF considers the articulation of open and modular tools supporting organizational interoperability, and appropriate functionalities, among three main areas, namely: *i)* informal care (e.g. life style, environmental and behavioral aspects, etc.), *ii)* formal care, and, *iii)* biomedical research.

Biomedical research (DHF-research) refers to all research levels from bench to clinical and to public health, using computer-based methods to bring research to clinical applicability at the individual patient level, both in the general community and when patients see healthcare professionals. To materialize such an ambitious vision this PhD thesis identified three key functional principles for the correct adoption of the DHF-research, namely:

- Data standardization strategies and open data policies, toward technical, syntactic and semantic (knowledge management) interoperability between clinical data systems and biomedical research platforms, taking into account the privacy challenges of biomedical data sharing.
- Profile-specific visual data mining functionalities covering the disparate needs and backgrounds of basic and clinical researchers.
- Profile-specific environments supporting multi-scale predictive modeling and several forms of complex data analytics.

However, the academic and research focus of this PhD thesis was better aligned with functional principles for data integration and knowledge management. For this reason, during the execution of this PhD thesis a previous COPD-specific knowledge base (COPDkb) has been extended to integrate over 40 public data sources on functional interaction (e.g. signal transduction, transcriptional regulation, protein-protein interaction, gene–disease association), and to interact with the Synergy-COPD simulation environment, which facilitates the user-friendly simulation of the Synergy-COPD multi-scale predictive models. The current COPDkb, freely available after registration at www.copdknowledgebase.eu, is the only publicly available knowledge resource dedicated to COPD combining genetic information with molecular, physiological and clinical data, as well as mathematical modeling.

Although the integrative functions of the COPDkb provide overviews about clinical trends and connections, and its semantically mapped content enables complex analysis approaches, further ICT developments, fostering convergence of open and proprietary approaches, should be considered as short-term priorities to generate user-friendly portals for clinicians devoted to translational research. Finally, a relevant area is the design of innovative business models providing sustainability of biomedical research platforms beyond specific research and/or infrastructure projects that triggered the initial settings.

Overall, for the correct deployment of any DHF-research initiative, both legal and ethical aspects ensuring privacy and security of data transfer and management delineate a crucial area to be properly handled. Data anonymization and encryption strategies have experienced a significant progress contributing to partially solving the problem. However, they show clear limitations in areas such as the management of genetic information wherein data anonymization is a challenge. In addition, the use of data for purposes other than the original data collection aims may generate limitations and activating communities of data donators for scientific purposes with a wider view than current practices is required. Clearly, evolving both legal frames and citizen cultural attitudes will be crucial to achieve a balance between social acceptation of anonymized data sharing together with reasonable levels of security and privacy of data transfer and management.

Within the Synergy-COPD lifetime, a first step for qualitative assessment of the current DHF-research proposal has been undertaken using a focus group strategy, and the conclusions were positive. Next steps are to generate structured interactions with well-known international experts in DHF-research to prioritize specific steps of the

deployment strategy, and, to plan collaborative interactions with selected on-going projects addressing similar aims.

Contributions of the PhD thesis to the overall Synergy-COPD results

Overall, the current PhD thesis generated knowledge that contributes to our understanding of underlying mechanisms of COPD heterogeneity, specially focusing on skeletal muscle dysfunction/wasting, and that supports the initial Synergy-COPD hypothesis. Specifically, the Synergy-COPD project generated evidence of abnormal regulations among relevant pathways in skeletal muscle, namely: cellular bioenergetics, inflammation and tissue remodeling. These findings were consistently observed in studies in humans, animal experiments and in cell culture assays. Moreover, the mechanistic modeling approaches undertaken during the current PhD thesis contributed to the analysis of the biological impact of changes in tissue oxygenation. However, model refinement should be a priority to be driven by the interplay with probabilistic modeling (Bayesian [85] and Thomas [86] networks) as a complementary strategy of experimental studies addressing the relationships between the O_2 pathway and ROS generation.

In addition, the technological developments of this study provided basic technological pillars for the deployment of integrated care management of chronic conditions, as a supporting tool for the real deployment of subject-enhanced and patient-specific health-risk assessment and stratification, the ultimate aim of Synergy-COPD.

Finally, one of the major conclusions of Synergy-COPD was the need for developing the Digital Health Framework (DHF) presented here as a proof of concept. The DHF as an operational setting should provide four major elements for optimization of the deployment in this type of projects: *i)* inclusion of covariates in the modeling, covering non-biological dimensions (behavioral, environmental, social, life style factors, etc.) and with important implications for health risk assessment; *ii)* introduction of dynamic enhancement of risk assessment and stratification; *iii)* provision of organizational and technical interoperability among actors at health system level, including informal care and healthcare; and, *iv)* coverage of the requirements for a systems-oriented biomedical research platform, including appropriate user-profiled interfaces.

Conclusions

1. The model integrating physiological determinants of the O_2 pathway and biochemical modulators of mitochondrial ROS formation provides, for the first time, a quantitative assessment of the relationships between cellular oxygenation and mitochondrial ROS production. The model generates consistent results in health, but parameter estimations when applied to COPD need refinement.

2. The ICT-platform supporting integrated care services (ICS) for chronic patients effectively covered the functional requirements for deployment within a single-provider environment. The challenges to be faced for regional deployment of the ICS were identified and strategies for adoption have been proposed.

3. The Digital Health Framework (DHF) conceptualizes a scenario for an effective cross talk between integrated care and systems-oriented biomedical research that should foster deployment of 4P medicine. Future steps for adoption of the DHF have been proposed.

4. The COPD-specific knowledge base (COPDkb), developed and assessed in the current PhD thesis, constitutes a pivotal component of systems-oriented biomedical research.

Background

The epidemics of non-communicable diseases and the need for cost-containment are triggering a profound reshaping of healthcare delivery toward adoption of the Chronic Care model, involving deployment of integrated care services (ICS) with the support of information and communication technologies (ICS-ICT). In this scenario, emerging systems medicine, with a holistic mechanism-based approach to diseases, may play a relevant role in health risk assessment and patient stratification.

The general aim of Synergy-COPD was to explore the potential of a systems medicine approach to improve knowledge on underlying mechanisms of chronic obstructive pulmonary disease (COPD) heterogeneity, focusing on systemic effects of the disease and co-morbidity clustering. The transfer of acquired knowledge to healthcare was also a core aim of the project. Moreover, Synergy-COPD explored novel cross talk between biomedical research and healthcare to foster deployment of 4P (Predictive, Preventive, Personalized and Participatory) Medicine for patients with chronic disorders.

The current PhD thesis contributed to Synergy-COPD focusing on two specific areas: *i)* a quantitative analysis of the relationships between cellular oxygenation and mitochondrial reactive oxygen species (ROS) generation; and, *ii)* different ICT developments addressing transfer of knowledge to healthcare and the interplay with biomedical research.

Hypothesis

The overarching hypothesis of this PhD thesis is that subject-specific health risk assessment and stratification may lead to novel and a more efficient patient-oriented healthcare delivery. Specifically, the current PhD studies hypothesize that predictive mechanistic modeling integrating oxygen pathway and mitochondrial function can contribute to assess the biological effects of cellular hypoxia and its role on skeletal muscle dysfunction in COPD. Moreover, it is hypothesized that a holistic design of the ICT support may contribute to a successful deployment of ICS-ICT for chronic patients fostering the transfer of the achievements of systems-oriented research into healthcare.

Objectives

To integrate physiological modeling of the O_2 pathway and biochemical modeling of mitochondrial ROS generation to quantitatively analyze the relationships between skeletal muscle oxygenation and mitochondrial ROS generation.

To develop ICT tools supporting Integrated Care Services (ICS-ICT) for chronic patients, as well as innovative cross talk between systems-oriented biomedical research and healthcare.

Main findings

Quantitative analysis between cellular oxygenation and mitochondrial ROS generation

The model analyzed the role of all the physiological determinants of the O_2 pathway. It was shown that a given degree of heterogeneity in the skeletal muscle reduces overall O_2 transfer more than does lung heterogeneity, but actually observed heterogeneity in lung is greater than in muscle, so that lung heterogeneity has a greater impact on overall O_2 transport. In addition, muscle heterogeneity showed to increase the range of skeletal muscle PmO_2 values, and in regions with a low ratio of metabolic capacity to blood flow, mitochondrial PO_2 (PmO_2) could exceed that of mixed tissue venous blood. Unfortunately, assessment of skeletal muscle functional heterogeneities is highly limited due to technological constraints.

The model indicates that the ratio between O_2 transport capacity and mitochondrial O_2 utilization potential determines PmO_2. The phenomenon might be highly relevant after high intensity resistance training in COPD patients with limitation of O_2 transport due to the pulmonary disease.

Simulations using data from healthy subjects during maximal exercise revealed that altitude triggers high mitochondrial ROS production in skeletal muscle regions with high metabolic capacity, but limited O_2 delivery, already evident at approx. 17,000 ft. above sea level. This is the altitude above which permanent human habitation does not occur, and the altitude above which humans experience inexorable loss of body mass. However, it is concluded that the use of the integrated model in disease conditions requires further refinement of mitochondrial parameter estimation.

ICT-support to the deployment of integrated care services (ICS-ICT) and to the cross talk between healthcare and systems-oriented biomedical research

An open and modular platform was developed to provide the common basic set of tools and technologies to support the implementation of ICS-ICT for chronic patients. The platform has effectively covered the four ICS developed and assessed within the NEXES European project (2008-2013, www.nexeshealth.eu) in one of Barcelona's Health Care Districts accounting for 540.000 inhabitants, and has shown potential for further deployment at regional level.

The concept of the Digital Health Framework (DHF) was articulated to provide linkage between healthcare and innovative systems-oriented biomedical research. The Synergy-COPD knowledge base was developed as a component of the DHF-research to enforce the transition toward 4P medicine.

Conclusions

1. The model integrating physiological determinants of the O_2 pathway and biochemical modulators of mitochondrial ROS formation provides, for the first time, a quantitative assessment of the relationships between cellular oxygenation and mitochondrial ROS production. The model generates consistent results in health, but parameter estimations when applied to COPD needs refinement.

2. The ICT-platform supporting integrated care services (ICS) for chronic patients effectively covered the functional requirements for deployment within a single-provider environment. The challenges to be faced for regional deployment of the ICS were identified and strategies for adoption have been proposed.

3. The Digital Health Framework (DHF) conceptualizes a scenario for an effective cross talk between integrated care and systems-oriented biomedical research that should foster deployment of 4P medicine. Future steps for adoption of the DHF have been proposed.

4. The COPD-specific knowledge base (COPDkb), developed and assessed in the current PhD thesis, constitutes a pivotal component of systems-oriented biomedical research.

Introducció

La proliferació de les malalties no contagioses i la creixent necessitat de reduir costos està desencadenant una remodelació estructural de l'atenció sanitària envers el model d'atenció a crònics, involucrant la implementació de serveis d'atenció integrada (SAI) amb el suport de les tecnologies de la informació i la comunicació (SAI-TIC). En aquest escenari, la emergent medicina de sistemes, amb un aproximació holística basada en els mecanismes de les malalties, juga un rol rellevant a l'avaluació del risc per la salut i la estratificació de pacients.

L'objectiu principal de Synergy-COPD ha estat la exploració del potencial de una aproximació de la medicina de sistemes per tal de millorar el coneixement dels mecanismes subjacents a la heterogeneïtat de la malaltia pulmonar obstructiva crònica (MPOC). Fent èmfasi als efectes sistèmics de la malaltia, així com en la comorbiditat. La transferència de nous coneixements a l'atenció sanitària ha estat també un dels objectius principals d'aquest projecte. A més, Synergy-COPD ha explorat noves interaccions envers la investigació biomèdica i l'atenció sanitària, amb la darrera finalitat de promoure la medicina 4P (predictiva, preventiva, personalitzada i participatòria) per a pacients amb malalties cròniques.

Aquesta tesi doctoral contribueix amb Synergy-COPD en dos aspectes específics:

1. Un anàlisi quantitatiu de la relació entre la oxigenació cel·lular i la producció de radicals lliures d'oxigen (ROS) a nivell mitocondrial.

2. Diversos desenvolupament tecnològics adreçats a la transferència de coneixement biomèdic envers a l'atenció sanitària i la investigació biomèdica.

Hipòtesis

La hipòtesi general d'aquesta tesi doctoral és que una personalització de l'avaluació del risc per a la salut i la estratificació de pacients ha de desencadenar en una atenció sanitària més eficient i orientada envers pacient. Específicament aquesta tesi doctoral planteja la hipòtesi de que el modelatge mecanicista del sistema de transport i utilització d'oxigen, tenint en compte la funció mitocondrial, pot contribuir a avaluar els efectes biològics d ela hipòxia cel·lular i el seu paper a la disfunció del múscul esquelètic a la MPOC. D'altra banda, aquesta tesi doctoral planteja també la hipòtesi referent a que un disseny holístic basat en les TIC pot contribuir a un desplegament efectiu de SAI-TIC

per a pacients crònics, fomentant l'aplicació dels assoliments de la investigació orientada a sistemes a l'assistència sanitària.

Objectius

La integració de un modelatge fisiològic del sistema de transport i utilització d'oxigen amb el modelatge bioquímic de la generació mitocondrial de ROS, amb la finalitat d'analitzar les relacions entre la oxigenació del múscul esquelètic i la producció mitocondrial de ROS.

El desenvolupament d'eines TIC que donin suport a Serveis d'Atenció Integrada (SAI-TIC) per a pacients crònics, i per tal de fomentar la interacció entre la investigació biomèdica basada en la medicina de sistemes i l'atenció sanitària.

Resultats principals

Anàlisi quantitatiu de la relació entre oxigenació cel·lular i la generació mitocondrial de ROS

El modelatge realitzat en aquesta tesi doctoral analitza tots els factor determinants del sistema de la cadena de transport d'oxigen. S'ha demostrat que donat un cert grau d'heterogeneïtat al múscul esquelètic es disminueix la transferència global d'oxigen més de lo que la redueix la heterogeneïtat pulmonar. D'altra banda, la heterogeneïtat observada actualment a nivell pulmonar es major que la observada al múscul, per tant la heterogeneïtat pulmonar en general té un impacte més gran sobre la transferència total d'oxigen.

A més, es demostra que la heterogeneïtat muscular incrementa el rang de nivells d'oxigenació cel·lular (PmO_2), i a regions del múscul esquelètic amb una major aportació sanguínia en comparació a la capacitat metabòlica, els valors de PmO_2 poden excedir els valors d'oxigenació venosa mixta. Malauradament, la mesura del nivell d'heterogeneïtat funcional al múscul esquelètic és molt insuficient degut a les limitacions tecnològiques.

El model indica que la relació entre la capacitat de transport d'oxigen i utilització d'oxigen determina principalment els valors d'oxigenació cel·lular PmO_2. Aquest fenomen, pot ser molt rellevant després d'un procés d'entrenament d'alta intensitat a pacients MPOC amb limitacions de transport d'oxigen degut a la malaltia pulmonar.

Les simulacions utilitzant dades mesurades en subjectes sans realitzant exercici màxim han desvelat que l'altitud desencadena una alta producció de ROS mitocondrial a les regions del múscul esquelètic amb una altra capacitat mitocondrial però amb una limitada capacitat d'aportació d'oxigen. Aquesta observació és evident a partir d'una altitud corresponent a uns 5000 metres sobre el nivell del mar. Per sobre d'aquesta altitud no existeix cap assentament humà permanentment habitat i els humans experimenten una pèrdua inexorable de massa corporal. Però, es conclou que l'ús del model integrat en condicions de malaltia requereix una millor estimació dels paràmetres mitocondrials.

Suport TIC per al desplegament de serveis d'atenció integrada (SAI-TIC) i la interacció entre l'atenció sanitària i la investigació biomèdica basada en la medicina de sistemes

S'ha desenvolupat una plataforma tecnològica modular que proporciona un conjunt bàsic d'eines i tecnologies per donar suport a la implementació de SAI-TIC per a pacients crònics. Aquesta plataforma tecnològica ha suportat de manera eficient els quatre SAI dissenyats i avaluats en el context del projecte europeu NEXES (2008-2013, www.nexeshealth.eu) a un dels districtes sanitaris de Barcelona, amb un total de 540.000 habitants, i ha mostrat potencial d'escalabilitat a nivell regional.

El concepte de "Digital Health Framework (DHF)" ha estat articulat amb la finalitat d'enllaçar l'atenció sanitària i a la investigació biomèdica basada en la medicina de sistemes. La base de coneixement de Synergy-COPD ha estat desenvolupada com a un component d'investigació del DHF per tal de fomentar la transició envers una medicina 4P.

Conclusions

1. El model que integra els determinants fisiològics de la cadena de transport d'oxigen i els elements bioquímics moduladors de la formació a nivell mitocondrial de ROS, ha proporcionat, per primera vegada, un anàlisi quantitatiu de la relació entre la oxigenació cel·lular i la producció mitocondrial de ROS. El model genera resultats consistents en salut, però una millor estimació dels paràmetres mitocondrials és necessària quan s'aplica a MPOC.

2. La plataforma tecnològica per al suport de serveis d'atenció integrada (SAI) per a pacients crònics ha cobert de forma efectiva els requisits funcionals per al desplegament d'un entorn amb un únic proveïdor. Els reptes que cal afrontar per a un

desplegament a nivell regional de SAI han estat identificats i s'han proposat estratègies per a la seva adopció.

3. El concepte de "Digital Health Framework (DHF)" representa un escenari on l'enllaç entre l'atenció integrada i la investigació biomèdica de medicina de sistemes han de promoure el desplegament de la medicina 4P. S'ha proposat les línies estratègiques per a una correcta adopció del DHF.

4. La base del coneixement específica per a MPOC (COPDkb) ha estat desenvolupada i analitzada en aquesta tesi doctoral, constitueix un component principal de la investigació biomèdica basada en la medicina de sistemes.

Introducción

La proliferación de enfermedades no transmisibles y la creciente necesidad de contención de costes están desencadenando un profundo rediseño de la atención sanitaria hacia la adopción de un modelo de atención a crónicos, involucrando la implementación de servicios de atención integrada (SAI) con el soporte de las tecnologías de la información y de la comunicación (SAI-TIC). En este escenario, la emergente medicina de sistemas, con una aproximación holística basada en los mecanismos de las enfermedades, juega un papel muy relevante en la evaluación del riesgo para la salud y la estratificación de pacientes.

El objetivo principal de Synergy-COPD ha sido la exploración del potencial de una aproximación de medicina de sistemas para mejorar el conocimiento de los mecanismos subyacentes a la heterogeneidad de la enfermedad pulmonar obstructiva crónica (EPOC). Haciendo énfasis en los efectos sistémicos de la enfermedad, así como en la comorbilidad. La transferencia de nuevos conocimiento a la atención sanitaria ha sido también un objetivo principal del proyecto. Por otro lado, Synergy-COPD ha explorado nuevas interacciones entre investigación biomédica y atención sanitaria, con la finalidad última de promover la medicina 4P (Predictiva, Preventiva, Personalidad y Participativa) para pacientes con enfermedades crónicas.

Esta tesis doctoral contribuye con Synergy-COPD en dos aspectos específicos: 1. Un análisis cuantitativo de la relación entre la oxigenación celular y la producción de radicales libres de oxígeno (ROS) a nivel mitocondrial. 2. Diversos desarrollos tecnológicos dirigidos a la trasferencia de conocimiento biomédico a la atención sanitaria y la investigación biomédica.

Hipótesis

La hipótesis general de esta tesis doctoral es que una personalización de la evaluación del riesgo para la salud y la estratificación, tiene que desencadenar una atención sanitaria más eficiente y orientada al paciente. Específicamente, esta tesis doctoral plantea la hipótesis de que un modelado mecanicista del sistema de transporte y utilización de oxígeno, teniendo en cuenta la función mitocondrial, puede contribuir a evaluar los efectos biológicos de la hipoxia celular y su papel en la disfunción del músculo esquelético en la EPOC. Por otra parte, se plantea la hipótesis de que un diseño

holístico basado en las TIC puede contribuir a una implementación exitosa de SAI-TIC para los pacientes crónicos, fomentando la transferencia de los logros de la investigación orientada a sistemas en la asistencia sanitaria.

Objetivos

La integración del modelado fisiológico del sistema de transporte y utilización de oxígeno con el modelado bioquímico de la generación mitocondrial de ROS, con la finalidad de analizar las relaciones entre la oxigenación del músculo esquelético y la producción mitocondrial de ROS.

El desarrollo de herramientas TIC que den soporte a servicios de atención integrada (SAI-TIC) para pacientes crónicos, y que fomenten la interacción entre la investigación biomédica basada en la medicina de sistemas y la atención sanitaria.

Resultados principales

Análisis cuantitativo de la relación entre oxigenación celular y la generación mitocondrial de ROS

El modelaje realizado en esta tesis doctoral analiza todos los factores determinantes de la cadena de transporte de oxígeno. Se ha mostrado que un determinado grado de heterogeneidad en el músculo esquelético reduce la transferencia global de oxígeno más de lo que la reduce la heterogeneidad pulmonar. Sin embargo, la heterogeneidad observada actualmente a nivel pulmonar es mayor que la observada en músculo, por lo tanto, la heterogeneidad pulmonar en general tiene un impacto mayor sobre la transferencia total de oxígeno.

Por otra parte, hemos mostrado que la heterogeneidad muscular incrementa el rango de niveles de oxigenación celular (PmO_2), y en regiones del músculo esquelético con un mayor aporte sanguíneo en comparación con la capacidad metabólica, los valores de PmO_2 pueden exceder los correspondientes valores de oxigenación venosa mixta. Desafortunadamente, la medición del nivel de heterogeneidad funcional en músculo esquelético es muy insuficiente debido a las limitaciones tecnológicas.

El modelo indica que la relación entre la capacidad de transporte y utilización de oxígeno determina principalmente los valores de oxigenación celular (PmO_2). Este fenómeno, puede que sea muy relevante después de un proceso de entrenamiento de alta

intensidad en pacientes EPOC con limitaciones de transporte de oxígeno debido a la enfermedad pulmonar.

Simulaciones utilizando datos medidos en sujetos sanos realizando ejercicio máximo han desvelado que la altitud desencadena una alta producción de ROS mitocondrial en las regiones del músculo esquelético con una alta capacidad metabólica pero con una limitada capacidad de aporte de oxígeno. Esta observación, es evidente a partir de una altitud correspondiente a 5000 metros sobre el nivel del mar. Por encima de esta altitud no existe ningún asentamiento humano permanentemente habitado y los humanos experimentan una perdida inexorable de masa corporal. Sin embargo, se concluye que el uso del modelo integrado en condiciones de enfermedad requiere una mejor estimación de los parámetros mitocondriales.

Soporte TIC para el despliegue de servicios de atención integrada (SAI-TIC) y la interacción entre la atención sanitaria y la investigación biomédica basada en la medicina de sistemas

Se ha desarrollado una plataforma tecnológica modular que proporciona un conjunto básico de herramientas y tecnologías para dar soporte a la implantación de SAI-TIC para pacientes crónicos. Esta plataforma tecnológica ha soportado de manera eficiente los cuatro SAI diseñados y evaluados en el contexto del proyecto europeo NEXES (2008-2013, www.nexeshealth.eu) en uno de los distritos sanitarios de Barcelona, con un total de 540.000 habitantes, y ha mostrado potencial de escalabilidad a nivel regional.

El concepto de “Digital Health Framework (DHF)” ha sido articulado con el fin de enlazar la atención sanitaria y la investigación biomédica basada en la medicina de sistemas. La basa de conocimiento de Synergy-COPD ha sido desarrollada como un componente de investigación del DHF para fomentar la transición hacia una medicina 4P.

Conclusiones

1. El modelo que integra los determinantes fisiológicos de la cadena de transporte de oxígeno y los elementos bioquímicos moduladores de la formación a nivel mitocondrial de ROS, ha proporcionado, por primera vez, un análisis cuantitativo de la relación entre la oxigenación celular y la producción mitocondrial de ROS. El modelo genera resultados consistentes en salud, pero una mejor estimación de los parámetros mitocondriales es necesaria cuando se aplica en EPOC.
2. La plataforma tecnológica para el soporte de servicios de atención integrada

(SAI) para pacientes crónicos ha cubierto de forma efectiva los requisitos funcionales para el despliegue en un entorno con un único proveedor. Los retos que se han afrontar un despliegue regional de SAI, han sido identificados y se han propuesto estrategias para su adopción.

3. El concepto de “Digital Health Framework (DHF)” representa un escenario en el que el enlace entre atención integrada e investigación biomédica de medicina de sistemas debe promover el despliegue de la medicina 4P. Se han propuesto líneas estratégicas para una correcta adopción del DHF.
4. La base de conocimiento específica para EPOC (COPDkb) que ha sido desarrollada y analizada en esta tesis doctoral, constituye un componente principal de la investigación biomédica basada en la medicina de sistemas.

Integrated model parameterization for the BioBridge subjects

To compute estimations of average muscle mitochondrial oxygen levels (PmO2) and Skeletal Muscle ROS generation for the BioBridge subjects the following set of oxygen transport and utilization parameters are needed:

Model parameter	Description	Units
TOTALVMAX	Maximal mitochondrial oxygen consumption when oxygen is in excess (Vmax) of overall exercising muscle	ml/min
TOTALQ	Total Cardiac Output	l/min
TOTALP50	Total muscle partial oxygen pressure at which speed of mitochondrial oxygen consumption is half maximal	mm Hg
EXS	Percent of TOTALQ that goes to exercising tissues (muscle)	%
VO2NEBP	Non-exercising body tissues oxygen uptake (VO2)	ml/min
VCO2NEBP	Non-exercising body tissues carbon dioxide uptake (VCO2)	ml/min
LOGSDVMAX	log SD Vmax (degree of muscle metabolism/perfusion heterogeneity)	real number
FIO2	Fractional Inspired Oxygen	mm Hg
TOTALVA	Total Alveolar Ventilation	l/min (BTPS)
TOTALDL	Total Lung Diffusion capacity	ml/min/mmHg
TOTALDM	Total Muscle Diffusion capacity	ml/min/mmHg
RQ	CO2/O2 exchange ratio	ratio
PB	Atmospheric barometric pressure	mm Hg
HB	Hemoglobin	mg/dl
TEMP	body temperature	degrees centigrade
P50	O2 hemoglobin dissociation curve P50	mm Hg
APH	PH of blood equilibrated with PCO2 of 30	mm Hg
BPH	PH of blood equilibrated with PCO2 of 60	mm Hg
SHUNT	cardiac shunt	Percentage
LOGSDQ	log SD Q (degree of lung ventilation/perfusion heterogeneity	real number
QSKEW	Modal perfusion skew	real number

Not all the above oxygen pathway parameters were measured in the BioBridge subjects so some estimation were performed. The approach used in this study is detailed in the following table, but briefly consisted on targeting for each subject measured VO_2max and measured PaO2 by changing simulated total cardiac output, log SD Q and muscle diffusion capacity:

Model parameter	Parameter estimation approach
TOTALVMAX	20% higher than measured VO2max
TOTALQ	Estimated for each subject, see Table I.
TOTALP50	0.14
EXS	80% for Controls and ((VO2max - VO2rest) / VO2max)*100 for COPD
VO2NEBP	300 for Controls and measured for COPD
VCO2NEBP	240 for Controls and 75% of measured VO2 for COPD
LOGSDVMAX	0.1
FIO2	0.21
TOTALVA	Measured VE – (deadspace as (PaCO2-PaCO2exp)/PaCO2*tidal volume)
TOTALDL	100 ml/min/mmHg.
TOTALDM	Estimated for each subject, see Table I.
RQ	Measured
PB	760
HB	Measured
TEMP	36.5
P50	26.8
APH	PH AND PaCO2 and use the Henderson Hasselbach nomogram.
BPH	PH AND PaCO2 and use the Henderson Hasselbach nomogram.
SHUNT	0
LOGSDQ	Estimated for each subject, see Table I.
QSKEW	0

To this end, for each subject, lung-diffusing capacity was set to 100ml/min/mmHg, so that no limitations on lung O2 diffusing capacity are considered as reported in the literature, and the lung log SD Q was changed in such a way that predicted PaO2 matched measured PaO2 with a threshold of ±1 mm Hg. The percent of total blood flow that goes to exercising tissues was set assuming a constant difference of 5ml/dl between CaO2 and CvO2, so that the blood flow that goes to non-exercising tissues is computed as the measured VO2 at rest divided by 50L/min. Finally, total cardiac output and total muscle diffusing capacity was set in such a way that predicted whole body VO2max matched measured VO2max (with a threshold of ±10ml/min) while still keeping the previous fitting restrictions to PaO2. Final parameters used are presented in **Table I** below.

With respect to the cell bioenergetics parameters, available data on changes in mitochondrial enzyme activity and gene expression in COPD patients has been analyzed and found that the most profound changes are in the activity of respiratory complex IV (0.5 of healthy subjects) and succinate dehydrogenase (0.7 of healthy subjects). So that this allowed going from a “healthy mitochondria”, used when simulating input data from healthy subjects, to a “COPD-like mitochondria”, used when simulating data from COPD patients. These changes result in essential changes of ROS production.

Table I: O_2 pathway model input parameter used to estimate unmeasured parameters. Before training (upper panel) and after training (lower panel).

Model parameter	C1	C2	C3	C4	C5	C6	C7	C8	C9	E1	E2	E3	E4	E5	E6	E7	E8	E9	E10	E11	E12	L1	L2	L3	L4	L5	L6
TOTALVMAX	2029	1788	1340	2289	1783	2167	2550	1079	2388	1584	1497	758	863	1319	1022	959	1066	1116	900	1002	1601	547	952	1218	864	1188	691
TOTALQ	20	11	9,5	16	18	18	18	8	18	9,8	9,8	5,6	7,1	7,5	8,5	8,2	8,2	8,3	7,3	8	10	6,8	7	9,2	7,5	10	6,6
TOTALP50	0,14	0,14	0,14	0,14	0,14	0,14	0,14	0,14	0,14	0,14	0,14	0,14	0,14	0,14	0,14	0,14	0,14	0,14	0,14	0,14	0,14	0,14	0,14	0,14	0,14	0,14	0,14
EXS	80,10	68,00	46,32	54,63	69,56	69,78	71,33	53,25	59,89	53,06	49,59	42,14	36,34	58,13	37,41	31,71	50,24	42,89	45,48	34,50	48,40	14,41	37,71	46,74	49,87	48,80	29,09
VO2NEBP	199	176	255	363	274	272	258	187	361	230	247	162	226	157	266	280	204	237	199	262	258	291	218	245	188	256	234
VCO2NEBP	149	132	191	272	206	204	194	140	271	173	185	122	170	118	200	210	153	178	149	197	194	218	164	184	141	192	176
LOGSDVMAX	0,1	0,1	0,1	0,1	0,1	0,1	0,1	0,1	0,1	0,1	0,1	0,1	0,1	0,1	0,1	0,1	0,1	0,1	0,1	0,1	0,1	0,1	0,1	0,1	0,1	0,1	0,1
FIO2	0,21	0,21	0,21	0,21	0,21	0,21	0,21	0,21	0,21	0,21	0,21	0,21	0,21	0,21	0,21	0,21	0,21	0,21	0,21	0,21	0,21	0,21	0,21	0,21	0,21	0,21	0,21
TOTALVA	88,94	52,00	43,08	51,70	60,29	49,02	84,17	29,76	66,90	40,72	39,19	28,32	26,46	29,21	20,44	38,73	27,01	32,47	20,25	30,87	50,34	19,05	29,10	39,24	22,24	29,90	16,23
TOTALDL	100	100	100	100	100	100	100	100	100	100	100	100	100	100	100	100	100	100	100	100	100	100	100	100	100	100	100
TOTALDM	41	53	37	59	29,5	39	52	24	43	80	38	25	50	40	20	45	25	50	23	28	45	20	40	40	19	50	35
RQ	1,06	1,22	1,14	1,22	1,26	1,13	1,31	1,36	1,12	1,24	1,07	1,00	0,99	1,21	1,07	1,10	1,17	1,10	0,88	1,01	1,16	0,99	1,13	1,14	1,02	1,20	0,93
PB	760	760	760	760	760	760	760	760	760	760	760	760	760	760	760	760	760	760	760	760	760	760	760	760	760	760	760
HB	13,4	13,4	14,9	13,7	14,6	14,7	15,8	13,4	16,7	15,2	15,7	15,1	14,5	16,6	14,5	14,9	14,6	14,3	13,0	15,8	17,3	14,3	16,1	13,0	12,2	11,3	13,5
TEMP	36,5	36,5	36,5	36,5	36,5	36,5	36,5	36,5	36,5	36,5	36,5	36,5	36,5	36,5	36,5	36,5	36,5	36,5	36,5	36,5	36,5	36,5	36,5	36,5	36,5	36,5	36,5
P50	26,8	26,8	26,8	26,8	26,8	26,8	26,8	26,8	26,8	26,8	26,8	26,8	26,8	26,8	26,8	26,8	26,8	26,8	26,8	26,8	26,8	26,8	26,8	26,8	26,8	26,8	26,8
APH	7,51	7,49	7,49	7,49	7,51	7,47	7,5	7,49	7,46	7,47	7,47	7,47	7,48	7,46	7,54	7,48	7,50	7,49	7,44	7,50	7,46	7,49	7,49	7,51	7,48	7,54	7,39
BPH	7,31	7,3	7,3	7,29	7,3	7,28	7,3	7,29	7,26	7,27	7,27	7,27	7,29	7,27	7,33	7,29	7,30	7,31	7,25	7,31	7,29	7,29	7,30	7,31	7,27	7,33	7,20
SHUNT	0	0	0	0	0	0	0	0	0	0	0	0	0	0	0	0	0	0	0	0	0	0	0	0	0	0	0
LOGSDQ	0,85	0,5	0,7	0,61	0,83	0,43	0,75	0,63	0,58	0,69	0,57	1,04	1,05	0,71	0,9	1,03	1	0,79	0,69	0,91	0,916	1,4	0,98	0,74	0,745	0,88	0,8
QSKEW	0	0	0	0	0	0	0	0	0	0	0	0	0	0	0	0	0	0	0	0	0	0	0	0	0	0	0
Model parameter	**C1**	**C2**	**C3**	**C4**	**C5**	**C6**	**C7**	**C8**	**C9**	**E1**	**E2**	**E3**	**E4**	**E5**	**E6**	**E7**	**E8**	**E9**	**E10**	**E11**	**E12**	**L1**	**L2**	**L3**	**L4**	**L5**	**L6**
TOTALVMAX	2247	1814	1778	3040	1892	2683	2813	1333	2880	2175	2019	984	794	1344	1080	998	1154	1265	1232	1354	2142	732	1303	1322	764	1285	689
TOTALQ	20	18	18	25	18	18	18	9	18	16	16	7,9	7,5	9	8,2	8,5	9	9	9,3	11	14	7,2	9	9,5	6,5	10,5	6,2
TOTALP50	0,14	0,14	0,14	0,14	0,14	0,14	0,14	0,14	0,14	0,14	0,14	0,14	0,14	0,14	0,14	0,14	0,14	0,14	0,14	0,14	0,14	0,14	0,14	0,14	0,14	0,14	0,14
EXS	71,90	83,00	72,56	74,56	62,33	76,11	63,00	55,78	66,44	66,38	74,75	55,19	27,73	58,00	48,54	40,00	37,56	49,78	49,03	48,73	66,57	26,94	54,00	50,74	44,00	48,00	33,55
VO2NEBP	281	153	247	318	339	215	333	199	302	269	202	177	271	189	211	255	281	226	237	282	234	263	207	234	182	273	206
VCO2NEBP	211	115	185	239	254	161	250	149	227	202	152	133	203	142	158	191	211	170	178	212	176	197	155	176	137	205	155
LOGSDVMAX	0,1	0,1	0,1	0,1	0,1	0,1	0,1	0,1	0,1	0,1	0,1	0,1	0,1	0,1	0,1	0,1	0,1	0,1	0,1	0,1	0,1	0,1	0,1	0,1	0,1	0,1	0,1
FIO2	0,21	0,21	0,21	0,21	0,21	0,21	0,21	0,21	0,21	0,21	0,21	0,21	0,21	0,21	0,21	0,21	0,21	0,21	0,21	0,21	0,21	0,21	0,21	0,21	0,21	0,21	0,21
TOTALVA	71,02	53,30	48,88	78,61	54,50	67,28	98,36	51,59	79,13	56,47	53,61	25,16	34,92	29,21	26,74	60,24	27,59	36,41	29,70	34,49	73,16	16,55	43,76	37,05	20,19	28,32	13,54
TOTALDL	100	100	100	100	100	100	100	100	100	100	100	100	100	100	100	100	100	100	100	100	100	100	100	100	100	100	100
TOTALDM	46	34	29.5	60	31	60	65	40	61	43,5	39	19	31	33	50	24	25	35	50	31	46	38	34	38	30	30	20
RQ	1,06	1,22	1,14	1,22	1,26	1,13	1,31	1,36	1,12	1,24	1,07	1,00	0,99	1,21	1,07	1,10	1,17	1,10	1,01	1,06	1,27	0,88	1,00	1,12	1,04	1,18	0,87
PB	760	760	760	760	760	760	760	760	760	760	760	760	760	760	760	760	760	760	760	760	760	760	760	760	760	760	760
HB	13,4	13,4	14,9	13,7	14,6	14,7	15,8	13,4	16,7	15,5	15,1	15,8	14,2	15,5	13,9	13,0	17,2	14,2	12,8	12,9	16,7	16,1	15,2	13,7	12,0	13,1	13,5
TEMP	36,5	36,5	36,5	36,5	36,5	36,5	36,5	36,5	36,5	36,5	36,5	36,5	36,5	36,5	36,5	36,5	36,5	36,5	36,5	36,5	36,5	36,5	36,5	36,5	36,5	36,5	36,5
P50	26,8	26,8	26,8	26,8	26,8	26,8	26,8	26,8	26,8	26,8	26,8	26,8	26,8	26,8	26,8	26,8	26,8	26,8	26,8	26,8	26,8	26,8	26,8	26,8	26,8	26,8	26,8
APH	7,51	7,49	7,49	7,49	7,51	7,47	7,5	7,49	7,46	7,49	7,48	7,47	7,5	7,51	7,5	7,38	7,47	7,49	7,49	7,48	7,46	7,48	7,49	7,52	7,49	7,5	7,42
BPH	7,31	7,3	7,3	7,29	7,3	7,28	7,3	7,29	7,26	7,29	7,28	7,27	7,31	7,31	7,29	7,19	7,29	7,29	7,29	7,27	7,28	7,29	7,3	7,32	7,28	7,29	7,23
SHUNT	0	0	0	0	0	0	0	0	0	0	0	0	0	0	0	0	0	0	0	0	0	0	0	0	0	0	0
LOGSDQ	0,79	0,75	0,68	0,68	0,81	0,57	0,71	0,81	0,58	0,85	0,74	0,79	1,4	0,92	1,12	1,22	1,05	0,85	0,77	0,82	0,98	1,45	1,05	0,71	0,9	0,85	0,88
QSKEW	0	0	0	0	0	0	0	0	0	0	0	0	0	0	0	0	0	0	0	0	0	0	0	0	0	0	0

References

1. Auffray, C., D. Charron, L. Hood, *Predictive, preventive, personalized and participatory medicine: back to the future.* Genome Medicine, 2010. **2**(8): p. 57. PMID: 20804580.
2. Hood, L., C. Auffray, *Participatory medicine: a driving force for revolutionizing healthcare.* Genome Med, 2013. **5**(12): p. 110.
3. WHO, *2008-2013 Action Plan for the Global Strategy for the Prevention and Control of Noncommunicable Diseases, ISBN: 9789241597418, URL:http://www.who.int/nmh/Actionplan-PC-NCD-2008.pdf. Accessed: 2013-08-20. (Archived by WebCite® at http://www.webcitation.org/6J0XGnHcJ)*.
4. Vestbo, J., S.S. Hurd, A.G. Agusti, P.W. Jones, C. Vogelmeier, A. Anzueto, P.J. Barnes, L.M. Fabbri, F.J. Martinez, M. Nishimura, R.A. Stockley, D.D. Sin, R. Rodriguez-Roisin, *Global strategy for the diagnosis, management, and prevention of chronic obstructive pulmonary disease: GOLD executive summary.* Am J Respir Crit Care Med, 2013. **187**(4): p. 347-65.
5. Murray, C.J.L., A.D. Lopez, *Measuring the Global Burden of Disease.* New England Journal of Medicine, 2013. **369**(5): p. 448-457.
6. Bousquet, J., J. Anto, P. Sterk, I. Adcock, K. Chung, J. Roca, A. Agusti, C. Brightling, A. Cambon-Thomsen, A. Cesario, S. Abdelhak, S. Antonarakis, A. Avignon, A. Ballabio, E. Baraldi, A. Baranov, T. Bieber, J. Bockaert, S. Brahmachari, C. Brambilla, J. Bringer, M. Dauzat, I. Ernberg, L. Fabbri, P. Froguel, D. Galas, T. Gojobori, P. Hunter, C. Jorgensen, F. Kauffmann, *Systems medicine and integrated care to combat chronic noncommunicable diseases.* Genome Medicine, 2011. **3**(7): p. 43.
7. WHO, *Innovative Care for Chronic Conditions: Building Blocks for Action. Geneva: World Health Organization (WHO/MNC/CCH/02.01). URL:http://www.who.int/chp/knowledge/publications/icccreport/en/. Accessed: 2013-08-20. (Archived by WebCite® at http://www.webcitation.org/6J0iTPMcg).* Geneva: World Health Organization, 2002.
8. EU, C., *Innovative approaches for chronic diseases in public health and healthcare systems. Council of the EU 3053rd Employment, social policy health and consumer affairs.*, 2010.
9. McCreary, L., *Kaiser Permanente's innovation on the front lines.* Harv Bus Rev, 2010. **88**(9): p. 92, 94-7, 126.
10. Atkins, D., J. Kupersmith, S. Eisen, *The Veterans Affairs experience: comparative effectiveness research in a large health system.* Health Aff (Millwood), 2010. **29**(10): p. 1906-12.
11. True, G., A.E. Butler, B.G. Lamparska, M.L. Lempa, J.A. Shea, D.A. Asch, R.M. Werner, *Open access in the patient-centered medical home: lessons from the Veterans Health Administration.* J Gen Intern Med, 2013. **28**(4): p. 539-45. PMID: Pmc3599018.
12. NEXES, *Supporting Healthier and Independent Living for Chronic Patients and Elderly.* CIP-ICT-PSP-225025, 2008-2013.
13. WB., R., *Health Care as a Complex Adaptive System: Implications for Design and Management.* The Bridge, 2008. **Spring**: p. 17-25.
14. Epping-Jordan, J.E., G. Galea, C. Tukuitonga, R. Beaglehole, *Preventing chronic diseases: taking stepwise action.* Lancet, 2005. **366**(9497): p. 1667-71.
15. Lowell, K.H., J. Bertko, *The Accountable Care Organization (ACO) model: building blocks for success.* J Ambul Care Manage, 2010. **33**(1): p. 81-8.
16. Goldsmith, J., *Accountable care organizations: the case for flexible partnerships between health plans and providers.* Health Aff (Millwood), 2011. **30**(1): p. 32-40.
17. Tol, J., I.C.S. Swinkels, J.N. Struijs, C. Veenhof, D.H. de Bakker, *Integrating care by implementation of bundled payments: results from a national survey on the experience of Dutch dietitians.* 2013, 2013.
18. EIP-AHA, *European Innovation Partnership for Active and Healthy Ageing. URL:http://ec.europa.eu/research/innovation-union/index_en.cfm?section=active-healthy-ageing. Accessed: 2014-06-19. (Archived by WebCite® at http://www.webcitation.org/6QRp7pXLY).*
19. *eHealth Action Plan 2012-2020. Green Paper on mobile health ("mHealth"). URL:https://ec.europa.eu/digital-agenda/en/news/green-paper-mobile-health-*

mhealth. Accessed: 2014-06-22. (Archived by WebCite® at http://www.webcitation.org/6QWamz0Y4). 2014.
20. Hood, L., J. Heath, M. Phelps, B. Lin, *Systems biology and new technologies enable predictive and preventative medicine.* Science, 2004. **306**: p. 640 - 643.
21. Oltvai, Z.N., A.L. Barabasi, *Systems biology. Life's complexity pyramid.* Science, 2002. **298**(5594): p. 763-4.
22. Beleut, M., P. Zimmermann, M. Baudis, N. Bruni, P. Buhlmann, O. Laule, V.-D. Luu, W. Gruissem, P. Schraml, H. Moch, *Integrative genome-wide expression profiling identifies three distinct molecular subgroups of renal cell carcinoma with different patient outcome.* BMC Cancer, 2012. **12**(1): p. 310.
23. Zhou, X., J. Menche, A.L. Barabasi, A. Sharma, *Human symptoms-disease network.* Nat Commun, 2014. **5**: p. 4212.
24. Tian, Q., N.D. Price, L. Hood, *Systems cancer medicine: towards realization of predictive, preventive, personalized and participatory (P4) medicine.* J Intern Med, 2012. **271**(2): p. 111-21. PMID: Pmc3978383.
25. Lee, D.-S., J. Park, K.A. Kay, N.A. Christakis, Z.N. Oltvai, A.-L. Barabási, *The implications of human metabolic network topology for disease comorbidity.* Proceedings of the National Academy of Sciences, 2008. **105**(29): p. 9880-9885.
26. Loscalzo, J., I. Kohane, A.L. Barabasi, *Human disease classification in the postgenomic era: a complex systems approach to human pathobiology.* Mol Syst Biol, 2007. **3**: p. 124. PMID: 1948102.
27. Park, J., D.-S. Lee, N.a. Christakis, A.-L. Barabási, *The impact of cellular networks on disease comorbidity.* Molecular systems biology, 2009. **5**: p. 262.
28. Vidal, M., Michael E. Cusick, A.-L. Barabási, *Interactome Networks and Human Disease.* Cell, 2011. **144**(6): p. 986-998.
29. Barabási, A.-L., *Network medicine--from obesity to the "diseasome".* The New England journal of medicine, 2007. **357**: p. 404-7.
30. Loscalzo, J., A.L. Barabasi, *Systems biology and the future of medicine.* Wiley Interdiscip Rev Syst Biol Med, 2011. **3**(6): p. 619-27. PMID: 3188693.
31. Barabasi, A.L., E. Bonabeau, *Scale-free networks.* Sci Am, 2003. **288**(5): p. 60-9.
32. van Riel, N.a.W., *Dynamic modelling and analysis of biochemical networks: mechanism-based models and model-based experiments.* Briefings in bioinformatics, 2006. **7**: p. 364-74.
33. Barabasi, A.-L., N. Gulbahce, J. Loscalzo, *Network medicine: a network-based approach to human disease.* Nat Rev Genet, 2011. **12**(1): p. 56-68.
34. Ghosh, S., Y. Matsuoka, Y. Asai, K.-Y. Hsin, H. Kitano, *Software for systems biology: from tools to integrated platforms.* Nature Reviews Genetics, 2011. **12**(12): p. 821-832.
35. Antezana, E., M. Kuiper, V. Mironov, *Biological knowledge management: the emerging role of the Semantic Web technologies.* Briefings in Bioinformatics, 2009. **10**(4): p. 392-407.
36. Seoane, J.A., G. López-Campos, J. Dorado, F. Martin-Sanchez, *New approaches in data integration for systems chemical biology.* Current topics in medicinal chemistry, 2013. **13**(5): p. 591-601.
37. Szalma, S., *Effective knowledge management in translational medicine.* J Transl Med, 2010. **8**: p. 68.
38. Cases, M., L.I. Furlong, J. Albanell, R.B. Altman, R. Bellazzi, S. Boyer, A. Brand, A.J. Brookes, S. Brunak, T.W. Clark, J. Gea, P. Ghazal, N. Graf, R. Guigo, T.E. Klein, N. Lopez-Bigas, V. Maojo, B. Mons, M. Musen, J.L. Oliveira, A. Rowe, P. Ruch, A. Shabo, E.H. Shortliffe, A. Valencia, J. van der Lei, M.A. Mayer, F. Sanz, *Improving data and knowledge management to better integrate health care and research.* J Intern Med, 2013. **274**(4): p. 321-8.
39. Maier, D., W. Kalus, M. Wolff, S.G. Kalko, J. Roca, I. Marin de Mas, N. Turan, M. Cascante, F. Falciani, M. Hernandez, J. Villa-Freixa, S. Losko, *Knowledge management for Systems Biology a general and visually driven framework applied to translational medicine.* BMC systems biology, 2011. **5**: p. 38.
40. Wyatt, J., D. Spiegelhalter, *Field trials of medical decision-aids: potential problems and solutions.* Proc Annu Symp Comput Appl Med Care, 1991: p. 3-7. PMID: Pmc2247484.
41. Shapiro SD, Reilly JJ Jr., R. SI, *Chronic bronchitis and emphysema. In: Mason RJ, Broaddus VC, Martin TR, King TE Jr., Schraufnagel DE, Murray JF, Nadel JA editors. .* Textbook of respiratory medicine, 5th edition, volume I. Saunders Philadelphia: Saunders Elsevier; 2010:919–967

42. Lopez, A.D., C.D. Mathers, M. Ezzati, D.T. Jamison, C.J. Murray, *Global and regional burden of disease and risk factors, 2001: systematic analysis of population health data.* Lancet, 2006. **367**(9524): p. 1747-57.
43. Salvi, S.S., P.J. Barnes, *Chronic obstructive pulmonary disease in non-smokers.* Lancet, 2009. **374**(9691): p. 733-43.
44. Tashkin, D.P., V.A. Clark, A.H. Coulson, M. Simmons, L.B. Bourque, C. Reems, R. Detels, J.W. Sayre, S.N. Rokaw, *The UCLA population studies of chronic obstructive respiratory disease. VIII. Effects of smoking cessation on lung function: a prospective study of a free-living population.* Am Rev Respir Dis, 1984. **130**(5): p. 707-15.
45. Fletcher, C., R. Peto, *The natural history of chronic airflow obstruction.* Br Med J, 1977. **1**(6077): p. 1645-8. PMID: Pmc1607732.
46. Brutsche, M.H., S.H. Downs, C. Schindler, M.W. Gerbase, J. Schwartz, M. Frey, E.W. Russi, U. Ackermann-Liebrich, P. Leuenberger, *Bronchial hyperresponsiveness and the development of asthma and COPD in asymptomatic individuals: SAPALDIA Cohort Study.* Thorax, 2006. **61**(8): p. 671-677.
47. Lange, P., J. Parner, J. Vestbo, P. Schnohr, G. Jensen, *A 15-Year Follow-up Study of Ventilatory Function in Adults with Asthma.* New England Journal of Medicine, 1998. **339**(17): p. 1194-1200.
48. Tager, I.B., M.R. Segal, F.E. Speizer, S.T. Weiss, *The natural history of forced expiratory volumes. Effect of cigarette smoking and respiratory symptoms.* Am Rev Respir Dis, 1988. **138**(4): p. 837-49.
49. Mannino, D.M., A.S. Buist, *Global burden of COPD: risk factors, prevalence, and future trends.* Lancet, 2007. **370**(9589): p. 765-73.
50. Coxson, H.O., I.H. Chan, J.R. Mayo, J. Hlynsky, Y. Nakano, C.L. Birmingham, *Early emphysema in patients with anorexia nervosa.* Am J Respir Crit Care Med, 2004. **170**(7): p. 748-52.
51. Black, P.N., R. Scragg, *Relationship between serum 25-hydroxyvitamin d and pulmonary function in the third national health and nutrition examination survey.* Chest, 2005. **128**(6): p. 3792-8.
52. Silverman, E.K., *Progress in chronic obstructive pulmonary disease genetics.* Proc Am Thorac Soc, 2006. **3**(5): p. 405-8. PMID: Pmc2658703.
53. Hogg, J.C., W. Timens, *The pathology of chronic obstructive pulmonary disease.* Annu Rev Pathol, 2009. **4**: p. 435-59.
54. Agusti, A., P.M. Calverley, B. Celli, H.O. Coxson, L.D. Edwards, D.A. Lomas, W. MacNee, B.E. Miller, S. Rennard, E.K. Silverman, R. Tal-Singer, E. Wouters, J.C. Yates, J. Vestbo, *Characterisation of COPD heterogeneity in the ECLIPSE cohort.* Respir Res, 2010. **11**: p. 122. PMID: Pmc2944278.
55. Casanova, C., J.P. de Torres, A. Aguirre-Jaime, V. Pinto-Plata, J.M. Marin, E. Cordoba, R. Baz, C. Cote, B.R. Celli, *The progression of chronic obstructive pulmonary disease is heterogeneous: the experience of the BODE cohort.* Am J Respir Crit Care Med, 2011. **184**(9): p. 1015-21.
56. Vestbo, J., A. Agusti, E.F. Wouters, P. Bakke, P.M. Calverley, B. Celli, H. Coxson, C. Crim, L.D. Edwards, N. Locantore, D.A. Lomas, W. MacNee, B. Miller, S.I. Rennard, E.K. Silverman, J.C. Yates, R. Tal-Singer, *Should we view chronic obstructive pulmonary disease differently after ECLIPSE? A clinical perspective from the study team.* Am J Respir Crit Care Med, 2014. **189**(9): p. 1022-30.
57. Soler-Cataluna, J.J., R. Rodriguez-Roisin, *Frequent chronic obstructive pulmonary disease exacerbators: how much real, how much fictitious?* Copd, 2010. **7**(4): p. 276-84.
58. Hurst, J.R., J. Vestbo, A. Anzueto, N. Locantore, H. Mullerova, R. Tal-Singer, B. Miller, D.A. Lomas, A. Agusti, W. Macnee, P. Calverley, S. Rennard, E.F. Wouters, J.A. Wedzicha, *Susceptibility to exacerbation in chronic obstructive pulmonary disease.* N Engl J Med, 2010. **363**(12): p. 1128-38.
59. Suissa, S., S. Dell'Aniello, P. Ernst, *Long-term natural history of chronic obstructive pulmonary disease: severe exacerbations and mortality.* Thorax, 2012. **67**(11): p. 957-63. PMID: Pmc3505864.
60. Maltais, F., M. Decramer, R. Casaburi, E. Barreiro, Y. Burelle, R. Debigare, P.N. Dekhuijzen, F. Franssen, G. Gayan-Ramirez, J. Gea, H.R. Gosker, R. Gosselink, M. Hayot, S.N. Hussain, W. Janssens, M.I. Polkey, J. Roca, D. Saey, A.M. Schols, M.A. Spruit, M. Steiner, T. Taivassalo, T. Troosters, I. Vogiatzis, P.D. Wagner, *An official american thoracic society/european respiratory society statement: update on limb*

muscle dysfunction in chronic obstructive pulmonary disease. Am J Respir Crit Care Med, 2014. **189**(9): p. e15-62.
61. Divo, M., C. Cote, J.P. de Torres, C. Casanova, J.M. Marin, V. Pinto-Plata, J. Zulueta, C. Cabrera, J. Zagaceta, G. Hunninghake, B. Celli, *Comorbidities and risk of mortality in patients with chronic obstructive pulmonary disease.* Am J Respir Crit Care Med, 2012. **186**(2): p. 155-61.
62. Van Hoyweghen, I., K. Horstman, *European practices of genetic information and insurance: lessons for the Genetic Information Nondiscrimination Act.* JAMA, 2008. **300**(3): p. 326 - 7.
63. Dustin, M.L., *Signaling at neuro/immune synapses.* J Clin Invest, 2012. **122**(4): p. 1149-55. PMID: Pmc3314453.
64. Poole, D.C., D.M. Hirai, S.W. Copp, T.I. Musch, *Muscle oxygen transport and utilization in heart failure: implications for exercise (in)tolerance.* Am J Physiol Heart Circ Physiol, 2012. **302**(5): p. H1050-63. PMID: Pmc3311454.
65. Vanfleteren, L.E., M.A. Spruit, M. Groenen, S. Gaffron, V.P. van Empel, P.L. Bruijnzeel, E.P. Rutten, J. Op 't Roodt, E.F. Wouters, F.M. Franssen, *Clusters of comorbidities based on validated objective measurements and systemic inflammation in patients with chronic obstructive pulmonary disease.* Am J Respir Crit Care Med, 2013. **187**(7): p. 728-35.
66. Fabbri, L.M., B. Beghe, A. Agusti, *COPD and the solar system: introducing the chronic obstructive pulmonary disease comorbidome.* Am J Respir Crit Care Med, 2012. **186**(2): p. 117-9.
67. Rennard, S.I., *COPD Heterogeneity: What This Will Mean in Practice.* Respiratory Care, 2011. **56**(8): p. 1181-1187.
68. Chen, X., X. Xu, F. Xiao, *Heterogeneity of chronic obstructive pulmonary disease: from phenotype to genotype.* Frontiers of Medicine, 2013. **7**(4): p. 425-432.
69. Rabe, K.F., S. Hurd, A. Anzueto, P.J. Barnes, S.A. Buist, P. Calverley, Y. Fukuchi, C. Jenkins, R. Rodriguez-Roisin, C. van Weel, J. Zielinski, *Global strategy for the diagnosis, management, and prevention of chronic obstructive pulmonary disease: GOLD executive summary.* Am J Respir Crit Care Med, 2007. **176**(6): p. 532-55.
70. Calverley, P.M., K.F. Rabe, U.-M. Goehring, S. Kristiansen, L.M. Fabbri, F.J. Martinez, *Roflumilast in symptomatic chronic obstructive pulmonary disease: two randomised clinical trials.* The Lancet, 2009. **374**: p. 685-694.
71. Vogelmeier, C., J. Vestbo, *COPD assessment: I, II, III, IV and/or A, B, C, D.* Eur Respir J, 2014. **43**(4): p. 949-50.
72. Celli, B.R., C.G. Cote, J.M. Marin, C. Casanova, M. Montes de Oca, R.A. Mendez, V. Pinto Plata, H.J. Cabral, *The body-mass index, airflow obstruction, dyspnea, and exercise capacity index in chronic obstructive pulmonary disease.* N Engl J Med, 2004. **350**(10): p. 1005-12.
73. Puhan, M.A., N.N. Hansel, P. Sobradillo, P. Enright, P. Lange, D. Hickson, A.M. Menezes, G.t. Riet, U. Held, A. Domingo-Salvany, Z. Mosenifar, J.M. Antó, K.G.M. Moons, A. Kessels, J. Garcia-Aymerich, f.t.I.C.C.C.W. Group, *Large-scale international validation of the ADO index in subjects with COPD: an individual subject data analysis of 10 cohorts.* BMJ Open, 2012. **2**(6).
74. Jones, R.C., G.C. Donaldson, N.H. Chavannes, K. Kida, M. Dickson-Spillmann, S. Harding, J.A. Wedzicha, D. Price, M.E. Hyland, *Derivation and validation of a composite index of severity in chronic obstructive pulmonary disease: the DOSE Index.* Am J Respir Crit Care Med, 2009. **180**(12): p. 1189-95.
75. Motegi, T., R.C. Jones, T. Ishii, K. Hattori, Y. Kusunoki, R. Furutate, K. Yamada, A. Gemma, K. Kida, *A comparison of three multidimensional indices of COPD severity as predictors of future exacerbations.* Int J Chron Obstruct Pulmon Dis, 2013. **8**: p. 259-71. PMID: Pmc3674751.
76. Vestbo, J., W. Anderson, H.O. Coxson, C. Crim, F. Dawber, L. Edwards, G. Hagan, K. Knobil, D.a. Lomas, W. MacNee, E.K. Silverman, R. Tal-Singer, *Evaluation of COPD Longitudinally to Identify Predictive Surrogate End-points (ECLIPSE).* The European respiratory journal : official journal of the European Society for Clinical Respiratory Physiology, 2008. **31**: p. 869-73.
77. Donaldson, G., H. Mullerova, N. Locantore, J. Hurst, J. Vestbo, A. Anzueto, J. Wedzicha, *Factors Associated With Change In COPD Exacerbation Frequency Phenotype.* J Respir Crit Care Med, 2011. **183**: p. A5362.
78. Barnes, P.J., B.R. Celli, *Systemic manifestations and comorbidities of COPD.* Eur Respir J, 2009. **33**(5): p. 1165-85.

79. Turan, N., S. Kalko, A. Stincone, K. Clarke, A. Sabah, K. Howlett, S.J. Curnow, D.A. Rodriguez, M. Cascante, L. O'Neill, S. Egginton, J. Roca, F. Falciani, *A Systems Biology Approach Identifies Molecular Networks Defining Skeletal Muscle Abnormalities in Chronic Obstructive Pulmonary Disease.* PLoS Comput Biol, 2011. **7**(9): p. e1002129.
80. Rodriguez, D.A., S. Kalko, E. Puig-Vilanova, M. Perez-Olabarria, F. Falciani, J. Gea, M. Cascante, E. Barreiro, J. Roca, *Muscle and blood redox status after exercise training in severe COPD patients.* Free Radic Biol Med, 2012. **52**(1): p. 88-94.
81. Klareskog, L., A. Catrina, S. Paget, *Rheumatoid arthritis.* Lancet, 2009. **373**(9664): p. 659 - 72.
82. Synergy-COPD, *Modelling and simulation environment for systems medicine: Chronic obstructive pulmonary disease (COPD) as a use case.* FP7-ICT-270086., 2011-2013.
83. François Maltais, Marc Decramer, Richard Casaburi, Esther Barreiro, Yan Burelle, Richard Debigare´ , P. N. Richard Dekhuijzen, Frits Franssen, Ghislaine Gayan-Ramirez, Joaquim Gea, Harry R. Gosker, Rik Gosselink, Maurice Hayot, Sabah N. A. Hussain, Wim Janssens, Micheal I. Polkey, Josep Roca, Didier Saey, Annemie, M. W. J. Schols, Martijn A. Spruit, Michael Steiner, Tanja Taivassalo, Thierry Troosters, Ioannis Vogiatzis, P.D. Wagner, *An Official American Thoracic Society/European Respiratory Society Statement: Update on Limb Muscle Dysfunction in Chronic Obstructive Pulmonary Disease.* Am J Respir Crit Care Med (in press), 2014.
84. Sala, E., J. Roca, R.M. Marrades, J. Alonso, J.M. Gonzalez De Suso, A. Moreno, J.A. Barbera, J. Nadal, L. de Jover, R. Rodriguez-Roisin, P.D. Wagner, *Effects of endurance training on skeletal muscle bioenergetics in chronic obstructive pulmonary disease.* Am J Respir Crit Care Med, 1999. **159**(6): p. 1726-34.
85. Richardson, R.S., B.T. Leek, T.P. Gavin, L.J. Haseler, S.R.D. Mudaliar, R. Henry, O. Mathieu-Costello, P.D. Wagner, *Reduced Mechanical Efficiency in Chronic Obstructive Pulmonary Disease but Normal Peak Vo2 with Small Muscle Mass Exercise.* Am J Respir Crit Care Med, 2004. **169**(1): p. 89-96.
86. Cases, M., L.I. Furlong, J. Albanell, R.B. Altman, R. Bellazzi, S. Boyer, A. Brand, A.J. Brookes, S. Brunak, T.W. Clark, J. Gea, P. Ghazal, N. Graf, R. Guigó, T.E. Klein, N. López-Bigas, V. Maojo, B. Mons, M. Musen, J.L. Oliveira, A. Rowe, P. Ruch, A. Shabo, E.H. Shortliffe, A. Valencia, J. van der Lei, M.A. Mayer, F. Sanz, *Improving data and knowledge management to better integrate health care and research.* Journal of internal medicine, 2013. **274**(4): p. 321-328.
87. ESF, *Personalised Medicine for the European Citizen – Towards more precise medicine for the diagnosis, treatment and prevention of disease (iPM). URL:http://www.esf.org/fileadmin/Public_documents/Publications/Personalised_Medicine.pdf. Accessed: 2014-06-19. (Archived by WebCite® at http://www.webcitation.org/6QRqm7B2R).* 2012.
88. Blanco, I., E. Gimeno, P.A. Munoz, S. Pizarro, C. Gistau, R. Rodriguez-Roisin, J. Roca, J.A. Barberà, *Hemodynamic and Gas Exchange Effects of Sildenafil in Patients with Chronic Obstructive Pulmonary Disease and Pulmonary Hypertension.* Am J Respir Crit Care Med, 2010. **181**(3): p. 270-278.
89. BioBridge, *Integrative Genomics and Chronic Disease Phenotypes: modelling and simulation tools for clinicians*, 2006-2009, FP6-2005-LIFESCIHEALTH-7, BioBridge project grant agreement nº 037909.
90. Van Hentenryck, K., *Health Level Seven. Shedding light on HL7's Version 2.3 Standard.* Healthc Inform, 1997. **14**(3): p. 74.
91. Thomas, R., M. Kaufman, *Multistationarity, the basis of cell differentiation and memory. I. Structural conditions of multistationarity and other nontrivial behavior.* Chaos, 2001. **11**(1): p. 170-179.
92. Trujillo, J., *An engineering process for developing Secure Data Warehouses.* Inf Softw Technol, 2009. **51**(6): p. 1033 - 1051.
93. Garcia-Aymerich, J., F.P. Gomez, M. Benet, E. Farrero, X. Basagana, A. Gayete, C. Pare, X. Freixa, J. Ferrer, A. Ferrer, J. Roca, J.B. Galdiz, J. Sauleda, E. Monso, J. Gea, J.A. Barbera, A. Agusti, J.M. Anto, *Identification and prospective validation of clinically relevant chronic obstructive pulmonary disease (COPD) subtypes.* Thorax, 2011. **66**(5): p. 430-7.
94. de-Torres, J.P., D. Blanco, A.B. Alcaide, L.M. Seijo, G. Bastarrika, M.J. Pajares, A. Munoz-Barrutia, C. Ortiz-de-Solorzano, R. Pio, A. Campo, U. Montes, V. Segura, J. Pueyo, L.M. Montuenga, J.J. Zulueta, *Smokers with CT detected emphysema and no airway obstruction have decreased plasma levels of EGF, IL-15, IL-8 and IL-1ra.* PLoS One, 2013. **8**(4): p. e60260. PMID: Pmc3618450.

95. de-Torres, J.P., C. Casanova, J.M. Marin, J. Zagaceta, A.B. Alcaide, L.M. Seijo, A. Campo, S. Carrizo, U. Montes, E. Cordoba-Lanus, R. Baz-Davila, A. Aguirre-Jaime, B.R. Celli, J.J. Zulueta, *Exploring the impact of screening with low-dose CT on lung cancer mortality in mild to moderate COPD patients: a pilot study.* Respir Med, 2013. **107**(5): p. 702-7.
96. Burrowes, K.S., J. De Backer, R. Smallwood, P.J. Sterk, I. Gut, R. Wirix-Speetjens, S. Siddiqui, J. Owers-Bradley, J. Wild, D. Maier, C. Brightling, *Multi-scale computational models of the airways to unravel the pathophysiological mechanisms in asthma and chronic obstructive pulmonary disease (AirPROM).* Interface Focus, 2013. **3**(2).
97. Pearl, J., *Probabilistic Reasoning in Intelligent Systems: Networks of Plausible Inference*1988: Morgan Kaufmann. ISBN: 9781558604797.
98. Burrowes, K.S., E.a. Hoffman, M.H. Tawhai, *Species-specific pulmonary arterial asymmetry determines species differences in regional pulmonary perfusion.* Annals of biomedical engineering, 2009. **37**: p. 2497-509.
99. Burrowes, K.S., M.H. Tawhai, *Computational predictions of pulmonary blood flow gradients: gravity versus structure.* Respiratory physiology & neurobiology, 2006. **154**: p. 515-23.
100. Wagner, P.D., *The multiple inert gas elimination technique (MIGET).* Intensive Care Med, 2008. **34**(6): p. 994-1001.
101. Wagner, P.D., *Determinants of Maximal Oxygen Transport and Utilization.* Annual Review of Physiology, 1996. **58**(1): p. 21-50.
102. Wagner, P.D., *Algebraic analysis of the determinants of VO2max.* Respir Physiol, 1993. **93**(2): p. 221-37.
103. Selivanov, V.a., T.V. Votyakova, J.a. Zeak, M. Trucco, J. Roca, M. Cascante, *Bistability of mitochondrial respiration underlies paradoxical reactive oxygen species generation induced by anoxia.* PLoS computational biology, 2009. **5**: p. e1000619.
104. Goh, K.-I., M. Cusick, D. Valle, B. Childs, M. Vidal, A.-L. Barabási, *The human disease network.* Proceedings of the National Academy of Sciences, 2007. **104**(21): p. 8685-8690.
105. De Las Mercedes Huertas Miguelanez, M., L. Ceccaroni. *A simulation and integration environment for heterogeneous physiology-models*. in *e-Health Networking, Applications & Services (Healthcom), 2013 IEEE 15th International Conference on*. 2013.
106. Vestbo, J., S. Hurd, A. Agusti, P. Jones, C. Vogelmeier, A. Anzueto, P. Barnes, L. Fabbri, F. Martinez, M. Nishimura, *Global Strategy for the Diagnosis, Management and Prevention of Chronic Obstructive Pulmonary Disease, GOLD Executive Summary.* Am J Respir Crit Care Med, 2013. **187**: p. 347 - 365.
107. Celli, B., C. Cote, J. Marin, C. Casanova, M. Montes De Oca, R. Mendez, V. Pinto Plata, H. Cabral, *The body-mass index, airflow obstruction, dyspnea, and exercise capacity index in chronic obstructive pulmonary disease.* N Engl J Med, 2004. **350**: p. 1005 - 1012.
108. Barberan-Garcia A, V.I., Golberg HS, Vilaró J, Rodriguez DA, Garåsen HM, Troosters T, Garcia-Aymerich J, Roca J and NEXES consortium, *Effects and barriers to deployment of telehealth wellness programs for chronic patients across 3 European countries.* Respir Med, 2014. **108**(4): p. 9.
109. Nexes, *Final workshop web page and video recordings. http://www.nexeshealth.eu/videos.html*, 2012.
110. Miller, W.G., J.R. Tate, J.H. Barth, G.R. Jones, *Harmonization: the sample, the measurement, and the report.* Ann Lab Med, 2014. **34**(3): p. 187-97. PMID: Pmc3999316.
111. Campbell, C.A., A.R. Horvath, *Harmonization of critical result management in laboratory medicine.* Clin Chim Acta, 2014. **432**: p. 135-47.
112. Uribe, G.A., D.M. Lopez, B. Blobel, *Towards automated biomedical ontology harmonization.* Stud Health Technol Inform, 2014. **200**: p. 62-8.
113. Kicinski, M., *Publication Bias in Recent Meta-Analyses.* PLoS ONE, 2013. **8**(11): p. e81823.
114. Brice, A., I. Chalmers, *Medical journal editors and publication bias.* Bmj, 2013. **347**: p. f6170.
115. Smulders, Y.M., *A two-step manuscript submission process can reduce publication bias.* J Clin Epidemiol, 2013. **66**(9): p. 946-7.
116. Pandey, J.P., *Genomewide association studies and assessment of risk of disease.* N Engl J Med, 2010. **363**(21): p. 2076-7; author reply 2077.

117. Barabasi, A.L., *Network medicine--from obesity to the "diseasome".* N Engl J Med, 2007. **357**(4): p. 404-7.
118. de Chassey, B., V. Navratil, L. Tafforeau, M.S. Hiet, A. Aublin-Gex, S. Agaugue, G. Meiffren, F. Pradezynski, B.F. Faria, T. Chantier, M. Le Breton, J. Pellet, N. Davoust, P.E. Mangeot, A. Chaboud, F. Penin, Y. Jacob, P.O. Vidalain, M. Vidal, P. Andre, C. Rabourdin-Combe, V. Lotteau, *Hepatitis C virus infection protein network.* Mol Syst Biol, 2008. **4**: p. 230. PMID: Pmc2600670.
119. Yeger-Lotem, E., L. Riva, L.J. Su, A.D. Gitler, A.G. Cashikar, O.D. King, P.K. Auluck, M.L. Geddie, J.S. Valastyan, D.R. Karger, S. Lindquist, E. Fraenkel, *Bridging high-throughput genetic and transcriptional data reveals cellular responses to alpha-synuclein toxicity.* Nat Genet, 2009. **41**(3): p. 316-23. PMID: Pmc2733244.
120. Bandyopadhyay, S., M. Mehta, D. Kuo, M.K. Sung, R. Chuang, E.J. Jaehnig, B. Bodenmiller, K. Licon, W. Copeland, M. Shales, D. Fiedler, J. Dutkowski, A. Guenole, H. van Attikum, K.M. Shokat, R.D. Kolodner, W.K. Huh, R. Aebersold, M.C. Keogh, N.J. Krogan, T. Ideker, *Rewiring of genetic networks in response to DNA damage.* Science, 2010. **330**(6009): p. 1385-9. PMID: Pmc3006187.
121. Saez-Rodriguez, J., L.G. Alexopoulos, J. Epperlein, R. Samaga, D.A. Lauffenburger, S. Klamt, P.K. Sorger, *Discrete logic modelling as a means to link protein signalling networks with functional analysis of mammalian signal transduction.* Mol Syst Biol, 2009. **5**: p. 331. PMID: Pmc2824489.
122. Ramirez, F., A. Schlicker, Y. Assenov, T. Lengauer, M. Albrecht, *Computational analysis of human protein interaction networks.* Proteomics, 2007. **7**(15): p. 2541-52.
123. Hare, J.M., *Nitroso–Redox Balance in the Cardiovascular System.* New England Journal of Medicine, 2004. **351**(20): p. 2112-2114.
124. West, J.B., *Highest permanent human habitation.* High Alt Med Biol, 2002. **3**(4): p. 401-7.
125. Naimi, A.I., J. Bourbeau, H. Perrault, J. Baril, C. Wright-Paradis, A. Rossi, T. Taivassalo, A.W. Sheel, R. Rabol, F. Dela, R. Boushel, *Altered mitochondrial regulation in quadriceps muscles of patients with COPD.* Clin Physiol Funct Imaging, 2011. **31**(2): p. 124-31.
126. Puente-Maestu, L., A. Lázaro, B. Humanes, *Metabolic derangements in COPD muscle dysfunction*. Vol. 114. 2013. 1282-1290.